September 26-29, 2010
Belfast, UK

Table of Contents

We would like to thank our sponsors and those who have made generous donations:

http://www.embs.org

http://www.ulster.ac.uk

http://www.medtronic.com

http://www.heartsine.com/

http://www.draeger.com

http://www.gehealthcare.com

http://www.mortara.com

www.THEW-project.org

http://www.zoll.com/

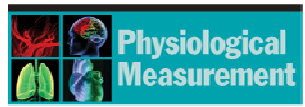

http://iopscience.iop.org/0967-3334/

http://www.ibm.com

The Engineering in Medicine and Biology Society of the IEEE advances the application of engineering sciences and technology to medicine and biology, promotes the profession, and provides global leadership for the benefit of its members and humanity by disseminating knowledge, setting standards, fostering professional development, and recognizing excellence.

The field of interest of the IEEE Engineering in Medicine and Biology Society is the application of the concepts and methods of the physical and engineering sciences in biology and medicine. This covers a very broad spectrum ranging from formalized mathematical theory through experimental science and technological development to practical clinical applications. It includes support of scientific, technological and educational activities.

Engineering in Medicine and Biology Society
445 Hoes Lane
Piscataway, New Jersey, USA 08854
Telephone: +1 732 981 3433
Facsimile: +1 732 465 6435
E-mail: emb-exec@ieee.org

www.embs.org

PUBLICATIONS
IEEE PULSE
Transactions on Biomedical Engineering Transactions on Biomedical Engineering Letters
Transactions on Information Technology in Biomedicine
Transactions on Neural Systems and Rehabilitation Engineering
Transactions on Medical Imaging
Transactions on NanoBioscience
Transactions on Computational Biology and Bioinformatics
Transactions on Biomedical Circuits and Systems
Reviews on Biomedical Engineering

ELECTRONIC PRODUCTS
EMBS Electronic Resource

CONFERENCES
Annual International Conference of the IEEE Engineering in Medicine and Biology Society (EMBC)
IEEE EMBS Special Topic Conference on Neural Engineering (NER)
International Symposium on Biomedical Imaging (ISBI)
International Conference on Biomedical Robotics and Biomechatronics (BIOROB) International Conference on Rehabilitation Robotics (ICORR) AMA/IEEE-EMBS Medical Technology Conference (MedTech)
Grand Challenges Conference Series (GCBE)

SUMMER SCHOOLS Sponsored by EMBS
International Summer School on Biomedical Imaging
International Summer School on Biomedical Signal Processing
International Summer School on Biocomplexity
International Summer School on Medical Devices and Biosensors
International Summer School on Information Technology in Biomedicine

Computing in Cardiology 2011

September 18th – 21st, 2011

Zhejiang University, Hangzhou, China

The 2011 Computing in Cardiology conference will be held in Hangzhou, China, from September 18th-21st. The meeting is affiliated with Zhejiang University.

Hangzhou is a noted ancient capital of China with famous natural beauty and cultural heritage. The city has many natural, cultural and historical landmarks including the famous West Lake, Grand Canal, Lingyin Temple, National Silk Museum, Tea Museum, Museum of Traditional Chinese Medicine and the Southern Song Dynasty Official Kiln Museum. Around Hangzhou there are also many places worth visiting, e.g. Wuzhen Ancient Town with thousands of years of history, Thousand Islets Lake with 1078 islets in a man-made lake, Tiantai Mountain Scenic Area (Tiantai Sect of Chinese Buddhism) and Mogan Mountai, which is one of the 'Four Best Summer Resorts in China'. The social programme will include visits to some of these sites.

Participants can fly:

- directly to Hangzhou on KLM from Amsterdam,
- to Shanghai and transfer to Hangzhou by bus or train (approximately 1 hour),
- to Beijing and then by internal flight to Hangzhou.

There will be the opportunity to travel inside China before and after the meeting and if there is enough interest, a short post conference tour may be organised, perhaps to Guilin in Gianxi Province or Xian in Shaanxi Province.

The first announcement will shortly be online at http://www.cinc2011.org

Board of Directors and Local Committee

BOARD OF DIRECTORS

President
Peter Macfarlane, DSc
University of Glasgow, UK

Secretary
Leif Sörnmo
Lund University
Lund, Sweden

Treasurer
Victor Mor-Avi, PhD
University of Chicago
Chicago, IL, USA

Past President
Harold Ostrow, MSEE
Gaithersburg, MD, USA

Willem Dassen, PhD
Maastricht University
Maastricht, The Netherlands

Paul Kligfield, MD
Weill Cornell Medical School
New York, NY, USA

Pablo Laguna, PhD
University of Zaragosa
Zaragosa, Spain

George Moody
Massachusetts Institute of Technology
Cambridge, MA, USA

Sheryl Prucka, MSEE
Park City, UT, USA

Ex-Officio ESC
Enno van der Velde, PhD
Leiden University Medical Center
Leiden, The Netherlands

Editor, Proceedings
Alan Murray, PhD
Freeman Hospital
Newcastle upon Tyne, UK

CinC 2010 SECRETARIAT ADDRESS
Dewar Finlay (d.finlay@ulster.ac.uk)
Chris Nugent (cd.nugent@ulster.ac.uk)
University of Ulster
Shore Road, Belfast
BT37 0QB

Web site: http://cinc2010.org

LOCAL COMMITTEE

Local Organsing Committee
Dewar Finlay (Conference Chair)
Chris Nugent (Conference Co-Chair)

Nicola Armstrong
Mark Beattie
Raymond Bond
Kyle Boyd
Cathal Breen
William Burns
Ian Cleland
Michael Daly
Steven Devlin
Rebecca Di Maio
Mark Donnelly
Leo Galway
Rachel Gawley
Daniel Guldenring
Regina Haughey
Colin Jamison
Heather McDonald
Sonja O'Neill
George Okeyo
Athanasia Panousopoulou
Darren Quinn
Jonathan Synnott
Shuai Zhang

Local scientific committee
Raymond Bond
Cathal Breen
Michael Daly
Rebecca Di Mio
Mark Donnelly
Omar Escalona
Dewar Finlay
Daniel Guldenring
Colin Jamison
Chris Nugent
Frank Owens
Peter Scott

International scientific committee
Jean-philippe Courderc
Johan Di Bie
Richard Gregg
Shen Luo
Stefan Nelwan
Peter van Dam
Joel Xue

Letter from the President

Dear Participant,

It is a pleasure for me to welcome you to the 37th Annual Conference of the organisation now known as “Computing in Cardiology”, this being the first meeting under the new title. The Board took a decision to change the name, given the view that “computers” were so pervasive nowadays, being integral to almost every electronic device. Computing in Cardiology seemed subtly more appropriate. Irrespective of the title, the tried and trusted format of the meeting remains the same this year.

Last year, there were concerns about the potential effect of swine flu and the economic situation on attendance at the meeting. This year, there have been concerns about the continuing economic situation, as well as the ash cloud and strikes potentially causing significant disruption to travel. I hope that you are reading this having reached Belfast without too much difficulty.

This year, approximately 350 abstracts were received for consideration. This is indeed a healthy number of submissions and the Board is extremely pleased that interest in participating in Computing in Cardiology remains high. One of the great features of the meeting is the networking which takes place throughout, whether this is at the scientific or social sessions!

Many of you will be aware that Bill Sanders decided to step down as Director of Information Systems after having loyally supported the conference organisation for over 30 years. Bill has served as President and Secretary of the Board in the past. Throughout the years, he has been faithfully supported by his wife Gary, who similarly has put an enormous amount of work into the organisation of the annual meeting. A special presentation will be made to Bill and Gary at the closing plenary session to acknowledge the tremendous service which they have given to Computers in Cardiology as was, virtually since its inception. On behalf of the Board, I wish to thank them for their unstinting efforts to promote Computers in Cardiology for over 30 years.

No conference could be organised without the support of the local organising committee. This year Dewar Finlay and Chris Nugent have played a major role in co- chairing the local organising committee and hence the meeting. If you have not organised a conference, then you will probably not appreciate the amount of work which goes on for up to 2 years beforehand. This begins with venue selection, proceeds with preparation of the Sunday Symposium and the social event, continues

with participation in selection of session chairs, and involves responding to numerous requests for invitations/support for visa applications etc. The Board would like to thank Dewar and Chris and their many colleagues for the huge effort which they have expended on organising this year's meeting.

I am confident that Computing in Cardiology 2010 will be well up to the usual high standard in respect of scientific content, social events and general enjoyment. Thank you for choosing Computing in Cardiology as a conference which you feel is worthy of attending.

Best Wishes
Peter Macfarlane
President

Welcome to Belfast

On behalf of the local organizing committee, we are delighted to welcome you to the 37th Annual Scientific meeting of Computing in Cardiology (formerly Computers in Cardiology) in Belfast, Northern Ireland. This is the first time that the conference has been held on the island of Ireland and we are delighted that you can join us for what we are sure will be an exciting meeting.

We received a large number of high quality abstract submissions and it has been our pleasure to work with the Computing in Cardiology (CinC) Board of Directors in the development of the conference program. In addition to the regular oral and poster sessions, this year's program will include a special plenary session devoted to Computing in Cardiac Safety**.** In addition to the standard scientific program, we are delighted to offer you the Sunday Symposium which this year will focus on Mobile Coronary Care.

We would like to express our sincere thanks to all those who have assisted in the organization of the meeting. We have benefited from huge support from the University of Ulster and from our Local Organizing Committee. We would also like to thank all those who have made generous financial donations to support the event. Finally we would like to thank you! Without your contributions and participation, this event would simply not be possible.

Dewar Finlay
Conference Chai

Chris Nugent
Conference Co-Chair

Map of Belfast

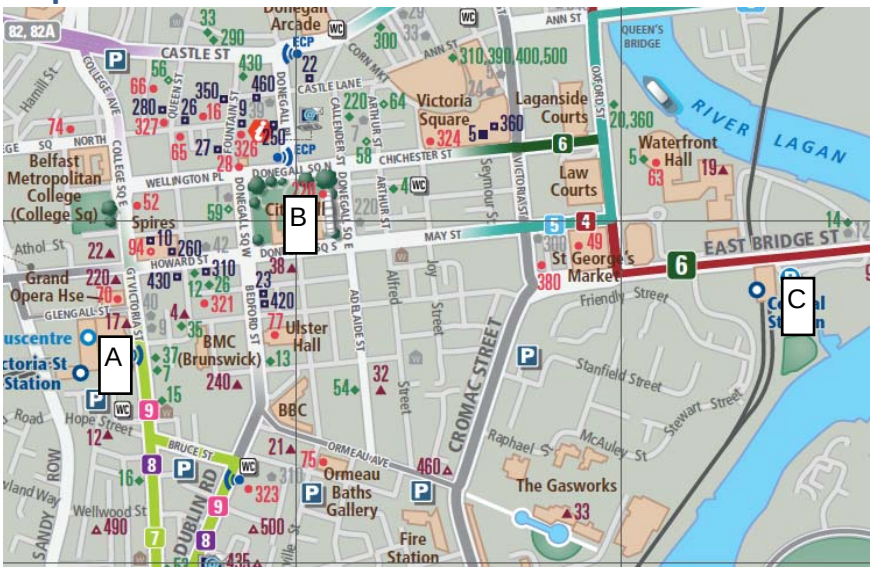

A: Europa Hotel
B: Belfast City Hall (Sunday symposium reception)
C: Belfast Central Station (Departure point for those taking train to Monday social)

General Information

Computing in Cardiology is one of the premier events focusing on computer applications in clinical cardiology and cardiovascular research. Annual meetings have been held for over three decades and attract scientists and professionals from the fields of medicine, physics, engineering and computer science. This year's meeting is hosted by the University of Ulster's School of Computing and Mathematics and the Computing Science Research Institute.

Belfast and Northern Ireland

Northern Ireland is a small country, which is a part of the United Kingdom, located on the north east of the island of Ireland. It shares a border with the Republic of Ireland and has a population of just under 2 million. Belfast is Northern Ireland's largest city located on the east coast. It is situated approximately 160 km north of Dublin.

Belfast is a vibrant city with a rich and varied heritage. The city has many cultural, political and historical landmarks including the famous Belfast murals and the dockland site where the infamous Titanic was constructed. Beyond the city, you can visit the various museums and tourist attractions that Northern Ireland has to offer. These include the Giant's Causeway, the Bushmills Whiskey Distillery and the Ulster American Folk Park, all of which are not more than 1.5 hours by road.

University of Ulster

The University of Ulster is a dynamic and innovative research and learning institute based in Northern Ireland (www.ulster.ac.uk). It has an international reputation for excellence, innovation and regional engagement and has built strong international partnerships across the globe.

The University currently has over 23,000 local, national and international students studying at undergraduate to postgraduate degree levels at one of the four campuses - Coleraine, Jordanstown, Belfast, and Magee. The School of Computing and Mathematics is based on the Jordanstown campus and has approximately 40 academic staff and 850 students. It offers courses at both undergraduate and postgraduate level, including opportunities for PhD study. The School delivers courses in multimedia, mathematics, ICT, computing science (with specialisms) and software engineering

Recognised as one of the leading research institutes in the UK, Ulster has consistently achieved international standard ratings in the UK Research Assessment Exercise (RAE), demonstrating its commitment to continuous high quality research. Research within the Faculty of

Computing and Engineering is managed by the Computer Science Research Institute (CSRI) (http://www.compeng.ulster.ac.uk/csri.php).

The CSRI is one of 17 University Research Institutes at Ulster. It fosters strategic objectives to produce high quality research output; expand international academic and industrial collaborations; expand a vibrant graduate programme; develop new infrastructure to support research; and stimulate and sustain regional development and economic regeneration. The area of medical informatics and computerized electrocardiology remains one of the key research topics within the CSRI.

Hotel and Conference Centre

The conference will be held at Belfast's landmark Europa hotel. The hotel boasts over 250 bedrooms and extensive conference facilities. It has historic significance in Northern Ireland's past and is the preferred choice of Prime Ministers, Presidents and many celebrities on their visits to Belfast. Located in the heart of the city the hotel offers visitors the opportunity to enjoy all that Belfast has to offer including the excellent shopping facilities and renowned nightlife. The hotel is a 10 minute drive from all major motorways and ferry and air terminals. It has a rail link next door and, just a few hundred meters from the front door, a direct coach link to Dublin Airport.

All scientific sessions of the conference and the Sunday Symposium will take place in the hotel. The Sunday symposium reception will be held in the Belfast City Hall and the social event will be held at the Ulster Folk and Transport museum. The social event will be followed by the conference dinner at the nearby Culloden hotel.

Transportation

During the conference, transportation will be provided to and from the social events. It is important that delegates are at transportation points at the correct times. This is outlined in the Social Program section of this booklet. The Sunday Symposium Reception will be held at Belfast City Hall which is within walking distance from the Hotel.

For travelling around at other times, there are several options. The conference Hotel sits adjacent to a bus and train station. Buses originating from this station travel to destinations throughout Northern Ireland. A local city bus service, know as 'Metro', is serviced from the side of Belfast City Hall (where the Sunday Symposium Reception will be held). All train and bus services are operated by Translink and more information, including timetables, can be found on their web site www.translink.co.uk. Private hire taxis can be booked in the hotel lobby

and public hire taxis operate from a taxi rank across the road from the hotel.

Registration

For the duration of the conference, the registration desk will be located at the entrance to the exhibition centre, which is through the main hotel lobby to the left hand side. The desk will be open at the following times:

Sunday (26th September)	12:00-18:00
Monday (27th September)	07:00-12:00
Tuesday (28th September)	07:30-18:00
Wednesday (29th September)	07:30-15:00

Internet Access

Wireless internet access is provided by BTOpenZone throughout the Hotel. Please contact the registration desk for further details of vouchers required.

Meals

The registration fee for attendees includes the following:

Sunday: A drinks reception will follow the Sunday Symposium. The reception will take place at 19:00 in Belfast City Hall.

Monday: Tea and Coffee will be served during the mid morning break. Lunch, a reception and gala dinner will be served as part of the social program.

Tuesday: Tea and Coffee will be served during the breaks throughout the day. A light lunch will be provided and during the poster session, in the evening, a light reception will be served.

Wednesday: Tea and Coffee will be served during the mid morning break. A light lunch will be served during the poster session.

Accompanying Persons

The accompanying person registration allows the guest to attend the Monday social event. This includes the Monday Lunch, reception at the transport museum and conference dinner at the Culloden Hotel – and of course participation as an activist or passivist in the activities. Guests are also welcome to attend the reception on Sunday evening at Belfast City Hall and the conference poster sessions.

For Authors and Speakers

Oral Presentations

The time allocated for each oral presentation is 10 minutes, followed by 5 minutes for discussion. Speakers are expected to adhere strictly to this schedule, which will be enforced by session chairs in order to finish sessions on time and to permit participants to move successfully from one parallel session to another. The only exception to the 10-minute limit for oral presentations is for the four finalists in the Rosanna Degani Young Investigator Award competition, who are each allotted 15 minutes for their talks, followed by 5 minutes for discussion.

All conference rooms will be equipped with a computer projection system (LCD projector and PC with Windows 7, Microsoft Office, Windows Media Player and Adobe Acrobat reader). Speakers are required to allow adequate time prior to their sessions to load and check their presentations on the designated computer. A member of the Local Organising Committee will be available in each parallel session to help. In addition, speakers are required to meet with their session chairpersons in the scheduled conference room at least 10 minutes before the beginning of the session.

Poster Presentations

Poster sessions will take place in the Exhibition Centre on Tuesday, 28th September, from 17:30 and on Wednesday, 29th September, from 12:00. The exhibition centre is located on the ground floor of the hotel, through the entrance lobby on the left hand side. Authors are required to be present at their posters during their assigned session in order to discuss their work with other conference attendees.

Check-in: Authors must check-in at the registration desk at the entrance to the exhibition centre during the 30 minutes prior to the poster session.

Hanging Posters: For the Tuesday poster session, authors may hang their posters at the location designated with the correct number between 14:00 and 17:30. For the Wednesday poster session, posters may be hung between 08:00 and noon. Subject areas for the poster sessions will be clearly marked and poster boards will be numbered with a card corresponding to the page number in this book. Mounting materials will be provided at check-in.

Rosanna Degani Young Investigator Award

Computing in Cardiology run an annual competition to encourage young investigators and provide a living memorial to Rosanna Degani. The

competition for the 2010 Rosanna Degani Young Investigator Award is open to persons under 36 years of age and in "training status" at the submission deadline of 1st May, 2010. Finalists in the competition will present their work in session M1, at 8:15 on Monday 27th September in the exhibition centre. The name of the winner will be announced during the closing plenary session on Wednesday.

PhysioNet / Computing in Cardiology Challenge 2010

Since 2000, Computing in Cardiology have annually issued a PhysioNet Challenge in cooperation with PhysioNet, part of the NIH sponsored Research Resource for Complex Physiologic Signals. The aim of this year's challenge is to develop robust methods for filling in gaps in multiparameter physiologic data (including ECG signals, continuous blood pressure waveforms, and respiration). Session S63 is devoted to the presentation of work from investigators who have attempted to address this problem. The Board of Directors of Computing in Cardiology provides a grant for challenge awards. In 2009 and 2010 the family of Solange Akselrod made it possible to increase the prize money available to be awarded to the winning participants. The winners will be announced during the closing plenary session on Wednesday.

Manuscripts

Computers in Cardiology will publish the conference proceedings containing the complete manuscripts of all presentations. A CD-ROM copy of the proceedings is usually available by the end of the year and will be mailed directly to all registrants. In addition, the complete proceedings will be freely available via the CinC web site (http://www.cinc.org).
For any questions about manuscripts, consult the CinC web site or contact

Alan Murray, Editor of the proceedings (Alan.Murray@nuth.nhs.uk).

Conference Overview

The conference begins on the afternoon of Sunday 26th with a special symposium entitled “Mobile Coronary Care”. A reception will be offered at the end of the symposium. The scientific sessions of the conference will begin on Monday morning. In the afternoon, the traditional social program will take place. Sessions will continue on Tuesday and Wednesday, including both oral presentations and poster sessions.

Sunday Symposium

The symposium will commence at 2pm on Sunday the 26th September at the Europa Hotel. The Sunday Symposium will be held in the Exhibition Centre in the Europa hotel with the following program:

14:00	Opening remarks – Professor Chris Nugent (University of Ulster, Belfast, UK)
14:10	Connected Health in Ireland – Dr Peter Donnelly (BioBusiness Northern Ireland, Belfast, UK)
14:50	The Design of Wearable Sensor Systems for Coronary Care – Professor Eric McAdams (INSA de Lyon, France)
15:30	Break
16:00	Defibrillation-Past, Present and Future – Professor John Anderson (HeartSine Technologies and University of Ulster (Professor Emeritus Medical Electronics), Belfast, UK)
16:40	Limitations of the 12 lead ECG and the Benefits of Body Surface Mapping in the Emergency setting of Mobile Coronary Care – Professor Jennifer Adgey (Royal Victoria Hospital, Belfast, UK)
17:20	State of mobile coronary care: An International Perspective – Professor Mary Carey (The State University of New York at Buffalo, USA)
18:00	Close

This will be followed by a civic reception in Belfast City Hall commencing at 19.00.

Scientific Sessions

The scientific sessions will begin on Monday, 27th September at 08:15 with the Rosanna Degani Young Investigator Award Competition. All sessions will be held either in the Exhibition Centre or the Grand Ballroom (which is split into four separate rooms).

Monday Social Program

Each year at CinC, the Monday afternoon is set aside to facilitate a social event. This is an important part of the conference program as it allows delegates to network and relax in a more informal setting away from the scientific sessions. This year's social program will be based at the Ulster Folk and Transport Museum (http://www.nmni.com/uftm) that is located approximately seven miles from Belfast city centre on the south shore of Belfast Lough. The museum covers a 170-acre site and comprises a wide range of activities and exhibits.

Located outdoors is Ballycultra village. This fully recreated village is made up of more than 30 historic buildings that have been brought from their original locations across Ireland and painstakingly restored at the museum site. The buildings, which include a corner shop, several houses, a carpenters workshop, silent cinema, school and bar, allow visitors to experience what life in Ireland would have been like over 100 years ago. The presence of guides dressed in traditional attire makes this experience all the more authentic.

Located indoors is the transport museum. This contains one of the best rail galleries in Europe as well as road and aviation galleries that illustrate the history of all forms of transport to the present day.

The social program will commence at noon on Monday. A long-standing tradition for the CinC social program is that delegates can chose between activist or passivist activities. This year will be no exception!

Activist program

At noon on Monday activists shall make their way to Belfast Central train station and board a vintage steam train that will take them on a scenic journey to the museum. Please note: **Activists must be at Belfast Central Station at 12:40.** The train has been specially chartered and must comply with the rail company's strict schedule of operation. It is not possible for the train to wait if delegates are delayed. You should allow 30 minutes to walk from the Europa Hotel to Belfast central station. We advise that you leave the hotel no later than 12:05. Public hire taxis are available for hire from outside the hotel for those not willing to make the 30-minute walk. If you do choose to hire a taxi you should also leave sufficient time for this journey (at least 15 minutes) as city centre traffic may be a factor.

Lunch packs will be provided on board the train. Upon arrival at the museum activists will be able to participate in a number of activities that will take place in Ballycultra village.

These will include:
Treasure Hunts
Penny whistle lessons
Story telling and harvest knot tying lessons in the school house
Guinness or whiskey tasting in McCusker's Pub

Passivist program

At noon on Monday passivists will assemble in the exhibition centre of the hotel. From there they will board transportation and take a scenic tour of sites of historical interest en-route to the Ulster Folk and Transport Museum. This will include an opportunity to view some of Belfast's famous murals and other political landmarks. Upon arrival at the museum, lunch will be available and passivists will have the opportunity to view the various buildings in Ballycultra village at their leisure. There will be an opportunity to interact with the museum guides who will be displaying traditional crafts in addition to cooking and serving traditional food in the various buildings.

Later in the afternoon
Later in the afternoon both activists and passivists will reconvene in the indoor transport museum for a drinks reception before departing, by coach, to the nearby Culloden hotel where the conference dinner will be held. Following dinner, busses will begin returning guests to Belfast City Centre (Europa Hotel).

Delegates should wear comfortable and informal clothing to the Social events and Conference dinner.

Scientific Sessions Program Overview

Monday, September 27, 2010

08:00	Welcome to CinC 2010	Exhibition Centre
08:15	M1: Rosanna Degani Young Investigator Finalist Presentations	Exhibition Centre
10:00	Coffee Break	Library bar
10:30	S21: Ischemia and Infarction I	Grand 3
	S22: Telemedicine I	Grand 1
	S23: Novel Techniques in HRV	Grand 4/5
	S24: Modeling & Simulation: Forward & Inverse Problems	Grand 2
12:00	Social Event	

Tuesday, September 28, 2010

08:00	S31: Arrhythmias	Grand 1
	S32: Cardiovascular Variability	Grand 4/5
	S33: Cardiovascular MRI	Grand 3
	S34: Ventricular Cell Modeling and Ischemia	Grand 2
09:30	Coffee Break	Library Bar
10:00	S41: Novel Techniques	Grand 1
	S42: Medical Informatics	Grand 2
	S43: Cardiovascular Imaging I	Grand 3
	S44: Baroreflex	Grand 4/5
11:00	Coffee Break	Library Bar
11:15	M5: Computing in Cardiac Safety – Plenary	Exhibition Centre
12:30	Lunch	To be Announced
14:00	S61: Ischemia and Infarction II	Grand 1
	S62: Lead Systems	Grand 4/5
	S63: PhysioNet/Computing in Cardiology Challenge	Grand 3
	S64: System Modeling & Instrumentation	Grand 2
15:30	Coffee break	Library Bar
16:00	S71: QT & Repolarisation	Grand 3
	S72: Cardiovascular Mechanics	Grand 2
	S73: CV Ultrasound Imaging	Grand 1
	S74: Atrial Cell Modeling	Grand 4/5
17:30	Poster session with light reception	Exhibition Centre
19:30	Poster session ends	

Wednesday, September 29, 2010

8:30	S91: Algorithms and Signal Processing	Grand 1
	S92: Clinical ECG	Grand 3
	S93: Heart Rate Variability	Grand 2
	S94: Electrophysiology	Grand 4/5
10:00	Coffee Break	Library Bar
10:30	SA1: Repolarisation at Rest and during Exercise	Grand 3
	SA2: Telemedicine II	Grand 1
	SA3: MRI: Ventricular Function	Grand 2
	SA4: Ventricular Cell Modeling	Grand 4/5
12:00	Poster Session with light lunch	Exhibition Centre
14:00	MC: Closing Plenary Session	Exhibition Centre
15:30	Closing Ceremony	
16:00	Conference Closes	

Scientific Program

Monday, September 27, 2010, 08:15

M1: Rosanna Degani Young Investigator Award

Room: Exhibition Centre

Chairs: Peter Macfarlane and Willem Dassen

1 **Correlation Between Time Domain Baroreflex Sensitivity and Sympathetic Nerve Activity**

Sónia Gouveia*, Ana Paula Rocha, Pablo Laguna and Philippe van de Borne

2 **Fully Automated Gating of Optical Coherence Tomography Data**

Kenji Sihan*, Charl Botha, Frits Post, Sebastiaan de Winter, Evelyn Regar, Patrick Serruys, Ronald Hamers and Nico Bruining

3 **MRI-Based Quantification of Myocardial Perfusion at Rest and Stress using Automated Frame-by-Frame Segmentation and Non-Rigid Registration**

Giacomo Tarroni*, Amit R Patel, Federico Veronesi, James Walter, Claudio Lamberti, Roberto M Lang, Victor Mor-Avi and Cristiana Corsi

4 **Simulating the Impact of the Transmural Extent of Acute Ischemia on the Electrocardiogram**

Mathias Wilhelms*, Olaf Dössel and Gunnar Seemann

Monday, September 27, 2010, 10:30

S21: Ischemia and Infarction I

Room: Grand 3

Chairs: Jennifer Adgey and Mary Carey

5 **Development and Comparison of Single-parameter Indices Characterizing Severity of Acute Myocardial Ischemia**

John Wang*, James Warren, Galen Wagner and Milan Horacek

6 **Validation of Electrocardiographic Criteria for Predicting the Culprit Artery in Patients with Acute Myocardial Infarction**

Niek van der Putten*, Peter Rijnbeek, Arnold Dijk, Gerard van Herpen, Enno van der Velde, Arie Maan, Jonathan Lipton and Jan Kors

7 **A Spatio-Temporal Study of Ischemia and the Time-Frequency Coupling Variations Between the ST Amplitude, Heart Rate and Dominant Angle**

Raul Llinares and Gari D Clifford*

8 **Enhancing the Acute MI Criteria in the Glasgow ECG Analysis Program to Include ST Depression**

Elaine Clark*, Maria Sejersten, Peter Clemmensen and Peter Macfarlane

9 **Graphic Visualization of ECG Estimated Myocardial Infarct Size using the 17 Segment Bull's Eye Presentation**

Richard Gregg*, Sophia Zhou and Eric Helfenbein

10 **Display of Heart-Surface Potentials Derived from 12-lead Electrocardiograms**

Milan Horacek*, James Warren and John Wang

Monday, September 27, 2010, 10:30

S22: Telemedicine I

Room: Grand 1

Chairs: Mark Donnelly and Michael Daly

11 **An Augmentative and Portable QTc-Observer(QTO-Q2) to Facilitate More Purposeful Outpatient Monitoring**

Thomas Chee Tat Ho* and Xiang Chen

12 **Non-Invasive Sensors Based Human State in Nightlong Sleep Analysis for Home-Care**

Magdalena Smolen*, Klaudia Czopek and Piotr Augustyniak

13 **Management of Non-uniform Data Transfer in Cardiac Monitoring Systems with Adaptive Interpretation**

Piotr Augustyniak*

14 **Optimization of the Alarm-Management of a Heart Failure Home-Monitoring System**

Marija Vukovic*, Mario Drobics, Dieter Hayn, Peter Kastner and Günter Schreier

15 **Multimedia Alarm Pages on Multiple Smartphone Platforms**

MJB van Ettinger*, JA Lipton, SP Nelwan, RJ Barendse, TB van Dam and N van der Putten

16 **Evaluation of Patients' Adherence and Satisfaction with a Self-Measurement Blood Pressure Telemonitoring Program**

Michele Triventi*, Giovanni Calcagnini, Federica Censi, Eugenio Mattei, Stefano Strano and Pietro Bartolini

Monday, September 27, 2010, 10:30

S23: Novel Techniques in HRV

Room: Grand 4&5

Chairs: Enno van der Velde and Peter Scott

17 **Heart Rate Variability Characterized by Refined Multiscale Entropy Applied to Cardiac Death in Ischemic Cardiomyopathy Patients**

José Fernando Valencia*, Montserrat Vallverdú, Rico Schroeder, Iwona Cygankiewicz, Rafael Vázquez, Antonio Bayés de Luna, Alberto Porta, Andreas Voss and Pere Caminal

18 **Assessing Sympatho-Vagal Balance in Schizophrenia through Tone-Entropy Analysis**

Ahsan Habib Khandoker*, Mami Fujibayashi, Toshio Moritani and Marimuthu Palaniswami

19 **RSA Component Extraction from Cardiovascular Signals by Combining Adaptive Filtering and PCA Derived Respiration**

Suvi Tiinanen*, Antti Kiviniemi, Mikko Tulppo and Tapio Seppänen

20 **New Representation of Heart Rate and Evaluation of Geometric Features Extracted From It**

Nader Jafarnia Dabanloo*, Sadaf Moharreri, Saman Parvaneh and Ali Nasrabadi

21 **A Hypotensive Episode Predictor for Intensive Care based on Heart Rate and Blood Pressure Time Series**

Joon Lee* and Roger Mark

Monday, September 27, 2010, 10:30

S24: Modeling & Simulation: Forward & Inverse Problems

Room: Grand 2

Chairs: Gunnar Seeman and Adriaan van Oosterom

22 **Differences in Non-Invasive Imaging of Atrial and Ventricular Recovery**

Peter M van Dam* and Adriaan van Oosterom

23 **Integrated Software Toolkit for Solving Bioelectric Field Problems**

Rob MacLeod*, Dana Brooks, Mike Steffen, Burak Erem, Darrell Swenson and Jeroen Stinstra

24 **An Iterative Method for Indirectly Solving the Inverse Problem of Electrocardiography**

J Pedron*, AM Climent, J Millet and MS Guillem

25 **A New Family of Variational-Form-Based Regularizers for Reconstructing Epicardial Potentials from Body-Surface Mapping**

Dafang Wang*, Robert Kirby, Rob MacLeod and Chris Johnson

26 **The Effect of Finite Element Mesh Quality on Electrical Bidomain Simulations**

Darrell Swenson*, Joshua Levine, Zhisong Fu and Rob MacLeod

27 **Accuracy of Estimates of Cardiac Action Potential Durations From Extracellular Waveforms Simulated by the Bidomain Model**

Simone Scacchi, Piero Colli Franzone, Luca F Pavarino* and Bruno Taccardi

Tuesday, September 28, 2010, 08:00

S31: Arrhythmias

Room: Grand 1

Chairs: Rebecca Di Maio and Roger Mark

28 **Susceptibility to Paroxysmal Atrial Fibrillation: A Study using Sinus Rhythm P Wave Parameters**

Aline Cabasson*, Lam Dang, Jean-Marc Vesin, Lukas Kappenberger, Roger Abacherli and Remo Leber

29 **Patient-Adaptive Ectopic Beat Classification using Active Learning**

Jenna Wiens* and John Guttag

30 **An Automated Algorithm for the Detection of Atrial Fibrillation in the Presence of Paced Rhythms**

Eric Helfenbein, Richard Gregg*, James Lindauer and Sophia Zhou

31 **A Mathematical Model of the Atrioventricular Node During Atrial Fibrillation**

Valentina DA Corino*, Frida Sandberg, Luca T Mainardi and Leif Sörnmo

32 **Modulation of ECG Atrial Flutter Wave Amplitude by Heart Motion: A Model-based and a Bedside Estimate**

Vincent Jacquemet*, Bruno Dubé, Peter van Dam, Aimé-Robert Leblanc, Réginald Nadeau, Marcio Sturmer, Teresa Kus and Alain Vinet

33 **Noninvasive Three-dimensional Cardiac Activation Imaging of Ventricular Arrhythmias in the Rabbit Heart**

Chengzong Han*, Steven Pogwizd, Cheryl Killingsworth, Jiajie Yan and Bin He

Tuesday, September 28, 2010, 08:00

S32: Cardiovascular Variability

Room: Grand 4/5

Chairs: Pablo Laguna and Luca Mainardi

34 **Respiration Differentially Modulates HRV Obtained from Arterial Pressure Wave and Electrocardiogram**

Salvador Carrasco-Sosa and Alejandra Guillén-Mandujano*

35 **Variability of the Systolic and Diastolic Electromechanical Periods in Healthy Subjects**

Salvador Carrasco-Sosa and Alejandra Guillén-Mandujano*

36 **Gender Related Differences in Scaling Structure of Heart-Rate and Blood-Pressure Variability as Assessed by Detrended Fluctuation Analysis**

Paolo Castiglioni* and Marco Di Rienzo

37 **Identification of Cardiovascular Baroreflex for Probing Homeostatic Stability**

Pedram Ataee*, Jin-Oh Hahn, Guy A Dumont and W Thomas Boyce

38 **Heart Rate Variability and Respiratory Sinus Arrhythmia Assessment of Affective States by Bivariate Autoregressive Spectral analysis**

Valentina Magagnin, Maurizio Mauri, Pietro Cipresso, Luca T Mainardi, Emery N Brown, Sergio Cerutti, Marco Villamira and Riccardo Barbieri*

39 **ECG-Derived Respiration: Comparison and New Measures for Respiratory Variability**

Devy Widjaja*, Joachim Taelman, Steven Vandeput, Marijke Braeken, RA Otte, Bea Van den Bergh and Sabine Van Huffel

Tuesday, September 28, 2010, 08:00

S33: Cardiovascular MRI

Room: Grand 3

Chairs: Rob Macleod and Philip Morrow

40 **Measurement of the Aortic Pulse Wave Velocity in MRI: Comparison of Transit Time Estimators**

Anas Dogui, Nadjia Kachenoura, Muriel Lefort, Alain De Cesare, Frédérique Frouin, Elie Mousseaux and Alain Herment*

41 **Feasibility of a Novel Approach for 3D Mitral Valve Quantification from Magnetic Resonance Images**

Francesco Maffessanti*, Marco Stevanella, Emiliano Votta, Massimo Lombardi, Oberdan Parodi, Daniele De Marchi, Carlo Conti, Alberto Redaelli and Enrico Caiani

42 **Rigid Registration of Delayed-Enhancement and Cine Cardiac MR Images using 3D Normalized Mutual Information**

Yasmina Chenoune*, Constantin Constantinides, Racha El Berbari, Elodie Roullot, Frédérique Frouin, Alain Herment and Elie Mousseaux

43 **Atrial Tissue Response to Radio Frequency Ablation: MRI Based Characterization of Injury**

Joshua Blauer*, Joshua Cates, Nassir Marrouche and Rob MacLeod

44 **Reproducible Evaluation of Diastolic Function using Phase-Contrast Magnetic Resonance Data**

Emilie Bollache*, Alban Redheuil, Stéphanie Clément-Guinaudeau, Carine Defrance, Ludivine Perdrix, Magalie Ladouceur, Muriel Lefort, Alain De Cesare, Frédérique Frouin, Alain Herment, Benoît Diebold, Elie Mousseaux and Nadjia Kachenoura

45 **Comparison of Aortic Lumen Area and Distensibility using Cine and Phase Contrast Acquisitions**

Alain Herment*, Muriel Lefort, Alain de Cesare, Nadjia Kachenoura, Frédérique Frouin and Elie Mousseaux

Tuesday, September 28, 2010, 08:00

S34: Ventricular Cell Modeling and Ischemia

Room: Grand 2

Chairs: Colin Jamison and Peter van Dam

46 **The Effect of the Shape of Ischemic Regions in the Heart on the Resulting Extracellular Epicardial Potential Distributions**

Josef Peter Barnes* and Peter Rex Johnston

47 **Re-Entry in a Model of Ischaemic Human Ventricular Tissue**

Richard Clayton*

48 **Simulation of ECG under Ischemic Condition in Human Ventricular Tissue**

Weigang Lu, Kuanquan Wang* and Henggui Zhang

49 **M-cell Heterogeneity Influence in Arrhythmic Pattern Formation in Sub-epicardial Regional Ischemia: A Simulation Study**

Oscar Alberto Henao Gallo, Carlos Alberto Ruiz Villa* and Jose Maria Ferrero de LomaOsorio

50 **Mechano-Electric Feedback Effects in a Ventricular Myocyte Model Subjected to Dynamic Changes in Mechanical Load**

Ivan Cenci*, Stefano Morotti, Jorge Negroni, Blanca Rodriguez and Stefano Severi

51 **Sarcoplasmic Reticulum Luminal [Ca] Regulates the Spontaneous Ca Release Events and Consequently Arrhythmia**

Luyao Lu, Ling Xia* and Xiuwei Zhu

Tuesday, September 28, 2010, 10:00

S41: Novel Techniques

Room: Grand 1

Chairs: Nico Bruining and Thomas Hilbel

52 **Impedimetric Point-of-Care Cardiac Marker System**

Eyad Hamad*, Paul Maguire and James McLaughlin

53 **Hybrid Edge Detection for Real-time Kalman Filter Based Left Ventricle Tracking in 3D+T Echocardiography**

Engin Dikici* and Fredrik Orderud

54 **Application of Novel Mapping for Heart Rate Phase Space and Its Role in Cardiac Arrhythmia Diagnosis**

Nader Jafarnia Dabanloo*, Sadaf Moharreri, Saman Parvaneh and Ali Nasrabadi

55 **ECG-Based Indices of Poincaré Plot Asymmetry Differ between Different Types of Athletic Training**

Hans Esperer*, Martin Oehler, Chris Esperer and René Schwesig

Tuesday, September 28, 2010, 10:00

S42: Medical Informatics

Room: Grand 2

Chairs: Stefan Nelwan and Peter Donnelly

56 **Dynamic Terminology Enhancement for Integrated ECG Resources**

Alexandra Kokkinaki*, Ioanna Chouvarda and Nicos Maglaveras

57 **EcgRuleML: A Rule-Based Markup Language for Describing Diagnostic ECG Criteria**

Raymond Robert Bond*, Dewar Darren Finlay, Chris Desmond Nugent and George Moore

58 **iCARDEA – an Approach to Reducing Human Workload in Cardiovascular Implantable Electronic Device Follow-Ups**

Maohua Yang, Christian Lüpkes*, Asuman Dogac, Mustafa Yuksel, Fulya Tunçer, Tuncay Namlı, Manuela Plößnig, Jürgen Ulbts and Marco Eichelberg

59 **Interoperability Challenges in the Health Management of Patients with Implantable Defibrillators**

Catherine Chronaki*, Manuela Plößnig, Fulya Tuncer, Mustafa Yuksel, Gokce Banu Laleci Erturkmen, Christian Lüpkes, Marco Eichelberg, Xavier Navarro, Wolfgang Pecho and Asuman Dogac

Tuesday, September 28, 2010, 10:00

S43: Cardiovascular Imaging

Room: Grand 3

Chairs: Mireille Garreau and Omar Escalona

60 **MRI to X-ray Fluoroscopy Overlay for Guidance of Cardiac Resynchronization Therapy Procedures**

YingLiang Ma, Simon Duckett, Anoopy Shetty, C Aldo Rinaldi, Kawal Rhode and Gang Gao*

61 **Automatic Quantification of Oedema from T2 Weighted CMR Image using Hybrid Thresholding Oedema Sizing Algorithm**

Kushsairy Kadir*, Alex Payne, John J Soraghan and Colin Berry

62 **Comparison of the Data Derived from Three-dimensional Reconstruction of Coronary Angiography and the Fractional Flow Reserve Measurements**

Balazs Tar, Peter Lugosi, Janos Santa, Tamas Ungvári, Sandor Ember and Zsolt Koszegi*

63 **Abilities of Cardiac MSCT Imaging to Provide Useful Anatomical and Functional Information for Cardiac Resynchronization Therapy Optimization**

Mireille Garreau*, Marie-Paule Garcia, François Tavard, Antoine Simon, Julien Fleureau, Dominique Boulmier, Pascal Haigron, Christine Toumoulin and Christophe Leclercq

Tuesday, September 28, 2010, 10:00

S44: Baroreflex

Room: Grand 4&5

Chairs: Michael Daly and Gari Clifford

64 **Effect of Physiological Changes in Heart Rate Turbulence using a Lumped Parameter Model**

Óscar Barquero-Pérez, Inmaculada Mora-Jiménez, Rebeca Goya-Esteban, Julio Ramiro-Bargueño, Arcadi García-Alberola and José Luis Rojo-Álvarez*

65 **Assessment of Coupling and Correlation Between Cerebral Autoregulation and Baroreflex in Stroke Patients**

Ben-Yi Liau*, Shoou-jeng Yeh and Chuang-Chien Chiu

66 **Joint Order Pattern Analysis to Asses Baroreflex Coupling of SBP and PI Series in Rats**

Tatjana Loncar Turukalo*, Sanja Milutinovic, Nina Japundzic Zigon and Dragana Bajic

Tuesday, September 28, 2010, 11:15

M5: Computing in Cardiac Safety - Plenary

Room: Exhibition Centre

Chairs: Peter Macfarlane and Dewar Finlay

67 **Electrocardiography and Repolarization Abnormalities: Benefits and Limitations of Fully Automated Methods for QT Measurement**

Paul Kligfield*

68 **Intracardiac Electrophysiology: Cellular Modelling of Abnormal Repolarisation**

Blanca Rodriguez*

69 **Cardiovascular Computer Devices: Balancing Novelty, Flexibility, Familiarity and Safety**

Alan Murray*

70 **Cardiac Computer Imaging: Intravascular Ultrasound and MRI Studies**

Nico Bruining*

Tuesday, September 28, 2010, 14:00

S61: Ischemia and Infarction II

Room: Grand 1

Chairs: Jim McLaughlin and Richard Gregg

71 **A Vectorial Approach for Evaluation of Depolarization Changes during Acute Myocardial Ischemia**

Daniel Romero Pérez*, Michael Ringborn, Pablo Laguna, Olle Pahlm and Esther Pueyo

72 **Model-Based Medical Expert System for Diagnosing Myocardial Ischemia Based on a Newly Developed Ischemia Parameter**

Hisham Alqysi*

73 **Research on Myocardial Ischemia Detection Based on Electrocardiogram R-S-T**

Jinzhong Song* and Hong Yan

74 **Body Surface Potential Mapping Improves Diagnosis of Acute Myocardial Infarction in those with Significant Left Main Coronary Artery Stenosis**

Michael John Daly*, Peter Scott, Colum Owens, Audrey Tomlin, Bernadette Smith and Jennifer Adgey

75 **Detection of Inferior Myocardial Infarction: A Comparison of Various Decision Systems and Learning Algorithms**

Jiří Spilka*, Václav Chudáček, Jakub Kužílek, Lenka Lhotská and Martin Hanuliak

76 **Combining Sgarbossa and Selvester ECG Criteria to Improve STEMI Detection in Presence of LBBB**

Richard Gregg*, Sophia Zhou and Eric Helfenbein

Tuesday, September 28, 2010, 14:00

S62: Lead Systems

Room: Grand 4&5

Chairs: John Wang and John Anderson

77 **Extended Multiple Linear Regression in the Derivation of Electrocardiographic Leads**

Daniel Guldenring*, Dewar Darren Finlay, Christopher Desmond Nugent and Mark Patrick Donnelly

78 **A Web-based Visualization Tool for Transforming the 12-lead ECG into a Body Surface Potential Map**

Raymond Robert Bond*, Dewar Darren Finlay, Chris Desmond Nugent and George Moore

79 **Real-Time Back-Projection of Fetal ECG Sources in OL-JADE for the Optimization of Blind Electrode Positioning**

Danilo Pani*, Stefania Argiolas and Luigi Raffo

80 **Short Distance Bipolar Electrocardiographic Leads in Diagnosis of Left Ventricular Hypertrophy**

Juho Väisänen*, Merja Puurtinen, Jari Hyttinen and Jari Viik

81 **Utilising a Genetic Algorithm to Minimise the Number of Leads in Body Surface Mapping for the Electrocardiographic Diagnosis of Myocardial Infarction**

Peter Scott*, Cesar Navarro, Marisol Giardina, Omar Escalona, John Anderson and Jennifer Adgey

82 **Fuzzy integrated Neural Network Classification of Body Surface Potential Contour Map to Detect Myocardial Infarction Location**

Hamid SadAbadi, Nader Jafarnia Dabanloo*, Masood Ghasemi and Sepideh Sabouri

Tuesday, September 28, 2010, 14:00

S63: PhysioNet/Computing in Cardiology Challenge

Room: Grand 3

Chairs: George Moody and Johan DeBie

83 **The PhysioNet/Computing in Cardiology Challenge 2010: Mind the Gap**

George B Moody*

84 **Estimation of Missing Data in Multi-channel Physiological Time-series by Reference Timing Channel and Average Substitution**

Philip Langley*, Susan King, Kun Wang, Dingchang Zheng, Roberto Giovannini, Marjan Bojarnejad and Alan Murray

85 **PhysioNet 2010 Challenge: A Robust Multi-Channel Adaptive Filtering Approach to the Estimation of Physiological Recordings**

Ikaro Silva*

86 **Reconstruction of Missing Physiological Signals using Artificial Neural Networks**

Adam Sullivan, Henian Xia, Joseph McBride and Xiaopeng Zhao*

87 **A Sensorless Kalman Estimator toward the Reconstruction of Physiologic Data**

Mohamed A Mneimneh* and Sahar Elturk

88 **Reconstruction of Missing Cardiovascular Signals using Adaptive Filtering**

Andras Hartmann*

Tuesday, September 28, 2010, 14:00

S64: System Modeling & Instrumentation

Room: Grand 2

Chairs: Anthony Fisher and Sally McClean

89 **Coupling the Guyton Model to Pulsatile Ventricles using a Multiresolution Modelling Environment**

Virginie Le Rolle*, David Ojeda, Raphaël Madeleine, Guy Carrault and Alfredo I Hernández

90 **Simulation of the Effect of Tachycardia on Atherosclerotic Plaque Development Based on the LDL Transport in Coronary Arteries**

Antonis Sakellarios*, Panagiotis Siogkas, Vasilis Tsakanikas, Lampros Michalis, Dimitrios Fotiadis, Katerina Naka, Nenad Filipovic and Kostas Stefanou

91 **Atrioventricular Delay Optimization in Cardiac Resynchronization Therapy Assessed by a Computer Model**

Kevin Tse Ve Koon*, Christophe Thebault, Virginie Le Rolle, Erwan Donal and Alfredo Ignacio Hernández

92 **Semi-Automated Extraction of Canine Left Ventricular Purkinje Fiber Network**

Kuanquan Wang*, Jie Li, Wangmeng Zuo, Henggui Zhang and Yongfeng Yuan

93 **A LabVIEW Based Multichannel Recording Architecture for High Density Electrical Mapping**

A Liberos*, MS Guillem, J Millet and AM Climent

94 **Predicting Unpinning Success Rates for a Pinned Spiral in an Excitable Medium**

Anna Behrend*, Philip Bittihn and Stefan Luther

Tuesday, September 28, 2010, 16:00

S71: QT & Repolarisation

Room: Grand 3

Chairs: Jean-Philippe Couderc and Kees Swenne

95 **Analyzing Thorough QT Study 1 & 2 in the Telemetric and Holter ECG Warehouse (THEW) using Hannover ECG System: A Validation Study**

Antoun Khawaja*, Ratko Petrovic, Anton Safer, Tobias Baas, Olaf Dössel and Ronald Fischer

96 **Torsadogenic Drug-induced Increased Short-term Variability of JT-area**

Xiao Jie*, Blanca Rodriguez and Esther Pueyo

97 **Electrocardiographic Markers Associated with Sotalol-induced Torsades de Pointes**

Jean-Philippe Couderc*, Xiajuang Xia, Stefan Kaab and Wojciech Zareba

98 **Comparison of three T-end Delination Algorithms based on Wavelet Filterbank, Correlation and PCA**

Tobias Baas*, Franz Gravenhorst, Ronald Fischer, Antoun Khawaja and Olaf Dössel

99 **QT/RR Coupling and Gender Differences**

Josef Halamek*, Pavel Jurak, Jolana Lipoldova and Pavel Leinveber

100 **Analysis of Heart Rate Adaptation in Long-Term ECG Recordings using RR-binning**

Lars Johannesen*, Ulrik Silvanus Lerkevang Grove, Jens Stampe Soerensen, Mick Lykkegaard Schmidt, Claus Graff and Jean-Philippe Couderc

Tuesday, September 28, 2010, 16:00

S72: Cardiovascular Mechanics

Room: Grand 2

Chairs: Natalia Trayanova and JJ Rieta

101 **Optimal Delineation of PCG Sounds via False-Alarm Bounded Segmentation of a Wavelet-Based Principal Components Analyzed Metric**

Mohammad Reza Homaeinezhad* and Ali Ghaffari

102 **The Evaluation of Methods in Determination of the Arterial Compliance for Real-Time Applications**

Weichih Hu*, Liang-Yu Shyu, Hou-Ming Cheng and Chen-Huan Chen

103 **Asymmetrical Oscillometric Pulse Waveform Envelopes in Normotensive and Hypertensive Subjects**

Dingchang Zheng*, Roberto Giovannini and Alan Murray

104 **Detection of Systolic and Diastolic Durations on Cardiac Output and Arterial Pressures**

Mick Lykkegaard Schmidt*, Lars Johannesen, Jens Stampe Soerensen, Kasper Lundhus, Samuel Emil Schmidt and Niels-Henrik Staalsen

105 **Comparison between Sample Entropy and AR-models for Heart Sound-based Detection of Coronary Artery Disease**

Samuel Schmidt*, John Hansen, Claus Holst Hansen, Egon Toft and Johannes Struijk

Tuesday, September 28, 2010, 16:00

S73: CV Ultrasound Imaging

Room: Grand 1

Chairs: Alain Herment and Cathal Breen

106 **An Automatic Media-Adventitia Border Segmentation Approach for IVUS Images**

Matheus Cardoso Moraes* and Sergio Shiguemi Furuie

107 **Quantitative Assessment of the Effects of Annuloplasty on Mitral Annulus Dynamic Geometry using Real-Time 3D Echocardiography**

Laura Fusini, Federico Veronesi, Cristiana Corsi, Paola Gripari, Francesco Maffessanti, Francesco Alamanni, Marco Zanobini, Moreno Naliato, Gloria Tamborini, Mauro Pepi and Enrico G Caiani*

108 **Heterogeneity of the Myocardial Strains as Revealed by Applying a Wavelet De-noising Process to the Myocardial Velocities**

Noa Bachner*, Offir Ertracht, Nir Zagury, Ofer Binah and Dan Adam

109 **Fusion of Electro-Anatomical Mapping and Speckle Tracking Echography for the Characterization of Local Electro-Mechanical Delays in CRT Optimization**

François Tavard, Antoine Simon, Erwan Donal, Alfredo Hernandez and Mireille Garreau*

110 **Myocardial Ischemia Detection Algorithm (MIDA): An Automated Echocardiography Sequence Analysis for the Diagnosis of Heart Muscle Damage**

Vijayalakshmi Ahanathapillai and John Soraghan*

111 **Segmentation of the Full Myocardium in Echocardiography using Constrained Level-Sets**

Martino Alessandrini*, Thomas Dietenbeck, Daniel Barbosa, Jan D'Hooge, Olivier Basset, Nicolo Speciale, Denis Friboulet and Olivier Bernard

Tuesday, September 28, 2010, 16:00

S74: Atrial Cell Modeling

Room: Grand 4&5

Chairs: Chema Ferrero and Leif Sornmo

112 **Potential Pharmacological Therapies for Atrial Fibrillation: A Computational Study**

Carlos Sánchez*, Alberto Corrias, Pablo Laguna, Mark Davies, Jonathan Swinton, Ingemar Jacobson, Esther Pueyo and Blanca Rodríguez

113 **Atrial Fibrillation-based Electrical Remodeling in a Computer Model of the Human Atrium**

Gunnar Seemann*, Paola Carrillo, Stefan Ponto, Mathias Wilhelms, Eberhard P Scholz and Olaf Dössel

114 **Functional Roles of Ionic Currents in A Mouse Sino-atrial Node Cell Model**

Sanjay Kharche*, Ming Lei and Henggui Zhang

115 **Wavefront-Obstacle and Wavefront-Wavefront Interactions as Mechanisms for Atrial Fibrillation: a Study Bbased on the FitzHugh-Nagumo Equations**

Claudia Lenk*, Mario Einax and Philipp Maass

116 **Anti-arrythmogenic Effects of Atrial Specific IKur Block: A Modelling Study**

Phillip Law, Sanjay Kharche* and Henggui Zhang

117 **Study the Effect of Tissue Heterogeneity and Anisotropy in Atrial Fibrillation Based on a Human Atrial Model**

Dongdong Deng* and Ling Xia

Tuesday, September 28, 2010, 17:30

P81: PhysioNet/CinC Challenge Posters

Room: Exhibition Centre

118 **Principal Component Analysis-based Method for Reconstruction of Fragments of Corrupted or Lost Signal in Multilead Data Reflecting Electrical Heart Activity and Hemodynamics**

Robertas Petrolis*, Renata Simoliuniene and Algimantas Krisciukaitis

119 **An Approach to Reconstructing Lost Cardiac Signals using Pattern Matching and Neural Networks via Related Cardiac Information**

Thomas Chee Tat Ho* and Xiang Chen

120 **Medical Multivariate Signal Reconstruction using Recurrent icial Neural Network**

Luiz Eduard Virgilio Silva, Juliano Jinzenji Duque, Isaias Soares, Renato Tinós and Luiz Otavio Murta Jr*

121 **HMMFIT: Using Hidden Markov Models to Reconstruct Missing Signals on Multi-parameter Physiologic Data**

Yanen Li*, Yu Sun, Chengxiang Zhai and Lui Sha

122 **Filling in the Gap: a General Method using Neural Networks**

Rui Rodrigues*

123 **Multi-parameter Physiologic Signal Reconstruction by Means of Wavelet Singularity Detection and Signal Correlation**

Wei Wu*

124 **PhysioNet/CinC Challenge**

Teresa Rocha*, Simão Paredes and Jorge Henriques

125 **Reconstruction of Multivariate Signals using Q-Gaussian Radial Basis Function Network**

Luiz Eduardo Virgilio Silva*, Juliano Jinzenji Duque, Renato Tinós and Luiz Otavio Murta Jr

Tuesday, September 28, 2010, 17:30

P82: Novel Techniques Posters

Room: Exhibition Centre

126 **Extracting Fetal ECG from a Single Maternal Abdominal Record**

Mohammad Ayat*, Khaled Assaleh, Hasan Al-Nashash and Moncef Gabbouj

127 **Image Registration of 3D Trans-Esophageal Echocardiography and X-ray Fluoroscopy for the Guidance of Trans-catheter Aortic Valve Implantation**

Gang Gao*, Geraint Morton, Jane Hancock, Simon Redwood, Martyn Thomas and Kawal Rhode

128 **Patient-Specific Correlation of Perfusion Defects to Coronary Arteries**

Constantine Zakkaroff*, Aleksandra Radjenovic, Derek Magee and Roger Boyle

129 **Categorization of Continuous ECG Based Risk Metrics using Asymmetric and Warped Entropy Measures**

Anima Singh* and John Guttag

130 **Obstructive Sleep Apnoea using Photoplethysmography-based Dynamic Features**

Lina María Sepúlveda-Cano*, Eduardo Gil-Herrando, Pablo Laguna and Germán Castellanos-Domínguez

131 **On the Measurement of Physiological Similarity Between Independent Components: Time-Structure Versus Frequency-Based Methods**

A Jimenez-Gonzalez* and CJ James

132 **Open-Source Teleconsulting System for International Cooperative Medical Decision Making in Congenital Heart Diseases**

Andrea Gori*, Alessandro Taddei, Alessio Ciregia, Debora Mota, Paolo Marcheschi, Nadia Assanta, Bruno Murzi and Giorgio Ricci

Tuesday, September 28, 2010, 17:30

P83: ECG Posters

Room: Exhibition Centre

133 **N-terminal Pro-brain Natriuretic Peptide in Combination with the 80-lead Body Surface Map Improves Detection of Acute Inferior Myocardial Infarction with Right Ventricular Involvement**

Michael John Daly*, Nicholas McKeag, Conor McCann, Christopher Cardwell, Ian Young and Jennifer Adgey

134 **Myocardial Infarction Localization using Combined Heart Vector Analysis and Neural Network Localizer**

Masood Ghasemi, Nader Jafarnia Dabanloo*, Sepideh Sabouri and Hamid SadAbadi

135 **A Comparison of IIR and Wavelet Filtering for Noise Reduction of the ECG**

Jens Stampe Soerensen*, Lars Johannesen, Ulrik Silvanus Lerkevang Grove, Kasper Lundhus, Jean-Philippe Couderc and Claus Graff

136 **Modified Rectangular Finite Impulse Response Filter for Stabilization of QT Measurement**

Jing Wu, Jean-Philippe Couderc* and Jean Xia

137 **Investigation on Two-year Peritoneal Dialysis Patients: Does the Cardiovascular Conditions Affect on ECG Biometrics?**

Tsu-Wang Shen, Shan-Chun Chang*, Chih-Hsien Wang and Te-Chao Fang

138 **Principal Component Analysis of the QRS Complex During Diagnostic Ajmaline Test for Suspected Brugada Syndrome**

Velislav Batchvarov, Ivaylo Christov, Giovanni Bortolan* and Elijah Behr

139 **Use of ECG Quality Metrics in Clinical Trials**

Martino Vaglio*, Lamberto Isola and Fabio Badilini

Tuesday, September 28, 2010, 17:30

140 **Study of Differences on Heart Rate in Patients with Apnea and Insomnia Syndromes**

Juan Guerrero, Antonio Benetó, Enriqueta Gómez, Manuel Bataller, Pilar Rubio and Alfredo Rosado*

141 **Evaluation of Methods for Estimation of Respiratory Frequency from the ECG**

Ainara Sobron, Inaki Romero* and Txema Lopetegi

142 **A Body Position Detection Method by Fusing Heterogeneous Information of Surface ECG**

Tsu-Wang Shen, Fang-Chih Liu, Ya-Ting Tsao, Shan-Chun Chang* and Yi-Ling Ou

143 **Design and Evaluation of an ECG Holter Analysis System**

Alberto Rodríguez*, Gemma Rodríguez, Raúl Almeida, Nelvy Pina and Gisela Montes de Oca

144 **Evaluation of a Shock Advisory System with Non-Shockable Pediatric Rhythms**

Jean-Philippe Didon*, Irena Jekova and Vessela Krasteva

145 **Investigation of the Autonomic Nervous System Control of Cardiovascular Variables using fMRI and Carotid Stimulation**

Giovanni Calcagnini*, Eugenio Mattei, Michele Triventi, Barbara Basile, Andrea Bassi, Marco Bozzali, Stefano Strano and Pietro Bartolini

146 **Accurate R Peak Detection and Advanced Preprocessing of Normal ECG for Heart Rate Variability Analysis**

Devy Widjaja*, Steven Vandeput, Joachim Taelman, Bea Van den Bergh and Sabine Van Huffel

147 **Blood Oxygen Level Measurement with a Chest-Based Pulse Oximetry Prototype**

Collin Schreiner*, Philip Catherwood, James McLaughlin and John Anderson

Tuesday, September 28, 2010, 17:30

148 **Personal Sensor-System Modalities Evaluation for Simplified ECG Recording in Self-Care**

Asta Krupaviciute*, Jocelyne Fayn, Eric McAdams, Christine Verdier, Chris Nugent and Paul Rubel

149 **An Alternative to Derive the Instantaneous Frequency of the Chest Compressions to Suppress the CPR Artifact**

Unai Ayala*, Elisabete Aramendi and Unai Irusta

150 **Impact of the Approximated On-Line Centering and Whitening in OL-JADE on the Quality of the Estimated Fetal ECG**

Danilo Pani*, Stefania Argiolas and Luigi Raffo

151 **A Beat-to-Beat P-Wave Analysis in a Healthy Population**

Valentina DA Corino*, Ioanna Chouvarda, Nicos Maglaveras and Luca T Mainardi

152 **ECG Motion Artefact Reduction Improvements of a Chest-based Wireless Patient Monitoring System**

Philip Catherwood*, Nicola Donnelly, James McLaughlin and John Anderson

153 **Low-cost Early Detection of Cardiovascular Disease on Chronic Kidney Disease Patients Based on Hybrid Heterogeneous ECG Features Including T-wave Altemans and Heart Rate Variability**

Tsu-Wang Shen, Chih-Hsien Wang*, Yi-Ling Ou, and Te-Chao Fang

Tuesday, September 28, 2010, 17:30

P84: Electrophysiology Posters

Room: Exhibition Centre

154 **Comparison of Voltage-Sensitive Dye di-4-ANEPPS Effects in Isolated Hearts of Rat, Guinea Pig and Rabbit**

Katerina Fialova*, Jana Kolarova, Ivo Provaznik and Marie Novakova

155 **Transcutaneous Dual Tuned RF Coil System Voltage Gain and Efficiency Evaluation for a Passive Implantable Atrial Defibrillator**

Omar Jacinto Escalona, Jose Jesus Velasquez, Lawrence Chirwa, Niall Waterman* and John Anderson

Tuesday, September 28, 2010, 17:30

P85: Cardiovascular Variability Posters I

Room: Exhibition Centre

156 **Changes of Heart Rate Complexity during Weaning from Mechanical Ventilation**

Vasilios Papaioannou, Ioanna Chouvarda*, Nicos Maglaveras and Ioannis Pneumatikos

157 **Estimation of Stress-Strain Relationships in Vascular Walls using a Multi-Layer Hyperelastic Modelling Approach**

Michel Edward Mickael*, Abbas Heydari, Roger Crouch and Sherri Johnstone

158 **A New and Fast Index for the Quantification of Short-Range Self-Similarity in RR Time Series**

Miguel Angel García-González*, Mireya Fernández-Chimeno and Juan Ramos-Castro

159 **Prediction of Ventricular Tachycardia by a Neural Network using Parameters of Heart Rate Variability**

Segyeong Joo*, Kee-Joon Choi and Soo-Jin Huh

160 **Frequency-domain Heart Rate Variability Analysis Performed by Digital Filters**

Tsung-Chieh Lee and Hung-Wen Chiu*

161 **Quantitative Analysis of the Relationship Between Chaotic Features of Surface ECG and an Intracardiac Electrogram**

Sakineh Yahyazadeh, Mohammad Firoozabadi*, Majid Haghjoo and Saman Parvaneh

162 **Gender-related Effects of Sucrose Ingestion and Hypoxia on Cardiac Autonomic Modulation in Young Subjects**

Tanja Princi*, Agostino Accardo, Petra Golja and Matjaz Klemenc

Tuesday, September 28, 2010, 17:30

163 **Perturbation in Parasympathetic Nervous System Activity Affects Temporal Structure of Poincaré Plot**

Chandan Karmakar, Ahsan Khandoker* and Marimuthu Palaniswami

164 **Heart Rate Asymmetry (HRA) in Altered Parasympathetic Nervous System Activity**

Chandan Karmakar, Ahsan Khandoker* and Marimuthu Palaniswami

165 **Using Cross-Correlation Function to Assess Dynamic Cerebral Autoregulation in Response to Posture Changes for Stroke Patients**

Ben-Yi Liau*, Shoou-Jeng Yeh and Chuang-Chien Chiu

166 **The Estimation of Arterial Stiffness Based on Analysis of Heart Rate**

Alexander Fedotov* and Lev Kalakutsky

167 **Web Site on Heart Rate Variability: Hrv-Site**

Mirian Álvarez González, Xosé Antón Vila Sobrino*, María José Lado Touriño, Arturo José Méndez Penín and Leandro Rodríguez Liñares

168 **Heart Rate Variability and QT Dispersion in a Cohort of Diabetes Patients**

Herbert Jelinek*, Ahsan Habib Khandoker and Marimuthu Palaniswami

Tuesday, September 28, 2010, 17:30

P86: Cell Modeling Posters

Room: Exhibition Centre

169 **Role of the Late Sodium Current in Arrhythmias Related to Low Repolarization Reserve**

Karen Cardona*, Beatriz Trenor, Lucia Romero, Jose Maria Ferrero and Javier Saiz

170 **A Biophysical Model of Atrial Fibrillation to Simulate the Maze III Ablation Pattern**

Catalina Tobon, Karen Cardona*, Jose Felix Rodriguez, Fernando Hornero, Jose Maria Ferrero Jr and Javier Sáiz

171 **Monophasic versus Biphasic Stimulation of Single Cardiomyocite Cell: a Simulation Study**

Monica Caselli*, Aldo Casaleggio and Stefano Severi

172 **Beta-Adrenergic Modulation of Heart Rate: Contribution of the Slow Delayed Rectifier K+ Current (IKs)**

Ronald Wilders*, Antoni CG van Ginneken and Arie O Verkerk

173 **Simulation of Cardiac Action Potential Propagation using Hybrid Models**

Matthew J Poole*

174 **Development of a Biophysically Detailed Model of the Rapid-Delayed Rectifier Potassium Channel**

Ismail Adeniran*, Jules Hancox and Henggui Zhang

175 **Gender and Age Based Differences in Risk of Proarrhythmia by Dofetilide : A Computational Model Study**

Rodolfo Gonzalez*, Julio Gomis-Tena, Alberto Corrias, Jose Maria Ferrero, Blanca Rodriguez and Javier Saiz

Tuesday, September 28, 2010, 17:30

176 **An Improved Model of Ba Current through L-type Ca Channels Including Voltage- and Ion-Dependent Inactivation**

Stefano Morotti*, Eleonora Grandi, Aurora Summa, Kenneth S Ginsburg, Donald M Bers and Stefano Severi

177 **Mathematical Modelling of Electrotonic Interaction between Stem Cell-Derived Cardiomyocytes and Fibroblasts**

Michelangelo Paci*, Laura Sartiani, Marisa Jaconi, Elisabetta Cerbai and Stefano Severi

178 **Interplay of Potassium Channels in Modulating the Action Potential of Human Ventricular Myocytes**

Chong Wang, Peter Beyerlein, Heike Pospisil, Antje Krause, Werner Dubitzky and Chris Nugent*

179 **The Role of the Transient Outward Current in Action Potential Repolarization: a Simulation Study**

Beatriz Carbonell, Lázló Virág, Norbert Jost, András Varró and Chema Ferrero*

180 **Slow Pulse Due to Calcium Current Induces Phase-2 Reentry In Heterogeneous Tissue**

Angelina Peñaranda*

Tuesday, September 28, 2010, 17:30

NN: New & Noteworthy Poster

Room: Exhibition Centre

181 **Time-Frequency Analysis of Cardio-Respiratory Response to Mental Task Execution**

Luigi Yuri Di Marco*, Roberto Sottile and Lorenzo Chiari

Wednesday, September 29, 2010, 08:30

S91: Algorithms and Signal Processing

Room: Grand 1

Chairs: Daniel Guldenring and Milan Horacek

182 **Moving Window Signal Concatenation for Spectral Analysis of ECG Waves**

Piotr Augustyniak*

183 **Heart Arrhythmia Detection using Continuous Wavelet Transform and Principal Component Analysis with Neural Network Classifier**

Ali Ghaffari, C Nat Nataraj*, Parham Ghorbanian and Ali Jalali

184 **Evaluation of Feature Models for 12-lead ECG Classification**

Mariano Llamedo*, Antoun Khawaja and Juan Pablo Martínez

185 **PCA-based Noise Reduction in Ambulatory ECGs**

Iñaki Romero*

186 **Filtering the Cardiopulmonary Resuscitation Artifact: an Analysis of the Influence of the Signal-To-Noise Ratio in the Accuracy of the Shock Advice Algorithm**

Sofia Ruiz de Gauna*, Jesus Ruiz, Unai Irusta and Unai Ayala

187 **Multi-Lead Discrete Wavelet-based ECG Arrhythmia Recognition via Sequential Particle Support Vector Machine Classifiers**

Mohammad Reza Homaeinezhad* and Ali Ghaffari

Wednesday, September 29, 2010, 08:30

S92: Clinical ECG

Room: Grand 3

Chairs: Raymond Bond and Shen Luo

188 **Characteristics of the Standard 12-lead Holter ECG in Professional Firefighters**

Mary G Carey*, Salah Al-Zaiti and Rachael Butler

189 **Effects of Sotalol on T-wave Morphology in 24-hour Holter ECG Recordings**

Thomas Brennan* and Lionel Tarassenko

190 **The ECG in the Normal Human Pregnancy**

Muti Goloba, Scott Nelson and Peter Macfarlane*

191 **QTc Analysis and Comparison in Pre-Diabetic Patients**

Pedro Virgilio Rivera Farina*, Javier Pérez Turiel, Francisco Javier Pagán Buzo, Enrique González Sarmiento, Alberto Herreros López and Carlos David Rodríguez Guerrero

192 **Comparison of QRS duration in African Blacks and European Caucasians**

Ibraheem Katibi, Brian Devine*, Elaine Clark, Suzanne Lloyd and Peter Macfarlane

193 **Quality of Electrocardiographic Records in Population Studies: What Can We Achieve?**

Siegfried Perz*, Roswitha Küfner, Karl-Hans Englmeier, Moritz F Sinner, Stefan Kääb, Christine Meisinger and H-Erich Wichmann

Wednesday, September 29, 2010, 08:30

S93: Heart Rate Variability

Room: Grand 2

Chairs: Sheryl Prucka and Ling Xia

194 **Repeatability Value in Heart Rate Associated with Experienced Zen Meditation**

Masaki Hoshiyama* and Asagi Hoshiyama

195 **Wavelet Transform Cardiorespiratory Coherence for Monitoring Nociception**

Christopher J Brouse*, Guy A Dumont, Dorothy Myers, Erin Cooke, Joanne Lim and J Mark Ansermino

196 **Respiratory Frequency Estimation from Heart Rate Variability Signals in Non-Stationary Conditions Based on the Wigner-Ville Distribution**

Eva Cirugeda, Michele Orini, Raquel Bailón and Pablo Laguna*

197 **Point Process Heart Rate Variability Assessment during Sleep Deprivation**

Luca Citi*, Elizabeth Klerman, Emery N Brown and Riccardo Barbieri

198 **Stress during Pregnancy: Is the Autonomic Nervous System Influenced by Anxiety?**

Joachim Taelman*, Steven Vandeput, Devy Widjaja, Marijke Braeken, RA Otte, Bea Van den Bergh and Sabine Van Huffel

Wednesday, September 29, 2010, 08:30

S94: Electrophysiology

Room: Grand 4&5

Chairs: Olaf Doessel and Jean-Marc Vesin

199 **Analysis of the Influence of Parasympathetic Postganglionic Neurons on Cardiac Response in Ventricular Fibrillation**

Juan Guerrero, Alfredo Rosado*, Antonio J Serrano, Manuel Bataller, Francisco J Chorro, Luis Such and Antonio Alberola

200 **Stability of Bipolar and Unipolar Endocardial Electrograms**

Paola Milpied*, Rémi Dubois, Pierre Roussel, Christine Henry and Gérard Dreyfus

201 **Spectral Analysis of Intracardiac Electrograms After PQRST Waves Removal**

Aldo Casaleggio*, Tiziana Guidotto, Vincenzo Malavasi and Paolo Rossi

202 **Predicting Transthoracic Defibrillation Shock Outcome in the Cardioversion of Atrial Fibrillation Employing Support Vector Machines**

Jose David Diaz, Omar Jacinto Escalona, Noel Camilo Castro*, John Anderson, Ben Glover and Ganesh Manoharan

203 **Three-dimensional Frequency Mapping from the Non-contact Unipolar Electrograms in Atrial Fibrillation**

Joao Salinet Jr*, Anita Ahmad, Peter Stafford, G André Ng and Fernando Schlindwein

204 **Automatic Location of Ventricular Arrhythmia using Implantable Defibrillator Stored Electrograms**

*Margarita Sanromán-Junquera, Inmaculada Mora-Jiménez, Jesús Almendral, Estrella Everss, Antonio Caamaño-Fernández, Felipe Atienza, Loreto Castilla and José Luis Rojo-Álvarez (MargaMargarita Sanromán-Junquerarita)

Wednesday, September 29, 2010, 10:30

SA1: Repolarisation at Rest and During Exercise

Room: Grand 3

Chairs: Willi Kaiser and Paul Kligfield

205 **Continuous Time Analysis Method for T–Wave Alternans Detection**

Manuel Blanco-Velasco*, Fernando Cruz-Roldán, Eduardo Moreno-Martínez, Juan Pablo Martínez, and Pedro Amo-López

206 **Automated QT Interval Measurement in Holter ECGs Recorded at 180 and 1000 Samples per Second**

Gopi Krishna Panicker, Vaibhav Salvi, Dilip Karnad, Peter Macfarlane*, Elaine Clark, Arumagam Ramasamy, Snehal Kothari and Dhiraj Narula

207 **Changes in The Ventricular Gradient Measured During Exercise Tests Predict Antiarrhythmic Therapy in Primary Prevention ICD Patients**

S Man*, PV De Winter, AC Maan, WPM Van Meerwijk, EE Van der Wall, MJ Schalij and CA Swenne

208 **Exercise Test Interpretation (XTI)**

Willi Kaiser* and Martin Findeis

209 **Evaluation of a Method for Quantification of Restitution Dispersion from the Surface ECG**

Ana Mincholé, Esther Pueyo, José Felix Rodríguez, Ernesto Zacur and Pablo Laguna*

210 **Evaluation of Restitution Properties using a Quasi-Stationary Exercise Protocol**

Joseph Starobin*, Vivek Varadarajan and Vladmir Polotski

Wednesday, September 29, 2010, 10:30

SA2: Telemedicine II

Room: Grand 1

Chairs: Leo Galway and Declan Bogan

211 **Enterprise Cardiovascular System to Support Multimodality Imaging and Clinical Effectiveness**

Neil Greenberg*, Robert Cecil, Fredrick Heupler and Richard Grimm

212 **Emergency Medical Care Information System for Fetal Monitoring**

Muhammad Ibn Ibrahimy*

213 **An Approach Towards a Heart Beat Sound Information Retrieval System**

Ehsan Safar Khorasani*, Shyamala Doraisamy, Azreen Azman and Masrah Azmi Murad

214 **Distinguishing Between Heart and Lung Sounds in Remote Auscultation of Patients**

Nausheen Mahmood, Aafreen Mahmood and Tanveer Syeda-Mahmood*

215 **Monitoring System for Forecasting Hypotensive Episodes**

Ricardo Jorge Santos*, Jorge Henriques and Jorge Bernardino

216 **Matching Data Fragments with Imperfect Identifiers from Disparate Sources**

Michael Craig*, Benjamin Moody, Sherman Jia, Mauricio Villarroel and Roger Mark

Wednesday, September 29, 2010, 10:30

SA3: MRI: Ventricular Function

Room: Grand 2

Chairs: Victor Mor-Avi and Christiana Corsi

217 **Semiautomatic Quantification of Left and Right Ventricular Functions in Magnetic Resonance Imaging**

L Masip*, PG Tahoces, M Souto, A Martínez and JJ Vidal

218 **Three-Dimensional Analysis of Septal Curvature from Cardiac Magnetic Resonance Images for the Evaluation of Severity of Pulmonary Hypertension**

Francesco Maffessanti, M Agustina Sciancaleopre, Amit R Patel, Mardi Gomberg-Maitland, Enrico G Caiani, Benjamin H Freed, Roberto M Lang and Victor Mor-Avi*

219 **Estimation of Right Ventricular Volume, Quantitative Assessment of Wall Motion and Trabeculae Mass in Arrhythmogenic Right Ventricular Dysplasia**

Massimo Lemmo*, Arshid Azarine, Giacomo Tarroni, Cristiana Corsi and Claudio Lamberti

220 **Evaluation of Semi-Automated Border Detection Algorithms for the Left Ventricular Endocardium from Magnetic Resonance Images**

Kun Wang*, Kieren Hollingsworth, Andrew J Sims, Andrew M Blamire and Alan Murray

221 **3D Evaluation of Myocardial End-Systolic Wall Stress From Cardiac Magnetic Resonance Cine Data**

Marion Senesi, Karine Defrance, Elie Mousseaux and Nadjia Kachenoura*

Wednesday, September 29, 2010, 10:30

SA4: Ventricular Cell Modeling

Room: Grand 4&5

Chairs: Blanca Rodriguez and Harold Ostrow

222 **Analysis and Improvement of a Human Ventricular Cell Model for Investigation of Cardiac Arrhythmias**

Jesús Carro*, José Félix Rodríguez, Pablo Laguna and Esther Pueyo

223 **Systems Biology in Drug Safety Assessment: Use of a Recalibrated Hund-Rudy Model to Predict the Effect of Novel Drug Compounds on Action Potential Duration**

Mark Davies*, Hitesh Mistry, Leyla Hussein, Najah Abi-Gerges, Chris Pollard and Jonathan Swinton

224 **In-Silico Evaluation of β-adrenergic Effects on the Long-QT Syndrome**

David U J Keller*, Andreas Bohn, Olaf Dössel and Gunnar Seemann

225 **Modelling of Intracellular Ca2+ Alternans and Ca2+-Voltage Coupling in Cardiac Myocytes**

Qince Li and Henggui Zhang*

226 **Mechano-Electrical Feedback during Cardiac Resynchronization Therapy?**

Nico Kuijpers*, Evelien Hermeling and Frits Prinzen

227 **Enhanced Computer Modeling of Cardiac Action Potential Dynamics using Experimental Data-Based Feedback**

Laura Munoz* and Niels Otani

Wednesday, September 29, 2010, 12:00

PB1: Forward/Inverse and System Modeling Posters

Room: Exhibition Center

228 **ECGSIM: Interactive Simulation of the ECG for Teaching and Research Purposes**

Peter M van Dam*, Adriaan van Oosterom and Thom Oostendorp

229 **Refined Estimate of the Dominant T Wave**

Roberto Sassi* and Luca T Mainardi

230 **Simulation of Fractionated Electrograms at Low Spatial Resolution in Large-Scale Heart Models**

Mark Potse* and Nico HL Kuijpers

231 **Implantable Cardioverter Defibrillator Predictive Simulation Validation**

Jess D Tate*, Jeroen G Stinstra, Thomas A Pilcher and Rob S MacLeod

232 **A Chaotic Model for Generating Heart Rate Variability Signal using Integral Pulse Frequency Modulation**

Mahdi Lak, Nader Jafarnia Dabanloo* and Seyed Kamaledin Setarehdan

233 **Towards the Cardiac Equivalent Source Models in ECG and MCG Problems: A Simulation Study**

Guofa Shou, Ling Xia*, Huilong Duan and Mingqi Qian

234 **The Inverse Problem of Phase Singularity Distribution: An Eikonal Approach**

Vincent Jacquemet*

235 **Estimating the Influence of Cardiac Motion on Simulations of Electrical Excitation**

Stefan Fruhner*, Harald Engel and Markus Bär

Wednesday, September 29, 2010, 12:00

236 **Role of the Fast Conduction System in Electrical Activation in Simple and Detailed Biophysical Heart Models**

Ali Pashaei*, Daniel Romero, Rafael Sebastian, Oscar Camara and Alejandro F Frangi

237 **Moving Equivalent Dipoles Derived from the Body Surface Potential Map by Solving the Inverse Problem**

Vito Starc*

238 **Study of the Static and Dynamic Characterization of the Biological Tissue to Obtain the Temperature Estimation in RF Ablation using Computer Modeling**

José Alba*, Macarena Trujillo, Ramón Blasco and Enrique J Berjano

Wednesday, September 29, 2010, 12:00

PB2: Imaging & Related Topics Posters

Room: Exhibition Center

239 **Three-Dimensional Analysis of Regional Left Ventricular Endocardial Curvature from Cardiac Magnetic Resonance Images**

Francesco Maffessanti*, Enrico G Caiani, Hans-Joachim Nesser, Johannes Niel, Regina Steringer-Macherbauer, Roberto M Lang and Victor Mor-Avi

240 **Characterization of Degenerative Mitral Valve Disease using Morphologic Analysis of Real-Time 3D Echocardiographic Images**

Sonal Chandra, Ivan S Salgo, Lissa Sugeng, Lynn Weinert, Masaaki Takeuchi, Wendy Tsang, Roberto M Lang and Victor Mor-Avi*

241 **Identifying Fetal Heart Anomalies using Fetal ECG and Doppler Cardiogram Signals**

Ahsan Habib Khandoker*, Yoshitaka Kimura, Marimuthu Palaniswami and Slaven Marusic

242 **Magnetic Resonance Imaging-Induced Heating on Patients with Implantable Cardioverter-Defibrillators and Pacemakers: Role of Lead Structure**

Eugenio Mattei*, Giovanni Calcagnini, Federica Censi, Michele Triventi and Pietro Bartolini

243 **Assessing Cardiac Phase Retrieval in IntraVascular UltraSound**

Aura Hernàndez-Sabaté*, Monica Mitiko Soares Matsumoto, Sergio Shiguemi Furuie and Debora Gil

244 **Noninvasive 4D Blood Flow and Pressure Quantification in Central Blood Vessels via PCMRI**

Sebastian Meier*, Anja Hennemuth, Ola Friman, Jelena Bock, Michael Markl and Tobias Preusser

Wednesday, September 29, 2010, 12:00

245 **A Computational Tool for Coronary Atherosclerotic Plaque Analysis of Virtual Histology Images**

Fernando Sales*, João Falcão, Breno Falcão, Sergio Furuie and Pedro Lemos

246 **Automated Heart Localization for the Segmentation of the Ventricular Cavities on Cine Magnetic Resonance Images**

Constantin Constantinides*, Yasmina Chenoune, Elie Mousseaux, Frédérique Frouin and Elodie Roullot

247 **A Method for Fast Browsing of Coronary Angiography Studies**

Aafreen Mahmood and Tanveer Syeda-Mahmood*

248 **Transmural Changes in Fibre Helix Angle in Normal and Failing Canine Ventricles**

Richard Clayton*, Samia Abdalhamid, Ryan Bloor, Kanna Kotagiri, Georgios Kyprianou, Jaeson Lee, Amruta Mane and Robert White

Wednesday, September 29, 2010, 12:00

PB3: Cardiovascular Variability Posters II

Room: Exhibition Center

249 **Poincaré Plot in Ischemic Rabbit Hearts**

Oto Janoušek*, Marina Ronzhina, Marie Nováková, Ivo Provazník and Jana Kolářová

250 **HRV in Isolated Rabbit Hearts and In Vivo Rabbit Hearts**

Oto Janoušek*, Marina Ronzhina, Peter Scheer, Marie Nováková, Ivo Provazník and Jana Kolářová

251 **Determination of the Frequency Bands for Heart Rate Variability: Studies on the Intact and Isolated Rabbit Hearts**

Marina Ronzhina*, Oto Janousek, Marie Novakova, Peter Scheer, Ivo Provaznik and Jana Kolarova

252 **Time Domain BRS Estimation: Least Squares versus Quantile Regression**

Sónia Gouveia*, Conceição Rocha, Ana Paula Rocha and Maria Eduarda Silva

253 **Relationship between Fractal Dimension and Power-Law Exponent of Heart Rate Variability in Normal and Heart Failure Subjects**

Monica Cusenza*, Agostino Accardo, Gianni D'Addio and Graziamaria Corbi

254 **Ventilatory Threshold Prediction by Spectral Analysis of Heart Rate Variability in Incremental Maximal Tests**

Adolfo Benítez-Herrera, Miguel A García-González*, Rosa Angulo-Barroso, Ferran Rodríguez-Guisado, Xavier Iglesias-Reig, Raul Bescós, Michel Marina and Josep M Padullés

255 **Modifications of Autonomic Activity and Baroreceptor Response During Tilt-induced Vasovagal Syncope**

Chun-An Cheng*, Jiunn-Tay Lee and Hung-Wen Chiu

Wednesday, September 29, 2010, 12:00

256 **Respiration Signal as a Promising Diagnostic Tool for Late Onset Sepsis in Premature Newborns**

Xavier Navarro*, Fabienne Porée, Alain Beuchée and Guy Carrault

257 **Identification of Sympathetic and Parasympathetic Nerves Function In Cardiovascular Regulation using NARX Model**

Ali Ghaffari, C Nat Nataraj*, Ali Jalali, Parham Ghorbanian and Fatemeh Jalali

258 **Tone-Entropy Analysis as a Cardiac Risk Stratification Tool**

Herbert Jelinek, Ahsan Habib Khandoker* and Marimuthu Palaniswami

259 **A New Parameter in the Nonlinear Dynamics of the Heart: The Higher Reconstruction Step**

Antônio Carlos da Silva Filho*, Fátima MHSP da Silva, Lourenço Gallo Júnior and Júlio Cesar Crescêncio

260 **Statistical Properties and Memory of Excursions in Heartbeat Intervals**

Israel Reyes Ramirez*, Lev Guzman Vargas and Ricardo Hernandez Perez

261 **Towards a Data Fusion Model for Predicting Deterioration in Haemodialysis Patients**

Yasmina Borhani*, Susannah Fleming, David Clifton, Sheera Sutherland, Lyndsay Hills, David Meredith, Chris Pugh and Lionel Tarassenko

262 **Heart Rate Variability using Poincare plots in 10 year old Healthy and Intrauterine Growth Restricted Children with Reference to Maternal Smoking Habits During Pregnancy**

Taher Biala*

Wednesday, September 29, 2010, 12:00

PB4: ECG Algorithms and Signal Processing Posters

Room: Exhibition Center

263 **QRS Morphological Analysis using Two Layered Self-Organizing Map for Heartbeat Classification**

Mutsuo Kaneko*, Fumiaki Iseri, Takafumi Gotoh, Hidehiro Ohki, Naomichi Sueda and Tatsuya Yoneyama

264 **Robust Delineation of High-Resolution Ambulatory Holter ECG Events via False-Alarm Controlled Segmentation of a Wavelet-Based Geometrical Decision Statistic**

Mohammad Reza Homaeinezhad* and Ali Ghaffari

265 **A Wavelet-based Algorithm for Delineation and Classification of ECG Waves**

Lars Johannesen*, Ulrik Silvanus Lerkevang Grove, Jens Stampe Soerensen, Mick Lykkegaard Schmidt, Jean-Philippe Couderc and Claus Graff

266 **Predicting Effectiveness of Cardiac Resynchronization Therapy Based on the Analysis of QRS Components using the Meyer Orthogonal Wavelet Transformation**

Xiaojuan Xia*, Jean-Philippe Couderc, Scott McNitt and Wojciech Zareba

267 **Automatic Electrocardiogram Delineator Based on the Phasor Transform of Single Lead Recordings**

Arturo Martínez*, Raúl Alcaraz and José Joaquín Rieta

268 **An Efficient Approach for Heartbeat Classification**

Stevan Jokić, Srđan Krčo, Dejan Sakač, Zoran Lukić, Vlado Delic and Tatjana Loncar Turukalo*

269 **Long-Duration Ambulatory Holter ECG QRS Complex Geometrical Templates Extraction by Non-Parametric Clustering of the QRS Virtual Close-up Extracted Feature Space**

Mohammad Reza Homaeinezhad* and Ali Ghaffari

Wednesday, September 29, 2010, 12:00

270 **A Fast and Robust Time-Series Based Decision Rule for Identification of Atrial Fibrillation Arrhythmic Patterns in the ECG**

Omar Jacinto Escalona* and Mauricio Enrique Reina

271 **Segment Clustering for Holter Recroding Analysis**

Jose Luis Rodríguez-Sotelo, Diego Peluffo-Ordóñez, David Cuesta-Frau, Germán Castellanos-Domínguez and Lina Sepúlveda*

272 **Optimal Delineation of Ambulatory Holter ECG Events via False-Alarm Bounded Segmentation of a Wavelet-Based Principal Components Analyzed Decision Statistic**

Mohammad Reza Homaeinezhad*

273 **Long-Duration ECG Signal Events Detection-Delineation via Segmentation of a Wavelet-Based Independent Components Analyzed Metric**

Mohammad Reza Homaeinezhad* and Ali Ghaffari

274 **Linear and Non-Linear Features for Intrapartum Cardiotocography Evaluation**

Václav Chudáček*, Jiří Spilka, Petr Janků and Lenka Lhotská

275 **Hidden Markov Tree-based Arrhythmia Classification**

Samar Krimi, Kaïs Ouni* and Noureddine Ellouze

276 **P Wave Delineation using Spatially Projected Leads from Wavelet Transform Loops**

Rute Almeida, Juan Pablo Martínez, Ana Paula Rocha and Pablo Laguna*

277 **BEATS: An Interactive Research Oriented ECG Marker System**

S Man*, AC Maan, EE van der Wall, MJ Schalij and CA Swenne

Wednesday, September 29, 2010, 12:00

PB5: ECG - Atrial Fibrillation Posters

Room: Exhibition Center

278 **Radial Basis Function Networks Applied to QRST Cancellation in Atrial Fibrillation Recordings**

Jorge Mateo, Ana Torres, César Sánchez and José Joaquín Rieta*

279 **Ectopic Beats Canceler for Improved Atrial Activity Extraction from Holter Recordings of Atrial Fibrillation**

Arturo Martínez*, Raúl Alcaraz and José Joaquín Rieta

280 **Simulation of Monitoring Strategies for Atrial Fibrillation Detection**

Federica Censi*, Giovanni Calcagnini, Eugenio Mattei, Michele Triventi and Pietro Bartolini

281 **Organization Analysis of Atrial Fibrillation Applied to the Improvement of Electrical Cardioversion Protocols**

Raúl Alcaraz, Fernando Hornero and José Joaquín Rieta*

282 **Study of Sample Entropy Ideal Computational Parameters in the Estimation of Atrial Fibrillation Organization from the ECG**

Raúl Alcaraz, Daniel Abásolo, Roberto Hornero and José Joaquín Rieta*

Wednesday, September 29, 2010, 12:00

PB6: T-Wave Alternans Posters

Room: Exhibition Center

283 **Sensitivity of T-Wave Alternans Identification Algorithms to Residual Physiological Noise Affecting the ECG after Preprocessing**

Silvia Bini*, Laura Burattini and Roberto Burattini

284 **Signal Processing Subsystem Validation for T wave Alternans Estimation**

Rebeca Goya-Esteban, Inmaculada Mora-Jiménez*, Manuel Blanco-Velasco, Óscar Barquero-Pérez, Antonio Caamaño-Fernandez, Arcadi García-Alverola and José Luis Rojo-Álvarez

285 **T Wave and QRS Complex Alternans During Standard Diagnostic Stress ECG Test**

Ivaylo Christov*, Giovanni Bortolan, Iana Simova and Tzvetana Katova

286 **T-Wave Alternans Quantification: Which Information from Different Methods?**

Laura Burattini*, Silvia Bini and Roberto Burattini

Wednesday, September 29, 2010, 12:00

PB7: Cardiovascular Mechanics Posters

Room: Exhibition Center

287 **Assessment of Autonomic Cardiac Control in Women with Cardiac Syndrome X using Time Related Autonomic Balance Indicator**

Mikhail Matveev, Svetlin Tsonev*, Rada Prokopova and Temenuga Donova

288 **Discrete Wavelet-Aided Delineation of PCG Signal Events via Analysis of an Area Curve Length-based Decision Statistic**

Mohammad Reza Homaeinezhad* and Ali Ghaffari

289 **Robust Arterial Blood Pressure Events Detection-Delineation via Segmentation of a Wavelet-Derived Stationary-Baseline Metric**

Mohammad Reza Homaeinezhad* and Ali Ghaffari

290 **Elimination of the Respiratory Effect on the Thoracic Impedance Signal with Whole-Body Impedance Cardiography**

Pavel Jurák*, Josef Halámek, Vlastimil Vondra, Ivo Viščor, Jolana Lipoldová and Martin Plachý

291 **Estimation of Hemodynamic Parameters from Seismocardiogram**

Kouhyar Tavakolian*, Andrew Blaber, Brandon Ngai, Bahman Yari Saeed Khanloo, Alireza Akhbardeh and Bozena Kaminska

292 **Mitral Valve Modelling in Ischemic Patients: Finite Element Analysis from Cardiac Magnetic Resonance Imaging**

Carlo A Conti, Marco Stevanella, Francesco Maffessanti*, Francesco Trunfio, Emiliano Votta, Alberto Roghi, Oberdan Parodi, Enrico G Caiani and Alberto Redaelli

293 **Long-Term Characterization of Arterial Blood Pressure Series**

Juan Carlos Perfetto*, Graciela Aurora Ruiz and Carlos Enrique D'attellis

Wednesday, September 29, 2010, 12:00

PB8: Informatics Posters

Room: Exhibition Center

294 **Displaying Computerized ECG Recordings and Vital Signs on Windows Phone 7 Smartphones**

Stefan Klug*, Kai Krupka, Hartmut Dickhaus, Hugo A Katus and Thomas Hilbel

295 **Transmural Exchange of Cardiology Related Information Between Two Academic Centres and Referring Hospitals using XDS(-I)**

Arnold Dijk*, Jan Peter Busman, Niek van der Putten and Willem Dassen

296 **Library for Managing and Processing ECG Signal Data: Design and Implementation in Delphi and C#**

Alberto Rodríguez*, Raúl Almeida, Gemma Rodríguez, Nelvy Pina and Gisela Montes de Oca

297 **A Personalised Self Management System for Chronic Heart Failure**

William P Burns*, Richard J Davies, Chris D Nugent, Paul J McCullagh, Huiru Zheng, Norman D Black and Gail A Mountain

Wednesday, September 29, 2010, 14:00

MC: Closing Plenary Session

Room: Exhibition Center

Chairs: Bill Sanders and Chris Nugent

298 **Nonhyperemic Intracoronary Pressure Waveform Analysis Predicts the Fractional Flow Reserve**

Peter Lugosi, Peter Santa, Zoltan Beres, Balazs Tar, Janos Santa and Zsolt Koszegi*

299 **Development and Validation of Automated Endocardial and Epicardial Contour Detection for MRI Volumetric and Wall Motion Analysis**

Enrico G Caiani*, Alberto Redaelli, Oberdan Parodi, Emiliano Votta, Francesco Maffessanti, E Tripoliti, Gaetano Nucifora, Daniele De Marchi, Giacomo Tarroni, Massimo Lombardi and Cristiana Corsi

300 **Polisomnography in Extreme Environments: the MagIC Wearable System for Monitoring Climbers Ascending on Mt Everest Slopes**

Paolo Meriggi*, Paolo Castiglioni, Carolina Lombardi, Francesco Rizzo, Andrea Faini, Marco Di Rienzo and Gianfranco Parati

301 **Investigation of Drowsiness while Driving utilizing Analysis of Heart Rate Fluctuations**

Gabriela Dorfman Furman and Anda Baharav*

302 **Features of Arterial Blood Pressure as Indicators of Impending Acute Kidney Injury in ICU Patients**

Li-wei Lehman*, Mohammed Saeed, George Moody and Roger Mark

303 **Development and Clinical Validation of a Physiological Data Acquisition Device Intended for Monitoring and Exercise Guidance of Heart Failure and Chronic Heart Disease Patients**

Athina Kokonozi, Alexander Astaras, Panagiotis Semertzidis, Emmanouil Michail, Dimitris Filos, Ioanna Chouvarda*, Olivier Grossenbacher, Jean-Marc Koller, Leopoldo Rossini, Jacque-André Porchet, Marc Correvon, Jean Luprano, Auli Sipilä, Chryssanthos Zambou

Abstracts

Correlation between Time Domain Baroreflex Sensitivity and Sympathetic Nerve Activity

M1

Sónia Gouveia*, Ana Paula Rocha, Pablo Laguna and Philippe van de Borne

Centro de Matematica da Universidade do Porto e Departamento de Matematica, Universidade de Aveiro, Portugal

Dysfunction of the autonomic nervous system (ANS) is evidenced by reduced baroreflex sensitivity (BRS), which can be quantified as the slope between SBP and RR values identified in baroreflex segments. However such BRS estimates do not distinguish fast/parasympathetic from slow/sympathetic ANS modulations. The traditional sequences technique is known to provide a BRS estimate based on short baroreflex sequences (BSs) reflecting essentially parasympathetic ANS activity. The alternative events technique is able to provide longer baroreflex events (BEs), besides BEs of the same length as BSs, and so it is more likely to additionally capture sympathetic modulation. The Muscle Sympathetic Nerve Activity signal (MSNA) has been used to directly investigate ANS modulations and it has been suggested that MSNA powers in LF and HF bands are respectively related with sympathetic neural excitation and inhibition. In this work, BRS estimates from short and long BEs are associated with MSNA powers, in order to test if the BRS estimates from the events are able to distinguish parasympathetic/sympathetic ANS modulations.

Simultaneous recordings of ECG, ABP, RESP and MSNA were acquired from 15 healthy subjects in supine rest condition. Short and long BEs are defined from a cutoff length adjusted to each subject, from the respiratory frequency estimated from RESP signal. The results indicate that BRS from short BEs are significantly correlated with MSNA powers in HF ($r=0.65$, $p<0.05$ for the hypothesis of no correlation) and not significantly correlated with MSNA powers in LF ($r=0.33$). On the other hand, BRS from long BEs are not significantly correlated with MSNA powers in HF ($r=0.40$) whereas they are significantly correlated with MSNA powers in LF ($r=0.61$, $p<0.05$). In conclusion, the results in this study evidence that short and long BEs may carry different information on ANS modulations in baroreflex regulation.

M1

Fully Automated Gating of Optical Coherence Tomography Data

K Sihan, C Botha, F Post, S de Winter, E Regar, PJWC Serruys, R Hamers, N Bruining

Erasmus MC, Rotterdam, the Netherlands

Objectives and background: images acquired of coronary vessels during a pullback of time-domain optical coherence tomography (OCT) are influenced by the dynamics of the heart. This study explores the feasibility of applying an in-house developed retrospective image-based gating method for OCT and the influence of catheter dislocation and luminal changes during the cardiac cycle on the outcome of quantitative OCT (QOCT).

Methods: The gating method was developed using Matlab (The Mathworks, Natick, MA, USA) and operates fully-automatic. OCT image data of 20 randomly selected patients, acquired with a commercially available system (Lightlab imaging, Westford, MA, USA), were pulled from our OCT database for development and validation.

Results: Twelve of the 20 datasets could be gated (an example is presented in the figure); the other 8 pullbacks could not be gated due to a lack of motion induced artefacts. Computations required approximately 30 minutes/dataset. Quantitative comparisons between the gated and the non-gated QOCT results showed significant differences for mean areas and volumes ($p < 0.001$) and mean relative differences of -11% (range -2 up to -20%) for lumen areas (gated) and -13% (range -5 up to -24%) for volumes.

Conclusion: Retrospective image-based time-domain OCT gating in the presence of motion induced artefacts is feasible. Significant changes in coronary lumen dimensions during the cardiac cycle were observed by OCT and in consequence, quantitative gated OCT analysis showed significant differences compared to non-gated QOCT analyses.

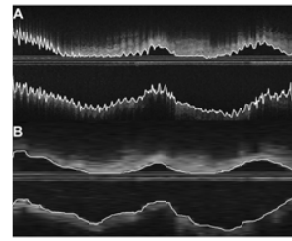

Panel A shows a non-gated data-set and panel B shows a gated data-set.

MRI-Based Quantification of Myocardial Perfusion at Rest and Stress using Automated Frame-by-Frame Segmentation and Non-Rigid Registration

M1

Giacomo Tarroni*, Amit R Patel, Federico Veronesi, James Walter, Claudio Lamberti, Roberto M Lang, Victor Mor-Avi and Cristiana Corsi

University of Bologna, Italy

The quantification of myocardial perfusion relies on manual tracing of myocardial regions of interest (ROIs) and repositioning the ROIs frame-by-frame throughout the contrast-enhanced image sequence. This tedious and potentially inaccurate methodology hinders widespread clinical use of imaging-based quantification of myocardial perfusion. Accordingly, we developed a technique for automated identification and registration of myocardial ROIs from cardiac magnetic resonance (CMR) images as a basis for perfusion quantification. Our approach uses region-based and edge-based level set techniques for endocardial and epicardial border detection combined with non-rigid registration, which is achieved by a 2D multi-scale cross-correlation and contour adaptation (fig., left). This approach was tested on 66 short-axis image sequences (Philips 1.5T) obtained in 11 patients at rest and during regadenoson stress at 3 levels of the left ventricle during first pass of a Gadolinium-DTPA bolus. Standard myocardial ROIs were automatically defined and registered to generate contrast enhancement curves throughout the image sequence. Analysis of one sequence required <1 min and resulted in endo- and epicardial boundaries that were judged accurate in all image sequences. Time-curves showed the typical pattern of first-pass perfusion with SNR of 15 ± 5 at rest and 19 ± 4 during stress. During stress, contrast inflow rate (0.031 ± 0.013 vs 0.014 ± 0.004 sec-1, $p<0.05$) and peak-to-peak amplitude (0.20 ± 0.05 vs 0.14 ± 0.03, $p<0.05$) were both increased compared to rest (fig., right). Despite the extreme dynamic nature of contrast enhanced image sequences and respiratory motion, fast automated detection of myocardial segments and quantification of tissue contrast results in curves with excellent noise levels, which reflect the expected effects of stress.

Simulating the Impact of the Transmural Extent of Acute Ischemia on the Electrocardiogram

M1

M Wilhelms, O Dössel, G Seemann

Institute of Biomedical Engineering, Karlsruhe Institute of Technology, Karlsruhe, Germany

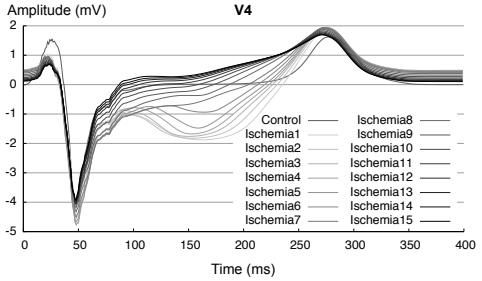

ECGs (lead V4) of control case and setups with different transmural extent of ischemia.

During acute cardiac ischemia, electrophysiological properties of the affected tissue are altered. Transmural heterogeneity of the metabolism and the greater distance to the coronary arteries lead to first appearance of the effects in the subendocardium. If the occlusion of the artery worsens, ischemia spreads transmurally towards the subepicardium. Diagnosis of cardiac ischemia is based on the ECG, especially shifts of the ST segment. Computer simulations help understanding the underlying effects and improving the early diagnosis of this pathology. In this work, we simulated the effects of ischemia, which were integrated in a human ventricular cell model, ten minutes after the occlusion of the left anterior descending coronary artery. The heterogeneous ischemic regions were modeled as ellipsoids with varying transmural extent. The excitation propagation was calculated using the monodomain equations in a heterogeneous model of complete ventricles. To obtain the corresponding ECG, the forward problem of electrocardiography was solved. In case of subendocardial ischemia (Ischemia1), small and short action potentials were initiated in the ischemic region causing a transmural gradient of the transmembrane voltage. Therefore, the ST segment was depressed in leads close to the ischemic region. An increase of the transmural extent of the ischemic region (Ischemia11) led to a conduction block in the center. Therefore, the transmembrane voltage exhibited a gradient from the ischemic zone towards the surrounding healthy tissue. Thus, the ST segment was a zero baseline, as in the healthy control case. During transmural ischemia (Ischemia15), the gradient of the transmembrane voltage was concentrated in direction of the ventricular wall leading to ST segment elevation. In this work, we showed that ST segment polarity can be dependent on the transmural extent of the ischemic region.

Development and Comparison of Single-parameter Indices Characterizing the Severity of Acute Myocardial Ischemia

John Wang*, James Warren, Galen Wagner and Milan Horacek

Philips Healthcare, Andover, MA, United States

Introduction: The aim of this study was to assess both the sensitivity and specificity of two single-parameter indices of ischemia severity (—ST— and ST-RMS) for 5 lead-triplets: Frank-leads/X,Y,Z; V2,V5,aVF; V2,V5,III; V3,V5, III; and V3,V6,III, each derived from 7 subsets of Mason-Likar (M-L) 12-lead ECG using only limb leads and two precordial leads (V1,V3; V1,V4; V1,V5; V2,V4; V2,V5; V3,V5; V3,V6). Our hypothesis was that a single-parameter index using derived Frank orthogonal leads would be the best. Methods: Regression coefficients for deriving 5 lead-triplets from 7 sets of predictor leads were developed from the Dalhousie Superset consisting of 120-lead ECGs from 892 subjects. The test dataset was the STAFF3 database, consisting of M-L 12-lead ECGs acquired for 99 patients before and during episodes of acute ischemia induced by balloon-inflation angioplasty. We compared the tested ischemic indices to detect ischemic state by varying their threshold values and constructing receiver operating characteristic curves (ROC). Ischemia-detection ability was assessed as an area under the entire ROC curve (AUC) and, in addition, as an area under the ROC curve in the useful range of specificity, between 80% and 90% (AUC80-90). Results: The averaged AUC performance results for the 5 triplets derived from the 7 sets of dual-precordial leads are (in the format of: Derived triplets/AUC from —ST—/AUC from ST-RMS): Frank-leads/88.36/88.84; V2,V5,aVF/88.62/86.47; V2,V5,III/89.40/87.51; V3, V5,III/90.38/90.33; and V3,V6,III/90.45/90.25. The best-performing triplets of derived leads are V3,V5,III and V3,V6,III. The ranking for AUC80-90 values is about the same. Conclusions: We conclude that the currently used indices of ischemia using pseudo-orthogonal triplet of leads V2,V5,aVF, as well as those using Frank orthogonal leads X,Y,Z are outperformed in ischemia detection by indices based on triplets V3,V5,III and V3,V6,III. It should be noted though that the differences in performance are small and thus our results should be corroborated on a larger study population.

Validation of Electrocardiographic Criteria for Predicting the Culprit Artery in Patients with Acute Myocardial Infarction

S21

Niek van der Putten*, Peter Rijnbeek, Arnold Dijk, Gerard van Herpen, Enno van der Velde, Jonathan Lipton and Jan Kors

Thoraxcenter, Erasmus Medical Center Rotterdam, Netherlands

Many criteria have been proposed to predict the culprit artery from the ECG in patients with ST-elevation acute myocardial infarction (STEMI). We previously presented the validation of two such criteria on a large independent data set. The objective of this study is 1) to compare seven criteria for predicting the culprit artery, and 2) to assess the performance of these criteria for patients with acute myocardial infarction (AMI) who do not meet the STEMI criteria. We performed a retrospective analysis of patients who underwent percutaneous coronary intervention of a single vessel for treatment of AMI. A digital ECG was made within two hours prior to the first balloon inflation. ECG measurements were obtained with the Modular ECG Analysis System. A variety of criteria for detecting the culprit artery, including recent criteria proposed by Fiol, Tierala, and Wang, were compared in patients with or without STEMI. The study population consisted of 475 patients (LAD 197, RCA 197, LCx 81) of whom 61.9% fulfilled STEMI criteria. Overall, the criteria of Tierala performed best on the STEMI cases with an accuracy of 97.5% for LAD, 91.4% for RCA, and 88.8% for LCx, but specificity for RCA (86.3%) was low and sensitivity for LCx (29.0%) disappointing. The performance significantly decreased on non-STEMI patients. For example, the accuracy of the Tierala criteria in this subgroup was 75.8% for LAD, 74.2% for RCA, and 78.8% for LCx (specificity LAD only 71.6%, sensitivity RCA 20.3%, and sensitivity LCx 2.3%). We conclude that the Tierala criteria have the highest accuracy for detecting the culprit artery in STEMI cases, but some specificity and sensitivity values were low. Moreover, accuracies significantly decrease in patients who do not meet the STEMI criteria. Improved criteria that better predict the culprit artery in the whole group of AMI patients are currently under investigation.

A Spatio-Temporal Study of Ischemia and the Time-Frequency Coupling Variations between the ST Amplitude, Heart Rate and Dominant Angle

Raul Llinares and Gari D Clifford*

Universidad Politecnica de Valencia, Valencia, Spain

An analysis of the Long Term ST Database (LTSTDB) was conducted to quantify the duration and magnitude of ischemic episode changes across leads and through time. An episode was defined to last as long as any single lead indicated clinically significant ST changes. We calculated that the LTSTDB contains 1135 episodes of ischemia and 360 episodes of non-ischemic rate-related ST changes in 86 recordings from 80 subjects. We calculated that the length of the ischemic episodes closely matched a log-logistic distribution with μ=5.56 and σ=1.01. For the 15 recordings that possess orthogonal (EASI) leads sets we derived the 12 standard leads and analyzed the spatial time course (from the j-point to j+120 ms) of each episode over time to identify dominant trends. Although the magnitude of the ischemic episodes did not reveal any inter-subject trend (except for generally exhibiting Brownian-like motion), there appeared to be strong correlations with the heart rate (HR). Wavelet cross-spectral coupling with significance testing was then applied to the ST-amplitude and HR evolution over the course of each episode. In all subjects significant cross-spectral correlations were found at very low frequencies ($<$0.04 Hz), as well as at respiration and baroreflex frequencies. This indicates that the ischemic episodes are modulated by blood pressure and activity or HR-related phenomena and that all episodes in the LTSTDB are of a 'mixed' type at some point in their duration. The dominant angle of the ischemic episodes was also calculated. Although this angle evolved over time, it generally drifted by only a few degrees even over long episodes. A few large angle changes were observed although no clear explanation for these shifts can be found. The dominant angle also showed significant correlation ($P<0.01$) with the ST amplitude and HR changes at similar frequencies to those described above.

Enhancing the Acute MI Criteria in the Glasgow ECG Analysis Program to Include ST Depression

Elaine Clark*, Maria Sejersten, Peter Clemmensen and Peter Macfarlane

Electrocardiology Section, University of Glasgow, Glasgow, United Kingdom

S21

Aims Extending the ACC/ESC criteria for STEMI to include new lead pairings has resulted in improved accuracy in some studies. The aim was to investigate if the age and sex dependent acute MI criteria in the University of Glasgow ECG analysis program (Uni-G) could be similarly enhanced.

Methods 912 prehospital 12-lead ECGs (601 male, 311 female, age 65.38 $\pm$ 13.89 years) from patients with acute coronary syndrome were recorded in Zealand, Denmark. 406 ECGs were randomly allocated to a training set and 506 to a test set. Both the ACC/ESC criteria and the Uni-G program were modified to include lead pairings -aVL,III, aVL,-III and -V2,-V3. The training set was used for evaluation. The hospital discharge diagnosis was the gold standard.

The training set was also used to explore alternative enhancements to the Uni-G criteria based on STEMI equivalence. The resulting extended criteria were evaluated on the test set.

Results For the training set, the original ACC/ESC criteria gave sensitivity (SE) 66.4% and specificity (SP) 89%; Uni-G criteria gave SE 74.8% and SP 93.9%. For the extended pairings, the ACC/ESC criteria gave SE 72% and SP 85.9% while Uni-G had SE 77.6% and SP 92.3%.

Using STEMI equivalent criteria to enhance the basic Uni-G criteria, the results were: for the training set, an increase in SE from 74.8% to 76.9% and no change in SP (93.9%); for the test set, SE was unchanged (80.1%) and SP decreased (93.2% to 92.9%).

Conclusion The improvement found by other investigators when using new lead pairings was evident using the ACC/ESC criteria but not the Uni-G criteria. The already sensitive Uni-G program gave better results than the expanded ACC/ESC criteria and all attempts at extending the criteria to other leads gave minor improvement in sensitivity at the expense of minor decrease in specificity.

Graphic Visualization of ECG Estimated MI Size using the 17 Segment Bull's Eye Presentation

RE Gregg*, SH Zhou, ED Helfenbein

Advanced Algorithm Research Center, Philips Healthcare
Andover, MA, USA

Background: The size of myocardial infarction (MI) presented as a proportion of the left ventricle (LV) can be estimated using the Selvester scoring system based on ECG. The method sums points assigned to 50 ECG criteria resulting in a final estimate of MI size. In this study we report our effort to automate and then visualize the MI size score on the 17 segment LV bull's eye common to cardiac imaging.

Method: The automated Selvester scoring algorithm was implemented based on the 50 criteria. The algorithm was then validated using a database. After excluding LBBB (n=17), the database contained 688 ECGs with and without MI. Each ECG was manually scored by two cardiologists. Two MI scores were averaged to serve as gold standard. Computer based measurements were redefined according to the definitions of the scoring algorithm but not adjusted for the data set. The automated and manual MI size scores were correlated to assess the accuracy of the automated algorithm. Visualization of the MI extent and location was accomplished by mapping the automated Selvester scores with corresponding locations in LV using the 17 segment bull's eye.

Results: The correlation between the automated and manual scores was 91%. The regression slope (m) and intercept (b) ($y = m x + b$) was 0.99 and 0.64 respectively. With 2 ms added to the duration criteria and exclusion of cases with rS pattern interpreted as Q wave due to 20μV R-wave (n=18), the results were improved to achieve a correlation of 94% with slope and intercept of 0.99 and 0.30

Conclusion: The bull's eye display of MI size is commonly used in cardiac imaging, including echocardiography, cardiovascular magnetic resonance and nuclear imaging. Automated ECG graphic display of MI size serves as a tool to assist cardiologists to visualize the MI size in LV.

Display of Heart-Surface Potentials Derived from 12-lead Electrocardiograms

Milan Horacek*, James Warren and John Wang

Medicine (Cardiology), Dalhousie University, Halifax, Nova Scotia, Canada

S21

We investigated whether the ischemic region due to occlusion of a coronary artery can be visualized on the bull's-eye display of the heart surface by using just ST measurements from the 12-lead ECG. Torso model with 352 body-surface and 202 heart-surface nodes was used. Coefficients for deriving 352 body-surface potentials from 8 independent potentials of 12-lead ECG were derived from Dalhousie Superset (n = 892) of 120-lead ECGs. The test set consisted of 120-lead ECGs acquired for 45 patients during ischemia induced by balloon-inflation angioplasty; three subgroups of equal size comprised patients whose LAD, LCx, and RCA were occluded, respectively. BSPMs at J point of each patient were reconstituted from the 12-lead ECG and similarity of original and reconstituted maps was assessed by a similarity coefficient SC (dot product of 352-dimensional vectors divided by the product of their lengths, in percent). We applied inverse-solution methodology (Tikhonov regularization with 2nd order regularizing operator) to calculate heart-surface potentials and visualize them on bull's-eye display. Reconstitution of known body-surface distributions from the 12-lead ECG achieved an overall SC 92.46 $\pm$ 6.95% (mean $\pm$ SD); SC for subgroups was: 89.79 $\pm$ 9.95% for LAD, 93.89 $\pm$ 2.86% for LCx, and 93.70 $\pm$ 5.77% for RCA group. All characteristic spatial features of maps were preserved. We calculated and displayed heart-surface potentials and found that the area of positive potentials on the heart surface corresponded, in general, with the underperfused territory caused by the occlusion of each specific vessel. For the LAD group 11/15 bull's-eye images indicated the correct territory; for the RCA and the LCx groups 10/15 and 12/15 images were correct (with incorrect classifications being RCA /LCx mix ups). Better-then-expected results can be attributed to the strongly dipolar character of distributions caused by injury current. Our approach shows promise for ischemia monitoring.

An Augmentative and Portable QTc-Observer(QTO-Q2) to Facilitate More Purposeful Outpatient Monitoring

Thomas Chee Tat Ho* and Xiang Chen

Signal Processing, Institute for Infocomm Research, Singapore

A tele-medical approach for monitoring and detecting prolonging QT-intervals via cellular equipments is proposed in this paper. Currently, the procedures for detecting Longed QT Syndrome (LQTS) involves taking a 1 time preliminary prognosis followed by a comprehensive long time hospital or laboratory bound monitoring; the latter is only conducted if and only if the former is tested positive. However, if the preliminary prognosis fails due to the absence of the symptoms during the instance of testing, the subject may be declared with a false clean bill of health. In this modern day and age where telemedicine is becoming a more important aspect of conventional medicine, it is sensible that the conventional methods be augmented with ambulatory long-term monitoring to better detect LQTS for people suspected of it. The QTc-Observer (QTO or Q2) is developed to monitor specifically QT intervals for the detection of LQTS. Built on top of the existing MobiCare System [1], the Q2 is connected to an all-day monitoring center for continuous observations by medical professionals. The electrocardiography (ECG) data is collected by a commercially available light and portable sensor. The data is forwarded onto the cellular phone for processing. The QT intervals with its corresponding RR-intervals are extracted for conversion to QTc intervals. The QTc intervals are plotted over time to form a trend line. The trend line formed over time is then analyzed for abnormalities. A sliding detection window is used to analyze consecutive segments for LQTS. Finally, a correlation measure is used to compare the trend lines in the consecutive windows for analysis.

Non-Invasive Sensors Based Human State in Nightlong Sleep Analysis for Home-Care

Magdalena Smolen*, Klaudia Czopek and Piotr Augustyniak

S22

Faculty of Physics and Applied Computer Science, AGH University of Science and Technology, 30 Mickiewicza Ave., 30-059 Krakow, Poland, Krakow, Poland

In this paper we present a non-invasive, easy-to-use and low-cost monitoring system for nightlong human sleep quantification. Our system uses simultaneous measurement of three different signals describing the activity of the human body: infrared video-recorded subject motion, audio-recorded acoustic effects and the three double-leads electrocardiogram. This study is aimed to show how sleep disorders influence a good night sleep. Acoustic characteristics of snoring sounds, which are approximately periodic waves with noise, were analyzed in this paper by using a multidimensional voice program MDVP. The ECG recordings were used to acquire electrocardiogram-derived respiratory (EDR) and the pattern of heart rate variability (HRV). The typical tachogram and its main parameters were calculated: RMSSD, SDANN. The square root of the mean squared differences of successive NN intervals (RMSSD) and the standard deviation of the average NN interval calculated over five minutes periods (SDANN) represented short-time and long-time variability respectively. Quantitative evaluation of the movements activity during nightlong sleep were carried out by means of processing the difference images from the consecutive video frames in respect to the background signal. During these studies several recordings of nightlong sleep were investigated. Characteristic pattern of each of the acquired signals and video frames were analyzed and final conclusions about the state and activity of every investigated patient were presented by setting-up the parameters corresponding to each of the signals. Our study shows the coincidence of respiratory sounds (snoring and breathing) with the subject motion and cardiovascular response. Both the value and frequency of the movements parameter revealed inter-subject motion variability as well as motion variability in time of the same patient. Increasing SDANN and RMSSD parameters are correlated with observed increased snoring sound intensity, which is above 65dB at any snoring event.

Management of Non-uniform Data Transfer in Cardiac Monitoring Systems with Adaptive Interpretation

P Augustyniak,

AGH University of Science and Technology
Krakow, Poland

Our research concerns the problem of data queuing in telemedical non-uniformly reporting surveillance systems, recently introduced to cardiology. In adaptive systems, sampling rates are individually set for each diagnostic parameter, what requires implementation of a reservation procedure managing the content of every packet in order to proper data delivery.

The reservation procedure considers changes in the data flow caused by time-variable requirements for the update rate of values in particular diagnostic data series. Automatic scheduling of reports was achieved with taking into consideration of two auxiliary data attributes in the information structure: the validity period and the priority, set individually for each ECG diagnostic measurement. The patient-side recorder-interpreter works in one of two reporting modes: in the immediate mode diagnostic packets are transmitted as promptly as implied by sampling requirements, while in the delayed mode the transmission is deferred until packets are filled with valid data. Switching between these modes allows the telediagnostic system to respond in short time in case of emergency, and to limit the usage of data carrier and energy for long-time regular reporting.

Data stream volume using rigid and adaptive reporting

component	volume [b]	interval [s]	rigid [bps]	adaptive [bps]
heart rate	1	0,3		
arrhythmia	5	3	181,5	65,67
ST segment	24	30		

The prototype is designed for cardiology-based surveillance of patients in motion and uses a star-shaped topology managed by the central server over a bi-directional digital data link. In the delayed reporting mode, the packet size limit was set to 20kB (6 minutes of recording). The wireless transfer session lasts for up to 10 seconds depending on the speed of data transfer (16kbps). The module is thus operating for 18s (including the management time) out of 360s reporting interval. The average energy is reduced below 3mA, i.e. to 6% of the value necessary for a seamless operation. In the immediate reporting mode, the minimum packet size of 256 bytes is collected within 4.63 seconds, which results in system response slightly worse than the delay in the interpretation process (typically 2s), but still acceptable as real time monitoring.

Optimization of the Alarm-Management of a Heart Failure Home-Monitoring System

S22

M Vukovic, M Drobics, D Hayn, P Kastner, G Schreier

Austrian Institute of Technology, Safety & Security Department
Vienna, Austria

MOBIle TELemonitoring (MOBITEL) was a study on home-based monitoring of heart failure patients after an episode of acute decompensations using mobile phone technology. Within the MOBITEL study it could be shown that by the use of home-monitoring with automated alarm generation not only the number of re-hospitalizations of heart failure patients can be significantly reduced, but also – in case of re-hospitalizations – the duration of the hospitalization is significantly decreased. These results might, however, be further improved by bringing down a relatively high number of false positive alarms generated during the MOBITEL.

In the present study we show by retrospectively evaluating the available data, how the existing MOBITEL algorithm can be improved. This is achieved by reducing the number of generated false alarms and by introducing a unique risk parameter, which can be used to indicate the patient's status.

We retrospectively analyzed data from 120 patients monitored between 2003 and 2008. For the analysis of historic treatment data and measurement tables, GNU-R statistical software was used. A computer based model was generated to optimize the alarm-management of a heart failure home-monitoring system.

The algorithm provides high sensitivity and specificity and shows a significant improvement to the previous model by reducing the number of false alarms, while obtaining nearly the same number of positive alarms.

The developed algorithm offers an opportunity to have a more efficient and precise telemonitoring system to support physicians, reduce hospitalizations, and decrease health care costs. Formulated concepts allow patient physician interaction as part of the control loop. Future works will focus on characterization and modeling of this control system with mathematical and computer science methods in order to find strategies for therapy optimization. Furthermore, the algorithm presented in this paper shall be applied in a prospective study for validation.

Multimedia alarm pages on multiple Smartphone platforms

MJB van Ettinger, JA Lipton, SP Nelwan, RJ Barendse, TB van Dam, N van der Putten

Erasmus MC
Rotterdam, The Netherlands

At the Critical Cardiac Care unit a patient is monitored closely by different devices. These devices generate alarms when an abnormality is detected. These alarms are typically provided by the patient monitor at the bedside or at the nurse desk. Caregivers aren't always at either of these locations. Additionally most alarms do not signify a life-threatening event.

At Department of Cardiology of the Erasmus MC patient monitors are connected to a central gateway. An application was developed to collect and manage alarms from the central gateway. The alarm manager stores the alarm messages; a web-interface provides access to the data. The web-interface can be used from many platforms including the following Smartphone platforms: iPhone, Android and Symbian. The web-interface provides the alarm messages to the caregiver. The interface can be configured to display alarms for each patient bed or for an entire care unit and is updated every 5 seconds. The alarms received by the Smartphone do not yet generate an audible alarm. However the current setting is that audible alarms can be heard within the ward. The user can look up the alarm on a Smartphone by clicking on it, the message and vital signs displayed by the monitor at the moment of the alarm are provided, enabling the user to make an informed decision regarding further action.

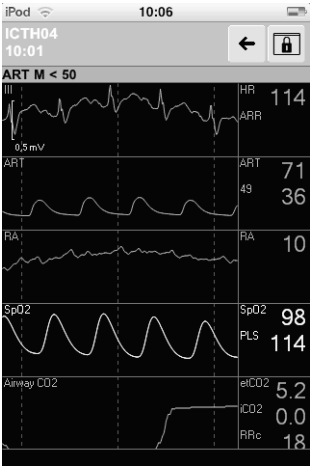

Screenshot made of the application on an iPod Touch

The system also provides a mechanism to add additional messages. For example lab results can be shown when new lab results are available, messages from a clinical decision support system could be integrated into the system as well as messages that aid nurses to follow clinical pathways.

The multimedia paging application allows delivery of alarms and clinical data directly to the caregiver on a portable electronic device, enables evaluation of alarm data and provides a platform for generating "smart" alarms.

Evaluation of Patients' Adherence and Satisfaction with a Self-Measurement Blood Pressure Telemonitoring Program

S22

Michele Triventi*, Giovanni Calcagnini, Federica Censi, Eugenio Mattei, Stefano Strano and Pietro Bartolini

Dept. of Technologies and Health, Italian National Institute of Health, Rome, Italy, Rome, Italy

Cardiovascular diseases are the world's leading killer, with extremely high costs, more than 50% of those caused by patient hospitalizations. Post-acute cardiovascular event patients, discharged by a health structure, have to follow a long and complex therapeutic/rehabilitation path, which involves either medical doctors and his/her own family. In this context, utilization of information and communication technologies in home monitoring applications is becoming more and more common. In the cardiological field, telemedicine projects include the monitoring of several parameters, for which the technology of the medical devices provides self-measurement methods. The aim of this study was to assess the evaluation of patients adherence and satisfaction with a self-measurement blood pressure telemonitoring program. The study enrolled patients dismissed from a health structure after the acute phase of a major cardiac or cerebro-vascular event. At dismission each patient received a telemedicine system equipped with an automatic blood pressure device, and a brief training, and it was asked to perform one blood pressure testing per day. Each patient was asked to complete a questionnaire at the end of the program. During the monitoring period, no feedback was given to the patients. 17 patients were monitored for an average of 75 days each. During a cumulative monitoring period of 1275 days, there were 1139 data transfer sessions. On average, the blood pressure measures received were 0.84 per day. 16/17 participants completed the feedback questionnaire. All patients (100%) scored installation, usability and quality of service as good or very good. The majority of patients (13/16) declared to feel comfortable with the self-measurement of blood pressure and the use of the telemonitoring system. Telemonitoring of blood pressure measurement can be considered a mature technology which find favour with patients dismissed after a acute cardiac or cerebro-vascular event.

Heart Rate Variability Characterized by Refined Multiscale Entropy Applied to Cardiac Death in Ischemic Cardiomyopathy Patients

José Fernando Valencia*, Montserrat Vallverdú, Rico Schroeder, Iwona Cygankiewicz, Rafael Vázquez, Antonio Bayés de Luna, Alberto Porta, Andreas Voss and Pere Caminal

Dept ESAII, Universitat Politècnica de Catalunya, Barcelona, Spain

The dynamics involved in the beat-to-beat variability of the heart occur over a large set of temporal scales. Due to this multiscale behavior, heart rate variability (HRV) cannot be completely characterized on a single time scale, and scaling techniques are required to characterize its behavior. Refined Multiscale Entropy (RMSE) was proposed as a refinement of Multiscale Entropy (MSE) since it offers a way to solve two shortcomings that produce the MSE dependence on variance and on the shape of the power spectrum of the considered series. In this work, RMSE was applied to characterize risk of cardiac mortality (CM) in ischemic cardiomyopathy patients, analyzing HRV by means of RR series of 24h holter-ECG during daytime and nighttime. The end-point was age-matched patients that suffered CM after a follow-up of three years. The study considered 30 patients with CM as high risk group and 192 survivor patients (SV) as low risk group. RMSE approach that takes into account an abroad range of time scales (tau) was based on: a) elimination of the fast temporal scales using antialiasing low-pass filter to focus progressively slower time scales; b) coarse graining procedure necessary to assess entropy rate; c) calculation of the entropy rate that was approximated by sample entropy. RMSE showed statistically significant differences ($p<0.05$) during daytime and nighttime only in middle time scales (tau=4-15). For these scales, RMSE was higher in SV group than in CM group. These indicated a reduction of the entropy-based complexity in high risk group when it was compared with low risk group. No statistical differences between SV and CM groups were presented at time scale tau=1 (unfiltered original RR series). It can be concluded that the dynamics in middle time scales should be considered to better describe the HRV of patients with CM.

Assessing Sympatho-Vagal Balance in Schizophrenia through Tone-Entropy Analysis

Ahsan Habib Khandoker*, Mami Fujibayashi, Toshio Moritani and Marimuthu Palaniswami

S23

Department of Electrical and Electronic Engineering, The University of Melbourne, Parkville, Victoria, Australia

Although schizophrenia patients more likely commit suicide, however, more than two thirds of patients with schizophrenia, compared with approximately one-half in the general population, die of coronary heart disease (CHD). Early screening and treatment of cardiovascular disease risk factors in those patients could prevent the adverse consequences. The aim of this study, therefore, is to determine whether Tone-Entropy (T-E) analysis method can determine how and to what extend the symaptho-vagal balance is altered with the severity of psychiatric disorders as determined by Global Assessment of Functioning (GAF) scale. Tone represents sympatho-vagal balance and entropy, the autonomic regularity activity. This study included 32 high-GAF, 32 low-GAF and 118 healthy control subjects. Evaluated tones [-0.0090$\pm$0.0111 (low-GAF); -0.0156$\pm$0.0173 (high-GAF); -0.0620$\pm$0.0476 (healthy)] and entropies [4.2744 $\pm$0.4205 (low-GAF); 4.8619$\pm$0.3070 (high-GAF); 5.0275$\pm$0.2140 (healthy)] are significantly ($P<0.01$) different among three groups. The curve-linear trend revealed in two-dimensional T-E space plot is consistent with standard T-E values obtained in an experiment of standard perturbations of autonomic function in healthy subjects obtained in our previous study [Khandoker et al, Med Engg & Phys, 32 (2010):161-167]. The significantly higher tone and lower entropy in the low-GAF group might suggest altered sympatho-vagal balance which could predict increasing risks of cardiovascular death.

RSA Component Extraction from Cardiovascular Signals by Combining Adaptive Filtering and PCA Derived Respiration

Suvi Tiinanen*, Antti Kiviniemi, Mikko Tulppo and Tapio Seppänen

Computer science and engineering laboratory, University of Oulu, Finland

S23

Respiratory sinus arrhythmia (RSA) is a phenomenon where heart rate changes synchronously with respiration. In non-laboratory environments and certain measurements protocols respiration rates may, however, alter in both low frequency range (LF, 0.04-0.15Hz) and high frequency range (HF, 0.15-0,4Hz) and thus distort the analysis of sympathetic and parasympathetic activity from the series of heart rate intervals (RRi) and systolic blood pressures (SBP). In addition, other spectrally calculated autonomic nervous system (ANS) indexes such as baroreflex sensitivity (BRS) may be biased due to respiration rate. Methods such as adaptive filtering have been applied to extract the RSA from cardiovascular time series. However, these methods require simultaneously measured respiration signal as a reference. This paper demonstrates how ECG derived surrogate respiration can be used as a reference signal in Least Mean Square (LMS) adaptive filter to extract RSA component from cardiovascular signals. Surrogate respiration signal is obtained by principal component analysis (PCA) applied for QRS complexes. A method minimizing residual energy is used to select an optimal PC component for the surrogate. Data set consists of 20 healthy males who performed spontaneous and controlled breathing at rest. Two cases were analyzed: 1) adaptive filtering with ECG derived surrogate respiration signal and 2) adaptive filtering with measured respiration. Results indicate that one PC is adequate as respiration reference for adaptive filter and that the ECG-based surrogate produces comparable results to the actual respiration signal. As a conclusion, ECG-based respiration surrogate is adequate to extract the RSA component.

New Representation of Heart Rate and Evaluation of Geometric Features Extracted From It

N Jafarnia Dabanloo*, S Moharreri, S Parvaneh, AM Nasrabadi

Islamic Azad University, Science and Research Branch, Tehran, Iran

S23

Heart rate is an indicator of heart's condition. Assessment of heart rate has been shown to aid clinical diagnosis and intervention strategies. It has been proved that nonlinear analysis of it might provide more valuable information for the physiological interpretation of heart rate fluctuations. However, the variety of contradictory reports in this field indicates that there is a need for a more rigorous investigation of methods as aids to clinical evaluation.

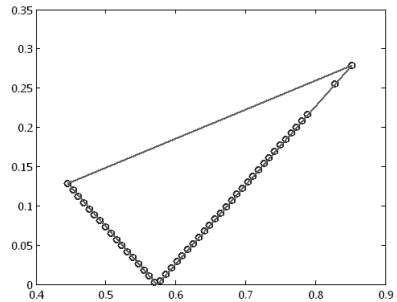

Estimation a triangle for point's distribution in HRV phase space.

In this paper, a novel method for representation of heart rate has been introduced which is obtaining by using RR interval time series signal to plot the Triangle mapping consist of all the ordered pairs: $(RR_i, \text{abs}\,(\overline{RR} - RR_i))$, $i = 1, \ldots, N$ where $\overline{RR}$ is the mean of RR intervals. We obtained a triangle from the distribution of these points and by analyzing it, we could extracted some geometric features which were evaluated in distinguishing four groups of subjects (Arrhythmia, Congestive Heart Failure (CHF), Atrial Fibrillation (AF) and Normal Sinus Rhythm (NSR)) obtained of Physionet database. Kruskal-Wallis test which is a nonparametric version of ANOVA analysis distribution was used to define the level of significance of each feature for different groups of subjects to demonstrate the usefulness of the proposed geometric features in biomedical applications. The results show that these features discriminate arrhythmia from NSR subjects by $p<2E\text{-}4$; CHF from NSR by $p<2E\text{-}3$; AF from NSR by $p<7E\text{-}4$; CHF from arrhythmia by $p<2E\text{-}2$; CHF from AF by $p<6E\text{-}4$; and arrhythmia from AF by $p<2E\text{-}3$.

Another advantage of this triangle mapping is that the points in this map overlapped with each other as a kind of compaction and so this map deletes the extra and useless information and just keeps the useful ones.

So it seems that this kind of mapping may be used as an efficient method for pathology detection.

A Hypotensive Episode Predictor for Intensive Care Based on Heart Rate and Blood Pressure Time Series

Joon Lee* and Roger Mark

Harvard-MIT Division of Health Sciences and Technology, Massachusetts Institute of Technology, Cambridge, MA, United States

In the intensive care unit (ICU), prompt therapeutic intervention to hypotensive episodes (HEs) is critical in order to avoid end-organ damage. In the stressful context of busy ICUs, advance alerts that can prospectively identify patients at increased risk of developing an HE in the next few hours would be of considerable value. Following this rationale, the objective of this study was to develop an automated, artificial neural network HE predictor for binary classification (normotensive vs. hypotensive) based on heart rate and blood pressure time series. Training and test data were compiled from 1,357 adult ICU stay records in the MIMIC II database. As many examples as possible were compiled from each record, provided that their time series quality was satisfactory. The gap between prediction time and the onset of the 30-minute target window was varied from 1 to 4 hours. A 30-minute observation window preceding the prediction time provided input information to the predictor. Various features were extracted from heart rate, mean arterial blood pressure, and pulse pressure time series. Feature space dimensionality was reduced via principal component analysis (PCA). While individual gap sizes were evaluated independently, weighted posterior probabilities based on different gap sizes were also investigated. The results showed that prediction performance degraded as gap size increased, and that the weighted voting scheme induced negligible performance improvement. Low PPVs were attributable to the overwhelming imbalance between the two groups. Overall prediction performance was promising with 1 hour gap, and the best mean area under ROC curve was 0.934. The nature of the data compilation and cross-validation promises similar prediction performance in a real-time clinical trial.

Differences in Non-Invasive Imaging of Atrial and Ventricular Recovery

S24

PM van Dam*, A van Oosterom

Radboud University Medical Center, Nijmegen, the Netherlands

Recently we have reported on progress made in a non-invasive method for imaging the timing of depolarization (*dep*) and repolarization (*rep*) based on observed body surface potentials. The method uses an equivalent double layer at the surface bounding the myocardium having a strength proportional to the local transmembrane potentials. The timing was found by minimizing the difference between observed body surface potentials and those based on the source description. The parameter estimation procedure involved is non-linear and, consequently, requires the specification of an initial estimate. For the timing of depolarization the initial estimate was found by using the fastest route algorithm, for the timing of repolarization the initial estimate additionally took into account electrotonic effects: with longer *ARI* (*ARI* = *rep* - *dep*) values at local minima in the timing of *dep* and shorter ones at locations exhibiting local maxima of *dep*.

We compared the application of the subsequently required regularization procedure, applied to either the timing of regularization, *rep*, or to the *ARI* values, in applications to atria and ventricles. The results are listed in the table shown below.

Ranges (in ms) of *ARI* and *rep* values found by regularizing either of these parameters

Regularized parameter applied to	Atria		Ventricles	
	ARI range	*rep* range	*ARI* range	rep range
ARI	75 - 119	100 - 215	186 - 281	268 - 327
rep	54 - 156	158 - 190	176 - 300	276 - 325

As can be seen, the estimated dispersion in *ARI* values is smaller if the regularization is applied directly to the *ARI* parameters. Those values for the atria are much smaller than those for the ventricles, as is in agreement with large-scale ion-kinetics modelling of the myocardium. Those of the ventricles are larger than those of atria due to the differences in wall thickness, the involvement of the Purkinje system and intrinsic differences of ion kinetics of left and right ventricle. These results indicate that for both the atria and ventricles the *ARI* is the preferred parameter to be regularized.

Integrated Software Toolkit for Solving Bioelectric Field Problems

Rob MacLeod*, Dana Brooks, Mike Steffen, Burak Erem, Darrell Swenson and Jeroen Stinstra

SCI Institute, University of Utah, Salt Lake City, UT, United States

The lack of robust, comprehensive, and integrated software remains a major impediment to the effective use of numerical simulation techniques in both basic cardiology and clinical practice. To be effective, simulations must provide an end-to-end solution, must require minimal tuning of parameters by the user, and must generate subject (patient) specific solutions in an acceptable time frame on realistically available computational resources. We have developed such a system for use in the simulation of bioelectric field problems in electrocardiology. This system consists of a set of software tools that are well coupled and well matched to both the sources of input data and the needs of biomedical scientists, engineers, and physicians. The input to the system is a set of medical images (MRI, CT), which are then segmented using a combination of automated tools and manual intervention. The segmentation then becomes the input for a polynomial mesh generation system, which creates either surface or volume geometric models suitable for computation. In this presentation, we will focus on recent progress specifically in the simulation toolkit that uses the geometric model and applied boundary conditions (measured electric potentials and tissue conductivities) to solve electrocardiographic forward and inverse problems. Within our problem solving environment, SCIRun, we have developed a complete set of open source tools for both boundary element and finite element approaches to both potential and activation-time based electrocardiographic source formulations. With this system, our biomedical and clinical collaborators are able, for example, to predict defibrillation fields from given device and electrode locations, to simulate epicardial and body surface potentials during acute myocardial ischemia from prescribed regions of poor perfusion, and to solve cardiac inverse problems in the setting of ventricular arrhythmias and reentrant tachycardias.

An Iterative Method for Indirectly Solving the Inverse Problem of Electrocardiography

J Pedron*, AM Climent, J Millet and MS Guillem

ITACA, Universidad Politecnica de Valencia, Valencia, Spain

S24

Solution of the inverse problem of electrocardiography is an ill-posed problem and noise sensitive, leading to non-physiological solutions under noise conditions. We propose the use of an indirect iterative method for solving the inverse problem in terms of multiple moving dipoles. A database of surface potentials generated by single dipoles was generated by solving by Boundary Element Method the forward problem in an eccentric spheres model of the human torso. The inverse problem was solved by iteratively searching the combination of surface potentials in our database most similar to the observed surface potentials in terms of their relative difference measure.

Simulated surface potentials generated by dipoles randomly located inside the myocardial wall were used to test the performance of the algorithm. Single dipoles were accurately located in 94% out of 1000 simulations. White noise with different signal to noise ratios (SNR) was added to simulated surface potentials in order to test noise sensitivity. Added noise with SNR down to 6dB allowed accurate location of single dipoles in 90% simulations. Double dipoles were accurately located in 78%, evidencing the effect of crosstalk errors. Noise, however, did not have a major effect on the performance of the algorithm, allowing accurate location of dipoles in 72% simulations in which 6dB noise was added. Computing times were dependent on the database resolution, number of nodes in the outer surface and number of dipoles searched. In either case, the presented iterative algorithm always reduced computing times for an exhaustive search (i.e. 0.35 vs. 369 s for locating a single dipole with a database size of 1632 dipole locations). An iterative algorithm to solve the inverse problem of electrocardiography based on comparison of stored surface potentials to recorded potentials has been implemented. The present method has shown to be accurate, time efficient and robust against noise.

A New Family of Variational-Form-Based Regularizers for Reconstructing Epicardial Potentials from Body-Surface Mapping

Dafang Wang*, Robert Kirby, Rob MacLeod and Chris Johnson

Scientific Computing and Imaging Institute, University of Utah, Salt Lake City, UT, United States

The potential-based inverse electrocardiographic problem aims to noninvasively recover epicardial potentials from body-surface recordings,with the torso volume conductor typically modeled using the finite element or boundary element method. This inverse problem is intrinsically ill-posed and commonly solved by the Tikhonov regularization, where discrete operators are needed to constrain certain properties of the epicardial potentials (amplitude, gradient or curvature). We propose a new family of regularizers within the classic Tikhonov framework, using the continuous basis functions and the variational principle underlying finite element methods. These variational-formed regularizers constitute an alternative to the traditional Tikhonov regularizers, but have four major advantages. First, if the discrete inverse problem is derived from the governing equations by finite element methods, the variational-formed regularizers automatically conform to certain variational principles inherently assumed by the discrete problem. Second, while traditional regularizers consider the discrete Euclidean norm, the variational-formed regularizers consider the L2-norm defined over a continuous domain, independent of discretization resolution, thereby achieving consistent regularization under multi-scale simulations. Third, the variational formulation enables an explicit matrix form of the discrete gradient operator over irregular meshes, which is difficult to obtain from traditional discretization. Fourth, the variational formulation allows simultaneous imposition of multiple constraints efficiently.

We validated the efficacy of the variational formulation through finite element simulations on a phantom experiment involving a live canine heart suspended in a human-torso-shaped electrolytic tank. When the finite element model was undergoing refinement, the variational-formed regularization maintained consistent regularization and improved reconstruction of epicardial potentials, whereas the traditional Tikhonov worsened the reconstruction. The variational-formed gradient regularizer notably outperformed the zero-order Tikhonov. The gradient regularizer also effectively captured epicardial potential features arising from ischemia. These early results suggest that the variational formulation may provide new improvements to the simulation of a broader range of potential-based electrocardiographic inverse problems.

The Effect of Finite Element Mesh Quality on Electrical Bidomain Simulations

Darrell Swenson*, Joshua Levine, Zhisong Fu and Rob MacLeod

Scientific Computing and Imaging Institute, University of Utah, Department of Bioengineering, Salt Lake City, UT, United States

S24

The simulation of electrical activity in the heart, such as normal and abnormal ventricular rhythms and ischemia, utilize computational methods that rely on an underlying geometric model, or polygonal mesh of cardiac tissues and boundaries. Because of the complex shape of many biological structures, it is often difficult to create meshes that conform to the boundaries between distinct regions. The resulting meshes can be non-conformal, ie., they have element faces that do not align with the surface tangents and the elements represent what is a smooth surface as a jagged boundary. We hypothesis that these jagged, non-conformal meshes produce local concentrations of current that lead to artifacts large enough to distort the resulting potential fields and generate misleading results. In simulations of acute ischemia, these artifacts can alter the location and severity of the epicardial elevations and depressions, which, in turn, can impact clinical diagnosis.

We used a bidomain simulation of ischemia to determine the effects of conformal versus non-conformal mesh boundaries on epicardial potentials. Within an anatomically correct heart geometry, we set elliptically shaped ischemic regions with elevated (30 mV) extracellular potentials. The ischemic regions were modeled using both conformal and non-conformal meshes.

Comparisons of epicardial potentials for both conformal and non-conformal meshes showed that when the ischemic region was located within 3 mm of the surface, there was greater than 200% difference in the resulting potential amplitudes. Although error decreased with distance from the epicardium, it always exceed 120%.

These results demonstrate that substantial errors in epicardial potentials from bidomain models can arise from jagged, non-conformal tissue boundaries in geometric models, underscoring the importance of geometric mesh quality in simulations of cardiac fields.

Accuracy of Estimates of Cardiac Action Potential Durations from Extracellular Waveforms Simulated by the Bidomain Model

Simone Scacchi, Piero Colli Franzone, Luca F Pavarino* and Bruno Taccardi

Dept of Mathematics, University of Milano, Milano, Italy

Objectives. Maps depicting the distribution of action potential durations (APD) on epicardial, endocardial and transmural surfaces provide important information for understanding normal and abnormal cardiac electrical activity. The goal of this work is to provide an extensive quantitative analysis of the accuracy level of the cardiac activation - recovery interval (ARI) distributions, obtained from extracellular electrogram markers, in comparison with a gold standard based on transmembrane APD distributions. Both heterogeneous and pathological (ischemic) conditions of the myocardial tissue are considered.

Methods. The analysis is based on large-scale 3D numerical simulations of the anisotropic Bidomain system coupled with the Luo-Rudy I membrane model. Activation and recovery sequences are simulated in myocardial blocks with homogeneous, heterogeneous and ischemic intrinsic cellular properties. ARI maps are determined from activation and repolarization time markers computed from either unipolar electrograms or from an alternative technique based on hybrid monophasic action potentials, obtained as the potential difference between a permanently depolarized site and an exploring site.

Results. The results show that on the whole the extracellular ARI and HMAP distributions considered are reliable and estimate the gold standard APD distributions with low relative mean discrepancies ($<= 2.1\%$) and good correlation coefficients ($>= 0.9$) in tissues with transmural heterogeneity. However, both ARI distributions can yield locally inaccurate APD estimates in regions where the curvature of the repolarization front changes abruptly (e.g near front collisions) or is negligible (e.g. where repolarization proceeds almost uniformly across fibers).

Conclusions. Even though the recovery maps based on extracellular repolarization time markers are very well correlated with maps of transmembrane recovery distributions, the associated ARI maps can have local inaccuracies and be weakly correlated with maps of APD distributions. In particular, both extracellular repolarization time markers generally underestimate the transmural repolarization time dispersion and consequently ARI measures underestimate the transmural APD dispersion.

Susceptibility to Paroxysmal Atrial Fibrillation: A Study using Sinus Rhythm P Wave Parameters

Aline Cabasson*, Lam Dang, Jean-Marc Vesin, Lukas Kappenberger, Roger Abacherli and Remo Leber

ASPG, Ecole Polytechnique Fédérale de Lausanne (EPFL), Lausanne, Switzerland

S31

Whereas many studies have used the signal-averaged P wave, this work aims to determine whether other electrocardiographic characteristics resulting from the analysis of the P wave in ECG recorded during sinus rhythm could be associated with paroxysmal atrial fibrillation susceptibility. Furthermore, the Euclidean distance between beat-to-beat P waves which has been rarely addressed in this context, is studied. The database used includes 42 two-minutes ECG recorded during sinus rhythm. It comprises 30 ECG from healthy male subjects (H group, mean age = 34 $\pm$ 13 years, mean heart rate = 67.5 $\pm$ 12.6 bpm) from the PTB database available in Physionet (sampling frequency 1 kHz) and 12 ECG from male patients subject to paroxysmal atrial fibrillation (PAF group, mean age = 61 $\pm$ 8 years, mean heart rate = 53.2 $\pm$ 7.9 bpm) from the Clinic Im Park in Switzerland (sampling frequency 977 Hz). Preprocessing was applied in order to reduce the noise and baseline wander. Several electrocardiographic characteristics were extracted on lead V1: average values of P width (from the P onset to the end of P) and P-R interval (from the P onset to the R peak) on all beats, and the Euclidean distance between beat-to-beat P waves. Means and standard deviations of each feature were computed for each group. Significant differences between the healthy and the PAF groups were observed on the P width (mean_H = 111.5 $\pm$ 15.8 ms and mean_PAF = 156.2 $\pm$ 26.3 ms; p-value$<$0.0005), on the P-R interval (mean_H = 210.8 $\pm$ 13.2 ms and mean_PAF = 259 $\pm$ 28 ms; p-value$<$0.0005), and on the variance of the Euclidean distance between beat-to-beat P waves (mean_H = 2.42e-2 and mean_PAF = 1.35e-1; p-value$<$0.1). Using P width and P-R interval parameters, the two groups are classified at 90% using Fisher's linear discriminant. In conclusion, the ECG recorded during sinus rhythm provides valuable markers for paroxysmal atrial fibrillation susceptibility, in particular the P width and the P-R interval. Moreover, the beat-to-beat variability of P wave parameters can be useful for this purpose, specially the variance of the Euclidean distance between beat-to-beat P waves. These preliminary results could be helpful in atrial fibrillation prevention.

Patient-Adaptive Ectopic Beat Classification using Active Learning

J Wiens, JV Guttag

Massachusetts Institute of Technology
Cambridge, MA, USA

A major challenge in applying machine learning techniques to the problem of heartbeat classification is dealing effectively with inter-patient differences in electrocardiograms (ECGs). Inter-patient differences create a need for patient-specific classifiers, since there is no *a priori* reason to assume that a classifier trained on data from one patient (or even many patients) will yield useful results when applied to a different patient. Unfortunately, patient-specific classifiers come at a high cost, since they require a labeled training set. Using *active learning*, we show that one can drastically reduce the amount of patient-specific labeled training data required to build a highly accurate patient-specific binary heartbeat classifier for identifying ventricular ectopic beats. Tested on all 48 half-hour ECG recordings from the MIT-BIH Arrhythmia database, our approach achieves an average sensitivity of 96.23% and specificity of 99.97%. The average number of beats needed to train each patient-specific classifier was only 37 beats, approximately 30 seconds of data.

We compare the classification performance of our algorithm to a classifier trained on the first portion of each record. This *passive* selection of the training set is common in the literature. The histogram shows the fraction of each record one must label when the training set is *actively* selected. If instead the training set were passively selected, one would have to label the first 90% of each record, to achieve the same average sensitivity as the proposed method.

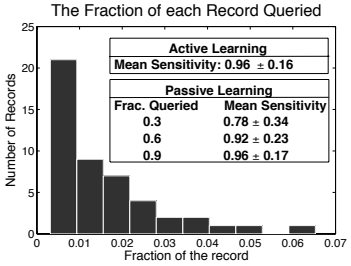

An Automated Algorithm for the Detection of Atrial Fibrillation in the Presence of Paced Rhythms

ED Helfenbein, RE Gregg*, JM Lindauer, SH Zhou

Advanced Algorithm Research Center, Philips Healthcare
Thousand Oaks, CA, USA

S31

Background: 2-5% of 12-lead diagnostic ECGs acquired in hospital are from patients with pacemakers. A significant percentage of these patients are in atrial fibrillation or flutter (AF). Many automated diagnostic algorithms abort analysis when paced rhythms are identified, so do not attempt detection of AF. In the presence of pacing, detection of AF can often be difficult, as there may only be subtle clues due to the pacing artifact and regular rhythm due to pacing. However, identification of AF is quite valuable, since the patient is at higher risk for stroke. The Philips DXL automated diagnostic algorithm contains logic for detection of AF in the presence of paced rhythms.

Method: The algorithm uses QRST subtraction with frequency domain analysis of the residual. A decision tree classifier uses features from the power spectrum, as well as RR irregularity measures from non-paced beats (if present).

A training database was developed containing 355 pacemaker ECG records with 265 presenting AF. The testing database was selected from an initial set of 42,817 sequential ECGs from the emergency department of a teaching hospital. All ECGs classified to have any ventricular pacing (intermittent, continuous, or dual) by the automated algorithm were used to create the testing subset of 1,057 ECGs. In this paced test set, 194 cases (18%) were identified by two expert readers to contain AF.

Results: On the training database of 355 paced ECGs, the algorithm had an AF detection sensitivity of 76%, positive-predictive value of 82%, and specificity of 73%. On the testing set of 1,057 paced ECGs, the algorithm had AF sensitivity of 71%, PPV 83%, and specificity 97%.

Conclusion: Automated detection of AF in the presence of pacing is a clinically important and valuable tool to assist cardiologists in ECG diagnosis, and can be done with a high degree of accuracy.

A Mathematical Model of Atrioventricular Node during Atrial Fibrillation

Valentina DA Corino*, Frida Sandberg, Luca T Mainardi and Leif Sörnmo

Department of Bioengineering, Politecnico di Milano, Milan, Italy

During atrial fibrillation (AF), a high number of atrial impulses bombard the atrioventricular (AV) node, that, acting as a filter, blocks some of them. Some models of the AV node during AF have been proposed, but all of them have certain limitations. The aim of this study is to present an AV node model which can be used on short-term surface ECGs to estimate AV node characteristics. The proposed AV node model is characterized by: the arrival rate of atrial impulses; two different refractory periods, corresponding to dual AV nodal paths; the probability of an atrial impulse choosing either of these pathways; a parameter modeling prolongation of the refractory period due to different physiological reasons. Atrial impulses are assumed to arrive to the AV node according to a Poisson process with a mean arrival rate, estimated by the AF frequency obtained from the surface ECG. Each atrial impulse is supra-threshold, i.e., it results in a ventricular contraction, unless it is blocked. The atrial impulses are blocked at the AV node according to a time dependent probability, which models the prolongation of the refractory period due to relative refractory period and concealed conduction. The smaller functional refractory period is obtained from the lower envelope of the Poincaré plot of the RR series; the other parameters of the model are obtained from the RR series by mean of maximum likelihood estimation. The model was tested on simulated signals (where convergence velocity was assessed) and on ECGs of 33 patients with AF. The average normalized absolute error between the normalized RR histogram and the estimated model probability density function (PDF), computed for bins of 20 ms size spaced between 0 and 2 s, was 0.0023 + 0.0016. These preliminary results are encouraging as AV nodal properties can be noninvasively assessed by a set of statistical parameters with a simple electrophysiological interpretation.

Modulation of ECG Atrial Flutter Wave Amplitude by Heart Motion: A Model-based and a Bedside Estimate

V Jacquemet, B Dubé, P van Dam, AR Leblanc, R Nadeau, M Sturmer, T Kus, A Vinet

Université de Montréal
Montréal, QC, Canada

S31

During atrial arrhythmia, ventricular contraction may modulate the morphology of the atrial contribution to the ECG by moving or constraining atrial geometry. We hypothesized that ventricular contraction induces only small changes in atrial signal amplitude on the thorax. Our aim is to estimate an upper bound for this effect as it could affect the interpretation of QRST cancellation.

Pseudo-orthogonal 3-lead ECG/VCG was recorded during 1 hour at rest in a patient with stable atrial flutter, atrio-ventricular block and a pacemaker programmed to deliver ventricular stimuli at a fixed rate of 40 bpm. Intervals between R waves and flutter waves were uniformly distributed (p=0.28; Kolmogorov-Smirnov test). Under the assumption that atrial signals are amplitude-modulated periodic waves, average beat subtraction eliminates the ventricular contribution to the ECG. Flutter wave amplitudes were extracted from the corrected VCG using min/max filters with window length of one flutter period. These amplitudes were analyzed over three intervals: during the T wave (320 ms), during the U wave (400 ms) and in the subsequent isoelectric interval (400 ms).

Flutter waves were also simulated using a previously-developed atrial model embedded into a time-dependent volume conductor model of the thorax in which atrial geometry was adjusted to MRI data acquired at 50 time instants during normal rhythm (worst-case estimate of geometrical effects).

Average flutter wave VCG magnitude in the three intervals was 309 ± 6 μV vs 308 ± 5 μV vs 314 ± 4 μV in the simulation, and 335 ± 36 μV vs 329 ± 28 μV vs 332 ± 24 μV in clinical data. Although variations of $>10\%$ were observed of some leads, results suggests that heart motion may be neglected for atrial activity cancellation.

Noninvasive Three-dimensional Cardiac Activation Imaging of Ventricular Arrhythmias in the Rabbit

C Han, SM Pogwizd, C Killingsworth, J Yan, B He

University of Minnesota
Minneapolis, MN, USA

Imaging myocardial activation is important for cardiovascular research and clinical medicine. The present study aims to rigorously assess the imaging performance of a physical-model based 3-dimensional cardiac electrical imaging (3-DCEI) approach with the aid of simultaneous 3-D intra-cardiac mapping from up to 200 intramural sites during ventricular arrhythmias induced by norepinephrine (NE) in the rabbit heart.

The physical-model based 3-DCEI approach is developed by modeling 3-D cardiac electrical activities using equivalent current densities (ECDs) and by mathematically solving a spatial-temporal linear inverse problem from body surface potential maps (BSPMs). In this study, BSPMs were obtained simultaneously with intramural bipolar recordings using plunge-needle electrodes in a closed-chest condition in four healthy rabbits. Ventricular arrhythmias including premature ventricular complexes (PVCs) and accelerated idioventricular rhythms (AIVRs) were induced by intravenous NE infusion. Computer tomography (CT) images were obtained after the mapping study for realistic heart-torso geometry models.

The non-invasively imaged activation sequence correlated well with the directly measured counterparts, with an averaged correlation coefficient of 0.73±0.03, and a relative error of 0.31±0.03 over 24 PVCs and 6 runs of AIVRs. The arrhythmia beats initiated by a focal (nonreentrant) mechanism as evident by 3-DCEI. The initiation sites covered both LV and RV, including outflow, apex, lateral, anterior and posterior walls. Sites of initial activation were well localized to within ~5mm for the ectopic beats.

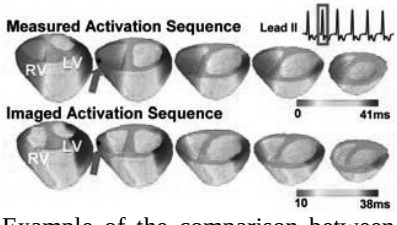

Example of the comparison between the measured and the imaged activation sequence of a ventricular arrhythmia beat in the rabbit heart.

The present result suggests that the 3-DCEI approach can non-invasively reconstruct 3-D ventricular global activation sequence and localize the origin of activation during focal ventricular arrhythmias. It also implies the potential application of 3-DCEI as a clinically useful tool to aid in localizing the origins of ventricular arrhythmias and understanding the mechanism of these arrhythmias.

Respiration Differentially Modulates HRV Obtained from Arterial Pressure Wave and Electrocardiogram

Salvador Carrasco-Sosa and Alejandra Guillén-Mandujano*

Departamento Ciencias de la Salud, Laboratorio de Fisiología Médica, Universidad Autónoma Metropolitana, Mexico City, Mexico

S32

The equivalence between the heart rate variability (HRV) derived from RR and systolic pressure to systolic pressure intervals (SPSP) remains controversial. To address this issue, we assessed the variability of the series resulting from the subtraction of the RR intervals from the SPSP intervals (SPSP-RR) and examined how it is affected by two maneuvers that modify the cardiac autonomic status. From ECG, noninvasive arterial pressure and respiratory movements recorded in 20 healthy subjects the RR, SPSP, SPSP-RR and respiratory series were computed, with a resolution of 0.5 ms, in three 5-min conditions: supine (S), postural change (P) and 100 W exercise (E). High (HF) and low (LF) frequency components were computed from the spectral analysis of the series, performed using the Welch periodogram method, and coherence function was obtained by cross-spectral analysis. While the HF component of SPSP intervals was larger than that of RR intervals in all conditions ($p<0.001$), their LF components were not different ($p>0.05$). In the three conditions power spectra of the SPSP-RR series showed a single component located in the HF band, highly coherent with the respiration spectra as indicated by a coherence of 0.88 ± 0.06. Averages of the HF component of SPSP-RR series were 6 ± 3 ms2, 9 ± 5 ms2 and 8 ± 6 ms2 in S, P y E respectively and were not different between conditions ($p>0.05$). The SPSP-RR HF to RR HF ratio was about 4% in S and P but of 420% during E. Our results indicate that the HRV obtained from RR and SPSP intervals are not equivalent because the respiratory influence is greater in the latter. This effect is clearly evidenced by the SPSP-RR series power spectra, especially during exercise. Moreover, they suggest that the respiratory modulation is produced by a non-neural mechanism, probably exerted mechanically onto the arteries.

Variability of the Systolic and Diastolic Electromechanical Periods in Healthy Subjects

Salvador Carrasco-Sosa and Alejandra Guillén-Mandujano*

Departamento Ciencias de la Salud, Laboratorio de Fisiología Médica, Universidad Autónoma Metropolitana, Mexico City, Mexico

Our aim was to assess: 1) the variability of the systolic and diastolic periods, using as estimators, of the first one, the electromechanical interval measured from the R wave maximum to the systolic peak of the pressure wave (RPre), and of the second, the interval from this pressure to the next R wave (PreR); 2) the effect of two cardiac autonomic activity modifying maneuvers on these estimators. ECG, noninvasive arterial pressure and respiratory movements were recorded from 21 healthy volunteers during three 5-min conditions: supine (S), 0.2Hz controlled breathing (CB) and 100W exercise (E). Spectral analysis of the RR, RPre, PreR and respiration series was performed using the Welch periodogram method to obtain the high (HF) and low (LF) frequency components. During the maneuvers both LF and HF components of PreR changed in parallel with those of RR intervals, but the HF of PreR was slightly greater ($p<0.001$). The HF component of PreR intervals increased from 473 ± 372 ms2 in S to 1854 ± 1263 ms2 ($p<0.001$) in CB and decreased drastically to 2 ± 1ms2 in E ($p<0.001$). In contrast, the maneuvers did not affect the LF component of RPre intervals ($p>0.05$) and had a minimal effect on its HF component, which increased from 3 ± 2ms2 in S to 15 ± 7ms2 in CB and decreased to 1 ± 0.5ms2 in E ($p<0.001$); these averages were very small in relation to those of PreR ($p<0.001$). From the fact that the maneuvers modify in an important and parallel manner both the HF and LF components of the RR and diastolic PreR intervals but not those of the systolic RPre intervals, our findings indicate that the cardiac autonomic modulation is evident in the diastolic period but not in the systolic one. In addition, they suggest that the systolic period is relatively constant, while the diastolic interval shows considerable flexibility.

Gender Related Differences in Scaling Structure of Heart-Rate and Blood-Pressure Variability as Assessed by Detrended Fluctuation Analysis

Paolo Castiglioni* and Marco Di Rienzo

Biomedical Technology Dept, Fondazione Don Gnocchi, Milan, Italy

S32

The fractal structure of heart rate variability (HRV) is traditionally described by two scale coefficients, the short- and the long-term self-similarity exponents, calculated by the Detrended Fluctuation Analysis (DFA) for box sizes shorter and longer than n=12 beats, respectively. Recently we showed, however, that the scale structure of Blood Pressure Variability (BPV) and HRV is better described by a spectrum of scale exponents, the alpha(n) function estimated for each box size n, rather than by the classic two-coefficient model. Aim of our study is to test whether gender may influence the fractal structure of HRV and BPV, as described by the DFA alpha(n) function. We enrolled 32 male (M) and 20 female (F) healthy volunteers matched by age (M:32.0 +7.6 yrs; F:31.1 +10.1 yrs, m+sd, p=0.71). We collected R-R intervals (RRI) from ECG, and systolic (SBP) and diastolic (DBP) finger blood pressures for 10 minutes in supine and sitting positions. For each beat-by-beat series, we calculated alpha(n) for n between 5 and 108 beats as described in (Castiglioni et al, IEEE Trans Biomed Eng. 2009). Alpha(n) spectra of male and female groups were compared separately for the supine and sitting positions (unpaired t-test). While we did not find any gender-related difference in sitting position, we observed significant changes in the alpha(n) patterns in supine positions. Indeed, for SBP, alpha(n) was close to 1 over all the box sizes in the female group, while in males it progressively decreased from 1.16 (at n=5) to 0.80 (at n=108). As to DBP and RRI, alpha(n) was significantly greater in males than in females for $n<8$. These results indicate marked gender differences in the cardiovascular response to the lying position presumably reflecting differences in the autonomic strategy to counteract the blood centralization occurring in clinostatic condition.

Identification of Cardiovascular Baroreflex for Probing Homeostatic Stability

Pedram Ataee*, Jin-Oh Hahn, Guy A Dumont and W Thomas Boyce

Electrical and Computer Engineering, University of British Columbia, Vancouver, BC, Canada

This paper presents a method to identify the cardiovascular baroreflex parameters that are useful for probing homeostatic stability. The work is built upon a physiology-based model of the closed-loop cardiovascular-baroreflex feedback system describing the regulation of heart rate and blood pressure. We propose a reduced-order system identification in which the model parameters having significant influence on the system responses are identified whereas the remaining model parameters are fixed at their typical values.

To this aim, parametric sensitivity analysis is conducted on the model to classify the model parameters into high-sensitivity, low-sensitivity, and invariant (constant within individual) groups based on their relative impacts on the system outputs. The baroreflex identification is formulated as a nonlinear optimization problem in which only high-sensitivity model parameters are identified whereas low-sensitivity and invariant parameters are fixed at their typical values. The possible advantage of the method is its computational efficiency without significant compromise in performance and accuracy.

The feasibility of the proposed strategy was validated using 500 Monte-Carlo system identification trials. Using heart rate, blood pressure and cardiac output measurements, the proposed method was able to accurately estimate high-sensitivity parameters even with low-frequency and invariant parameters fixed at their typical values.

The method was also applied to the experimental data of 10 individuals in the MIMIC Database in the PhysioBank. It was observed that the sympathetic and parasympathetic responses on heart rate and total peripheral resistance estimated by the proposed method were consistent with our a priori knowledge on the behavior of cardiovascular-baroreflex system. Overall, results suggest potential of the proposed method in probing homeostasis based on the estimates of sympathetic and parasympathetic tones. The method may also be useful for a variety of diagnostic applications involving sympathetic and parasympathetic activities.

Heart Rate Variability and Respiratory Sinus Arrhythmia Assessment of Affective States by Bivariate Autoregressive Spectral Analysis

Valentina Magagnin*, Maurizio Mauri, Pietro Cipresso, Luca T Mainardi, Emery N Brown, Sergio Cerutti, Marco Villamira and Riccardo Barbieri

Istituto Ortopedico IRCCS Galeazzi, Milano, Italy

S32

The impact of computational devices in modern everyday life has raised an increasing interest on the study of emotions elicited by human-computer interactions. Our motivating research hypothesis is that an automated system for affective states detection can rely on non-invasive acquisition and processing of biological signals, such as the Electrocardiogram and Respiration. In this study we evaluate the autonomic nervous system response and the mechanical and autonomic effect of respiration on heart rate during PC-mediated stimuli eliciting targeted affective states. To this extent, we use multivariate autoregressive (AR) spectral methods to estimate standard heart rate variability (HRV) measures, as well as the interaction between R-R interval and respiration time series, a measure of respiratory sinus arrhythmia (RSA). We further assess significance of the linear cardio-respiratory coupling by use of surrogate series. A group of 35 young healthy volunteers is considered. Each subject was monitored during four experimental conditions: Baseline (stare at a white screen, 3 minutes), Relaxation (sequence of panoramas, 10 minutes), Stress (perform a Stroop task, 4 minutes), and Engagement (read a detective tale, 10-15 minutes). In order to account for possible effects due to the sequential order of the emotion-induced conditions, the sample was split into two groups: half of the subjects (RES group) were exposed to Engagement before Stress, the other half (RSE group) to Stress before Engagement. Resulting HRV measures clearly separate the autonomic nervous system response among all three conditions. Of note, less significant differences are found between Engagement and Stress in the RSE group, suggesting that Stress stimuli may cause a lasting response possibly affecting the following Engagement period. Results from bivariate analysis further indicate a substantial disruption of the cardio-respiratory coupling during non-relaxing conditions, as corroborated by significantly lower levels of coherence (although still above the surrogate zero threshold) and RSA gain.

Derived Respiration: Comparison and New Measures for Respiratory Variability

Devy Widjaja*, Joachim Taelman, Steven Vandeput, Marijke Braeken, RA Otte, Bea Van den Bergh and Sabine Van Huffel

Department of Electrical Engineering, Katholieke Universiteit Leuven, Leuven, Belgium

Respiration can be measured in different ways, by using impedance sensors, pressure sensors or just by a thermistor in the nose. However, respiration can often also be extracted from the pure ECG signal having the advantage that no extra equipment is needed. This study first examines which ECG derived respiration (EDR) method is the most accurate.

Simple ECG filtering, R or RS amplitude based techniques and information in QRS areas are compared with each other. Data of simultaneously recorded ECG and respiration during a stress test were obtained for this analysis. The mean-squared error (MSE) quantified the difference between the obtained breath-to-breath intervals of the EDR signals and the actual respiratory signal. The R peak amplitude (MSE = 0.63) and the RS amplitude (MSE = 0.72) gave the best approximation and have the advantage over the filtered ECG (MSE = 1.53) and QRS areas (MSE = 2.15) that even sighs can be detected.

In a second part of the study, this R peak amplitude based respiration signal is now used to investigate respiratory variability (RV). Analogously to HRV, some new measures (rMSSD, SDSD, pNN1 and pNN2) for breath-to-breath interval analysis are proposed. These parameters were applied on data coming from a 25 minute stress test, being 5 minutes of rest alternated with 5 minutes of arithmetic tasks. These new measures showed that RV was significantly lower during rest than during arithmetic tasks. Also, significant differences were found between the first resting period and the 5 minutes following the arithmetic tasks. The standard deviation of successive differences (SDSD) also managed to differentiate between the 2 arithmetic tasks ($p < 0.01$).

To conclude, breath-to-breath intervals can be extracted accurately based on the R peak amplitude in the ECG and new efficient measures for respiratory variability are proposed.

Measurement of the Aortic Pulse Wave Velocity in MRI: Comparison of Transit Time Estimators

A Dogui, N Kachenoura, M Lefort, A Cesare, F Frouin, E Mousseaux, A Herment*

INSERM U678 UPMC, Paris, France

S33

Introduction. The aortic pulse wave velocity (PWV) is calculated as the ratio between the distance separating two aortic locations and the transit time (Δt) needed for the flow wave to cover this distance. While the distance can be accurately estimated from MR Cine images, the determination of Δt from Phase Contrast (PC) acquisitions remains more difficult. The aim of this study was to describe a new method (MSeg) for Δt estimation and to compare it with three previously described methods (MUpslope, MFoot, MPoint), in terms of correlation with aging and reproducibility.

Methods. We studied forty volunteers (42±15 year) who had cine and PC acquisitions at the level of the aortic arch. The 3D length of the aortic arch was calculated from axial and coronal acquisitions. Δt was defined as the time shift between the flow curves of the ascending (CA) and descending (CD) aorta and calculated with: 1) MSeg by minimizing the area delimited by two sigmoid curves fitted to the systolic up-slope of CA and CD, 2) MUpslope by minimizing the area between the systolic up-slope of CA and the CD curve, 3) MFoot using CA and CD feet, 4) MPoint using the half maximum of CA and CD.

Results. PWV linearly increased with aging: results of Pearson coefficient (r) and PWV values are summarized in the following table. Transit time estimation by two operators introduced a variability of 6.04% (MSeg), 7.13% (MUpslope), 6.62% (MFoot), and 6.67% (MPoint).

Results of Pearson coefficient of the linear regression and Mean ± SD of PWV

		Mean ± SD PWV (m/s)		
Methods of Δt estimation	r of the linear regression	All subjects (n=40)	Subjects <40 years (n=21)	Subjects≥40 years (n=19)
MSeg	0.85	4.53±1.29	3.82±0.6	5.33±1.41
MUpslope	0.85	4.6±1.4	3.86±0.69	5.42±1.55
MFoot	0.65	4.72±1.53	4±1.27	5.53±1.41
MPoint	0.76	4.97±1.52	4.32±0.99	5.69±1.7

Conclusion. All Δt estimators provided the expected trend of PWV according to aging. However, MSeg resulted in a better correlation with aging, higher reproducibility, and less overlap between the <40 and ≥40 years groups.

Feasibility of a Novel Approach for 3D Mitral Valve Quantification from Magnetic Resonance Images

Maffessanti F, Stevanella M, Votta E, Lombardi M, Parodi O, De Marchi D, Conti CA, Redaelli A, Caiani EG

Department of Biomedical Engineeing, Politecnico di Milano
Milan, Italy

Mitral annulus (MA) assessment is of great importance for the diagnosis and treatment of mitral valve (MV) disease. Standard CMR image acquisition allows to obtain only a limited number of measurements. We propose a different way to study the MV by multiple CMR long-axis cine images, followed by 3D reconstruction and quantification. Our aim was to test the reproducibility of this approach.

CMR cine imaging of 18 long-axis planes (55 frames/cardiac cycle; spatial resolution: 0.78 mm; slice thickness: 8mm), rotated every 10° along the left ventricular long-axis, was performed in 12 patients with myocardial infarction. Custom software was used for MV quantitative analysis (Figure): 1) in the end-diastolic (ED) and end-systolic (ES) frames, in each plane, the position of the MA annulus and papillary muscles (PM) tips were manually identified; 2) the MA geometry and PM position were automatically reconstructed in a 3D space; 3) several parameters were then computed: MA perimeter, antero-posterior and intercommissural diameters, MA height, MA 3D and projected area, the angle between PM, the distance from PM to the MA. To assess the reproducibility of the procedure, two operators repeated the analysis: the inter-operator variability was evaluated as the coefficient of variation (CV(%)=100*SD/mean).

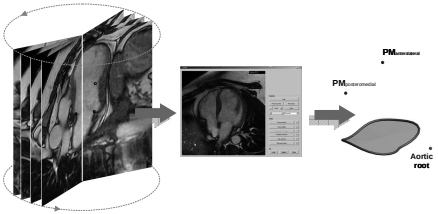

Schematic of the workflow

Analysis of MA was feasible in all patients, showing good inter-operator agreement for MA perimeter (CV_{ED}=1.9%; CV_{ES}=1.8%), antero-posterior (CV_{ED}=3.0%; CV_{ES}=5.8%) and intercommissural diameters (CV_{ED}=1.8%; CV_{ES}=2.0%), 3D (CV_{ED}=3.4%; CV_{ES}=4.3%) and projected areas (CV_{ED}=2.8%; CV_{ES}=3.7%), and the distance from PM and MA (CV_{ED}=4.1%; CV_{ES}=4.6%). MA height (CV_{ED}=9.9%; CV_{ES}=16.1%) and the angle between PM (CV_{ED}=6.8%; CV_{ES}=10.6%) were less reproducible, in particular at ES.

Quantitative information on MA and PM morphology and function is feasible from CMR imaging n multiple long-axis planes. The proposed approach is highly reproducible and could constitute the basis for in-depth evaluation of the MV and for the planning of surgical procedures.

Rigid Registration of Delayed-Enhancement and Cine Cardiac MR Images using 3D Normalized Mutual Information

Yasmina Chenoune*, Constantin Constantinides, Racha El Berbari, Elodie Roullot, Frédérique Frouin, Alain Herment and Elie Mousseaux

LIF, Inserm UMR 678, UPMC, Paris, France

S33

Delayed-Enhancement Cardiac MRI (DE-CMRI) is nowadays the imaging technique of choice for visualizing and quantifying the myocardial infarction extent. In clinical routine, segmental evaluation of myocardial gadolinium uptake in infarcted zones is visually performed by blinded observers. However, the hyperenhancement causes a loss of contrast between myocardium and ventricular cavity, making difficult myocardial contours delineation and accurate image interpretation. In this paper, we propose a method to take advantage of the good contrast of Cardiac MR Images (Cine-CMRI) to resolve this difficulty. First, epicardium and endocardium contours of the left ventricular cavity were automatically segmented from breath-hold Cine-CMRI, which present high intensity contrast between muscle and cavity. The obtained contours were then superimposed on DE images, acquired in a second breath-hold, to localize the hyperenhancement information obtained from the DE-CMRI on the Cine-CMRI corresponding images. A global spatiotemporal alignment was performed to correct spatial misalignment resulting from potential patient movement between the two acquisitions and to temporally synchronize DE and Cine images. An automated rigid registration method which uses the maximization of 3D Normalized Mutual Information (NMI) was developed to locally register the cardiac images. This method was applied to 3D data, acquired through short-axis views, from the apex to the base of the heart. Ten patients with proven myocardial infarction were studied and for each patient, three different DE-CMRI exams, obtained at 5, 6 and 7 minutes after contrast agent injection were processed. The registration accuracy evaluation was qualitatively performed by superimposing segmented endocardic and epicardic contours on DE images and quantitatively using the Sum-of-Squared intensity Differences (SSD). The proposed rigid registration method showed high-quality alignment results for more than 92 % of the processed data, with a mean displacement value of 2.66 ± 2.45 mm in the short-axis plane and inter-slice maximal displacement value of 9 mm.

Atrial Tissue Response to Radio Frequency Ablation: MRI Based Characterization of Injury

Joshua Blauer*, Joshua Cates, Nassir Marrouche and Rob MacLeod

CARMA center, University of Utah, Salt Lake City, UT, United States

Introduction

Atrial fibrillation (AF) can be treated via percutaneous catheter ablation. However, when ablation does fail the cause can be difficult to determine. Recent advances in late gadolinium enhanced (LGE) MR imaging can aid the assessment of ablation induced lesions non-invasively. To capitalize on the information available in these images, lesions must be accurately detected and displayed in a manner that will allow interpretation of lesion extent and continuity. Our group and others have found that mapping the 3D MRI data onto a surface model of the left atrium (LA) provides an intuitive visualization for clinical interpretation. However, detection of ablation injury has largely depended on pixel intensity thresholding strategies that do not account well for noise and are subject to the arbitrary selection of thresholds. We sought to generalize the detection of scar by characterizing the shape of profiles transverse to the LA tissue in the LGE-MRI images.

Methods

The LA endocardial border was defined in 3 LGE-MRI scans acquired 3 months post ablation. These segmentations were used to generate triangulated surface models of the LA in the MRI coordinate space. A line profile of the LA tissue was generated at each node of the models by sampling the MRI at regularly space intervals orthogonal to the surface (+/- 4 mm). Additionally, an experienced reader manually segmented regions of scar in the LA wall. Applying Principal Component Analysis (PCA), we projected each profile onto the first and second components in order to identify those profiles that crossed regions of scar.

Results and Discussion

The projection of profiles onto the first PCA component showed a significant difference ($p < 0.05$) between scar profiles and the entire population of profiles. Early evidence indicates that PCA of line profiles can effectively categorize scar and normal tissue.

Reproducible Evaluation of Diastolic Function Using Phase-Contrast Magnetic Resonance Data

E Bollache*, A Redheuil, S Clément-Guinaudeau, C Defrance, L Perdrix, M Ladouceur, M Lefort, A De Cesare, F Frouin, A Herment, B Diebold, E Mousseaux, N Kachenoura

INSERM U678/UPMC, Paris, France

S33

Left ventricular diastolic dysfunction is an early sign of heart failure; thus, its early detection is crucial for patients management. Its clinical estimation is currently performed using Doppler echocardiography, which allows estimating conventional diastolic parameters based on blood flow and myocardial velocities. Despite recent developments in trough-plane velocity-encoded Magnetic Resonance (MR) using phase-contrast (PC) imaging, MR evaluation of diastolic function in clinical routine is not established yet. Accordingly, our aim was to provide a robust, fast and reproducible technique to estimate diastolic parameters from PC MR images.

We studied 40 healthy volunteers (23 women, 17 men, age: 33 ± 12 years), who had a transmitral flow and a mitral annulus longitudinal velocity sequences. To analyze these data, we developed a semi-automated segmentation process based on: 1) pixels connectivity, in terms of velocity sign, for the transmitral and aortic flows, and 2) a k-means clustering of the myocardial velocity profiles. Diastolic parameters were automatically extracted from velocity and flow rate curves. For variability evaluation, the segmentation, as well as the curves analysis, were achieved by two operators on a sub-group of 20 subjects.

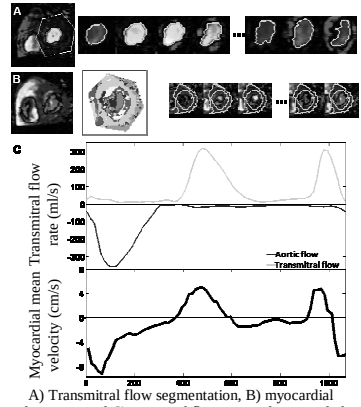

A) Transmitral flow segmentation, B) myocardial clustering, and C) extracted flow rate and myocardial velocity curves

The flows segmentation was reproducible as reflected by a mean percentage of overlap between the two segmentations of 99.5 ± 2.1%, resulting in a slight functional parameters variability (<3.7%). For tissue maximal velocities, the inter-operator variability was 2.4 ± 3.2%. Furthermore, our conventional parameters were consistent with echographic literature and our new flow rate-related parameters were well related to those with a high prognostic value.

A reproducible and robust method was proposed and successfully tested on 40 subjects in terms of inter-operator variability and consistency of the derived diastolic parameters. The addition of such developments to MR tools may prove clinically useful.

Comparison of Aortic Lumen Area and Distensibility using Cine and Phase Contrast Acquisitions

Alain Herment*, Muriel Lefort, Alain de Cesare, Nadjia Kachenoura, Frédérique Frouin and Elie Mousseaux

U678, Inserm, Paris, France

Introduction Aortic distensibility is calculated as (Ss-Sd)/Sd/dP, where Ss and Sd are the systolic and diastolic lumen areas and dP the pulse pressure. To assess distensibility values obtained from Cine and Phase Contrast (PC) sequences, we first implemented an automatic segmentation method and validated it against experts manual contouring of the lumen. Then, the distensibility values obtained for both Cine and PC sequences were compared.

Material and methods Data were acquired using a thoracic section perpendicular to both ascending and descending aorta at the level of the pulmonary artery bifurcation. The brachial pressure was recorded simultaneously in the magnet. To test the segmentation algorithm, PC aorta sections (860) were collected from 12 datasets acquired on three different (1.5T and 3T) scanners. Then, data from 50 subjects acquired on a GE Signa-Excite scanner were used to compare Cine and PC distensibility values in the ascending aorta.

Results The mean and worst Dice overlap measures were $0.945\pm$ 0.014 and 0.84, respectively. The manual intra- and inter- and the automated inter-operator variabilities were $8.43\pm6.58\%$, $10.09\pm8.29\%$ and $0.59\pm0.92\%$, respectively. Slope (a), offset (b) and Pearsons coefficient (r) of the linear regression and, mean (m) and standard deviation (SD) of the Bland Altman test were respectively: a=0.95, b=0.35 cm2, r=0.96, m=0.03 cm2, SD=0.66 cm2 when comparing PC lumen areas to Cine lumen areas; and a=0.47, b=1.27 1000mmHg-1, r=0.57, m=-1.07 1000mmHg-1, SD=2.01 1000mmHg-1 when comparing PC distensibility to Cine distensibility. The average values of distensibility obtained with Cine (4.42 1000mmHg-1) were higher than for PC sequences (3.34 1000mmHg-1), but both appeared quite consistent with those previously presented in the literature.

Conclusion Despite very similar Cine and PC estimations of the aortic area lumen, derived distensibility values in the ascending aorta appeared larger using Cine sequences.

The Effect of the Shape of Ischemic Regions in the Heart on the Resulting Extracellular Epicardial Potential Distributions

Josef Peter Barnes* and Peter Rex Johnston

Griffith University, Australia

S34

Recently, computer simulations have been used to model the electrical behaviour of ischemia in the heart in an attempt to better understand the processes involved and increase accuracy in patient diagnosis. The vast majority of these studies assume ischemia progresses from the endocardium towards the epicardium and the ischemic region is rectangular in shape. The presence of sharp edges in these models has been found to play a significant role in the determination of ST segment epicardial potential distributions, with current loops forming around the sharp edges. This numerical study looks at ischemic geometries in which some or all of these sharp edges are removed and how this affects the resulting extracellular epicardial potentials during the ST segment. The two key ischemic region geometries studied are cylindrical and semi-ellipsoidal in shape.

Using a simple anisotropic model for the cardiac geometry and realistic conductivity values, results for the rectangular ischemic shape show a central depression over the ischemic region which separates into three depressions (one centred over the ischemic region and two on its lateral borders) as the ischemic thickness is increased. For ischemic thicknesses above 70%, elevation appears over the ischemic region which increases in magnitude as the ischemia becomes transmural. The cylindrical ischemic shape gives almost identical results due to the continued presence of similar current loops as in the rectangular model. Results from the semi-ellipsoidal shape, however, differ from the previous results for medium thicknesses of ischemia (30%-70%), with the central depression separating into only two depressions as the thickness increases. Elevation again occurs over the ischemic region when the ischemic thickness is above 70%. Here the potential distributions are quantitatively similar to the other shapes.

This study therefore shows that epicardial potential distributions depend both on the thickness of the ischemic region and its shape.

Re-Entry in a Model of Ischaemic Human Ventricular Tissue

Richard Clayton*

Department of Computer Science, University of Sheffield, Sheffield, United Kingdom

BACKGROUND: Ventricular fibrillation in the human heart generally induces global ischaemia, and so the aim of this study was to understand how ischaemia modulates the stability and period of re-entry in models of human ventricular tissue. METHODS: Tissue simulations used a monodomain model with a diffusion coefficient of 1.171 cm2/ms. Membrane excitability was described using the 2006 version of the TNNP model for human ventricular cells, with parameters set to give steep APD restitution and unstable re-entry. To simulate ischaemia, extracellular K+ concentration was increased from a normal value of 5.4 mM to 7.0 and 8.0 mM, maximum L type Ca2+ channel conductance decreased to 90% and 80% of its default level, and an ATP dependent K+ current was activated with intracellular ATP concentrations reduced from a normal value of 6.8 mM to 5.5 and 5.0 mM. Action potential duration (APD) and conduction velocity (CV) restitution were measured with an S1S2 protocol in thin 2D strips of simulated tissue, and the stability of re-entry was assessed in a square domain representing a 25 x 25 cm 2D sheet. RESULTS: Increasing extracellular K+ concentration to 8.0 mM reduced the minimum diastolic interval supporting S2 propagation from 380 to 340 ms, and reduced CV from 64 to 49 cm/s. Changes in maximal L type Ca2+ channel conductance and intracellular ATP led to modest changes in APD and CV. Combining these changes resulted in flatter APD and CV restitution curves in simulated ischaemic tissue. Re-entry was unstable in simulated normal tissue with a period varying between 300 and 230 ms, but stable in simulated ischaemic tissue with a period of around 400 ms. Simulated ischaemic tissue with extracellular K+ set to 8.0 mM converted unstable re-entry to re-entry, but simulated ischaemic tissue with extracellular K+ set to 7.0 mM did not. CONCLUSION: In these models, simulated ischaemia acted to flatten APD and CV restitution, reduced CV and increased the period of re-entry, but did not always result in the conversion of unstable re-entry to stable re-entry. The characteristics of fibrillation in normal and globally ischaemic ventricular tissue are likely to be different.

Simulation of ECG under Ischemic Condition in Human Ventricular Tissue

Weigang Lu, Kuanquan Wang* and Henggui Zhang

Harbin Institute of Technology, China, and University of Manchester, United Kingdom

S34

Myocardial ischemia is the foremost precursor of cardiac arrhythmias, which is caused by reduced coronary blood flow to the heart. However, the functional effects of ischemia-induced electrical properties of cardiac cells on ventricular electrical wave conduction have not been fully understood yet. In this study, to simulate ischemic effects, we developed a human ventricular cell and tissue models, which take into account three main pathophysiological consequences of ischemia: elevated extracellular potassium ([K+]o), acidosis, and anoxia. An ATP sensitive K+ current (IKATP) formulated by Ferrero et al. was adapted in the models. Using the model, we first simulated action potentials of endocardial, midmyocardial and epicardial cells with acute ischemic condition and measured respective action potential duration (APD90). Then we quantified the effects of ischemia on the waveform of ECG, particularly on ST segment depression or elevation by using a 2D model of human left ventricular tissue based on the anatomical structure of the human heart. In the ventricular tissue model, different transitional border zones mimicking the heterogeneity created by acute myocardial ischemia were considered. Effects of variation in local ischemic site and size in epicardial, transmural and endocardial regions were modeled respectively. At cell level, simulations showed that under acute ischemic condition, the resting membrane potential was elevated, and the APD was abbreviated by about 15 22% in endocardial cells, 16% 25% in midmyocardial cells and 14% 21% in epicardial cells. At tissue level, ischemia produced a depressed ST segment and change in the profile of ECG. The larger the size of the ischemic region, the more dramatic the changes in the amplitude of ST and T-wave were observed. With transmural ischemia, a double T-wave was formed. These simulation results matched to clinical data. Our model can be successfully implemented to simulate the electrical activity of human ventricular tissue affected by myocardial ischemia.

M-cell Heterogeneity Influence in Arrhythmic Pattern Formation in Sub-Epicardial Regional Ischemia: A Simulation Study

Oscar Alberto Henao Gallo, Carlos Alberto Ruiz Villa* and Jose Maria Ferrero de LomaOsorio

Physiology Group, Technological University of Pereira, Pereira, Risaralda, Colombia

Ventricular arrhythmias and myocardial ischemia are inseparable. The occurrence of lethal arrhythmia was related with myocardial injury, alterations of ionic conductance and metabolite concentrations. Ischemia altered in differential form the wall heterogeneity, the epicardium and M cell is more affected that endocardium. In this computational study, we calculate the vulnerability of reentry during different stages of regional sub-epicardial ischemia in dissimilar islands configurations of M cell intro the cardiac wall (Antzelevitchs Hypothesis). For this purpose, a modified version of the Luo-Rudy model (2000) was used to simulate cardiac action potentials. The main components of ischemia (hypoxia, acidosis and hyperkalemia) were considered in the model. The tissue comprises 150x300 cells, which include different islands of M cells up to 55% tissue area, 20% for epicardial cells and the rest of endocardial zone. An S1-S1 stimulation protocol was used, and the vulnerable window (VW) for re-entry was quantified for different degrees of acute ischemia. We show that re-entrant pattern arise in the tissue after an extrastimulus is delivered. The wavefront invade virtual tissue through the epicardial zone. The core of re-entrant front remains within the central ischemic zone. The value of the VW, measured as the window of coupling intervals which elicit re-entry, is dependent on the degree of ischemia and the distribution of M cell clusters. Under conditions which mimiqued the first 8.0 minutes of ischemia, VW=5 milliseconds (ms). The VW reached 10 ms the 8.25 minute, increasing to 18 ms at the 8.5 minute, and further to 28 ms in t=8.75 minutes, this values of VW are means in different distributions of M cell. The VW abruptly decreases to zero in the ninth minute. In conclusion, the model predicts that the VW for re-entry has a logistic behaviour during sub-epicardial ischemia, with re-entry paths comprising midmyocardial islands of tissue.

Mechano-Electric Feedback Effects in a Ventricular Myocyte Model Subjected to Dynamic Changes in Mechanical Load

Ivan Cenci*, Stefano Morotti, Jorge Negroni, Blanca Rodríguez and Stefano Severi

Computing Laboratory, University of Oxford, Oxford, UK

S34

The effect of mechano-electric coupling on myocytes action potential (AP) has been largely studied considering constant stretches. This study examined the role of mechano-electric feedback (MEF) in a more physiologic setting, in which sarcomere length varies following cardiac work loops (WLs) and affects the stretch-modulated currents (Ism) in real time. A model of mammalian myocyte contraction was incorporated into a complete mathematical description of AP, ionic currents and Ca2+ transient of the guinea pig ventricular cell. In addition, the effect of myocytes strain on stretch-modulated channels was implemented by integrating a modified version of the MEF model proposed by Gurev et al. This new coupled model simulates the four phases of the cardiac cycle as a sequence of isometric and isotonic contractions/relaxations. Intracellular Ca2+ controls contraction and half sarcomere length (Lm) is used as input to MEF, that in turn affects the AP through Ism. Simulations were conducted to investigate the role of MEF in modulating electrical activity during WL for different length preloads and force afterloads. Results were in agreement with experimental WL and MEF studies. Moreover, considering varying resting half sarcomere length (Lmo), our simulations showed that under basal conditions (Lmo=0.855 micrometers), Ism activation during the WL has a limited impact on AP. However a progressive increase in the strain sensed by Ism, induced by decreasing Lmo, results in DADs during WL phase 4 (Lmo=0.75 micrometers), ectopic activations (Lmo=0.70 micrometers) and triggered activity (Lmo=0.68 micrometers). To our knowledge, our model is the first to integrate cardiac cell electrophysiology and mechanics with physiological details such as ionic membrane currents, intracellular Ca2+ handling, cross-bridge formation and WL implementation. On the base of simulation results, it can be asserted that the generation of arrhythmogenic phenomena could arise when the strength of the MEF is increased, as under heavy myocardium stress conditions.

Sarcoplasmic Reticulum Luminal [Ca^{2+}] Regulates the Spontaneous Ca^{2+} Release Events and Consequently Arrhythmia

Luyao Lu, Ling Xia, Xiuwei Zhu

Department of Biomedical Engineering, Zhejiang University, Hangzhou 310027, China

The intracellular Ca^{2+} release from sarcoplasmic reticulum (SR) provides the major Ca^{2+} source required in cardiac excitation-contraction coupling. The important role that SR luminal Ca^{2+} concentration plays in regulating ryanodine receptors (RyRs) has been demonstrated by many experimental observations. However, the precise relationships between the Ca^{2+} loading status of SR and intracellular Ca^{2+} dynamics as well as electrophysiological characteristic are not completely clear.

In this paper, we developed a multi-scale mathematical model by coupling a two-dimensional spatially Ca^{2+} reaction-diffusion model with an action potential model of the ventricular myocyte. The proposed multi-scale model was applied to study the effects of changes in SR Ca^{2+} content on subcellular spatiotemporal Ca^{2+} cycling, and on the possible membrane potential changes caused by aberrant Ca^{2+} release events. The simulation results showed that 1) the spontaneous sparks increased when SR Ca^{2+} content was elevated in a diastolic myocyte, and vice versa, which suggested a positive regulating effect of SR luminal [Ca^{2+}] on Ca^{2+} release; 2) under the conditions that SR Ca^{2+} was overloaded, spontaneous Ca^{2+} sparks and waves might also occur without any external stimulus, and 3) once formed, the propagation of Ca^{2+} waves was accelerated as the SR Ca^{2+} content increased. Moreover, those spontaneously occurred Ca^{2+} release events elevated cytoplasmic $[Ca^{2+}]_i$ and then activated Na^{+}-Ca^{2+} exchange current that depolarized the sarcolemma transiently, which might cause a delayed afterdepolarization (DAD).

These findings suggest that regulation of RyRs by SR luminal [Ca^{2+}] plays an important role in formation and propagation of Ca^{2+} waves and consequently heart arrhythmia with overloaded SR Ca^{2+} content.

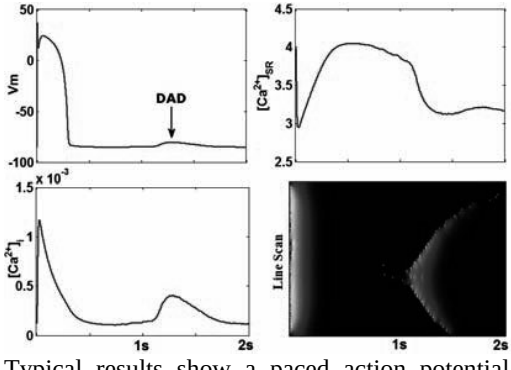

Typical results show a paced action potential, followed by a spontaneously Ca wave which causes a DAD when SR Ca^{2+} was overloaded.

Impedimetric Point-of-Care Cardiac Marker System

Eyad Hamad*, Paul Maguire and James McLaughlin

Nanotechnology and Integrated Bioengineering Centre (NIBEC),
University of Ulster, Newtownabbey, Antrim, United Kingdom

S41

The requirement for fast identification, with accurate and reliable diagnostics for acute myocardial infarction has generated what can be called Point-of-Care (POC) devices. POC is a developed technology; providing diagnosis and analysis of clinical measurement at the patients bedside [1]. Using just a few drops of blood in such a device can lead to an accurate diagnosis [2] within minutes. Additionally, it may avoid a fatal situation [3]. This work describes the development and characterisation of a novel electrical impedance spectroscopy (EIS) immunosensor for application in point-of-care cardiac marker detection. EIS is a sensitive, label-free, real time technique however, the underlying source of the observed EIS response is poorly characterised. A full understanding of the relationship between target binding and impedance response could significantly improve both detection limits and sensitivity. The development of micro-structured interdigitated electrodes (IDEs) for multi-frequency EIS offers advantages over traditional macro-structured systems leading to the generation of knowledge on similar length scales to that of the bio-recognition components. Figure 1. Real-time detection of Ab-Ag interaction at 130 Hz. (50 ng/mL of antigen was injected each 2 minutes) In this work, we use interdigitated electrodes (IDEs) as EIS platform for monitoring the cardiac enzyme in real-time, our results showed evidences of detection within less than 2 minutes . This detection based on antibody-antigen interaction onto the IDEs surface. Immunosensors were constructed by immobilising myoglobin antibodies onto the surface of the IDEs via alkanethiol SAM. The response related to antigen binding was monitored at a fixed frequency 130 Hz. As a result, improved signal-to-noise ratios were obtained affording greater sensitivity, low detection limits (ng.mL-1) and fast detection times. Ongoing research aims to develop EIS IDE arrays to achieve point-of-care cardiac enzyme detection within less than 5 minutes. We anticipate this will have high impact in the diagnosis of cardiac events and allow faster delivery of emergency medical care.

Hybrid Edge Detection for Real-time Kalman Filter Based Left Ventricle Tracking in 3D+T Echocardiography

Engin Dikici* and Fredrik Orderud

Faculty of Medicine, Norwegian University of Science and Technology, Trondheim, Norway

Endocardial border segmentation in 3D echocardiography is a challenging problem, since the trabeculated structure of the endocardium leads to intensity profiles that change over the cardiac cycle. This study introduces a novel Max Flow/Min Cut based edge detector (MFMC), and its combined usage with an existing step edge detector (STEP) for improving edge detection throughout the cardiac cycle.

The real-time left ventricular tracking framework uses an extended Kalman filter to recursively predict and update a deformable subdivision surface, based on a combination of edge measurements and a kinematic model. Edge detection is performed using normal-displacement measurements in sampled intensity profiles, and are processed using an information-filter formulation of the Kalman filter. For a given set of intensity profiles, MFMC based normal displacements are found as; (1) a graph is formulated where each voxel of each profile is represented by a node, (2) edges are set between consequential voxels within the same profile and, the neighboring profiles same-index voxels, with weights inversely proportional to the intensity gradients, (3) nodes corresponding to innermost and outermost profile voxels are connected to source/sink super-nodes respectively, (4) The minimal cut corresponding to maximum flow between source/sink is used to determine MFMC normal-displacements. Since MFMC solves the normal-displacement problem simultaneously for all profiles, results are smooth and consistent. Also, MFMCs low-order polynomial computational complexity does not threaten real-time tracking.

MFMC outperforms STEP for endocardial border detection at end-diastole (ED), while STEP works best at end-systole (ES). A hybrid method based on a weighted sum of MFMC and STEP, where the weight factors are set based on mesh size, outperforms both pure MFMC and STEP.

10 manually segmented 3D echocardiograms are used for validation. For ED, surface errors are, Hybrid: 2.50$\pm$1.61(mm), STEP: 3.07$\pm$1.93(mm), MFMC: 2.62$\pm$1.58(mm). For ES, Hybrid: 3.02$\pm$1.70(mm), STEP: 3.11$\pm$1,82(mm), MFMC: 3.70$\pm$1.81(mm). For ejection fraction, the percentage errors are, Hybrid: 3.83$\pm$5.88(%), STEP: 6.29$\pm$7.15(%), MFMC: 8.36$\pm$5.97(%).

Application of Novel Mapping for Heart Rate Phase Space and Its Role in Cardiac Arrhythmia Diagnosis

N Jafarnia Dabanloo*, S Moharreri, S Parvaneh, AM Nasrabadi

Islamic Azad University, Science and Research Branch, Tehran, Iran

S41

The nonlinear analysis of Heart Rate Variability (HRV) is a valuable tool in both clinical practice and physiological research reflecting the ability of the cardiovascular system. Poincare plot is a geometrical representation of RR time series to demonstrate patterns of heart rate dynamics resulting from nonlinear processes.

In this paper, by using Poincare plot points we introduced a novel mapping for heart rate phase space which consists of all the ordered pairs: $(RR_i, \quad (\overline{RR} - RR_{i+1})^2)$, $i = 1, \dots, N-1$ where $\overline{RR}$ is the mean of RR intervals. By analyzing the point's distribution in this new map, we could estimate a two degree polynomial equation in the form of $y = Ax^2 + Bx + C$ in which y is $(\overline{RR} - RR_{i+1})^2$ and x is RR_i. The useful features obtaining of this map are the coefficients *A*, *B*, and *C*. For evaluating them, we try to distinguish three groups of subjects using the Physionet database (Arrhythmia, Congestive Heart Failure (CHF), and Atrial Fibrillation (AF)) with Normal Sinus Rhythm (NSR). Kruskal-Wallis test was used to define the level of significance of each feature for different groups of subjects to demonstrate the usefulness of the proposed method in cardiac arrhythmia diagnosis. The results show that these features discriminate CHF from NSR subjects by $p<E\text{-}4$; arrhythmia from NSR by $p<E\text{-}5$; and AF from NSR by $p<E\text{-}5$.

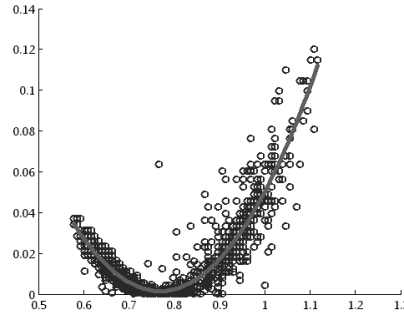

Estimation of a quadratic equation for point's distribution in HRV phase space.

In this novel method, we have used the function between current data of time series and the following one. Hence, it seems that this kind of mapping and the resulted quadratic equation has the capability of being used as a prediction method for some kinds of cardiac arrhythmia. So this method would be evaluated in most cases and compared with clinical results to detect its more advantages in cardiac arrhythmia diagnosis.

ECG-based Indices of Poincaré Plot Asymmetry Differ between Different Types of Athletic Training

Hans Esperer*, Martin Oehler, Chris Esperer and René Schwesig

Internal Medicine - Cardiology, Otto-von-Guericke University Magdeburg, Germany

Heart rate varability (HRV) is a promising technique to evaluate the effects of physical training (PT) on the cardiac autonomic nervous system. However, traditional HRV methods have produced contradictory results. We hypothesized that, at the elite level, novel ECG-based indices of Poincaré plot (PoP) asymmetry would significantly differ between different PT types. 36 male elite athletes aged 23 ± 5 years with a training history of 2 years of running (R, n=12), or triathlon (T, n=12), or cycling (C, n=12), and 12 age- matched untrained controls (Co), underwent 24-hour ECG monitoring. The following PoP asymmetry indices were determined: (1) relative frequency of episodes of sudden increases in cycle lenghth (SIC); (2) relative frequency of episodes of sudden decreases in cycle length (SDC); (3) decay rate of SIC duration (lambda_SIC), and (4) decay rate of SDC duration (lambda_SDC). The SIC-related indices served as measures of left-sided, and the SDC-related indices of right-sided asymmetry regarding the PoPs bisector. SIC(%)was smallest in C differing significantly ($p< 0.01$) with both R and T. SDC(%)did not differ between PT groups. Whereas lambda_SIC differed significantly ($p<0.01$) between R and C, lamba_SDC differed significantly ($p<0.05$) between R and T. Of note, each PT group differed significantly ($p< 0.001$) with contols regarding all the asymmetry indices investigated. In conclusion, different types of PT induce different effects on heart rate dynamics, and the novel PoP asymmetry indices allow for differentiation of PT types. This may be important as to the design of high performance PT.

Dynamic Terminology Enhancement for Integrated ECG Resources

Alexandra Kokkinaki*, Ioanna Chouvarda and Nicos Maglaveras

Lab of Medical Informatics, The Medical School, Aristotle University of Thessaloniki, Thessaloniki, Greece

S42

Public Biosignal Resources, containing signals and annotations, can serve an important role in biomedical research and education, provided that an appropriate framework allows for population, querying and data/metadata access of these resources. In this paper, we present Dynamic Terminology Enhancement Method (DTEM) to support enrichment and extensibility in a biosignal integration system called ROISES (Research Oriented Integration System for ECG signals), which integrates diversely encoded ECG signals and the corresponding annotation and metadata. The DTEM method manipulates the ontological structure of the system whose taxonomy is based on UMLS and ecgML, to dynamically enhance its terminology from the newly added sources. The method is performed in two successive steps. The first step investigates the suitability of the term to constitute a class in the ontologys hierarchy, by comparing it with UMLS Metathesaurus terms. To perform the comparison, the system engages Support Vector Machines and employs semantic and syntactic measures based on UMLS characteristics. The second step determines the most suitable point in the ontologys taxonomy to place the previously selected terms. The method constructs a vector whose elements constitute similarity indices of the terms UMLS ancestor hierarchy list compared to the required ontology, and adopts decision tree algorithms to decide upon the most suitable hierarchy to be subsumed by the ontology. DTEM was applied to ROISES to support the extensibility of its schema. In the first step, the testing dataset contained a set of medical terms originating from medication, medication categories and free text entries for medical history, not present in the global ontology. The procedure resulted in 98.6% sensitivity and 77.7% specificity and classified the suitable from the inapt classes. The second step trained a decision tree with a dataset of ancestor hierarchies related to the previously acquired terms. The testing procedure resulted in 100% sensitivity and 96.0% specificity.

EcgRuleML: A Rule-Based Markup Language for Describing Diagnostic ECG Criteria

Raymond Robert Bond*, Dewar Darren Finlay, Chris Desmond Nugent and George Moore

School of Computing and Mathematics, University of Ulster, Belfast, Antrim, United Kingdom

Computerized interpretation of the ECG is usually carried out in a black box. That is, the rules used to make the decisions are not immediately accessible to the clinician. This is due to the fact that expert systems are built by a knowledge engineer who develops rules from the clinicians description of ECG criteria and compiles them into unreadable machine code. In this study we propose the ECG Rule Markup Language (ecgRuleML) as a way to externalize decision rules used to interpret the ECG.

EcgRuleML uses the eXtensible Markup Language (XML) to provide a framework for articulating quantitative rules for measuring intervals, segments, widths, peaks, heart rate and the cardiac axis. A structure has also been set in place for articulating calculative rules, e.g. if the S wave in V1 + R wave in V5 is more than 35mm then LVH. Abstract rules such as a slurred S wave can be articulated using codes.

In this study, ecgRuleML has been used to define rules to assess ST Elevation Myocardial Infarction (STEMI) in a Lux-192 Body Surface Potential Map (BSPM). An algorithm has been integrated into a BSPM viewer where the rules have been parsed from an ecgRuleML file and executed in 63ms (mean from 10 trials) on a PC (3GHz CPU, 3GB RAM).

EcgRuleML provides a means to encapsulate rules readable to both the computer and the human. Its external nature means that identical rules can be managed and shared amongst different systems and research communities. In this regard, it promotes standardization and avoids duplication of work. Further development will involve the design of an interface where clinicians can graphically define rules, which are automatically converted into the ecgRuleML format for use in a decision support system. This work will give clinicians more control and trust over computerized decision making.

iCARDEA - an Approach to Reducing Human Workload in Cardiovascular Implantable Electronic Device Follow-Ups

Maohua Yang, Christian Lüpkes*, Asuman Dogac, Mustafa Yuksel, Fulya Tunçer, Tuncay Namli, Manuela Plößnig, Jürgen Ulbts and Marco Eichelberg

R&D Division Health, OFFIS, Oldenburg, Germany

S42

More than 800,000 patients in Europe have an implanted cardiovascular implantable electronic device (CIED) today, causing 5.8 million follow-up visits for patients per year, and both numbers are quickly rising. This calls for new methods of long-term surveillance with a view to optimizing patient safety and care, alleviating the burden of caregivers, and lowering health care costs through IT support. The iCARDEA Project aims at developing an intelligent platform to semi-automate the follow-up of CIED patients using adaptable computer interpretable clinical guideline models. For this purpose, data from hospitals electronic health records (EHR), from patient maintained personal health records (PHR) and the CIED device readouts themselves, provided by the remote monitoring services offered by all major vendors for the current generation of devices, are collected and correlated. The CIED data is provided in or converted into a vendor independent standard format (based on the IHE Implantable Device Cardiac Observation Profile), and EHR and PHR data are converted to HL7 Clinical Document Architecture (CDA) format. This permits CIEDs from multiple vendors as well as different health record systems to be connected to the iCARDEA system. The PHR component furthermore enables patients to take an active role in the management of their own healthcare. Patients can manage their medication summaries, dietary information, prescriptions, etc. through the system and receive educational information and feedback. Furthermore, the correlated data from all sources is presented to the caregivers in an intelligent way to reduce the workload. The data presented is enriched by automatically generated patient-specific warnings and suggestions based on statistically valid patterns extracted using state-of-the-art data analysis techniques applied to reference case knowledge bases. The article describes the approach and system architecture of this project, which has started in February 2010.

Interoperability Challenges in the Health Management of Patients with Implantable Defibrillators

Catherine Chronaki*, Manuela Plößnig, Mustafa Yuksel, Gokce Banu Laleci Eturkmen, Christian Lüpkes, Marco Eichenberg, Xavier Navarro, Wolfgang Pecho and Asuman Dogac

Institute of Computer Science, FORTH, Heraklion, Crete, Greece

An increasing number of patients make the choice to accept an Implantable Cardioverter-Defibrillator (ICD) to alleviate the risk of life-threatening conditions such as dangerous arrhythmias, sudden death, heart failure, etc. Technology empowered patients and their families access online educational resources, maintain Personal Health Records (PHRs), engage in social networking relating to their condition, use wireless activity and lifestyle monitoring devices. Electronic Health Records (EHRs) and decision support tools assist cardiologists in follow-up of ICD patients typically 3 times per year based on current clinical guidelines. Recent CIED models support remote monitoring and clinical trials show reduction of in-office visits and improved quality of care. The CIED device transfers data on the health status of the device and the patient to proprietary vendor databases. The attending cardiologist may receive alerts and remotely access the vendors database to review the patients and devices health status. In this paper we report on current status of relevant interoperability initiatives. IHE is working on the (Implantable Device Cardiac Observation) IDCO profile, using HL7 and ISO/IEEE11073 standards including the Rosetta Terminology mapping to facilitate interoperability at the device level. Other IHE profiles address EHRs to leverage provider data (e.g. diagnostic examinations, lab results, progress reports) and PHRs to capture activity and lifestyle data. Continua Health Alliance works on interoperability guidelines for personal health devices. However, a widely acceptable solution for ECG interoperability is still not available despite the efforts of the OpenECG network. The iCARDEA (An Intelligent Platform for Personalized Remote Monitoring of the Cardiac Patients with Electronic Implant Devices) project has engaged a multidisciplinary group in addressing this challenge offering automated computer interpretable personalized guidelines based on PHR, EHR, and ICD data as a Decision Support tool for cardiologists hoping to improve quality of life of ICD patients in a secure, unobtrusive and transparent way.

MRI to X-ray Fluoroscopy Overlay for Guidance of Cardiac Resynchronization Therapy Procedures

YingLiang Ma*, Simon Duckett*, Anoop Shetty*, C. Aldo Rinaldi†, Tobias Schaeffter* and Kawal S. Rhode*

*Division of Imaging Science, King's College London, UK
† Department of cardiology, Guy's and St Thomas' Hospitals, UK

S43

Cardiac resynchronization therapy (CRT) can be an effective procedure for patients with heart failure but 30% of patients do not respond. This may be partially caused by the sub-optimal placement of the left ventricular lead.

We demonstrate how pre-procedural cardiac MR images can be used to assist CRT by integration of anatomical and functional information with live X-ray images. We evaluated our approach in 7 patients. Each patient underwent pre-CRT MRI (Philips 1.5T Achieva) using MultiHance contrast. This included whole heart imaging using a cardiac and respiratory gated bSSFP sequence; 3D tagged and cine imaging for function; and late enhancement imaging for scar.

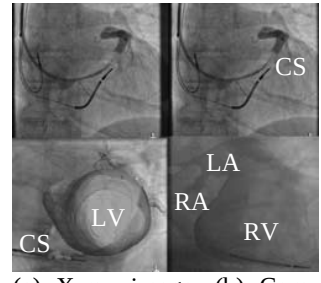

(a) X-ray image. (b) Coronary venous overlay. (c) 16 segment AHA model. (d) Complete anatomical model.

The MRI data were processed to yield a detailed anatomical model. Whole heart segmentation was achieved automatically using the Philips EP Planner and the coronary venous anatomy was manually segmented by a clinical expert. Functional information was derived using the Tomtec 4D LV-Analysis. The left ventricle was segmented into the standard 16 segment AHA model and the functional information could be added to this. If scar was present, this was segmented by an expert and added to the model.

The implant was carried out using a Philips Allura X-ray system and the detailed cardiac model was registered to the X-ray fluoroscopy using multiple views of a catheter looped in the right atrium. There was complete freedom of movement of the X-ray system and respiratory motion compensation was achieved by tracking the diaphragm. The software framework was a specially modified version of the Philips EP Navigator.

We validated the registration using balloon occlusion coronary venograms. The mean 2D target registration error for 7 patients was 1.3±0.68mm. Furthermore, left lead deployment was successful in all patients.

In conclusion, we demonstrate a complete software/workflow solution for guidance of CRT by using pre-procedural MRI data combined with live X-ray fluoroscopy.

Automatic Quantification of Oedema from T2 Weighted CMR Image using Hybrid Thresholding Oedema Sizing Algorithm

Kushsairy Kadir*, Alex Payne, John J Soraghan and Colin Berry

Dept of Electronic and Electrical Engineering/Centre for Excellence in Signal and Image Processing(CeSIP), University of Strathcylde, Glasgow, United Kingdom

Oedema is fluid retention within the myocardial tissue due to damage tissue causing swelling in the affected area after myocardial infarction (MI). Thus quantification of oedema area after an MI is an important step in medical diagnosis to differentiate between viable and death myocardial tissue. A novel automatic quantification of oedema is proposed in this work. It is based on hybrid thresholding where image morphological operation is combined with statistical thresholding to classify oedema tissue. First an image morphology opening operation is first performed to remove the spurious small positive bright object on the myocardial wall. Next the mean value of the normal tissue is estimated by the maximum value of the lower part of the intensity profile of the image. Threshold value is then calculated as a 2 standard deviation (SD) above the mean value. The segmented oedema is then further processed to remove any disjointed false positive bright region by labelling all segmented region and removing any region area below a certain threshold which is empirically determined. Once the segmentation of the oedema has been achieved additional post processing step is applied to take into account of dark pixel region that may account for microvascular obstruction (MVO). An iterative dilation operation is performed to joint the remaining oedema area and finally remaining isolated dark pixel is analysed to identify potential MVO. Each dark region is classified as MVO if the border is completely encompassed by oedema pixel. The method is then applied to cardiac magnetic resonance (CMR) images of eight patients, for each patient between nine to twelve slices of T2 weighted MR image were acquired. All short axis images were used except for the extreme basal and apical slices. The result for oedema quantification is very encouraging with correlation score of 81.1% when compare to manual segmentation.

Comparison of the Data Derived from Three-dimensional Reconstruction of Coronary Angiography and the Fractional Flow Reserve Measurements

Balazs Tar, Peter Lugosi, Janos Santa, Tamas Ungvári, Sandor Ember and Zsolt Koszegi*

Invasive Cardiology Laboratory, Jósa A. County Hospital, Nyíregyháza, Hungary

S43

The measurement of the fractional flow reserve (FFR) of intermediate coronary lesions is reasonable because the uncertainty of the hemodynamic information of the conventional coronary angiography. Our aim was to compare the data calculated from the 3D reconstruction of a given stenosis with the FFR values measured on the same coronary segment. 22 patients (age : 61 ± 9.73 years) were evaluated by the IC30 software of the Axiom Artis X-ray machine. 3D reconstruction was successfully carried out on 23 coronary arteries (14 LAD, 4 CX, 5 RCA). Regression analysis demonstrated significant relationship between the cross-sectional area percentage stenosis (AS) calculated based on the 3D measurement and the FFR (r : -0.566, p: 0.008), as well as between the 3 D derived plaque volume(PV) and the FFR (r : -0.501, p: 0.018). On the other hand, the diameter stenosis (DS) and the mean lumen diameter (MLD) did not correlate with the FFR values. The correlation between the 3 D derived MLA and the FFR did not reach the significant level, either. According to the Receiver Operating Characteristic (ROC) analysis the rank of the areas under the ROC curves (AUC) were the following: 1. PV (0.76), 2. AS (0.74), 3. DS (0.62), 4. MLA (0.55), 5. MLD (0.51).The difference between the AUC of the PV and MLA was found to be significant (p=0.02). The best agreement with the FFR was found when the PV was $> 44\%$ (sensitivity 66.67 %, specificity 82.35) and the 3D AS was $>60\%$ (sensitivity 100%, specificity 47 %). Quantification of the intermediate coronary artery stenoses in 3D provides more precise evaluation of the hemodynamic significance. In our opinion beside the 3D AS, the calculated PV characterizing the entire lesion is also an important predictor of the flow consequence of the stenosis.

Abilities of Cardiac MSCT Imaging to Provide Useful Anatomical and Functional Information for Cardiac Resynchronization Therapy Optimization

Mireille Garreau*, Marie-Paule Garcia, François Tavard, Antoine Simon, Julien Fleureau, Dominique Boulmier, Pascal Haigron, Christine Toumoulin and Christophe Leclercq

LTSI, INSERM - Université de Rennes 1, Rennes, France

A main limit of biventricular Cardiac Resynchronization Therapy (CRT) is the high rate of non-responder (30%). Improvement in patient selection and device implantation strategy may reduce this rate. A challenging task to carry out remains both the identification of the most effective pacing sites and the left ventricular lead positioning (by a venous access). This paper aims to show how cardiac Multislice-CT (MSCT) imaging, from only one exam, can be helpful for the clinician to analyse venous system and cardiac function before the device implantation. 4D CT data have been analyzed in order to extract global and local left ventricle (LV) function and coronary vein anatomy. The proposed process is decomposed in four steps: (1) the 3D tracking of coronary veins based on minimum-cost path computation and on fast-marching technique; (2) the 3D extraction of the LV along the cardiac cycle by using a fuzzy connectedness algorithm, providing a surface mesh representation and volume variation along the cycle; (3) the cardiac LV motion estimation based on a multi-resolution surface matching method, giving access to functional parameters associated to anatomical segments (e.g. radial and longitudinal motion components); (4) the fusion of extracted data with adapted modes of visualization such as 3D dynamic and color-coded surfaces and synthetic bull-eye representations combining anatomical (LV endocardium and veins) and functional (endocardium motion) descriptions. Although the three first parts of this process have been presented in earlier works, the integration of the overall set of available information with adapted modes of visualization may represent an advance towards the optimal use of MSCT imaging in CRT planning. This approach has been tested on three patients. Results show that combined anatomical and functional information, concerning in particular the characterization of the venous network and the LV most delayed region, are of high interest for CRT optimization.

Effect of Physiological Changes in Heart Rate Turbulence using a Lumped Parameter Model

Óscar Barquero-Pérez, Inmaculada Mora-Jiménez, Rebeca Goya-Esteban, Julio Ramiro-Bargueño, Arcadi García-Alberola and José Luis Rojo-Álvarez*

Signal Theory and Communications, Universidad Rey Juan Carlos, Fuenlabrada, Madrid, Spain

S44

Heart Rate Turbulence (HRT) is a strong risk stratification criterion in patients with cardiac disorders. Several physiological factors affect HRT, e.g, heart rate, circadian rhythm, prematurity. However, the relationship between these factors and HRT still needs to be further clarified. We propose to use a modified version of a detailed lumped parameter model, capable of handling the generation of ectopic beats and the subsequent hemodynamic regulation, to study the relationship between different physiological factors and the HRT. We started from the detailed model of cardiac regulation previously developed by Ursino and Magosso. Unlike previous models using time-counters and electrical description, we modified ventricle activation function phi [1 maximum contraction, 0 complete relaxation], in order to generate the hemodynamic effect of ectopic beats. We described the ectopic beat with three parameters: complementary prematurity CP (percentage of the original rr-interval), maximum contraction (MC), and systole duration (Tsys, sec).

In order to characterize the relationship between the HRT and phi parameters, we computed TS and TO parameters for three different combinations among them: (1)MC=0.5, Tsys = 0.3 sec, and CP=[10,20,30,40,50]%; (2)MC = 0.5, P=20%, and Tsys = [0.1, 0.2, 0.3, 0.4, 0.5]; (3)Tsys=0.3, P=20%, MC=[0.1, 0.2, 0.3, 0.4, 0.5, 0.6, 0.7]. HRT was reduced as CP increased: TS=[75.3, 72.4, 70.6, 69.8, 68.9]ms/beat, and TO=[-22.8, -21.3, -20, -18.9, -17.9]. Increasing Tsys yielded a reduction in HRT pattern: TS=[89.0, 79.4, 72.4, 67.3, 64.2]ms/beat, and TO=[-26.1, -23.4, -21.3, -19.7, -18.4]. Finally, increasing MC of the ventricle activation also yielded a reduction in HRT pattern: TS=[104.1, 106.4, 100.1, 86.2, 72.4, 60.6, 51.1]ms/beat, and TO=[-30.4, -30.2, -28.2, -24.6, -21.3, -18.4, -15.9]. Nevertheless, a general trend could be observed to TS and TO being slightly larger than those reported in the literature. Relationships between different physiological factors and HRT can be analyzed by using a detailed lumper parameter model of cardiac regulation, by including the hemodynamic effect of ectopic beats. Changes in prematurity, systole duration and contraction, modify the resulting HRT pattern. This issue should be taken into account when quantifying it by TS and TO parameters.

Assessment of Coupling and Correlation between Cerebral Autoregulation and Baroreflex in Stroke Patients

Ben-Yi Liau*, Shoou-jeng Yeh and Chuang-Chien Chiu

Department of Biomedical Engineering, Hung Kuang University, Taichung, Taiwan

Stroke, one of the cardiovascular diseases, has been the leading causes of mortality in Taiwan, even in the world for decades. According to previous research, the causes of cardiovascular diseases are highly related to the change of physiological parameters. Stroke can be resulted from unstable cerebral blood flow due to the cerebral autoregulation (CA) and baroreflex mechanisms being unable to work in effect. CA and baroreflex are important mechanisms for protection in human body. However, the relationship or function between CA and baroreflex is not clear in the past studies. Therefore, if the related physiological parameters cab be monitored as well to make the coupling between CA and baroreflex clear, it would be helpful for diagnosing of stroke in clinical practice. The main purpose of this research is to integrate the analysis of blood pressure, cerebral blood flow and heart rate to evaluate coupling effect. There are 10 stroke patients (56 ± 10.6 years) included in this study. Results of blood pressure and cerebral blow velocity values in stroke are lower than those in healthy persons ($p<0.05$). Low frequency power of blood pressure and cere-bral flow velocity are also decreased more than those in healthy subjects ($p<0.05$), it might be the effect of sympathetic nerve system. K2 means chaoticness. K2 values of cerebral flow velocity and mean heart rate in stroke subjects are higher than those in healthy subjects significantly ($p<0.05$), it might indicate cerebral flow and heart rate in stroke are more chaotic. The values of baroreflex sensitivity in healthy subjects are also higher significant ($p<0.05$). The values of independence of complexity and predictability of blood pressure, cerebral flow and heart rate between 0 and 1 indicate they are highly coupled. Therefore, if the correlation of blood pressure, cerebral flow and heart rate can be observed simultaneously, and the coupling degree of cerebral autoregulation and baroreflex can be investigated, the effect of diag-nosis of cardiovascular diseases can be improved.

Joint Order Pattern Analysis to Asses Baroreflex Coupling of SBP and PI Series in Rats

[1]T Loncar-Turukalo, [2]S Milutinovic, [2]N Japundzic Zigon, [1]D Bajic

[1]Faculty of Technical Sciences, University of Novi Sad,Serbia
[2]School of Medicine, University of Belgrade, Serbia

S44

INTRODUCTION: Insight in complex heart rate (HR) and blood pressure (BP) interactions reveals important aspects of baroreceptor reflex (BRR) control of short-term BP fluctuations. The symbolic method of order pattern analysis is enhanced to represent BP and pulse interval (PI) joint dynamics within four consecutive heart beats. The synchronization between source, SBP (systolic) series and target, PI series was assessed using probability density function (pdf) of permutations /transcriptions/ which map SBP changes into PI responses. The deviation of transcription pdf from uniform pdf was measured by Kullback-Leibler divergence (KLD).

EXPERIMENT: The BRR loop was opened at different levels using pharmacological blockade of β-adrenergic (by prazosine), α-adrenergic (by metoprolol) and M-cholinergic (by atropine) receptors. Experiments were done in conscious telemetred Wistar out bred male rats.

METHOD: The stationary time series of SBP and PI of length 1024 were preprocessed to remove respiration induced variability. The symbolization procedure is shown in Fig.1. The symbol associated with four consecutive samples is vector of their rank-ordered indices, yielding 4! different patterns. The permutations mapping SBP into PI symbolic words were analyzed and the presence of higher order permutations was evaluated reflecting dissimilarity between the source and target symbols. KLD was calculated for different time-delays between SBP and PI series, in order to evaluate the time-delay from change in SBP to BRR mediated PI response.

RESULTS: The pdf of transcription changes clearly reveals the increase of higher order transcriptions in open BRR loop (Fig.2), revealing more dissimilarity and random like behavior. KL divergence in control protocol reached maxima 0.22 for delay of 3, 4 and 5 beats between SBP and PI. KLD gradually decreases in opened BRR loop to 0.05 due to β-adrenergic blockade and 0.02 due to α-adrenergic and M-cholinergic blockade. Besides, KLD dependence on time delay was lost in open BRR loop.

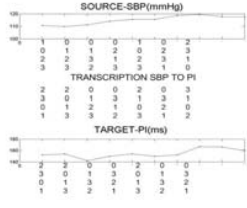

Fig.1

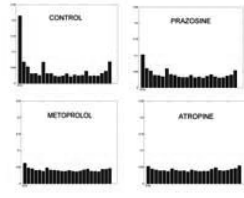

Fig.2

Electrocardiography and Repolarization Abnormalities: Benefits and Limitations of Fully Automated Methods for QT Measurement

Paul Kligfield*

Weill Cornell Medical College, Cornell University, New York, NY, United States

During early phase trials of new drug safety in humans, prolongation of the rate-corrected QT interval has become a surrogate marker for heterogeneity of ventricular repolarization that can cause potentially fatal arrhythmic events. Thorough QT studies have been designed to test for clinically significant QT prolongation by the new drug in comparison with placebo, using a positive control such as moxifloxacin in addition to demonstrate adequate test sensitivity of the method used for QT determination. Measurement of QT may be done manually, automatically, or by adjudication of selected automated samples. Although full automation of QT measurement might lead to cost-effective benefits, several important problems limit the fully automated evaluation of QT. Variability and ambiguity of T wave morphology when repolarization becomes abnormal limits precision of QT measurement by all methods. Automated measurement of QT is improving, but in the absence of a universally accepted ECG definition of the end of the T wave, QT measurements have become proprietary engineering solutions that differ among ECG core labs and among algorithm developers. Significant differences of QT measurements occur between different single ECG leads, between single leads and global intervals of duration (from the earliest onset in any lead to the latest offset in any lead), and between and within different generations of automated algorithms in digital electrocardiographs from different manufacturers. Looking toward the future, it should be appreciated that prolongation of the unidimensional QT duration is not necessarily equivalent to complex heterogeneity of repolarization, and we are likely to move beyond evaluation of the QT interval alone as a marker of arrhythmogenicity. Alternative measures of repolarization such as T wave symmetry, T wave notching, and PCA of the T wave loop might further increase the benefit of fully automated ECG algorithms in drug safety testing.

Intracardiac Electrophysiology: Cellular Modelling of Abnormal Repolarisation

Blanca Rodríguez*

Computing Laboratory, University of Oxford, Oxford, United Kingdom

M5

Abnormalities in cardiac repolarization have been implicated in cardiac arrhythmogenesis caused by disease, mutations and drugs. Of particular concern for regulatory agencies, pharmaceutical industry and society is the fact that certain drugs, in particular those not designed to affect the heart, can exhibit cardio-toxicity (i.e. unwanted side effects), which can put patients with otherwise healthy hearts at risk of developing lethal arrhythmias. Drug cardiotoxicity is often related to abnormalities in repolarization caused by drug-induced alterations at the ionic level. Given the limitations of in vitro and in vivo testing in preclinical prediction of drug cardiotoxicity, there is increasing interest in computational methods to complement experimental findings. This presentation will describe the state-of-the-art in computational cardiac electrophysiology and how this technology can be used to investigate the mechanisms of cardiac electrophysiological function and the implications of abnormalities in repolarization, from the ionic to the ECG level. Our main aim is to unravel the mechanisms of drug-induced arrhythmic risk in the context of high inter-subject electrophysiological variability, and to propose novel arrhythmic risk biomarkers based on this research.

Cardiovascular Computer Devices: Balancing Novelty, Flexibility, Familiarity and Safety

Alan Murray*

Cardiovascular Physics & Engineering Research Group, Freeman Hospital and Newcastle University, Newcastle upon Tyne, United Kingdom

Without cardiovascular devices the success of modern medicine would be poorer and many lives now saved would be lost. Many devices now rely on computers, either in their standard recognisable format, or hidden in devices ready to run at the push of a button and without any need to load or start a program. This invasion by computing into cardiology has brought with it many advantages. Diagnoses and treatments not possible several years ago are now indispensible. The ability to introduce novelty, user flexibility and diversity, as well the clear presentation of results has reaped many advantages.

Nevertheless, computers have brought with them problems, many of which have a direct bearing on patient safety. In the UK the National Patient Safety Agency collates all reports of medical safety incidents in the UK, and the Medicines and Healthcare products Regulatory Agency (MHRA) deals with incidents specifically involving medical devices. Most other countries have similar bodies. In their latest report the MHRA indicated that there had been over 8000 UK device incidents in the previous year, of which over 1000 involved a serious injury and over 200 a death. Of the total incidents, 12% were life support and 3% imaging.

Specific computer problems can relate to the device not behaving as planned in the design, either because the device was not correctly programmed, or unexpected conditions appeared, or because of external interference or other influences. Also, clinical staff can often use devices in unintended ways, either because the functions were not clear, or because staff became lost in the many layers of user interaction. Versatility is not always a positive feature. There is much that can be learnt, either as a clinical user, developer or manufacturer of cardiovascular computer devices by reviewing safe design.

Cardiac Computer Imaging: Intravascular Ultrasound and MRI Studies

Nico Bruining*

Thoraxcenter, Erasmus MC, Rotterdam, Netherlands

M5

During the past 20 years, great progress has been made in the diagnosis and treatment of cardiovascular diseases in which imaging plays an important role. It is used for diagnosis, during treatment (intervention) and to help in evaluating new therapeutic strategies. Where in the early days only invasive angiography was available, today there is a whole array of imaging modalities to choose from - both invasive as well non-invasive.

One of the major breakthroughs in the treatment of acute coronary problems was the development of coronary angioplasty (PTCA), later followed by the implantation of permanent metallic stents to avoid acute lumen narrowing after PTCA. Today, these stents are coated with drugs to avoid the problem of scar tissue growth within the stents. The latest development is the bioabsorbable stent, which is designed to be absorbed after having done its healing job. To evaluate the safety and efficacy of these new treatment methods, intravascular ultrasound (IVUS) and optical coherence tomography (OCT) are used in addition to angiography. Both are invasive catheter-based modalities which can visualize coronary artery disease in great detail. The availability of computer-assisted software allows the use of these imaging modalities to quantify the effects of the treatment methods.

However, a follow-up angiogram is a major inconvenience for patients. Therefore, the hope is that in the near future this could be performed non-invasively by computed tomography or even by MRI. Although promising results have been reported using these two modalities, especially for diagnosis, unfortunately they are not yet capable of visualizing the coronary arteries with the same level of detail as the invasive imaging techniques. Hopefully, new computer algorithms can help to close this gap as this would have a major impact on further studies that aim to prevent cardiac related diseases.

A Vectorial Approach for Evaluation of Depolarization Changes during Acute Myocardial Ischemia

Daniel Romero Pérez*, Michael Ringborn, Pablo Laguna, Olle Pahlm and Esther Pueyo

Communications Technology Group (GTC), Aragón Institute for Engineering Research (I3A), Zaragoza, Spain

Changes in the repolarization phase (ST-T segment) of the electrocardiogram (ECG) are conventionally used to detect acute myocardial ischemia. Previous studies have also reported changes in the depolarization phase (QRS complex) during acute ischemia. Among those, a method based on QRS slope measurements in the 12 standard leads has been proposed to characterize ischemia induced QRS changes. In the present study we evaluated the upslope (IUS) and downslope (IDS) of the R wave of the QRS complex in ECG leads obtained from spatial QRS loops of 79 patients undergoing prolonged, elective percutaneous coronary intervention (PCI). The QRS loops were obtained by two methods: i) from orthogonal ECG leads X, Y and Z corresponding to the vectorcardiogram (VCG); ii) from the first three orthogonal leads derived after applying principal component analysis (PCA) over the 12-lead ECG. The dominant direction of each QRS loop was determined, and a new lead, denoted by VCG or PCA, was generated by projecting the corresponding QRS loop onto that dominant vector. For each patient, the slope indices IUS and IDS were evaluated in the PCI recording as well as in a control recording acquired before the PCI procedure, and relative factors of change during PCI were calculated. We showed that IUS and IDS computed over VCG and PCA leads present higher sensitivity to the ischemia-induced changes than the same indices evaluated over the standard 12-lead ECG. Mean relative factors of change were 10.5 and 12.4 for IUS and IDS in PCA, and 7.87 and 13.7, respectively, in VCG, representing an increase in sensitivity of up to 103% for IUS and 46% for IDS compared to measurements obtained in lead V3 of the standard ECG, which was the lead showing the most marked changes among the 12 standard leads. We conclude that evaluation of slope indices in leads derived from QRS loops significantly increases their potential value for detection of acute myocardial ischemia.

Model-Based Medical Expert System for Diagnosing Myocardial Ischemia Based on a Newly Developed Ischemia Parameter

Hisham Alqysi*

Clinical Analysis Dept, Hawler Medical University, Erbil, Iraq

The documented ECG parameters such as ST-shift and T-wave inversion are weakly related to the presence and the extent of myocardial ischemia. Therefore, their presence is not always indicative specifically of the myocardial ischemia. In this study, a new parameter called ischemia parameter has been developed based on the differences in electrical conductivities between normal and ischemic tissue. Equations are derived in a new model to determine this ischemia parameter. The model is incorporated in a medical expert system which is interfaced with measuring device. All the required ECG measurements are listed in scp file for analysis by the expert system.

Clinical trial of this noninvasive technique (expert system + measuring device) shows that this technique can accurately (sensitivity $>$93.6% and specificity 80.4%) diagnose chronic, acute (angina) and silent myocardial ischemia and determine its numerical severity.

This medical system can differentiate between cardiac and noncardiac chest pain.

Accurate and noninvasive diagnosis can find many clinical applications including the assessment of the open heart surgery CABG, the efficiency of the stent ,the need of angiography .etc

Research on Myocardial Ischemia Detection Based on the Electrocardiogram R-S-T

Jinzhong Song* and Hong Yan

State Key Laboratory of Space Medicine Fundamentals and Application, China Astronaut Research and Training Center, Beijing, China

Electrocardiogram (ECG) is an economic and convenient detecting tool in myocardial ischemia(MI), whose clinical appearance is mainly exhibited by ST-T complex change. However, it is highly sensitive to interferences(axis deviation, heart rate, electrode interference, postural changes, etc), which causes ST-T complex feature points difficult to detect accurately. In this paper, a new detection approach of myocardial ischemia was proposed based on ECG R-S-T, which just needed to locate three feature points R-wave peak, S-wave peak, and T-wave peak. Some vectors derived from the triangle RSTs were calculated, and they were RT(RT length), TS(ST length, the distance between S-wave peak and T-wave peak), RS(RS length), Area(the area of triangle RST), Rate1(the amplitude ratio of T-wave peak and R-wave peak), Rate2(the length ratio of RT and RS). The means, variances, and approximate entropys of these vectors were regarded as estimation parameters, as a result, significant differences ($P<0.05$) of five parameters RTrv, TSrv, RSrv, ArearE, and Rate1rE were obtained after the long-term ST database(LTST) verification. The proposed method provided a simple and reliable basis for clinical diagnosis of myocardial ischemia.

Body Surface Potential Mapping Improves Diagnosis of Acute Myocardial Infarction in those with Significant Left Main Coronary Artery Stenosis

Michael John Daly*, Peter Scott, Colum Owens, Audrey Tomlin, Bernadette Smith and Jennifer Adgey

The Heart Cente, Royal Victoria Hospital, Belfast, United Kingdom

Non-invasive diagnosis of LMCA stenosis is challenging. Acute myocardial infarction (AMI) as a consequence of LMCA obstruction has a poor prognosis and thus early diagnosis is essential to expedite prompt revascularisation.

Methods: Patients presenting pre- and in-hospital between 2000-9 with acute chest pain were analysed. Those included had a 12-lead ECG and body surface potential map (BSPM) recorded at presentation, cardiac troponin T (cTnT) assessed 12 hours and coronary angiography. AMI was defined as cTnT 0.03g/L. STE on 12-lead ECG was defined using the Minnesota criteria. STE in aVR was 0.5mm, STD was 1mm and TWI was 3mm in 2 contiguous leads. STE on BSPM was defined as 1mm in the anterior, lateral, inferior, right ventricular or high right anterior territories and 0.5mm in the posterior territory. Significant LMCA stenosis was defined as 70% luminal narrowing at angiography.

Results: One hundred and eight patients had significant LMCA stenosis and were aged 67 $\pm$ SD 11 yrs (84% male). Eight were excluded due to lack of BSPM. Of the remaining 100 patients, AMI occurred in 83 (83%). Of these 83 patients, STE on 12-lead ECG occurred in 9: sensitivity 11%, specificity 88% for AMI. STE in aVR occurred in 17/83 (sensitivity 20%, specificity 88%), TWI in 26/83 (sensitivity 31%, specificity 76%) and STD in 41/83 (sensitivity 49%, specificity 71%). STE on BSPM occurred in 77/83: sensitivity 93%, specificity 71% for AMI diagnosis. Of those with STE on BSPM, STE occurred in either the high right anterior, right ventricular or posterior territories in 60 (78%) patients. Of these 60, 35 (58%) patients had STE in the high right anterior region (positive predictive value 91% for AMI diagnosis).

Conclusion: In patients with acute chest pain and significant LMCA stenosis, STE on BSPM has an improved sensitivity (93%) over 12-lead ECG in the diagnosis of AMI.

Detection of Inferior Myocardial Infarction: A Comparison of Various Decision Systems and Learning Algorithms

Jiří Spilka*, Václav Chudáček, Jakub Kužílek, Lenka Lhotská and Martin Hanuliak

Biodat Research Group, FEE, CTU in Prague, Prague 2, Czech Republic

Myocardial infarction (MI) is one of the most common causes of death or disability in the Western world. It could be a minor event, perhaps not even recognized, or it may be a major attack with results varying from acute pains, hemodynamic deterioration to sudden death. Nevertheless, detection of an infarction greatly improves patient's chances of surviving and returning to health, therefore the task is of great importance. In this work we focused on detection of inferior MI. Our database consisted of 6350 ECG records and interpretation was made by cardiologist; 512 records were assessed as inferior MI and 1598 as normal sinus rhythm the rest contained other types of pathologies. We evaluated the three most known decision systems, the Selvester QRS score, the Novacode, and the Siemens 440/740 with respect to prediction accuracy of inferior MI. In addition, we compared their performance to learning algorithms, such as Ripper, C4.5, SVM, and Naive Bayes. Then, we chose the best performing decision system and, according to data distributions, modified decision rules to improve performance. We found performance of the decision systems questionable even when only records of normal sinus rhythms and inferior MI were used. The best results were achieved by the Selvester and Siemens. The Selvester, while having great specificity of 0.99, achieved low sensitivity of 0.41. On the contrary, Siemens had good sensitivity of 0.80 but lacked specificity 0.87. Better results were achieved using Ripper with 0.83 sensitivity and 0.92 specificity. The modification of the Selvester improved sensitivity from 0.58 to 0.85, on the other hand specificity lowered from 0.93 to 0.90. In this work we showed that decision systems for prediction of inferior MI need further improvements; by modifying parameters in the Selvester QRS score we improved results that were comparable to those of Ripper.

Combining Sgarbossa and Selvester ECG Criteria to Improve STEMI Detection in Presence of LBBB

RE Gregg*, SH Zhou, ED Helfenbein

Advanced Algorithm Research Center, Philips Healthcare
Andover, MA, USA

Background: ECG detection of ST-segment Elevation Myocardial Infarction (STEMI) in presence of left bundle-branch block (LBBB) has long been a challenge. The Sgarbossa ECG criteria have been validated and tested by researchers in a number of studies, but criticized due to low sensitivity. The purpose of this study was to compare Sgarbossa criteria with Selvester criteria (the 10% rule) and propose a new algorithm with combined Sgarbossa and Selvester criteria for improved detection of STEMI in LBBB.

Method: The study population (n = 382) with 144 acute MI and 238 controls includes data from multiple sources. One was computer algorithm selected LBBBs (n = 209) from patients with discharge diagnosis of acute MI (n = 100) and non- acute MI (n=109). The second set included acute MI (n = 43) and control (n=70) cases with selection criteria similar to the first set. Additional controls were added from the CSE diagnostic set (n=12) and a community based population (n=48). Elements of the Sgarbossa criteria (discordant ST elevation of 5mm, concordant ST elevation of 1mm, ST depression in V1-V3) and Selvester criteria (discordant ST elevation $\geq$ 10% of |R-S| plus STEMI limits) were tested separately and in a combination with the Sgarbossa discordant ST elevation replaced by the Selvester discordant ST elevation 10% rule. ECG criteria were compared by sensitivity, specificity, positive likelihood ratio (LR+) and negative likelihood ratio (LR-).

Results: Applying Sgarbossa criteria alone resulted a 30% sensitivity, 88% specificity, 2.5 LR+ and 0.80 LR-. Combined Sgarbossa and Selvester criteria increased the sensitivity to 39% with a specificity of 89%, 3.6 LR+ and 0.68 LR-.

Conclusion: Replacing the Sgarbossa discordant ST elevation criterion with the Selvester 10% rule improves the sensitivity without losing specificity. The ST elevation threshold relative to QRS amplitude works better than an absolute ST elevation threshold.

Extended Multiple Linear Regression in the Derivation of Electrocardiographic Leads

Daniel Guldenring*, Dewar Darren Finlay, Christopher Desmond Nugent and Mark Patrick Donnelly

Computer Science Research Institute, University of Ulster, Carrickfergus, Northern Ireland, United Kingdom

In this study, we investigate the performance of an approach for deriving electrocardiographic leads with the aim of improving derivation accuracy. We focus our attention on a limited lead system that uses leads I, II, V2 and V5 to derive the remaining precordial leads. Our extended multiple linear regression based lead transformation approach (EMLRLT) extends the standard multiple linear regression (MLR) approach by combining the data from the recorded leads with quadratic and cross product terms from the same leads. The study dataset consisted of 180 12-lead ECGs extracted from the PTB Diagnostic ECG Database (publicly available via PhysioNet). A computerized algorithm was used to identify QRSonset, QRSoffset and T-end. Patient specific lead transformations for the standard MLR and EMLRLT approaches were calculated via multiple linear regression analysis. In both approaches, 50 QRST complexes from each recording were used to develop the transformations. Subsequently, data from 50 unseen complexes were used to compare estimation accuracy of both approaches. Median RMS error values were calculated for QRS complexes, ST-T segments and for the entire QRST. It was found that all missing leads were more accurately estimated using the EMLRLT approach. Using the standard MLR, the median RMSEs for the QRST were found to be 44.2V, 42.7V, 40.3V and 19.3V for leads V1, V3, V4 and V6, respectively. Using the EMLRLT approach, the median RMSEs for the QRST were found to be 28.2V, 29.3V, 25.1V and 13.4V for leads V1, V3, V4 and V6, respectively. According to the sign test, all differences were statistically significant with $p<0.05$. This study has demonstrated that alternative methods for lead transformation have the potential to improve lead derivation accuracy. Further research is required in order to assess whether or not these improved performance metrics translate into an improved diagnostic accuracy.

A Web-based Visualization Tool for Transforming the 12-lead ECG into a Body Surface Potential Map

Raymond Robert Bond*, Dewar Darren Finlay, Chris Desmond Nugent and George Moore

School of Computing and Mathematics, University of Ulster, Belfast, Antrim, United Kingdom

The 12-lead ECG is the most commonly used technique for assessing cardiac activity. With just six precordial electrodes, it is often criticized for its lack of right sided and posterior leads. In contrast, the Body Surface Potential Map (BSPM) can use over 200 electrodes to capture information from the entire surface of the torso. Although BSPMs have been shown to be more sensitive in detecting cardiac pathologies, a large number of electrodes are impractical in routine clinical practice. This reality has lead to the development of reduced lead sets, where a small number of leads are recorded and a mathematical solution is used to derive additional leads. In this study, we have developed a web based ECG viewer that provides a platform to transform the 12-lead ECG into a BSPM.

The viewer was developed using lossless vector graphics technology (Adobe Flash). A user can load a Health Level Seven Annotated Electrocardiogram (HL7 aECG) 12-lead ECG. A set of pre-stored coefficients can be selected or a new set can be uploaded. Subsequently, the 12-lead ECG is transformed into a BSPM, which can be further explored using isopotential and isointegral tools. The BSPM can also be saved using an open storage format called XML-BSPM.

This tool was tested by transforming 20 12-lead aECG files into 192 lead BSPMs (Lux format). This was performed using transformation coefficients developed from an existing set of 192 lead BSPMs. The average transformation time on a PC (3GHz CPU, 3GB RAM) was 1.35 seconds. This included the time to parse coefficients from the XML, perform the transformation and to generate the XML-BSPM file.

This tool presents more information than would be available with the 12-lead ECG. It could outperform current methods used to display ST elevation (24-lead view) and could therefore improve the accuracy of a diagnosis.

Real-Time Back-Projection of Fetal ECG Sources in OL-JADE for the Optimization of Blind Electrode Positioning

Danilo Pani*, Stefania Argiolas and Luigi Raffo

DIEE - Dept. of Electrical and Electronic Engineering, University of Cagliari, Cagliari, Italy

Fetal electrocardiogram (FECG) extraction from non-invasive biopotential recordings is strongly affected by the intensity of the FECG contribution to the input signals. The higher the FECG contribution the higher the SNR and consequently the quality of the separation. The definition of a subject-specific good electrodes positioning is an open issue, sometimes addressed performing ultrasound-based preliminary examinations. In this paper we present a blind technique potentially exploitable for the real-time interactive electrodes placement, embedded into the OL-JADE extraction algorithm, a 2-stage online ICA algorithm. The underlining idea is that an estimate of the FECG power at the electrodes (lost in the estimated sources due to ICA scaling ambiguity) could be achieved inverting the blind extraction process only for the FECG estimated sources, exploiting this information for an iterative arrangement of the electrodes positions in order to find a good placement for a specific subject, improving SNR. When using OL-JADE, the main problem is that the recursive sample-by-sample nature of the first stage (whitening) prevents the identification of a single whitening matrix for a block of input samples. A good approximation of the inverse of such process can be found as a Least Squares solution obtained by the method of normal equations. On the contrary, the inversion of the second stage of OL-JADE is exact. FECG sources are virtually back-projected at the electrodes so that the input FECG power levels can be estimated. From simulations on real and synthetic signals we found that the approximated back-projection is effective in producing an FECG contributions power ranking. An optimized version of the proposed method has been integrated with OL-JADE on a floating point DSP. The real-time performance is achieved with wide margin, opening to the realization of a blind interactive electrodes positioning procedure in real scenarios.

Short Distance Bipolar Electrocardiographic Leads in Diagnosis of Left Ventricular Hypertrophy

J. Väisänen, M. Puurtinen, J. Hyttinen and J. Viik

Tampere University of Technology, Tampere, Finland

Novel small and wearable electrocardiogram (ECG) devices offer new means of recording cardiac activity in different applications. Our objective was to evaluate the performance of closely separated (6 cm) bipolar leads in differentiating subjects with left ventricular hypertrophy (LVH) from normal subjects.

The study population consists of 236 healthy subjects, 116 pure LVH patients having either pure left-sided valvular disease or sustained hypertension (150/90 mmHg or higher) and 189 complex LVH patients with various cardiac conditions frequently associated with LVH.

A total of 36 vertical, 30 horizontal and 66 diagonal bipolar leads located on the anterior thorax were analyzed. The QRS amplitudes of bipolar leads were calculated for each patient and the overall diagnostic performance of the bipolar leads was assessed by receiver operating characteristic (ROC) analysis. In addition the sensitivities of leads were calculated at equal specificity of 90%. As a reference Sokolow-Lyon criteria was applied to the data.

The ROC areas and sensitivities for the best bipolar leads in group comparisons of normal subjects vs. pure LVH subjects and normal subjects vs. complex LVH subjects are listed in Table 1. The best leads differentiating normals from pure and complex LVH subjects are vertical leads located on lower anterior thorax and mid-thoracic region, respectively. These leads have better performance and are more sensitive than clinically applied Sokolow-Lyon criteria. It should also be noted that the cut off point criteria for complex LVH is reversed.

As a conclusion the new short distance bipolar leads are efficient in discriminating subjects with LVH from normal subjects based on QRS amplitude.

Table 1. ROC areas, sensitivities and cut off points at 90 % specificities for the best bipolar leads and for Sokolow-Lyon criteria. Group comparisons were normal subjects vs. pure LVH and normal vs. complex LVH. Note that the diagnostic criteria for bipolar lead in case of complex LVH is reversed.

Method	ROC area	Sensitivity at 90% specificity	Cut off point (μV) at 90% specificity
Sokolow-Lyon (pure)	0.73	42 %	> 4255
Best bipolar (normal vs. pure)	0.81	59 %	>765
Sokolow-Lyon (complex)	0.67	39 %	< 1766
Best bipolar (normal vs. comp)	0.85	65 %	< 816

Utilising a Genetic Algorithm to Minimise the Number of Leads in Body Surface Mapping for the Electrocardiographic Diagnosis of Myocardial Infarction

Peter Scott*, Cesar Navarro, Marisol Giardina, Omar Escalona, John Anderson and Jennifer Adgey

Cardiology, West Wing, Royal Victoria Belfast, Belfast, Antrim, United Kingdom

Introduction: The 80-lead Body Surface Map (BSM) is a diagnostic tool utilised by clinicians for the diagnosis of myocardial infarction (MI) at our centre. The optimum number and placement of leads on the BSM is uncertain. We used Genetic Algorithm analysis to determine a reduced lead system for the optimal diagnosis of MI. Method: 1106 cases presenting to our centre with ischaemic type chest pain (576 ST Segment Elevation MI, 244 Atypical ECG and 286 Non-MI) were recorded using the 80-lead BSM. All recordings were made within 12 hours of symptom onset. MI was confirmed by elevation of Troponin T $>$ 0.09 umol/l and BSM diagnosis and recording quality confirmed by retrospective analysis by two physicians. A Genetic Algorithm was developed to determine a subset of reduced number of leads, with their associated anatomical position within the 80-lead BSM system, while maintaining sensitivity and specificity for MI diagnosis. Additional weighting was included in the fitness function to encourage leadsets containing fewer electrodes as well as leadsets closer together on the torso (to aid lead placement). The Genetic Algorithm was run on two separate occasions (Run A and Run B) and the output compared with the 80-Lead BSM. Results: Run A produced a 24 lead system. The sensitivity and specificity for MI diagnosis was 86.40% and 97.55% respectively. Received Operator Characteristic (ROC) curve c-statistic was 0.805. Run B produced a 21 lead system with sensitivity and specificity of 84.84% and 98.25% respectively. ROC curve c-statistic was 0.811. This compares favourably with the 80 lead BSM (sensitivity 90%, specificity 92%, ROC c-statistic 0.850). Conclusion: We have developed a novel genetic algorithm based approach, in determining the optimal number ($<$25) and position of leads from the 80-lead BSM for the electrocardiographic diagnosis of MI.

Fuzzy integrated Neural Network Classification of Body Surface Potential Contour Map to Detect Myocardial Infarction Location

H. SadAbadi [1], N. Jafarnia Dabanloo [2*], M. Ghasemi [3], S. Sabouri [2]

[1] Department of Mechanical Engineering, Concordia University, Montreal, Qc, Canada
[2] Faculty of Biomedical Eng, Science and Research Branch, Azad University, Tehran, IR
[3] Dept. of Mechanical Engineering, K.N. Toosi University of Technology, Tehran, IR

Abstract:

Because of the absence of comprehensive understanding of fundamental basic science of the ischemic heart disease, there are still some mismatches between the diagnostic methods and the therapeutic interventions. This paper addressed this issue by presenting an automatic Neuro-fuzzy method for characterizing the location of MI applied to the standard 17-segment model of the heart.

This work is relying on the idea that already has presented by the same authors[1] in CinC/PhysioNet Challenge 2007 and has ranked second[2]. The data that is used here is 352-electrode BSPM data for four cases (two training cases and two test cases). First, some horizontal/vertical lines are considered on torso surfaces. Then the ECG contour map on torso surface is plotted and the behavior of some ECG features on these lines is calculated. These ECG features includes maximum positive QRS peak, maximum negative QRS peak and QRS integral. In this paper, a method of fuzzy decision-making applied for characterization of infarcted elements. The proposed method in the first level uses a neural network classifier to characterize a region on torso surface. Next, the method of dealing with the uncertainties present in the data using the fuzzy approach to map these regions to the heart surface.

The results of two test subjects are the estimated infarcted elements. These results are compared to a gold standard that consists of expert analysis of gadolinium-enhanced MRI data. Given the estimated and gold standard sets of infarct segments, "overlap" (SO) can be defined as the number of segments in both sets divided by the number of segments in either set (a value between 0 and 1, where 1 is a perfect match and 0 indicates that the sets are completely disjoint). The proposed method reached SO=0.44 and SO=0.26 for two test subjects so far. This method can estimate the location of both cases medially and need more adjustments in the parameters. By implementing other ECG features one can detect the location of infarcted area more precisely.

Table 1: Comparison between the results of the proposed method and our previous method

Test subjects	Overlapped Segments (SO)	
	The proposed method	Previous Semi –Automatic method
#3	0.44	0.50
#4	0.26	0.444

[1] SadAbadi, H., et. al., "Variation of ECG features on torso plane: An innovative approach to myocardial infarction detection", In proceeding of Computers in Cardiology, 2007; pp. 629 - 632.

[2] http://www.cinc.org/challenge.shtml

The PhysioNet/Computing in Cardiology Challenge 2010: Mind the Gap

George B Moody*

Harvard/MIT Division of Health Sciences and Technology,
Massachusetts Institute of Technology, Cambridge, MA, United States

In settings ranging from sleep studies to surgery to sports medicine to intensive care, real-time monitoring of a variety of physiologic signals has become an essential tool for clinicians and researchers. Transient corruption or loss of one or more signals, common in all of these settings, can be disruptive, especially when continuous observations are required in order to rule out rare events or as a basis for forecasting. Signal corruption can be particularly challenging when it mimics features that are associated with pathologic states.

The aim of this year's challenge is to develop robust methods for filling in gaps in multiparameter physiologic data (including ECG signals, continuous blood pressure waveforms, and respiration). In a real-world monitoring application, these methods can be applied for many purposes, including: robust estimation of parameters such as heart rate, mean arterial pressure, and respiration when the primary signals used to derive these parameters become unavailable or unreliable; detection of changes in patient state, when the relationships between signals remain consistent even as individual signals change their behavior; and recognition of intervals of signal corruption, when a signal becomes inconsistent not only with respect to its previous history but also with respect to its relationships with other signals.

In this Challenge, participants are asked to reconstruct, using any combination of available prior and concurrent information, segments of signals that have been removed from multiparameter recordings of patients in intensive care units (ICUs).

Estimation of Missing Data in Multi-channel Physiological Time-series by Reference Timing Channel and Average Substitution

P Langley, S King, K Wang, D Zheng, R Giovannini, M Bojarnejad, A Murray

Newcastle University & Freeman Hospital, Newcastle upon Tyne, UK

Physiological data continuously acquired from the clinical environment is often corrupted by noise, artifact or interruption so that sections of data are un-analysable. If sufficiently accurate estimations of these sections of data could be derived then a more complete analysis could be achieved. Our hypothesis was that reconstruction of missing data could be accurately achieved using average substitution if an appropriate reference timing channel without missing data was available.

Physiological data from the Computing in Cardiology Challenge 2010 were analysed. Reference timing was determined by an automatic beat detection algorithm from a channel without missing data. This was preferably the ECG channel, or if not available, a channel containing pulsatile data (eg blood pressure). For the channel with missing data the average beat across the recording was determined and this average provided the estimate of each missing beat at each beat time provided by the reference timing channel. Baseline offset estimate was achieved by ensuring the mean of the reconstructed data was equal to the mean of the 10 s of data prior to loss of signal. This algorithm would be ineffective for missing data which is non-pulsatile (eg respiration) so we implemented an algorithm based on PCA estimation of the respiratory data from the ECG channel. Results are shown in table 1.

	Event 1			Event 2			
Set	Basic	+Baseline	+Respiration	Basic	+Baseline	+Respiration	Attempted
A	50.1	52.9	54.3	65.1	65.1	66.5	100
B			67.8			78.0	100

Table 1. Score for each event and dataset for the basic algorithm, basic algorithm plus baseline estimation and the addition of the respiratory algorithm.

The final algorithm achieved scores of 54 (event1) and 67 (event 2) for set A and 68 (event 1) and 78 (event 2) for set B when providing estimates for missing data in all 100 recordings in each set. The algorithm does not take account of beat to beat changes in amplitude and consistently achieved higher scores based on correlation (event 2) than amplitude (event 1).

PhysioNet 2010 Challenge: A Robust Multi-Channel Adaptive Filtering Approach to the Estimation of Physiological Recordings

Ikaro Silva*

Laboratory for Computational Physiology, MIT, Cambridge, MA, United States

The 2010 PhysioNet Challenge was to predict the last 30 seconds (the g̈ap̈) of a physiological waveform given 9 minutes and 30 seconds of its previous history and 10 minutes of N different concurrent physiological recordings (sampled at 125 Hz). A robust approach was implemented by using a set of adaptive filters to predict the desired channel. In all, N+2 channels (the N original signals, and 2 signals derived from the first 9 minutes and 30 seconds of the signal preceding the gap) were used to estimate the missing data. For each of the N+2 individual channels, a gradient adaptive lattice Laguerre filter (GALL) was trained to estimate the desired channel. The GALL filter was chosen because of its fast convergence, numerical robustness, stability, and ability to model a very long response using relatively few parameters. A learning factor was applied to each GALL in order to account for changes in the environment and/or in the relationship between the channels. The prediction of each of the N+2 channels (the output of each of the N+2 GALL filters) was then linearly combined using time-varying weights determined through a Kalman filter with a learning factor optimized over a training region. At the time of this writing, an average score of 80% on Set B (Event 2) was obtained. The performance of the procedure was found to be roughly dependent on the type of recording, number of channels available, and the ranking of the final weights given by the Kalman filter. This suggests that the tracking of the Kalman weights might provide further insight into how specific changes in a physiological state affect the selected recording. The approach is extensible to recordings with any number of signals, other types of signals, and other problem domains.

Reconstruction of Missing Physiological Signals using Artificial Neural Networks

Adam Sullivan, Henian Xia, Joseph McBride and Xiaopeng Zhao*

Nonlinear Dynamics Lab, University of Tennessee, Knoxville, TN, United States

Real-time monitoring of vital physiological signals is of significant clinical relevance. Disruptions in the signals are frequently encountered and make it difficult for precise diagnosis. Thus, the ability to accurately predict/recover the lost signals could greatly impact medical research and application. In response to the PhysioNet/CinC Challenge 2010: Mind the Gap, we develop an algorithm based on artificial neural networks to predict the missing signals in one channel using the measurements in other channels. An artificial neural network model is created for each record, which consists of 6, 7, or 8 signals acquired from bedside ICU patient monitors. We first train the network using data from the beginning 9.5 minutes of the record. Then, we reconstruct the missing data in the subsequent 30 seconds for a specific channel. A few techniques are utilized to improve the performance of the model. Principle component analysis is used to reduce complexity and computational cost. Noisy signals are smoothened using a wavelet-based de-noising algorithm before training and testing. We explored three different neural networks: focused time-delayed neural network, distributed time-delayed neural network, and nonlinear autoregressive network with exogenous inputs. The focused time-delayed neural network is more computationally efficient while the other two networks provide slightly more precise predictions. For highly correlated data sets, all three networks are able to produce accurate predictions; however, predictions of chaotic and highly noisy data sets are less satisfactory.

A Sensorless Kalman Estimator toward the Reconstruction of Physiologic Data

Mohamed A Mneimneh* and Sahar Elturk

Marquette University, Scottsdale, AZ, United States

The aim of the 2010 Physionet/ Computers in Cardiology challenge titled Mind the Gap is to robustly reconstruct missing signal from multiparameter physiologic data. Real-time monitoring of physiological signals is an essential method used by clinicians and researchers during sleep studies, surgeries, and intensive care units. However, corruption or loss of some of the signals could occur during monitoring. Such signal corruption could be disruptive especially when signals are required for predicting or monitoring rare events. This work uses a Kalman Filter based approach to estimate the missing signals from concurrently available physiologic signals. The Mind the Gap challenge is divided into two events. The first is to determine the best estimate of the missing signal. The second is to determine the best estimate which correlates with the missing signal. Three sets of data are provided for this challenge: Set-a, Set-b, Set-c consisting of 100 records each. The first two data sets are used for testing, and Set-c will be used toward the final score of both events. The method used in this work estimates the missing signal using measurements from signals occurring simultaneously. The Kalman Filter determines the optimal coefficients which transform concurrent signals to the missing one. The Scoring of the first event is the maximum between 0 or 1 - sum of squares of the error between the estimated signal and original signal normalized by the energy of the residual. The scoring of the second event is defined as the maximum between 0 and the correlation coefficient between the estimated and the actual signal. The final score of each event is the sum of scores across all submitted records. The Kalman filter based estimator approach presented in this work is applied to set-b of the challenge yielding scores of 56.6996 and 70.6656 for events 1 and 2, respectively.

Reconstruction of Missing Cardiovascular Signals using Adaptive FIltering

Andras Hartmann*

Institute of Human Physiology and Clinical Experimental Research, Semmelweis University, Budapest, Hungary

This work is addressed to The PhysioNet/Computing in Cardiology Challenge 2010: Mind the Gap. The aim of the challenge is to develop robust methods for filling in gaps in multiparameter physiologic data. Our approach to identify the 30 seconds of missing ICU data (target signal) was a gray-box technique. Using the signals' history we identified the connection in form of a Multi-Input/Single-Output (MISO) system, where the output is the prior of the target signal, the inputs are all the other signals. Assuming that the connection is time-invariant, we were able to make a prediction of the target by using the identified filter on the available parallel measured signals. Third order Infinite Impulse Response (IIR) filters were used in the model, the filtered signals were summarized in a linear model. The filter coefficients were estimated using a genetic algorithm with a fitness function containing both Mean Squared Error (MSE) and correlation coefficient to the target prior. This was found to maximize both Q1 and Q2 scores. Since the above assumption only holds for short time period, we restricted the identification of the transfer function to 2s, 10s and 30s of prior, and chose the best fit. Our current results show promise on the datasets where the reconstructions can be tested: Q1=64.045, Q2=79.7993, Q1=64.9604, Q2=77.8366 of 100 attempts on each A and B datasets respectively. The algorithm converged in every case to a stable filter, a good fit to the prior ensured good identifiability. We conclude that this approach can be efficient in reconstructing lost cardiovascular signal waveforms. As next step we will consider further analysis of the found transfer functions.

Coupling the Guyton Model to Pulsatile Ventricles using a Multiresolution Modelling Environment

Virginie Le Rolle*, David Ojeda, Raphaël Madeleine, Guy Carrault and Alfredo I Hernández

LTSI Université de Rennes 1, INSERM U642, Rennes, France

The pioneering work of Guyton, Coleman, and Granger (1972) provided an interesting multi-organ, lumped-parameter model of the global cardiovascular system and its regulation. However, this model (G72) does not include a pulsatile representation of the cardiac function and thus cannot be used for a beat-to-beat analysis. Within the framework of the SAPHIR project, the G72 model has been re-implemented by using an object-oriented multiresolution modeling tool, developed in our laboratory (M2SL). In this paper, we propose the substitution of the original, non-pulsatile cardiac sub-model of the G72 model by an elastance-based pulsatile model of the heart, including interventricular interaction through the septum. This substitution process is not simple, as it requires the identification of the pulsatile model parameters that will preserve the stability and physiological properties of the G72 model, as well as and the appropriate handling of the heterogeneous time-scales that will be involved within the new model. An identification algorithm has been thus applied to reproduce benchmark data from the original G72 model with the modified, pulsatile version of the model. The error function being minimized has been defined as the mean square error of eight physiological variables calculated between the outputs from both models (urinary output, muscle venous oxygen pressure, muscle cell oxygen pressure, mean arterial pressure, sympathetic stimulation, cardiac output, muscle blood ow and rate of oxygen usage by muscle cells). After parameter identification, the mean square error for the eight signals is equal to 0.0108. Results show how a higher-resolution model allows the simulation of realistic pulsatile ventricular pressures while keeping the main physiological properties of the original model. Besides, this is an example of how multiorgan models such as those proposed by Guyton could be used as a c̈ore-modelẗo integrate higher-resolution models, allowing for a better representation of appropriate boundary conditions.

Simulation of the Effect of Tachycardia on Atherosclerotic Plaque Development Based on the LDL Transport in Coronary Arteries

Antonis Sakellarios*, Panagiotis Siogkas, Vasilis Tsakanikas, Lampros Michalis, Dimitrios Fotiadis, Katerina Naka, Nenad Filipovic and Kostas Stefanou

Unit of Medical Technology and Intelligent Information Systems, Dept. of Materials Science and Engineering, University of Ioannina, Ioannina, Greece

S64

The formation of the atherosclerotic plaque is associated with the accumulation of lipids, monocytes and macromolecules into the arterial wall, which loses its elasticity and is gradually fattened. The process is influenced by the local hemodynamic environment. Furthermore, it is reported that tachycardia or high heart rate affects the physiology of the arterial wall enhancing the pro-atherosclerotic conditions. Especially, the endothelium is exposed to extended low shear stress of the systolic phase. In this work, the effect of high heart rate on the LDL transport and the development of atherosclerosis are examined using the finite element method. The simulation is performed on two case studies i.e. 3D reconstructed right coronary artery with and without atherosclerotic plaque. The velocity profile is pulsatile, while the tachycardia case is assumed to have 40% increased flow rate and 25% increased velocity than the normal case. The Navier-Stokes equations are used to model the blood flow and LDL transfer is modeled using convection-diffusion equation. The accumulation of the LDL is based on the Kedem-Katchalsky equations and is considered to be shear stress dependent. The results indicate the role of hemodynamics on the accumulation of LDL. Moreover, high heart rate enhances the influence of blood flow lengthening the exposure to low shear stress during systole. It is found that the area of low wall shear stress (0-2 Pa) which is critical for the formation of plaque is about 8% greater in the tachycardia case than the normal case. That means that the penetration of LDL on the arterial endothelium is increased at the systolic phase. In addition, comparing the two arterial models, the results depict that atherosclerotic plaque is formed not locally at the lowest values of shear stress, but at regions where low shear stress dominates. Lowering the heart rate, the pro-atherosclerotic environment is reduced.

Atrioventricular Delay Optimization in Cardiac Resynchronization Therapy Assessed by a Computer Model

Kevin Tse Ve Koon*, Christophe Thebault, Virginie Le Rolle, Erwan Donal and Alfredo Ignacio Hernández

LTSI, Université de Rennes 1, Rennes, France

Clinical studies have shown that patient response to Cardiac Resynchronization Therapy (CRT) is highly dependent on the pacing configuration namely the atrioventricular (AVD) and interventricular (VVD) delays; the former being the most sensitive parameter. Current research in this field is oriented towards individualization of AVD and VVD, in order to maximize patient response. Different echocardiographic indicators have been proposed to optimize CRT delivery. Maximizing left ventricular filling is widely regarded as the optimization target to achieve, with respect to AVD selection. This feature can be obtained through the pulsed-wave Doppler (PWD) recording of the mitral inflow. A lumped-parameter model of the cardiovascular system made of three interacting modules (an electrical heart model, an elastance-based mechanical heart model and a circulatory system), previously proposed by our team was used to analyze the mitral flow during AVD optimization. A sensitivity analysis of different model parameters is first carried out, showing that left ventricular diastolic compliance, electro-mechanical delay and elastance function forms are the most important model features affecting mitral flow. Patients undergoing CRT at the Pontchaillou University Hospital were included in a device optimization protocol. For different AVDs, the audio signal corresponding to the PWD of the mitral flow was acquired for at least three cardiac cycles and processed by short-term FFT. A contour-tracing algorithm was applied to the average recorded mitral flow to obtain its profile. Finally, parameter identification of the proposed model was performed to minimize a relative mean squared error (rmse) calculated between the observed and the simulated mitral flows (for all AVD). Data from three patients provided rmse values of 0.049, 0.13 and 0.18. This model is capable of reproducing the main mitral flow profiles observed clinically and may be useful in performing AVD optimization in a postoperative context.

Semi-Automated Extraction of Canine Left Ventricular Purkinje Fiber Network

Kuanquan Wang*, Jie Li, Wangmeng Zuo, Henggui Zhang and Yongfeng Yuan

Harbin Institute of Technology, China

The purkinje fiber network (PFN) is a very important conduction system in the endocardial surface of the ventricle, which is crucial in modeling ventricular tachycardia and fibrillation. Traditional medical imaging methods such as magnetic resonance imaging (MRI) or computed tomography (CT) fail to reveal the PFN information well especially when individual fibers are in dense fibrous regions or under noisy conditions. Another kind of method is to construct the PFN by the modeling method. i.e. modeling using the fractal structure of the endocardial surface photographs. However, among steps of the construction, PFN is extracted by the threshold value of the gray scale before the visualization, which needs the gray scale modification at some points to differentiate them from background points. In this work, we will introduce a semi-automated method for extracting PFN in the left ventricle, which is increasingly concerned in the pattern recognition and is proved to be feasible and efficient in the visualization and simulation of the heart. In the proposed method, a bank of filters with different orientations and scales is first used to lift the 2D image in a 4D orientation space, which is effective in disambiguating the crossing configuration problem of other lifting method. Then we use a geodesic based method to compute optimal paths in this 4D space, leading to a robust global segmentation of fibers. Our method can directly and naturally compute both centerlines and radii of fibers. With this method, a semi-automated scheme can be used to extract PFN conveniently by only manually providing the starting and ending points of purkinje fibers.

A LabVIEW Based Multichannel Recording Architecture for High Density Electrical Mapping

A Liberos*, MS Guillem, J Millet and AM Climent

ITACA, Universidad Politecnica de Valencia, Valencia, Spain

Introduction. The goal of our work is to describe and test a novel multichannel recording equipment architecture for cardiac mapping based on LabVIEW: the Reconfigurable Architecture for Electrical Mapping (RAEM). Methods. The RAEM architecture implements the communication between a generic analog acquisition hardware and a computer (PC) by means of a Field Programmable Gate Array (FPGA) and a Real-Time Controller (RTC). The first step of a RAEM system involves the temporal storage of a certain number of samples acquired from the analog block into a temporal memory installed in the FPGA. The second step of a RAEM system involves sending the data stored in the temporal memory to a PC by the Transmission Control Protocol (TCP). The third step of a RAEM system is the reassembling of the information into the PC in order to store and to represent it. Evaluation of the performance, versatility and limitations of the presented architecture was done by using three different National Instruments (NI) hardware solutions (Single-BoardRIO-9631, Single-BoardRIO-9642 and the CompactRIO-9024+CompactRIO-9104). Throughput for each hardware solution will be measured for an increasing cadence in TCP packet generation, or Data Readout Period (DRP). Results. RAEM architecture programmed in LabVIEW was executable for the three evaluated NI solutions independently of the hardware. In order to obtain the maximum throughput, a compromise between temporal memory size of the FPGA, RTC processor capability and DRP is required. Maximum data throughput achievable for each hardware solution were 19, 22 and 51 Mbps, obtained for DRPs equal to 13, 20 and 30 ms, respectively. Conclusion. The design of the RAEM system, based on LabVIEW and RIO hardware, allows migration to new hardware platforms keeping the same architecture.

Predicting Unpinning Success Rates for a Pinned Spiral in an Excitable Medium

A Behrend*, P Bittihn, S Luther

Max Planck Institute for Dynamics and Self-Organization
Goettingen, Germany

Today, the only robust technique for terminating ventricular fibrillation is an electrical shock of up to 400 joules. A reliable alternative to this procedure is desirable, as the strong currents of the shock may result in cardiac lesions and therefore may increase the risk of further arrhythmias. To understand how other, more gentle, pacing protocols could lead to a termination of ventricular fibrillation, it is crucial to clarify the underlying mechanisms.

Fibrillation and other life-threatening cardiac arrhythmias are associated with the existence of spiral waves in the tissue. Their termination by conventional anti-tachycardia pacing (ATP) is substantially limited by anchoring of these waves at natural heterogeneities. Far-field pacing (FFP) is a control strategy that has been shown to be capable of unpinning waves from obstacles. For the application of several periodic pulses, the success of unpinning is determined by the initial position of the spiral as well as by the pacing frequency. Therefore, we systematically study the response of a pinned spiral wave to a series of periodic FFP-pulses in a generic model of excitable media for a broad range of pacing frequencies. From the phase response of the spiral to a single pulse only, we construct an iterative map for the response to multiple pulses. For pacing frequencies lower than the spiral frequency, the map accurately predicts the phase response and the unpinning success rate for further pulses. For high pacing frequencies, however, the phase response predicted by the iterative map deviates from the results obtained by direct numerical simulations due to the interactions of consecutive pulses. We identify and discuss the mechanisms underlying this frequency-dependent deviation.

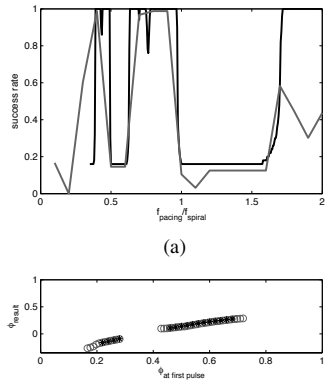

Prediction of (a) the success rate for 8 periodic FFP stimuli for different pacing frequencies (b) the resulting phase ϕ after 2 pulses ($f_{\mathrm{pacing}}/f_{\mathrm{spiral}} = 0.8$). Black: prediction by the iterative map. Red: success rate determined by direct simulation (in steps of 0.1).

Analyzing Thorough QT Study 1 & 2 in the Telemetric and Holter ECG Warehouse (THEW) using Hannover ECG System: A Validation Study

Antoun Khawaja*, Ratko Petrovic, Anton Safer, Tobias Baas, Olaf Dössel and Ronald Fischer

Biosigna GmbH /CareFusion Research Services, Munich, Germany

Following the ICH E14 guideline, the measurement of QT/QTc prolongation has become the standard surrogate biomarker for cardiac drug safety evaluation. The focus is on reliability and precision of the evaluation, as the low threshold level of just about five to ten milliseconds may decide on the faith of a drug development. Attempts to automate ECG evaluation meet concerns that algorithms might fail under challenging conditions. Therefore, validation of automated ECG algorithms is needed to build trust in their reliability and precision. Hannover ECG System (HES) is one of the well-renowned and well-reputed ECG analysis and interpretation programs worldwide. In this work we demonstrate the ability of HES to assess drug effects by detecting QT/QTc prolongation as mentioned, using THEW database studies Thorough QT (TQT) 1 and 2. For the assessment of drug effect, calculation of double delta parameters was performed for RR, QT/QTc changes from the baseline in both studies. Baseline was considered from start of recording to the time of drug administration and was characterized by the median of parameters. The single delta differences are calculated by baseline subtraction from all time segments. Furthermore, double delta difference was built by subtracting placebo single delta from Moxifloxacin single delta for each study subject. Finally, double delta differences were characterized by mean, median, SEM and 95% CI per hour. For brevity only results from TQT1 and the maximum effects are reported here. Results: double delta difference means [ms] (SEM [ms]; maximum effect time[h]); QT: 12.0 (2.56; 3 to <4); QTcB: 14.0 (1.88; 2 to <3); QTcF: 12.9 (1.68; 3 to <4) and QTcI: 12.3 (1.88; 3 to <4). Similar results have been reported from comparable studies. We conclude that HES algorithm is capable to evaluate TQT studies according to the requirements specified by ICH E14 guideline.

Torsadogenic Drug-Induced Increased Short-term Variability of JT-area

Xiao Jie*, Blanca Rodríguez and Esther Pueyo

Computing Laboratory, Oxford University, Oxford, United Kingdom

It is well recognized that QT prolongation alone is inadequate for assessment of drug-induced cardiac toxicity. Increased beat-to-beat variability of repolarization (BVR) has been suggested to indicate increased susceptibility to drug-induced arrhythmia. The goal of this study is to characterize BVR in patients before and after administration of sotalol, a torsadogenic antiarrhythmic drug, in the search for new biomarkers of proarrhythmic risk. Two electrocardiogram (ECG) datasets, consisting of individuals with (group I, n=16) and without (group II, n=17) history of drug-induced torsades de pointes, were employed. Identification of peaks and limits for individual P, QRS and T waves was performed via quadratic spline wavelet transform of the ECG signal. QT interval was measured as the interval between the onset of QRS wave and the end of the T wave. JT-area (total T wave area) was computed as the area between the curve and the baseline from J-point to the end point of the T wave. BVR was evaluated by short-term variability (STV, the mean orthogonal distance from each point in the Poincaré plot to the diagonal) of QT interval and JT area. We found that in both groups, sotalol injection resulted in significant increase in STV of JT-area (from 3.1 ± 2.3 to 4.8 ± 2.6 mVms in group I, p=0.008; from 3.5 ± 1.6 to 4.5 ± 2.3 mVms in group II, p=0.009), while no significant change occurred in STV of QT interval (from 16.3 ± 18.0 to 17.6 ± 17.9 in group I, p=0.7; from 12.2 ± 9.6 to 16.4 ± 19.0 ms in group II, p=0.4). In conclusion, STV of JT-area, as an indicator of BVR, has the potential to be a biomarker for drug toxicity. Further evaluation is needed in order to establish its predictive value.

S71

Electrocardiographic Markers Associated with Sotalol-induced Torsades de Pointes

Jean-Philippe Couderc*, Xiajuang Xia, Stefan Kaab and Wojciech Zareba

University of Rochester Medical Center, Rochester, NY, United States

Background: Recent recommendations from the AHA, ACCF and the ISCE have highlighted the need for monitoring in-hospital patients with a risk for drug-induced QT prolongation and torsades de pointes (TdPs). In this work, we compared repolarization prior to the occurrence of drug-induced TdPs in three cases of sotalol-induced TdPs (+TdPs) to the ECG patterns preceding maximum QTc prolongation in healthy individuals exposed to sotalol who did not develop TdPs (-TdPs). Method: Based on data from the Telemetric and Holter ECG Warehouse (THEW), we implemented a computer-based analysis of the repolarization signal (ST-T-wave) on 10-min intervals just prior to the arrhythmia (for the group with TdPs-n=3) and just prior maximal QTc prolongation (in the individuals without sotalol-induced TdPs-n=3). We computed the delta values using baseline values one hour prior to the first interval (10-min off drug). We investigated QT/QTc prolongation, QT variability, ventricular ectopic beats (VPBs) frequency, T-wave amplitude, T-peak to Tend interval, T-wave complexity and macro T-wave alternans. Results: The table below describes the baseline differences between the two groups. The analysis of changes of these parameters in reference to baseline revealed primarily an increased QTc variability prior to the event, presence of VPCs prior to TdPs, and profound changes in T-loop morphology in patients developing TdPs.

+TdPs (N=3) -TdPs (N=3) RR (msec) 1038±119 1038±91 QTcF (msec) 555±34 478±21 TpTe (msec) 118±9 107±28 madQTc* (n.u.) 0.93±0.64 0.23±0.08 T-wave magnitude (mV) -0.36±0.35 0.22±0.17 Macro T-Wave alternans No No T-wave complexity (n.u.) 0.29±0.18 0.18±0.04 VPCs (n/10 min.) 60±20 0±0

Conclusion: The individuals who developed sotalol-induced TdPs exhibit longer baseline QTc interval. There was no difference in the magnitude of sotalol-induced prolongation of QTc between the groups with and without TdPs. Individuals with TdPs reveal larger beat-to-beat variability of the QT intervals, lower T-wave amplitude and presence of VPBs.

Comparison of Three T-end Delineation Algorithms Based on Wavelet Filterbank, Correlation and PCA

Tobias Baas*, Franz Gravenhorst, Ronald Fischer, Antoun Khawaja and Dössel

Institute of Biomedical Engineering (IBT), Karlsruhe Institute of Technology (KIT), Karlsruhe, Germany

There is a large interest in analyzing the QT-interval, as a prolonged QT-interval can cause the development of ventricular tachyarrhythmias such as Torsade de Points. One major part of QT-analysis is T-end detection. Three T-end delineation algorithms have been developed and applied to Physionet QT database (2-Lead 250Hz) and Through QT Study #2 from Telemetric and Holter ECG Warehouse (THEW) (24-Hour 12 Leads 1000Hz). First method (WTDM) is wavelet based, detecting the maximum of the T-wave by evaluating detail coefficients of a stationary wavelet transform. Starting from the detected maximum, T-end is calculated by a linear tangential approach to the ECG baseline. Methods, based on correlation (CTDM) and PCA (PTDM) need a template for T-end detection. This template, generated by a window starting at the R-peak of an RR-interval and ending at 70% of the RR-interval is cut out for a lage number of heart beats. These T-wave containing signals are used to calculate the template as the mean. Thus, a patient related template is found, in which a precise T-end can be marked. For CTDM the template is correlated to every RR-interval in the ECG-record, while it is stretched and shifted. The best correlation in the interval is used to mark T-end as T-end of the template. PTDM uses PCA to get the best stretch- and shift factors for every heart beat. T-end can than be calculated by the stretched and shifted template similar to CTDM. All algorithms were tested at Physionet QT database with good results, while PTDM produced better results than WTDM and CTDM got best results. Standard derivation in sampling points (fs=250Hz) have been 33.4 WTDM, 8.1 PTDM and 7.8 CTDM. In a second validation we were able to detect 5-10ms QTc-prolongation in a double delta QTc study from THEW with Moxifloxacin. It could be seen that WTDM is prone to interference while CTDM works most stable even under bad conditions.

QT/RR Coupling and Gender Differences

Josef Halamek*, Pavel Jurak, Jolana Lipoldova and Pavel Leinveber

Magnetic Resonance and Bioinformatic, Institute of Scientific Instruments, ASCR, Brno, Czech Republic

Data from the THEW database (72 men, 55 women) was used to test various QT/RR models and gender differences. Three dynamic models (transfer function model TRF, exponential weighting EXP, and EXP with added direct coupling with RR EXPDC) and a static nonlinear model (NONLIN) were tested. Two records (30 min) were analyzed for each subject. Sets of RR and QT intervals together with the moving average of RR and QT intervals were analyzed. The tested parameters were: QTc, QT/RR slope (GainS, slope is QT gain for slow RR variability), time constant of QT adaptation, QT gain for fast RR variability (GainF) and error signal between measured and model QT (RMS). Results: A) Gender differences: Women have longer QTc $p<0.0001$, higher level of GainS and GainF and faster QT adaptation, all $p<0.05$. B) Model differences: NONLIN has significantly higher RMS and lower QTc ($p<0.001$) relative to dynamic models. NONLIN has higher intersubject parameter differences and higher dependency on the number of averaged intervals. Dynamic models: QTc differences (paired tests) are minimal (2.4 ± 4 ms). The EXP model has significantly higher RMS $p<0.01$ than the TRF or EXPDC model. Conclusion: i) Dominant QT/RR coupling is dynamic. The nonlinear static model does not assess the proper QTc even with averaging. ii) The EXP model overestimates random QT variability (RMS); its step response differs from known QT step response. The best models are TRF and EXPDC according to the mathematical test (minimal RMS) and physiological test (shape of step response). If only QTc is analyzed, the choice of dynamic model is not important. iii) The longer QTc and steeper GainS in healthy women are compensated to an extent by higher GainF and faster QT adaptation. GainF is an important parameter. The QT dynamic differences from steady state are proportional to GainS - GainF. We hypothesize that an analysis of the influence of drugs on QT dynamic properties may explain why cardiac arrhythmias and drug-induced Torsades de Pointes are more prevalent in women. Such analysis supposes the standardization of the QT model and measurement with defined significant excitation of RR.

Analysis of Heart Rate Adaptation in Long-Term ECG Recordings Using RR-Binning

Lars Johannesen*, Ulrik Silvanus Lerkevang Grove, Jens Stampe Soerensen, Mick Lykkegaard Schmidt, Claus Graff, Jean-Philippe Couderc

Health Science and Technology, Aalborg University, Aalborg, Denmark

Understanding how the heart rate (HR) affects different ECG segments is required to assess the presence of abnormalities in the ECG. The 24-hour Holter offers an opportunity to investigate this relationship. We propose two methods to investigate this relationship using RR-binning: a subject specific and a population based profile. We used daytime recordings (7 am to 11 pm, lead X) from 157 healthy subjects (78 males, aged 37 $\pm$ 15 years) and (79 females, aged 38 $\pm$ 16 years) from the Telemetric and Holter ECG Warehouse. The subject specific ECG profile was created by grouping the cardiac beats according to the previous RR-interval and calculating a median beat for each RR-interval. The population based profile was generated as the median of subject specific profiles. The same procedure was applied for 51 AMI subjects grouped by location of infarction. Group 1 (anterior/ant. lateral) included 23 subjects (17 males, aged 52 $\pm$ 14 years) and (6 females, aged 68 $\pm$ 15 years). Group 2 (inferior/inf. lateral) included 28 subjects (22 males, aged 55 $\pm$ 12 years) and (6 females, aged 62 $\pm$ 15 years). Both AMI groups had acute and stable phase recordings. The profiles were used to assess T-wave adaptation to HR. Population based T-wave adaptation to HR was observed for healthy subjects (R^2=0.90) but was less less pronounced for AMI subjects (group 1: R^2=0.08, acute and R^2=0.31, stable) and (group 2: R^2=0.23, acute and R^2=0.20, stable). At the subject level, T-wave adaptation to HR was R^2=0.78 for healthy subjects, and for AMI subjects: (group 1: R^2=0.92, acute and R^2=0.62, stable) and (group 2: R^2=0.85, acute and R^2=0.79, stable). There was a difference in T-wave amplitude adaptation to HR between AMI and healthy subjects for population-based profiles, which was not present at the subject-specific level.

Optimal Delineation of PCG Sounds via False-Alarm Bounded Segmentation of a Wavelet-Based Principal Component Analysis Metric

Mohammad Reza Homaeinezhad* and Ali Ghaffari

Department of Mechanical Engineering, KN Toosi University of Technology, Tehran, Iran

The aim of this study is to describe a new false-alarm probability (FAP) bounded unified framework for segmentation of the phonocardiogram (PCG) signal sounds registered by an electronic stethoscope board. To meet this end, after application of appropriate pre-processings, a fixed sample size sliding window is moved on the selected scale and in each slid, six feature vectors namely as summation of the nonlinearly amplified Hilbert transform, summation of absolute first order differentiation, summation of absolute second order differentiation, curve length, area and variance of the excerpted segment are calculated to construct a newly proposed principal components analyzed geometric index (PCAGI) (to be used as the segmentation decision statistic (DS)) by application of a linear orthonormal projection. Next, using an adaptive smoothing filter (ASF), the obtained metric is modulated and is freed from the fast fluctuations. Afterwards, histogram parameters of the filtered DS metric are used to regulate the -level Neyman-Pearson classifier for FAP-bounded delineation of the PCG events. To assess performance quality of the proposed PCG segmentation algorithm, the method was applied to all 85 records of Nursing Student Heart Sounds database (NSHSDB) including stenosis, insufficiency, regurgitation, gallop, septal defect, sound split, rumble, murmur, clicks, friction rub and snap disorders with different sampling frequencies. Also, the method was applied to the records obtained from an electronic stethoscope board designed for fulfillment of this study in the presence of high-level power-line noise and external disturbing sounds and as the results, no false positive (FP) or false negative (FN) errors were detected.

The Evaluation of Methods in Determination of the Arterial Compliance for Real-Time Applications

Weichih Hu*, Liang-Yu Shyu, Hou-Ming Cheng and Chen-Huan Chen

Dept. of Biomedical Engineering, Chung Yuan Christian University, Chung Li, Taiwan

Using pulse wave velocity (PWV) to determinate the arterial stiffness was generally accepted. However, using the arterial system relaxation constant with the Windkessels model to index the arterial stiffness may simplify the procedure. To accurate evaluation of arterial compliance is importance in its common index for the determination the arterial stiffness. In comparison the indexes of arterial stiffness such as pulse wave velocity (PWV) and the arterial system relaxation constant using Windkessels model, the compliance is a common dominator. There were two locations that were generally used to acquire the blood pressure waveform noninvasively. One is at carotid artery with the tonometry device or at the brachial artery with pressure volume relation method. There were two methods of calculating the compliance. One was using the area proportion under pressure waveform (C1). And, the other method could be using the formulas of arterial system relaxation constant (C2). Both methods have assumed a hypothetical stoke volume and using a mean arterial pressure. We have acquired and examined blood pressure waveform using tonometry at carotid artery and pressure volume relation at brachial artery from 581 subjects. The pulse velocity has also acquired at the same situation. The compliance of carotid artery calculated using area method was 1.41 ± 0.548. And, the compliance using relaxation constant was 1.41 ± 0.527. The correlation was 0.8 and the R2 was 0.7. For brachial artery, the compliance calculated from area proportion was 1.14 ± 0.4288. And, the compliance calculated using relaxation constant was 0.97 ± 0.36. The correlation of compliance was 0.76 and R2 was 0.82. The correlation of compliance between two pressure locations was 0.64 and R2 was 0.68 using area proportional methods. The correlation of compliance using relaxation constant was 0.5 and R2 was 0.58. The correlation of compliance at both locations and the methods of calculation were high. This result means that the measurement of compliance could be carried out at brachial artery with a simpler instrument such as using oscillometric blood pressure method.

S72

Asymmetrical Oscillometric Pulse Waveform Envelopes in Normotensive and Hypertensive Subjects

Dingchang Zheng*, Roberto Giovannini and Alan Murray

Regional Medical Physics Department, Newcastle University, Newcatle upon Tyne, United Kingdom

Blood pressures in automated oscillometric measurement devices are determined by analysing different features from the oscillometric waveform. This study investigated the symmetry of the oscillometric waveform shape in normotensive and hypertensive subjects.

Ten normotensive (SBP$<$140 mmHg) and ten hypertensive subjects (SBP140 mmHg) were studied with three repeat measurements. The oscillometric cuff pressure was deflated linearly and recorded digitally. Auscultatory SBP and DBP were obtained during cuff deflation. The oscillometric waveform envelope was related to cuff pressure and constructed from the sequential peaks of the oscillometric pulses extracted from the recorded cuff pressure. The cuff pressure corresponding to the maximum oscillometric pulse amplitude was taken as the automated MAP. The cuff pressures corresponding to 30%, 50% and 70% of the maximum oscillometric pulse amplitude in each envelope were measured for both the high and low pressure regions. At each amplitude level, the cuff pressure widths (absolute difference to the automated MAP) in the high and low pressure regions were compared. The average pressure widths from the three repeat measurements were used as the reference value for that subject.

For the normotensive group, the overall mean$\pm$SD of the cuff pressure widths in the high and low pressure regions for the normalised amplitude levels of 30%, 50% and 70% were 43$\pm$6 vs 36$\pm$9 mmHg, 29$\pm$6 vs 17$\pm$7 mmHg, and 22$\pm$5 vs 10$\pm$4 mmHg respectively. For the hypertensive group, the corresponding values were 52$\pm$10 vs 47$\pm$10 mmHg, 40$\pm$9 vs 28$\pm$10 mmHg, and 28$\pm$8 vs 19$\pm$8 mmHg. For both groups, the cuff pressure widths in the high pressure region were significantly larger than in the low pressure region at the normalised amplitude levels of 50% and 70% (all P$<$0.01).

In conclusion, the asymmetrical feature of the oscillometric waveform envelope has been confirmed in both normotensive and hypertensive groups.

Detection of Systolic and Diastolic Durations on Cardiac Output and Arterial Pressures

Mick Lykkegaard Schmidt*, Lars Johannesen, Jens Stampe Soerensen, Kasper Lundhus, Samuel Emil Schmidt and Niels-Henrik Staalsen

Health Science and Technology, Aalborg University, Aalborg, Denmark

In coronary artery bypass graft patency research, the graft quality is often quantified by analysis of simultaneously recorded physiological signals such as graft flow, electrocardiogram, arterial pressure and cardiac output. From these recordings the diastolic filling and the pulsatility index can be estimated giving an indication of the quality of the graft and anastomosis. In this paper we present two methods to measure systolic and diastolic durations from arterial pressure and cardiac output recordings. The methods located the systolic and diastolic start which was defined as extrema or zero-crossings. The signals were initially baseline filtered and a ruleset was applied to determine whether to choose the extrema or zero-crossing. The methods were evaluated by comparing the systolic and diastolic durations between the two methods in 96 measurement sets from 8 pigs undergoing bypass surgery. Furthermore we compared diastolic filling and pulsatility index. We obtained a mean difference between arterial pressure and cardiac output, in systolic and diastolic duration of -119.84ms ($\pm$78.82ms) and 118.57ms ($\pm$ 97.49). The correlation between systolic and diastolic duration was 30.97% and 80.54% respectively. For diastolic filling and pulsatility index we obtained a mean difference between arterial pressure and cardiac output of -13.36% ($\pm$ 11.47) and -0.03 ($\pm$1.90) respectively, with correlation coefficients of 56.19% and 56.29%. The results indicate a correspondence between the systolic and diastolic detection of cardiac output and arterial pressure, which indicates that the developed methods work. However, there is a better correlation between the diastolic durations and a bias between the two measurements, which is expected as systolic start for arterial pressure signals is delayed and the systolic period is shorter compared to cardiac output. The use of more than one technique to detect the systolic and diastolic can be used to ensure more stable results when performing coronary graft patency assessments.

Comparison between Sample Entropy and AR-models for Heart Sound-based Detection of Coronary Artery Disease

Samuel Schmidt*, John Hansen, Claus Holst Hansen, Egon Toft and Johannes Struijk

Department of Health Science and Technology, AAU, Aalborg So, Denmark

The first reported observations of rare diastolic murmurs in patients with coronary artery disease (CAD) dates back to the late sixties. Several studies have subsequently examined various signal processing methods for identification of weak heart murmurs. Two such methods are autoregressive (AR) modeling and sample entropy. The aim of the current study is to analyze the relationship between features from an AR-model and features describing signal entropy. Sample entropy and the poles of a 6th order AR model were calculated from diastolic intervals in heart sound recordings randomly selected from a database of high quality stethoscope recordings. In total 100 recordings were analyzed (50 patients with two recordings each). The patients were referred for coronary angiography and the percentages of artery occlusions were collected from the angiography. The stethoscope recordings were made from the left 4th intercostal space on the chest of patients. The recordings were sampled at 4000 Hz and band-pass filtered with a 6 order Chebyshev filter with pass-band edge frequencies at 50 Hz and 500 Hz. The parameters for Sample entropy was m=2 and r=0.5 x STD. The angle of the first AR pole was the best AR feature for discriminating CAD patients from non CAD patients. CAD patients (N=23) were defined as patients having at least one coronary stenosis with a minimum of 50% diameter reduction. The area under the receiver operating characteristic curve was 0.765 (95% CI: $\pm$0.09) for the AR pole and 0.762 (95% CI: $\pm$0.09) for Sample entropy. The spearman correlation between the two measures was 0.92.

An Automatic Media-Adventitia border Segmentation Approach for IVUS images

Matheus Cardoso Moraes[1], Sergio Shiguemi Furuie[1]

[1] Department of Telecommunication and Control - School of Engineering, University of São Paulo, Brazil

In image processing, segmentation is considered one of the most important and hardest operations. The media-adventitia segmentation, in Intravascular Ultrasound (IVUS) images (Figure), is one of the first steps for a vase 3D reconstruction, and it is an important operation for many applications: measurements of its border circumference, area and radius; for studies about the mechanical properties and anatomical structures of vessels; which consequently will infer about therapy plans and evaluations; localization of pathologies. The purpose here is to segment the media-adventitia in IVUS images with high accuracy by combining a set of imaging-processing techniques: Speckle Reducing Anisotropic Diffusion (SRAD), Wavelet, Otsu and Mathematical Morphology. Firstly, SRAD is applied to attenuate the speckle noises. Next, the vessel and plaque features are extracted by performing Wavelet Transform. Optimal thresholding is carried out by Otsu to create a binarized version of these features. Then, Mathematical Morphology is used to obtain an adventitia shape. Finally, this approach is evaluated by segmenting 100 challenging images, obtaining an average of True Positive (TP), False Positive (FP(%)), False Negative (FN(%)), Max False Positive (Max_{FP} (mm)), Max False Negative (Max_{FN} (mm)) (Table). Furthermore, its effectiveness is demonstrated by comparing this result with a recent one in the literature.

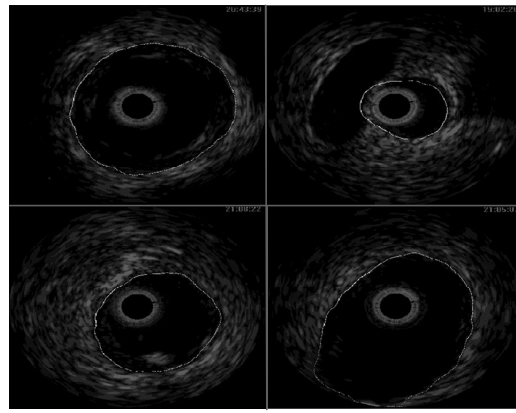

Figure. Segmentation result.

Table. Assessment of the proposed approach

TP (%)	FP (%)	FN (%)	Max.$_{FP}$ (mm)	Max.$_{FN}$ (mm)
92.83±4.91	3.43±3.47	7.17±4.91	0.27 ±0.22	0.31±0.2

Quantitative Assessment of the Effects of Annuloplasty on Mitral Annulus Dynamic Geometry using Real-Time 3D Echocardiography

Laura Fusini, Federico Veronesi, Cristiana Corsi, Paola Gripari, Francesco Maffessanti, Francesco Alamanni, Marco Zanobini, Moreno Naliato, Gloria Tamborini, Mauro Pepi and Enrico G Caiani*

Biomedical Engineering Dpt., Politecnico di Milano,

Mitral valve (MV) repair is the preferred treatment for mitral regurgitation associated with organic MV prolapse (MVP) . Our goal was to describe the dynamic changes in mitral annulus (MA) geometry following MV repair with annuloplasty, using custom software for MA tracking from transthoracic real-time 3D echocardiography (RT3DE). Methods. Forty-four patients (62 ± 11yrs) with organic MVP and ejection fraction (EF)$>55\%$ were studied by RT3DE the day before MV repair (23 received a complete rigid ring - RIG, 21 an incomplete flexible one - FLEX), and 3 and 6 months after. An age-matched group of 20 normal (NL) subjects (57 ± 9yrs) was studied as control. After manual initialization, the MA was tracked frame-by-frame in the 3D space, and several parameters were computed: min and max 3D surface area (A), delta area (DA=maxA-minA), 2D projected vs 3D surface area ratio (A2D/A3D), max longitudinal displacement (LD), mean height (H) and delta height (DH=maxH-minH). Differences vs pre-surgery, and in MVP vs NL values were tested ($p<.05$). Results. As expected, MVP had an enlarged MA resulting in greater area and height during the cardiac cycle, leading to a reduced planarity compared to NL. Annuloplasty resulted in: 1) reduced area in both RIG and FLEX, with minimal DA during the cardiac cycle; 2) more planar MA shape, as depicted by a reduced H and an increased A2D/A3D. Interestingly, at 3- and 6-months, FLEX height was greater than RIG, due to the lower planarity associated with incomplete ring design compared to the complete one. At 6-months, all values were found unchanged. Conclusions. MA dynamic analysis from RT3DE was feasible in patients undergoing MV repair, giving new insights in the in-vivo performance of the implanted annular prosthesis. This would constitute a new useful tool for the surgeon in the clinical decision process and in follow-up monitoring.

Heterogeneity of the Myocardial Strains as Revealed by Applying a Wavelet De-noising Process to the Myocardial Velocities

Noa Bachner*, Offir Ertracht, Nir Zagury, Ofer Binah and Dan Adam

Faculty of Biomedical Engineering, Technion-Israel Institute of Technology, Haifa, Israel

Introduction One of the novel tools in echocardiography is the measurement of 2D strain, based on speckle tracking. The tracking provides the myocardial velocities, in time and space domains, from standard echo cines. Since the measured velocities are noisy, currently only global measures are obtained. In this study we propose using a validated wavelet de-noising process for filtering the raw velocities, as this process allows preserving the high frequency spatial and temporal components of the signals. Methods Echocardiography was applied to 27 normal adult Sprague-Dawley rats, and 3 short axis scan levels were obtained. The cines were analyzed by a commercial echocardiography speckle tracking program, and the myocardial velocities were de-noised by a novel 3 dimensional wavelet de-noising process. The circumferential and radial strains were calculated from the de-noised velocities for 6 segments. Single factor analysis-of-variance was performed to determine whether heterogeneity of the strain exists among the different segments. Results The circumferential strain was found to be heterogeneous at the apex and base levels ($P<0.001$); while it was homogeneous at the mid-ventricular level. At the apical level, the anterior-septum exhibited circumferential strain of -10.3$\pm$8.4%, whereas the lateral wall exhibited -27.4$\pm$7.2%. The radial strain was found to be heterogeneous at all scan levels (apex $P<0.01$, base and mid-ventricle $P<0.001$), while the radial strain at the septum (apex 18.1$\pm$12.3%, mid-ventricle 22.9$\pm$9.1%, base 8.2$\pm$10.3%) was smaller than the one at the free wall (apex 29.5$\pm$13.8%, mid-ventricle 29.9$\pm$12.4%, base 16.3$\pm$13.9%) for all scan levels (apex $P<0.001$, mid-ventricle and base $P<0.05$). Conclusions Wavelet de-noising of the myocardial velocities reveals heterogeneity of the circumferential and radial strains that was never reported before, which is important for understanding myocardial function. Identifying this heterogeneity is crucial when attempting to diagnose abnormal segmental myocardial function.

Fusion of Electro-Anatomical Mapping and Speckle Tracking Echography for the Characterization of Local Electro-Mechanical Delays in CRT Optimization

François Tavard, Antoine Simon, Erwan Donal, Alfredo Hernandez and Mireille Garreau*

LTSI, Université de Rennes 1 and INSERM, RENNES, France

Cardiac Resynchronization Therapy (CRT) has been shown to improve cardiovascular function and reduce mortality rates in a specific subpopulation of patients suffering from heart failure. However, about 1/3 of the patients implanted do not respond appropriately to this therapy. One way to decrease this non-response rate would be to better select the candidates to a CRT. A characterization of the electro-mechanical activation periods of each region of the left ventricle (LV) could be useful for this selection process. This study aims to perform this characterization by the fusion of electrical, mechanical and anatomical information acquired from Electro-Anatomical Mapping (EAM), Speckle Tracking Echocardiography (STE) and Multislice CT (MSCT) imaging, respectively. LV surfaces automatically extracted from 4D MSCT images are chosen as a reference for the registration and fusion of EAM and STE data. EAM provides 3D anatomical points of the LV and associated local activation time (LAT) delays. STE produces 2D contours of the LV and their displacements and strains. In a previous work, we proposed a semi-automatic rigid registration method for the fusion of EAM and MSCT LV-surfaces. In this paper, we propose an additional automatic rigid registration method of STE and MSCT data, based on the minimization of a metric calculated between STE contours and 2D contours extracted from MSCT surfaces. This metric includes distance terms, weighted according to anatomical a priori knowledge. After registration, local electrical and mechanical activation times can be compared in the same space through 2D quantitative maps, providing means to compute and to characterize local electro-mechanical couplings on the LV. Correlation ratios (r) between local and global electro-mechanical delays from 6 different LV regions were computed for two patients (Patient 1: r=0.978; Patient 2: r=0.783). The complementary information obtained from the local electro-mechanical indexes may be useful for a better patient selection for CRT.

Myocardial Ischemia Detection Algorithm (MIDA): An Automated Echocardiography Sequence Analysis for the Diagnosis of Heart Muscle Damage

Vijayalakshmi Ahanathapillai and John Soraghan*

Centre for Excellence in Signal & Image Processing, University of Strathclyde, Glasgow, United Kingdom

Myocardial Ischemia or damaged heart muscle does not contract as much as the healthy muscle, resulting in abnormal heart wall movement. Myocardial Ischemia Detection Algorithm (MIDA) is developed to analyze the echocardiography sequences automatically in order to detect the presence of such heart muscle damage within the heart chamber. Firstly, the proposed algorithm involves applying a wavelet transform based speckle noise reduction followed by contrast enhancement using Delaunay triangulation technique to enhance the heart wall boundary. Following this, a Fuzzy multi resolution edge detection method is used to obtain both the inner and outer heart wall boundaries from each Echo scan frame and are subsequently combined to form a composite image. This image contains useful information regarding the movement of the heart wall from the contracted phase to the relaxed phase. Parameters which describe the heart function such as Ejection Fraction, LV Volume, and Cavity area are also determined from heart wall boundaries. Finally, statistical pattern recognition techniques such as Principal Component Analysis (PCA) and Independent Component Analysis (ICA) are applied to extract features which are then classified using a combined k-nearest neighbour (Combined kNN) classifier to identify the abnormal heart wall movement. This Combined kNN classifiers combines different kNN classifier outputs in a way to increase the sensitivity and better classification, when compared with SVM, Naive Bayes and linear classifiers. The total number of patient data used for testing was 62, out of which 27 hearts had normal wall movement and 35 hearts possessing varying levels of abnormal wall movement in different wall segments. A correct recognition of 83.87% was observed with a sensitivity of 82.85% and specificity of 85.18%. The results to date indicate clearly that the proposed feature extraction and classification technique can be used as an effective tool for automatically diagnosing Myocardial Ischemia.

Segmentation of the Full Myocardium in Echocardiography using Constrained Level-Sets

Martino Alessandrini*, Thomas Dietenbeck, Daniel Barbosa, Jan D'Hooge, Olivier Basset, Nicolo Speciale, Denis Friboulet and Olivier Bernard

ARCES, University of Bologna, Bologna, Italy

In echocardiography, left ventricle detection is a common practice in order to retrieve indexes of myocardial health. Although a great attention has been given to the segmentation of the endocardium, a very limited literature addresses the detection of both endo- and epicardial contours. Nevertheless, a trustful detection of both boundaries is fundamental in order to estimate clinical parameters like the ventricular mass.

Hereto, the aim of this work is to propose an original active contour model based on level-set technique specifically designed for the detection of the whole myocardium in short-axis ultrasound scans.

The proposed segmentation flow proceeds by seeking the maximal statistical separation between target, i.e. the myocardium, and background. In order to deal with low-contrast or missing boundaries, a localized version of standard region-based methods is adopted. Moreover, shape prior information is efficiently embedded in the evolution equation, forcing the active contour to be approximately annular. This prevents the detection of undesired small structures, like papillary muscles. With the resulting formalism the detection of both endo- and epicardium is addressed efficiently with a single level-set function.

Forty B-mode short-axis images were acquired from 5 different patients. Both endo- and epicardium were manually segmented by two expert physicians. We assessed the performances of the algorithm by measuring Mean Absolute Deviation (MAD) and Hausdorff Distance (HD) between automatic and manual contours, as well as the correlation coefficient (R) between the areas they enclose. Six points were placed by the user for initialization.

We obtained MAD = 3.1 ± 0.5 pixels and HD = 9.2 ± 2 pixels. These values fall within the intra-observer variability between the two experts, given by MAD = 3.7 ± 1.2 and HD = 10.6 ± 3.7. The correlation coefficient was R = 0.98.

The presented method is shown to be a reliable and accurate tool for full myocardium segmentation on ultrasound images.

Potential Pharmacological Therapies for Atrial Fibrillation: A Computational Study

Carlos Sánchez*, Alberto Corrias, Pablo Laguna, Mark Davies, Jonathan Swinton, Ingemar Jacobson, Esther Pueyo and Blanca Rodríguez

University of Zaragoza, Zaragoza, Spain

Persistent atrial fibrillation (AF) is mainly sustained by reentrant wavelets which propagate through excitable tissue, but its underlying ionic mechanisms are still unclear. In this study we: 1) quantify the sensitivity of properties related with arrhythmic risk to changes in human atrial ion channel properties; 2) investigate alternative methods to prevent AF from propagating. Simulations are performed using the Maleckar action potential (AP) model and its extension to tissue, and validated using experimental data from the literature. The sensitivity analysis shows that IK1 inhibition by 30% results in an anti-arrhythmic increase in action potential duration (APD) (from 197 ms under control conditions to 318.2 ms) and Vrest (from -73.75 mV to -64.7 mV). Regarding APD rate adaptation, overexpression of either ICaL or INaK causes at least a 1.5-fold anti-arrhythmic decrease of the time constants associated with both fast and slow adaptation phases. Overexpression of IK1 or inhibition of INaK implies shallower APD restitution slopes that favor reentry stability but prevent wave-breaks from happening. Tissue simulations show that 30% block of INa leads to a significant slowing of conduction velocity (CV) (from 48.5 cm/s to 36.38 cm/s). Besides, 30% block of IK1 and INaK lead to anti-arrhythmic increases in both effective refractory period (ERP) (from 223 ms to 287 ms and 272 ms, respectively) and wavelength (WL=ERP*CV) (from 10.82 cm to 14.28 cm and 13.45 cm, respectively). Simulations are also conducted to evaluate the role of electrical remodeling caused by sustained AF, resulting in lower ERP (151 ms), CV (45.95 cm/s) and WL (6.94 cm), and higher reentrant dominant frequency (from 4.39 Hz under control to 6.84 Hz). Sensitivity of parameters related to both reentry stability and reentrant properties to changes in ion channel electrophysiology as provided here can help in the design and screening of new multi-channel action anti-AF drugs.

Atrial Fibrillation-based Electrical Remodeling in a Computer Model of the Human Atrium

Gunnar Seemann*, Paola Carrillo, Stefan Ponto, Mathias Wilhelms, Eberhard P Scholz and Olaf Dössel

Institute of Biomedical Engineering, Karlsruhe Institute of Technology, Karlsruhe, Germany

Atrial fibrillation (AF) is a common cardiac pathology affecting 10% of the older population. AF is characterized by an abnormal rapid and irregular activation. Sustained AF contributes to congestive heart failure, ventricular arrhythmia, cardiac mortality and thromboembolic stroke. Additionally, AF modifies the atrial electrical properties (electrical remodeling) promoting the occurrence and maintenance of AF.

Electrical remodeling includes changes in the L-type calcium as well as the inward rectifier, the acetylcholine regulated and the outward rectifier potassium channels. These effects were integrated in the human atrial model of Courtemanche et al.. Electrical remodeling further includes a decrease in connexin40 expression. This was considered in the conductivity for the utilized monodomain equation calculating excitation propagation. As geometrical model, a 2D rectangle was used. To analyze the bahavior of physiology and remodeling, the action potential duration (APD), effective refractory period (ERP), conduction velocity (CV), wave length (WL) and their restitution curves were investigated. Furthermore, the number of spirals and the power spectrum of the pseudo ECG were analyzed.

APD in tissue was reduced from 322ms to 144ms for remodeling. Similarly, ERP was reduced from 330ms to 103ms. Both effects are due to the ion channel changes. CV was lowered from 755mm/s to 608mm/s mainly based on the conductivity reduction. As the WL is the product of ERP and CV, its reduction is even higher (from 249mm to 63mm) leading to a higher chance of occurrence and maintenance of AF. In the physiological case, no spirals could be initiated because of the long WL. For remodeling, a maximum of 7 spirals were initiated leading to a peak in the power spectrum of 10.32Hz.

The model shows the potential risk of electrical remodeling and can further be used in computational studies of AF treatment planning like RF ablation or drug design.

Functional Roles of Ionic Currents in A Mouse Sino-atrial Node Cell Model

S Kharche, M Lei, H Zhang

University of Manchester, UK

Introduction: Functional roles of ion currents in a mouse sino-atrial node (SAN) cell model were simulated by ion current block.

Methods: In the Mangoni et al. mouse SAN model, ionic currents were blocked to study their roles in pacemaking. $[Ca^{2+}]_i$ was buffered simulating effects of ryadonine. Effects of these simulations were quantified as alterations in cell action potential (AP) characteristics, *i.e.*, cycle length (CL), AP duration at 90% repolarisation (APD_{90}), maximum diastolic potential (MDP), and maximal upstroke velocity (dV/dt_{max}).

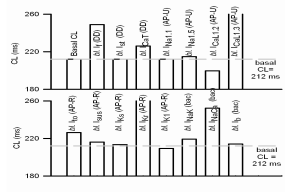

CL changes due to various ion channel blocking.

Results: Table 1 summaries AP basal properties. Phase plane analysis shows the diastolic depolarization (DD) is regulated by hyperpolarization activated (I_f), sustained inward (I_{st}), and T-type Ca^{2+} (I_{CaT}) currents. AP upstroke is regulated by the fast Na^+ ($I_{Na1.1}$ and $I_{Na1.5}$) and the L-type Ca^{2+} currents ($I_{CaL1.2}$ and $I_{CaL1.3}$). AP repolarisation is regulated by the transient outward (I_{to}), sustained outward (I_{sus}), rapidly and slowly activating delayed rectifying (I_{Kr} and I_{Ks} respectively) and the inward rectifier (I_{K1}) currents. The Na^+-K^+ pump (I_{NaK}) and Na^+-Ca^{2+} exchanger (I_{NaCa}) are background currents. As shown in Figure, I_f blocking increased CL by 17.4%. I_{CaT} block caused a 6% CL increase. Blocking $I_{CaL1.3}$ or I_{Kr} arrested pacemaking. Blocking I_{NaCa} caused an 18% CL reduction. Reducing $[Ca^{2+}]_i$ (0.1 μM to 0.001 μM) increased CL by 5.1%. A small 20% increase of $[Ca^{2+}]_i$ arrested pacemaking.

Conclusions: I_{st}, $I_{Na1.1}$, $I_{Na1.5}$ are not functional in the pacemaking. I_{NaCa} and I_{NaK} are functionally background currents rather than regulators of intracellular ionic concentrations. The model has limited predicative potential and requires further development.

Table 1. Experimental range and model AP features.

	CL (ms)	APD_{90} (ms)	MDP (mV)	dV/dt_{max} (V/s)	TOP (mV)
Exp. range	106 ~ 232	45.8 ~ 107.1	-70 ~ -52	8.2 ~ 45.2	-54.6 ~ -40
Model	212.31	121.1	-66.87	5.31	-47.3

Wavefront-Obstacle and Wavefront-Wavefront Interactions as Mechanisms for Atrial Fibrillation: A Study Based on the FitzHugh-Nagumo Equations

Claudia Lenk*, Mario Einax and Philipp Maass

Institute of Physics, Ilmenau University of Technology, Ilmenau, Germany

Atrial fibrillation (AF) is the most common arrhythmia of the heart in the industrialized countries. Understanding the mechanisms that lead to AF is at the root for improving existing or developing new therapies. In this work we investigate, based on the FitzHugh-Nagumo (FHN) equations for excitable media, certain generating mechanisms for AF that were suggested in the literature. In particular, we study the influence of locally modified cell properties (obstacles) on the propagation of initially planar excitation waves. In contrast to earlier studies, which considered passive or insulating obstacles, we consider areas where the cell properties vary gradually over some finite correlation length. We find that a transition from functional to anatomical reentry occurs in dependence of both the reduction strength of excitability and the size of the correlation length. This behaviour is characterized in terms of dynamical phase diagrams.

In order to tackle the question how regular self-excitatory sources as stable spiral waves in the left atrium can possibly lead to irregular, fibrillatory excitation patterns in the right atrium, we furthermore investigate the perturbation of regularly paced waves, representing, for example, those emanating from the sinus node, by regular waves emanating from another pacemaker, as, for example, a spiral wave. Both sources of the excitation waves are located in two distinct regions of the simulation area and are connected by a small bridge only. Here we find from the solutions of the FHN equations that the perturbation of the regularly paced waves by the waves emanating from the self-excitatory pacemaker can lead to fibrillatory states, thus confirming corresponding conjectures discussed in the literature. The extent of irregularity of these fibrillatory states is quantified in terms of an entropic measure in dependence of the frequency of the perturbing self-excitatory pacemaker.

Anti-arrythmogenic Effects of Atrial Specific Ultra Rapid Potassium Current Block: A Modelling Study

Phillip Law, Sanjay Kharche, Henggui Zhang

The University of Manchester, Manchester, UK

Introduction: The atrial specific ultra rapid potassium current (I_{Kur}) provides an attractive target in the management of AF. In this study we investigate *in silco* the anti-arrhythmogenic effects of pharmacological blocking of I_{Kur} under sinus rhythm (SR) and atrial fibrillation (AF) conditions.

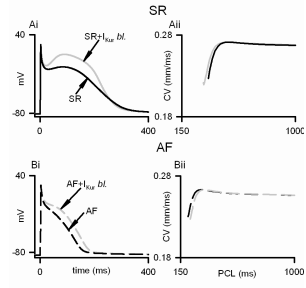

AP profiles and CVr curves under SR and AF conditions with and without I_{Kur} block.

Methods: Reduction of I_{Kur} by 80% based on experimental data was incorporated into a computer model of human atrial action potential (AP) developed by Courtemanche *et al.* under normal (*i.e.* sinus rhythm) and AF conditions, that considered the AF-induced ion channel remodelling in human atrial cells. The effects of I_{Kur} block on atrial AP were quantified by changes in the characteristics of APs that include the AP duration (APD), APD restitution (APDr), effective refractory period (ERP) and ERP restitution (ERPr). Using 1D strand models, intra-atrial conduction velocity (CV), CV restitution (CVr) and temporal vulnerability window (VW) of tissue to genesis of uni-directional conduction block by an extra-stimulus were computed. Re-entrant wave behaviour in idealized 2D sheets and realistic 3D anatomical model was simulated.

Results: As shown in the figure, under SR conditions, I_{Kur} block prolonged the AP plateau phase, but marginally shortened APD (by 4.8%) and ERP (by 2.5%). In the AF-remodeled tissue, I_{Kur} block increased APD (by 16.2%) and ERP (by 15.4%). I_{Kur} block did not affect CV at low pacing rates (0.27 mm/ms under SR, 0.25 mm/ms under AF), but modulated tissue's ability to support excitation wave conduction at high pacing rate. The cut off pacing cycle length (PCL) (i.e. the maximal PCL at which the tissue can sustain propagation) was reduced from 320 ms to 313 ms in the normal tissue, but was increased from 198 ms to 217 ms in the AF-remodeled tissue. I_{Kur} block augmented tissue's VW by 7.5% in the normal tissue, but reduced it by 19.2% in the AF-remodeled tissue. In 2D idealized sheets and in the 3D simulations, blocking I_{Kur} did not affect re-entrant wave or scroll wave dynamics.

Conclusions: Simulation data shows the pro-arrhythmicity of block I_{Kur} under SR, but anti-arrhythmic effects in the AF case. Since I_{Kur} is atrial specific, it is an attractive potential target for AF drug therapy treatment.

Study of the Effect of Tissue Heterogeneity and Anisotropy in Atrial Fibrillation Based on a Human Atrial Model

Dongdong Deng* and Ling Xia

Department of Biomedical Engineering, Zhejiang University, Hangzhou, Zhejiang, China

Atrial fibrillation (AF) is the most common cardiac arrhythmias in clinic, it is characterized by multiple waves of excitation coursing through myocardial tissue. AF disrupts the normal sinus rhythm and may arise from ectopic foci. In right atrium, there are many different conduction bundles which have different action potential morphology, and they provide a substrate for reen-trant activity during AF. Fibre orientation is important in electric propagation and maintaining AF, however, most previous simulation studies didn't con-sider the fibre orientation. In this paper we studied the effect of tissue hetero-geneity and anisotropy on initiation and maintaining of AF based on a realis-tic human atrial model with fibre orientation and detailed conduction system. Two atrial cell models were used to simulate AF, the first one was based on the model developed by Courtemanche et al, the second one was an AF-induced electrical remodeling cell model which is based on Courtemanche et al and was modified to incorporate the experimental data measured by Bosch et al. Two pacing protocols were used to initiate AF, the first one was the cross-field protocol, and the second one was the ectopic focus stimulation. The results showed that tissue heterogeneity and anisotropy are important for AF, and in some cases AF is transient due to the lack of anisotropy. Another finding is that fiber orientation is very important in sustaining of re-entry waves. Furthermore, different pacing protocols influence the AF patterns, the cross-field protocol will get a more chaos re-entry waves than that of the ectopic focus stimulation method. This investigation suggests that a detail atrial anatomical model should be necessary for AF simulation.

Principal Component Analysis-Based Method for Reconstruction of Fragments of Corrupted or Lost Signal in Multilead Data Reflecting Electrical Heart Activity and Hemodynamics

Robertas Petrolis*, Renata Simoliuniene and Algimantas Krisciukaitis

Institute for Biomedical Research, Kaunas University of Medicine, Kaunas, Lithuania

P81

Multilead signals reflecting electrical activity of the heart and hemodynamics give comprehensive, but usually redundant representation of the processes. Therefore fragments of transient corruption or loss of data in one or more leads can be restored substituting them by the signals reconstructed using information carried by the other leads. Multivariate analysis methods, particularly Principal Component Analysis is successfully used for optimal representation of quasiperiodic biomedical signals as ECG or ICG. Concatenated arrays of particular fragments of all registered leads are used to represent processes during each heart beat. Every such array can be represented by finite sum of Principal Components (eigenvectors of covariation matrix formed from these concatenated arrays) multiplied by coefficients calculated for each particular cardiocycle. Principal Components calculated from enough long learning set can be used as universal basis functions too. Using such basis functions for fragments of corrupted or lost data in one lead it is possible to reconstruct the data if coefficients are calculated ignoring fragments of lost or corrupted data in concatenated cardiocycle array. Our elaborated method performs structural analysis of ECG to find fiducial time point of every cardiocycle (peak of R wave). Excerpts of samples around fiducial time point in all registered leads are concatenated to form one dimensional array representing cardiocycle. Universal basis functions (Principal Components) are calculated using the arrays formed from the part of recording free of corrupted or lost data. Coefficients of the basis functions for corrupted or lost data fragments are calculated ignoring data of corrupted or lost leads. Corrected data fragments are formed firstly substituting corrupted or lost fragments by interpolated baseline adding to it reconstructed data using basis functions in particular time points according previously detected fiducial points. Our investigations showed that not only the variation in shape of one of corrupted or lost leads of ECG, but also variation in shape of signals reflecting hemodynamics can be pretty good restored using other synchronically registered signals.

An Approach to Reconstructing Lost Cardiac Signals using Pattern Matching and Neural Networks via Related Cardiac Information

Thomas Chee Tat Ho* and Xiang Chen

Signal Processing, Institute for Infocomm Research, Singapore

An approach to reconstruct the missing signals by pattern matching and neural networks is proposed in this paper for The Physionet Challenge 2010, Mind the Gap. The hypothesis used in this approach in the reconstruction of the missing signals is that the different cardiac signals originating from the same heart should exhibit the same signs of stress acting upon it. The level of stress in the different cardiac signals can and may vary. Based on the hypothesis, the last 30 seconds of data in all the available channels should exhibit the same signs of stress as the missing 30 seconds. Hence the last 30 seconds would serve as labels to be pattern-matched against prior signals in its own respective channel. This pattern matching is for the purpose of searching for similar precursors in the data. The neural network is built via pattern matching and cross-reference scoring of data set A. Reconstruction of the missing signal in data set B and C is based on its own prior signal data and using the trained neural network to determine the most likely segment for the missing segment. The initial 11 submissions have given results of 0.9529 for event 2 and 0.0475 for event 1 for the reconstruction of ECG channels in data set B. In the next few months up to September, more research would be done to maximize the results for event 1 without or minimal compromise to the results for event 2.

P81

Medical Multivariate Signal Reconstruction using Recurrent Artificial Neural Network

Luiz Eduard Virgilio Silva, Juliano Jinzenji Duque, Isaias Soares, Renato Tinós and Luiz Otavio Murta Jr*

Computing Signals and Images in Medicine Group (CSIM), University of São Paulo, Ribeirão Preto, São Paulo, Brazil

This work proposes a method for reconstruction of multivariate signals with missing parts of the data. The proposal consists in employing an artificial neural network (ANN), specifically recurrent multilayer perceptron (RMLP), to restore the missing intervals of the multivariate signals. In RMLP network, every neuron receives inputs from every other neuron in the network.

In this approach, a RMLP was trained for each multivariate signal in dataset. The network input patterns consist of a number of attributes which is number of channels available, except for the channel with missing data. At each discrete time sample RMLP has input patterns and one desired output that is the channel with missing data. For that channel with missing data, the input pattern contribution is the previous output from RMLP. The time variable ranges from the beginning to just before the missing data. Each pattern is presented to ANN more than once, as an iteration process. After training, this ANN is used to predict the missing values, with time within the missing part of the signal.

P81

The training was done in several situations, varying the number of iterations for training and the learning rate. Looking at results obtained from testing dataset, in general, optimal results were observed for good quality signals. On the other hand, signals which most of the channels are low quality, with low SNR, it was observed that when missing data channel had a moderate quality, the reconstruction was still good. However, if missing data channel was noisy, the reconstruction, in general, was not good. This could be explained by the fact that ANN is strongly dependent on the desired output channel, getting to learn with certain efficiency even when some of the inputs are noisy.

HMMFIT: Using Hidden Markov Models to Reconstruct Missing Signals in Multi-Parameter Physiologic Data

Yanen Li*, Yu Sun, Chengxiang Zhai and Lui Sha

Department of Computer Science, University of Illinois at Urbana-Champaign, Urbana, IL, United States

Real-time monitoring of physiologic signals is an important clinical tool for intensive care of patients. However, transient corruption or loss of one or more signals could prevent accurate interpretation of the signals and mislead the downstream analysis. Robust reconstruction of physiologic signals utilizing multi-parameter information remains a research challenge. The successful reconstruction of physiologic signals relies on the accurate detection of changes in patient state as well as the precise estimation of intervals of signal corruption. To address this problem, we assume that the time series of multi-parameter signals follow Common Hidden States (Normal, Abnormal and Critical), which can be modeled by the continuous-density Hidden Markov Models (HMMs). The multi-modal signals are modeled as conditional probability density functions given the Common Hidden States of a patient. Yet effective, traditional HMMs are inherently limited in that the given parametric form for the probability density functions is arbitrary. Moreover, there is no successful discriminative training procedure and regularization technique for standard HMMs parameter estimation. Here we propose HMMFIT, a Non-parametric Hidden Markov Model to jointly model the correlation be-tween different modality of multi-parameter signals as well as the temporal correlation of the signal to be reconstructed. A fast learning algorithm using stochastic gradient decent is designed to estimate the model. Results on the Physionet/CiC Challenge 2010 data set A and B (100 series of records for each set) show that the HMMFIT model significantly outperforms the baseline models. We achieve average score of 0.58 and 0.66 at event 1 and event 2 in Set A by 10-fold cross validation; and we achieve score of 0.55 and 0.63 in average at event 1 and event 2 in 100 series of records of Set B, respectively.

Filling in the Gap: a General Method using Neural Networks

Rui Rodrigues*

Dep Mathematics, FCT/Universidade Nova de Lisboa, Monte da Caparica, Portugal

P81

When a set of medical signals has redundant information it is sometimes possible to recover one signal from its past and the information provide by the other signals. In this work we present a general method to accomplish this task. For a long time it was known that multilayered networks are universal approximators but, even with the backprop algorithm, it was not possible to train in a reasonable amount of time such a network to realize complex real life tasks. In the last years Geoffrey Hinton proposed a training method that is able to overcome the previous difficulties. Pretraining a multilayered perceptron, layer by layer as a restricted boltzmann machine first and then as an autoencoder enables the backprop algorithm to find satisfactory weights for a complex neural network. So, if ecg leads II and V are available and lead AVR is missing for a while, we first train, using past information, an autoencoder on leads II and V and another on lead AVR. The higher layer of the first autoencoder will provide features that will allow, with an extra perceptron, to match the higher layer of the second autoencoder. Now this higher layer of the second autoencoder can be seen as a code that enables us to reconstruct lead AVR. We applied the same procedure to reconstruct, for example, missing intracranial pressure signal when pleth, abp and respiration signals are available or missing CVP when pleth, respiration and some ecg leads are present. Moreover, the autoencoder we train sucessfully on the past of a signal can be used to judge if present signal suffered significant changes: when the autoencoder reconstruction error is big on the the present time signal, something changed on the signal and that might be for example noise degradation or alteration in the heart rate.

Multi-parameter Physiologic Signal Reconstruction by Means of Wavelet Singularity Detection and Signal Correlation

Wei Wu*

WEIWU INFO Portugal, Porto, Portugal

Reconstructing corrupted data from multi-parameter physiologic signals becomes essential for a real-world monitoring application. Our investigation has discovered that multi-parameter physiologic signals coming from a single human body are strongly correlated and synchronized, and it is possible to predict the waveform peaks of one signal by observing peak distribution at another signal. The Wavelet singularity analysis at signals can exactly detect the waveform rising and falling that occur in the same periodical way as the peaks occur, confirming the singularities of multi-parameter physiologic signals are also strictly synchronized. Based on the phenomenon mentioned above, we propose a novel method to reconstruct corrupted data. We use Wavelet to detect the singularity of the target signal, resulting at a time distribution curve of singularity peaks that accord with the rising and falling edge of the signal. The singularity peaks are further used to find out a basic waveform unit that appears periodically throughout the signal. Also the singularity peak distribution curve of other signals are calculated and among them, one bearing the most similar singularity peak period as the target signal bears is chosen as a reference signal. The corrupted data at the target signal is reconstructed by laying the basic waveform units one by one according to the singularity peek distribution of the reference signal at the time duration where the target data is corrupted, then, the time delay between the target signal singularity peak and the reference signal singularity peak is calculated and is used to align the reconstructed data with target signal. The reconstructed signal can reach above 99% accuracy in timing and 98% accuracy in amplitude for a target signal corrupted randomly, and variable accuracy for a target signal not only corrupted but also distorted due to the basic waveform unit extracted from the target signal may also be distorted. The reconstruction accuracy can be further improved by manually choosing the basic waveform unit that is sensitive to amplitude accuracy and by refining the reference selection that is sensitive to timing accuracy and by optimizing computation algorithm.

P81

PhysioNet/CinC Challenge

Teresa Rocha*, Simão Paredes and Jorge Henriques

Departamento de Engenharia Informática e de Sistemas, Instituto Superior de Engenharia de Coimbra, Coimbra, Portugal

This work proposes a wavelet scheme to reconstruct missing data in physiologic signals that have been removed from multiparameter recordings of patients in intensive care units. The key idea consists of the decomposition of the signal into two compo-nents, approximation and detail, through wavelet transform. In the case of the signal with missing data is an ECG (ECG*), it is taken advantage of the fact that there are two other ECG signals in the record. In a first phase, a section of the ECG* signal before the prediction period is mod-eled as a combination of the approximation and detail coefficients of the other two ECG in the same period. Then, the determined model parameters are used to reconstruct the missing ECG* data, based on the combination of the other two ECG signals available in the forecast period. In the case of the signal to be reconstructed is not an ECG (ABP, RESP,), two auxiliary signal sections are generated in order to apply the same strategy described above. Firstly, a segment of the signal before the missing period is considered as a template. Then, using a wavelet coefficients correlation approach, the two sections of the remaining signal that best match the template, constitute the referred auxiliary sections. The approximation and detail coefficients of these sections are used to model the template. Finally, the determined model parameters, together with the 30 seconds after the sections, are employed to reconstruct the missing signal. Applied to all records of set A, this strategy provided results of 45% and 56%, for scores 1 and 2, respectively. For all records of set B, results were of 46% and 54%, for scores 1 and 2, respectively. Although these preliminary results are promising, future work will consist in the optimization of the parameters involved in the proposed strategy.

P81

Reconstruction of Multivariate Signals using a Q-Gaussian Radial Basis Function Network

Luiz Eduardo Virgilio Silva*, Juliano Jinzenji Duque, Renato Tinós and Luiz Otavio Murta Jr

Computing Signals and Images in Medicine (CSIM), University of São Paulo, Ribeirão Preto, São Paulo, Brazil

Radial basis function Networks (RBFNs) have been successfully employed in different Machine Learning problems. The use of different radial basis functions in RBFN has been reported in the literature. Here, we discuss the use of the q-Gaussian function as a radial basis function employed in RBFNs. An interesting property of the q-Gaussian function is that it can continuously and smoothly reproduce different radial basis functions, like the Gaussian, the Inverse Multiquadratic, and the Cauchy functions, by changing a real parameter

q. In addition, we discuss the mixed use of different shapes of radial basis functions in only one RBFN. For this purpose, a Genetic Algorithm is employed to select the number of hidden neurons, width of each RBF, and q parameter of the q-Gaussian associated with each radial unit.

Network training is the search for optimal values of the radius and the q-parameter of each radial basis Gaussian. The minimum and maximum numbers of basis function in the mid layer are defined a priori. The k-means clustering algorithm was employed to calculate each set of center positions of the q-Gaussians. In training stage with a multivariate signal with n variable, the network inputs are the n samples of each channel at once, except for the channel which part of the data is missing, which was used as desired output.

Results from testing dataset were precise for good and moderate quality signals. However, if channel which part is missing is very noisy, the reconstruction, in general, was not so good. This fact could be explained by the artificial network training that is strongly dependent on the desired output channel, getting to learn with certain efficiency even when some of the inputs are noisy.

Extracting Fetal ECG from a Single Maternal Abdominal Record

Mohammad Ayat[*, **], Khaled Assaleh[**], Hasan Al-Nashash[**] and Moncef Gabbouj[*]

[*]Tampere University of Technology, Finland
[**]American University of Sharjah, UAE

Fetal ECG (FECG) is the electrical activity of fetal heart muscles and it can reveal vital information of fetal heart status. This signal can be recorded non-invasively during pregnancy from the abdomen of a pregnant woman. However, such a recording of the FECG would be useless since it is largely overwhelmed by the maternal ECG and other sources of noise. Nonetheless, if the abdominal recording is properly processed then a useful FECG can be extracted and it can provide a very good and simple means for detecting and diagnosing fetal heart diseases.

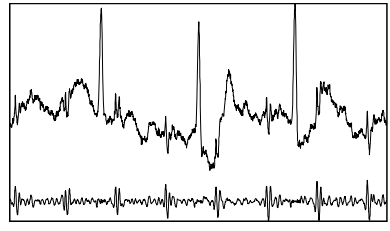

Upper plot shows real abdominal record, Lower one shows extracted FECG with proposed method.

P82

Many methods have been proposed for FECG extraction from abdominal signals. They usually need multi-channel input; hence, they require complex lead structure.

In this work, we introduce a novel two-tier technique for extracting fetal ECG from a single abdominal record. The proposed method in its first tier extracts an estimate of the maternal ECG by processing the abdominal signal through a Savitzky-Golay smoothing filter. The estimated maternal ECG is then nonlinearly aligned with the abdominal signal using polynomial networks to extract the fetal ECG signal. Results on synthetic and real abdominal ECG data show that the proposed method can extract fetal ECG with signal quality comparable or better than that extracted by multi-channel based methods.

Image Registration of 3D Trans-Esophageal Echocardiography and X-Ray Fluoroscopy for the Guidance of Trans-Catheter Aortic Valve Implantation

Gang Gao*, Geraint Morton, Jane Hancock, Simon Redwood, Martyn Thomas and Kawal Rhode

Division of Imaging Sciences, King's College London, London, United Kingdom

Trans-catheter aortic valve implantation (TAVI) is an alternative to conventional open aortic valve replacement and is becoming more widespread. The procedure is performed by delivering the new valve via a catheter inserted either via the femoral artery or through the apex of the heart. Current-ly, TAVIs are routinely guided using X-ray fluoroscopy and 3D trans-oesophageal (TOE) echocardiography. X-ray fluoroscopy is excellent for device visualization and TOE is excellent for visualizing the anatomy of the heart. Correct positioning of the new valve is critical. In this study, we demonstrate a robust and efficient method to register TOE and X-ray images and validate this using data from 3 TAVI patients. We hypothesize that real-time fused data will be a powerful combination to guide valve implants. Three TAVI procedures were performed using a GE Innova 2100IQ X-ray system. Echo images were acquired using a Philips iE33 echocardiography system and a X7-2t 3D TEE probe. For each patient, multi-view X-ray im-ages were acquired simultaneously with 3D TEE images during the proce-dure. The image data were processed off-line for co-registration. The registra-tion was achieved using a combination of calibration of the TOE probe and localization in the X-ray images. Localization was carried out by GPU-accelerated 2D-3D registration of a nano-CT-derived 3D model of the TOE probe to the X-ray data. The registration accuracy was assessed by manual expert localization of the implanted devices in both the TOE and X-ray data. The target registration error was 2.7 ± 1.8mm, 4.2 ± 3.0mm, 2.3 ± 2.1mm respectively for the 3 different patient data. In conclusion, we demonstrate a novel technique for registration of 3D TEE and X-ray fluoroscopy images for the guidance of TAVI procedures. We have evaluated our approach off-line and shown clinically acceptable accuracy. Once developed as a real-time solution, this approach is likely to have a significant clinical impact.

P82

Patient-Specific Correlation of Perfusion Defects to Coronary Arteries

Constantine Zakkaroff*, Aleksandra Radjenovic, Derek Magee and Roger Boyle

School of Computing, University of Leeds, United Kingdom

Patient-specific correlation of perfusion defects to coronary arteries responsible for blood supply in the affected territories has the potential to improve accuracy of diagnosis and intervention planning. Cardiac cycle phase difference between perfusion and angiography datasets explains the vast variation of the shape of the myocardium between these datasets and precludes the use of standard methods of 2D/3D registration. Research published to date does not provide a reliable method of registering 2D perfusion and 3D coronary angiography datasets.

This paper presents a work-flow for non-rigid registration of 2D perfusion series and 3D angiography volumes; the solution of the registration problem relies on the use of the 4D wall motion series (spanning the complete cardiac cycle) as a mediator for non-rigid registration perfusion and angiography datasets. The work-flow assumes the availability of the localisation/segmentation of the main coronary arteries in the angiography dataset. In the first two steps the phases corresponding to perfusion and angiography datasets are determined through rigid registration of those datasets to the cine series. In the next step, an Eulerian framework-based sequential non-rigid phase-by-phase registration of the 4D cine series provides a transform spanning the phase difference between perfusion and angiography datasets. Finally, the phase-difference transform from the previous step is used to transform the angiography dataset containing the localised/segmented main coronary arteries into the corresponding perfusion phase where coronary arteries can be directly associated with perfusion defects.

The presented work-flow for mediated spatiotemporal registration is first validated on synthetic cine series derived from clinical data; the second part of the evaluation is carried out on clinical data. The results of the evaluation show the utility of the method in this particular context while highlighting its potential applicability to other areas of cardiac image analysis.

P82

Categorization of Continuous ECG-based Risk Metrics for Cardiovascular Death using Asymmetric and Sample Size Entropy-Based Method

Anima Singh* and John Guttag

EECS, MIT, Cambridge, MA, United States

Categorization of continuous clinical variables into groups such as high, medium or low risk is useful for risk stratification and to guide therapy in patients. In this study, we investigated an asymmetric entropy-based approach to select cutoffs for such categorizations. The proposed asymmetric entropy based method automatically selects cutoffs while addressing the problems of unbalanced class representation in the data set and the asymmetric misclassification costs of false negatives and false positives. We tested the algorithm for categorization of three electrocardiographic based risk metrics for prediction of cardiovascular mortality, heart rate variability (HRV LF-HF), morphological variability (MV) and deceleration capacity (DC). The number of cutoffs derived using asymmetric entropy was same as those used in the literature for risk stratification for cardiovascular deaths. We evaluated the categorization performances of each set of cutoffs using a composite score derived from the product of sensitivities and specificities between any two risk-groups. We derived the cutoffs using a training set containing 1067 patients, and evaluated them on a separate set of 1066 patients. Both the training and test sets were drawn from a study of patients with non-ST-elevation ACS. For MV, the literature based cutoff, 52.5, had a mean score of 0.655. Our method yielded a mean cutoff value of 45 with a mean score of 0.656. For DC, the literature-based cutoffs, 2.5 and 4.5, had a mean score of 0.60, while our method generated 4.2 and 6.0 as the two cutoffs with a significantly higher ($p<0.05$) mean score of 0.73. For HRV LF-HF the performance of the single cutoff drawn from the literature (cutoff: 0.95; score: 0.62) was significantly ($p<0.05$) better than that of the cutoff derived using asymmetric entropy (mean cutoff: 1.8; score: 0.56). However, when asymmetric entropy was used to derive two cutoffs, it yielded cutoffs of 0.8 and 2.0 with a mean score of 0.75. This suggests that a three-way categorization based on cutoffs identified by our proposed method might be of clinical utility.

P82

Obstructive Sleep Apnoea using Photoplethysmography-based Dynamic Features

Lina María Sepúlveda-Cano*, Eduardo Gil-Herrando, Pablo Laguna and Germán Castellanos-Domínguez

Universidad Nacional de Colombia, Sede Manizales, Colombia

Recently, photopletysmography (PPG) signal has been developed for home Obstructive sleep apnea (OSA) monitoring, being an easily acquired measurement, that provides a measure of the tissue blood volume, in particular, whenever an apneic episode occurs, sympathetic activity increasingly produces vasoconstriction that is reflected by decreases in the PPG amplitude fluctuation. Therefore, PPG events can indirectly quantify apneas during sleep. However, other physiological events such as artifacts, movements and deep inspiratory gasp produce sympathetic activation, and consequently, decrements in PPG envelope amplitude, which are unrelated to apnea. As a result, its high sensitivity can produce misdetections and overestimate apneic episodes. To cope with this shortage, nonstationary techniques of signal processing are required to analyze the time evolution of the autonomic control mechanism. Even that different approaches have been developed (Time Frequency, TimeVarying, and Time Scale analysis, etc.), still without accurate models to describe sympathetic activation, the application of aforementioned approaches often fails to provide satisfactory results because of imposed stationary assumptions. Mostly, it is assumed that each extracted feature is generated independently and identically, instead of treating the data as stochastically dependent, and thus providing a possible approach, capable of capturing the evolving information of the structure. This paper explores the training methodology for OSA detection, which is based on relevance analysis of dynamic features extracted from nonparametric time-frequency representation of PPG envelope. The methodology consists of four phases: (1) preprocessing is carried out, with a segmentation process, followed by an artifacts removal and a clustering algorithm; (2) the dynamic features are extracted from nonparametric timefrequency representation based on spectrogram; (3) both linear transformations (namely, Principal Component Analysis and Partial Least Squares) are used to perform dimensionality reduction; (4) the results are validated through cross validation using a k-nn classifier. For two classes (normal, apnea) the results for PCA are: specificity 81:82%, sensibility 100% and for PLS specificity 81:82%, sensibility 88:57%. Achieved results related to performed accuracy and dimension reduction are comparable with respect to outcomes reported, and clearly show that the proposed methodology can be focused on finding alternative methods for OSA diagnosis.

P82

On the Measurement of Physiological Similarity Between Independent Components: Time-Structure Versus Frequency-Based Methods

A Jiménez-González*, CJ James

University of Southampton, Southampton, UK
Universidad Autónoma Metropolitana-Iztapalapa, México City, México

This work explored two methodologies to quantify physiological similarity between independent components (ICs) extracted from abdominal phonograms by single-channel independent component analysis (SCICA).

ICs were processed to produce (a) one index about time-structure (through rhythmicity calculation) and (b) one index about frequency content. The rhythmicity index (R) was calculated by: (1) envelope generation, (2) autocorrelation, and (3) autospectrum to quantify the frequency of the dominant rhythm (i.e. R). The frequency content index (S) was obtained from the IC power spectral density, where the central frequency of its single-peak spectrum was taken as S.

The criteria to recognise similar rhythmicities were established by considering physiological rates. Thus, since the physiological ICs in the abdominal phonogram correspond to maternal respiratory (MR), maternal cardiovascular (MC), and foetal heart sounds activities (FHS), four ranges of similarity were proposed for R: R_{MR}= [0.1–0.6] Hz, R_{MC}= [0.83–1.7] Hz, R_{FHS}= (1.7–3.0] Hz, and R_N for noise. The criteria for similar frequency content were only based on our empirical observations, which led to ranges of similarity for S as: S_{MR}= (0–2] Hz, S_{MC}= (2.0–19.0] Hz, S_{FHS}= (19.0–44.5] Hz, and S_N> 44.5 Hz for noise.

Both methodologies were tested on a dataset of 750 ICs (preclassified as MR, MC, FHS, and noise) by quantifying their sensitivity (Se) and specificity (Sp). The ICs were extracted from 25 abdominal phonograms recorded between 29 and 40 weeks of gestational age.

These methods are fast and easily implemented since they are based on autocorrelation and/or spectral analysis. Particularly, results showed optimal Se-Sp values of 0.75 for the R-based methodology, and 0.93 for the S-based methodology, which means that S is better than R to recognise similar ICs. On the other hand, R is more complete since rhythmicity not only recognises similar ICs, but also identifies their physiological origin, which is a desired quality. Thus, both methodologies are promising for automatic classification purposes. Most importantly, they lead to the possibility of enhancing the classification of physiological ICs extracted by SCICA. Future work will aim for such an enhancement by combining these two approaches to exploit their advantages.

P82

Open-source Teleconsulting System for International Cooperative Medical Decision Making in Congenital Heart Diseases

Andrea Gori*, Alessandro Taddei, Alessio Ciregia, Debora Mota, Paolo Marcheschi, Nadia Assanta, Bruno Murzi and Giorgio Ricci

Medical Informatics, CNR Institute of Clinical Physiology, Massa, Italy

A project was developed by Heart Hospital in Massa, supported by Cuore un Mondo Association and Tuscany Region, for medical cooperation with Balkan Countries in diagnosis and care of congenital heart diseases. First step was to set up a telemedicine network aimed at multi-center cooperative medical decision making. While echography studies allow to recognize abnormalities in newborns or in the fetus, operators are not sufficiently skilled in many remote hospitals. Frequently it is necessary to transfer urgently to specialized cardiac units newborns suffering by critical cardiac disorders while early care planning, possibly before delivery, would limit both risks and costs. Tele-echocardiography was initially implemented at pediatric clinical centres of Banja Luka, Rijeka and Tirana, using videoconference equipment for transmitting over Internet sequences of medical images. Upload network transfer rate of 512 kbps was provided for achieving real time transmission without significant loss of diagnostic information. Actually videoconference systems are expensive, use proprietary technology and have limited functions. To overcome these limitations we developed a low-cost device using Open-Source software and standard hardware. This system allows both real time and off-line teleconsultation as well as videoconference interconnection. Mini-ITX low-power motherboard was chosen to achieve small size equipment. LAMP frame-work was implemented (Open Source software bundle consisting of Linux operating system/Apache web server/MySQL RDBMS database/PHP scripting language). Ekiga (open source application supporting both H323 and SIP protocols over Internet) was applied for enabling on-line operator interaction. Real time transmission of medical images was achieved by VLC (free media player supporting common audio/video codecs and file formats as well as protocols for streaming over network). DCM4CHE (Open Source Clinical Image and Object Management software) was implemented for storage and distribution of DICOM image studies provided by imaging equipment. Flash Video format was applied to deliver not-DICOM images over the Internet, using buffering for limiting loss of information.

P82

N-Terminal Pro-Brain Natriuretic Peptide in Combination with the 80-Lead Body Surface Map Improves Detection of Acute Inferior Myocardial Infarction with Right Ventricular Involvement

Michael John Daly*, Nicholas McKeag, Conor McCann, Christopher Cardwell, Ian Young and Jennifer Adgey

The Heart Centre, Royal Victoria Hospital, Belfas, United Kingdom

Right ventricular myocardial infarction (RVMI) with an acute inferior infarction (AIMI) remains a diagnostic challenge and is associated with increased rates of morbidity and mortality necessitating rapid myocardial reperfusion for their reduction.

Methods: Consecutive patients presenting to our unit with acute chest pain between 2003-6 were enrolled if they had blood sampled for NT-proBNP, a standard 12-lead ECG and body surface map (BSM) recorded at first medical contact. AIMI was defined as 1mm ST-elevation in at least two contiguous leads of the standard 12-lead ECG, i.e. II, III or aVF in combination with a peak Troponin T 0.03g/L. Definition of RVMI was by angiographic occlusion of the RCA proximal to the origin of the first major RV branch. Patients were excluded if they had LVEF $<55\%$, severe valvular disease, renal impairment or did not undergo coronary angiography.

Results: Enrolled were 407 patients (age 62 ± 13 yrs; 70% male). Of these 407, 72 had STEMI at presentation. AIMI occurred in 39/72 (54%). Of those 39 patients, 24 (62%) had RVMI. On the basis of ROC analysis, a NT-proBNP of 373ng/L provided the best discrimination of patients with and without RVMI (sensitivity 71%, specificity 67%). In diagnosis of RVMI, BSM had a sensitivity 79% and specificity 87%. NT-proBNP levels were significantly higher in those with RVMI compared to non-RVMI (996 ng/L v 305 ng/L, p=0.006). Of those with AIMI, the c-statistic for distinguishing RVMI from non-RVMI using NT-proBNP alone was 0.761 (95% CI: 0.609 - 0.913) and BSM alone was 0.807 (95% CI: 0.713-0.882). Using the combination of BSM and NT-proBNP the c-statistic was 0.861 (95% CI: 0.728 - 0.995; $p<0.001$).

Conclusion: In patients with acute inferior STEMI, the combination of NT-proBNP and BSM identifies those with RVMI (c-statistic = 0.861, $p<0.001$), thus identifying a group where early reperfusion is paramount.

P83

Myocardial Infarction Localization using Combined Heart Vector Analysis and Neural Network Localizer

Masood Ghasemi, Nader Jafarnia Dabanloo*, Sepideh Sabouri and Hamid SadAbadi

Biomedical Engineering, Science & Research Branch, Islamic Azad University, Tehran, Iran

The development of accurate methods for characterization of Myocardial Infarction (MI) is of major importance, especially for diagnosis purposes. To assess the recent developments and to encourage the scientists to much more focus on this issue, the CinC/Physionet Challenge 2007 was held on the same topic. Since, the data-sets of the challenge were limited to four subjects; the proposed methods were not evaluated very well. Therefore, in this paper, we reconsider the VCG-based method proposed by Ghasemi et al. in the CinC/Physionet Challenge 2007 and develop a multi-layer perceptron (MLP) neural network (NN) to automatically perform MI localization at its decision-making stage. To perform this task, we first implement the VCG-based method to generate a part of the activation front's surface which is induced by MI. Then, the resulting vector is fed into the neural network MI localizer consisting of one hidden layer. The output of the neural network will be the segment(s) in which MI has occurred. In order to evaluate the method, we use the PTB diagnostic database. The selected MI subjects were divided into two sets; the training set and the test set. Note that the subjects with bundle branch block and hypertrophy were excluded from our data-sets. Finally, we examined the neural network MI localizer with the test set and the method approached the accuracy of about 67.5%. Since, the performance of the neural network is connected to its input vector i.e. MI-induced activation front; the generating mathematical model should be more investigated in future works.

P83

A Comparison of IIR and Wavelet Filtering for Noise Reduction of the ECG

Jens Stampe Soerensen*, Lars Johannesen, Ulrik Silvanus Lerkevang Grove, Kasper Lundhus, Jean-Philippe Couderc and Claus Graff

Health Science and Technology, Aalborg University, Aalborg, Denmark

Baseline wander and powerline noise both have confined power spectra making the use of narrowband linear time-invariant filters (IIR) ideal. For transient ECG noise, wavelet filtering has been proposed as a potential filtering alternative to IIR filtering. This study compares the ability to preserve information and reduce noise contaminants for five wavelet filters and three IIR filters. Two 3-lead Holter ECGs from healthy subjects were obtained from the Telemetric and Holter ECG Warehouse. A one minute noise-free segment was identified from lead X of the first ECG and replicated to 24 h duration. White Gaussian noise (15 dB SNR) was added to the noise free ECG in increments of 10% coverage. The second ECG was a 2.5 minute segment with alternating muscle transients (70% total) and noise-free segments (30% total) of approximately 10 s durations. Computation times and improvements in SNR for different noise coverages were calculated for all filters and compared. RMS errors were calculated from noise-free segments on the ECG with transient muscle noise. Wavelet filters improved SNR more than IIR filters when the signal was covered by more than 50 % noise. In contrast, the computation times were shorter for IIR filters (6 s) than for wavelet filters (88 s). There was no difference between wavelet and IIR filtering with respect to RMS errors on the ECG with transient muscle noise. In a clinical setting where the amount of noise is unknown, we recommend using IIR filters over wavelet filtering for consistent performance and low computation time.

P83

Modified Rectangular Finite Impulse Response Filter for Stabilization of QT Measurement

Jing Wu, Jean-Philippe Couderc* and Jean Xia

Department of Electrical and Computer Engineering, University of Rochester, Rochester, USA

Instruction: In drug-safety studies, the measurements of QT intervals require to have a level of precision to detect small drug-induced prolongation. This paper discusses a modified approach of -shaped FIR Filter to optimize the quality of signal and improve the stability of QT/QTc interval measurements.

Methods: the proposed filter is designed to have a time-dependent frequency characteristic based on pre-defined fiducial points of the EKG. The radius of regular -shaped FIR filter is modified to obtain different frequency characteristics within QRS and the repolarization interval. This optimal filter is compared to its simple forms (including 5 radiuses). We compared the standard deviation of QT/QTc interval between the optimal filter and the single-radius filters (radius N=5, 10, 15, 20). The evaluation of QTc stability was based on the standard deviations of QTc interval when measured from Holter ECG signals from 20 healthy subjects filtered with the proposed five versions of the -shaped FIR filter.

Results: We included Holter ECG signal recorded at 1000Hz sampling frequency and 16 bit amplitude resolution. The study population included 6 females (45$\pm$9 yrs) and 14 males (40$\pm$10 yrs). The corresponding low-pass filters had a cutoff frequency equal to 110, 72, 47, 39, 26 Hz for N=3, 5, 8, 10, 15, respectively. The optimal filters combined frequency characteristics of the -shaped FIR filter for N=15 for the repolarization interval and N=3 for the QRS interval. The variability of QTc duration of filtered signal with regular filter N=5, 10, 15, 20 were calculated by averaging the standard deviation of QTc which was 10, 13, 10, 10 msec, respectively. These results correspond to 42%, 76%, 37% and 45% decrease stability in reference to the optimal filter.

Conclusion: The standard deviation of QTc interval with optimal filter revealed an averaged 50% increase of stability in comparison to other proposed filter.

P83

Investigation on Two-year Peritoneal Dialysis Patients: Does the Cardiovascular Condition Affect ECG Biometrics?

Tsu-Wang Shen, Shan-Chun Chang*, Chih-Hsien Wang and Te-Chao Fang

Medical Informatics, Tzu Chi University, Hualien, Taiwan

Introduction: Biometrics is anatomical, physiological or behavioral characteristics different from person to person. Electrocardiogram is previously verified as a new biometric for human identification. However, it is still unclear if any internal, external or temporal factors may affect the biometric. Previous evidence indicates that ECG biometric is robust from 1-3 year observation for healthy subjects. However, it is uncertain if changes of cardiovascular conditions may cause any difference. In general, end-stage renal disease patients provide an accelerated process on vascular calcification, atherosclerosis and peripheral arterial disease. Hence, the research investigates if cardiovascular conditions may impact ECG biometrics. Method: Twenty-three peritoneal dialysis patients were monitored for two year period (2007-2009) under IRB regulation at Tzu-Chi General hospital, Taiwan. The cardio-ankle vascular index (CAVI) and ankle-brachial index (ABI) were measured to evaluate cardiovascular conditions. Then, their ECG signals have been recorded for 5 minutes at supine position for two years, which are sampled at 500 sps and filtered for bandwidth from 0.01Hz to 50 Hz. Seventeen fracture features (Shen 2005) were extracted and the template matching method is applied for observing the difference on ECG morphology. Our ECG templates were generated at first year and tried to match the signal at two year after. Total of 25% outliner heartbeats were eliminated on 5 min recordings for all subjects. Results and conclusions: From above population, the average ABI increased 5.2% and the average CAVI decreased 14.9%. All features demonstrated no significant, except the feature, RS amplitude divided by TS amplitude. It correlates ABI significantly for two year period (-.627 and -.497, $p<0.05$). Our results show that ECG is still able to identify individuals, even the average correlation coefficients decreased from 0.985 to 0.877 after two years. Hence, we suggest that ECG biometric may calibrate after years on peritoneal dialysis patients.

P83

Principal Component Analysis of the QRS Complex During Diagnostic Ajmaline Test for Suspected Brugada Syndrome

Velislav Batchvarov, Ivaylo Christov, Giovanni Bortolan* and Elijah Behr

Centre of Biomedical Engineering, Bulgarian Academy of Sciences

Background: The Brugada syndrome (BS) is often associated with intraventricular conduction disturbances which may worsen the prognosis. We used principal component analysis (PCA) of the QRS complex in order to assess ventricular depolarisation heterogeity during diagnostic ajmaline test in patients with suspected BS. Methods: Digital 10-second 15-lead electrocardiograms (ECG) (500 Hz, 4.88 V resolution, 12 standard leads + leads V1, V2 and V3 recorded one intercostal space higher, V1h to V3h) were acquired in 96 patients with suspected BS and visibly non-diagnostic resting ECGs (60 men, age 39.4±16.7 years) before, during and after administration of ajmaline (1 mg/kg for 5 minutes). PCA was performed on a beat-to-beat basis on the automatically delineated QRS-onset to J-point interval using 3 different sets of leads: a) V1, V2 and V3 (QRS-PCAstand), b) V1h, V2h and V3h (QRS-PCAhigh), and c) V1, V2, V3 plus V1h, V2h and V3h (QRS-PCAtotal). The mean PCA (ratio of 2nd to 1st eigenvalue) of all individual complexes within a 10-s ECG was analysed. Results: There were 23 patients with positive tests (14 male (61%), age 43±17 years) and 73 with negative tests (46 male (63%), age 38±17 years). Among patients with positive tests, those with symptoms (2 of them with syncope and 4 with aborted cardiac arrest) had higher QRS-PCAhigh both before the test (0.39±0.27 vs 0.13±0.11, p=0.003), as well as during maximum effect of the drug (0.32±0.19 vs 0.12±0.06, p=0.001) compared to those without symptoms (n=17). QRS-PCAstand and QRS-PCAtotal were not significantly different between patients with and without symptoms. Following ajmaline, QRS-PCA decreased significantly compared to baseline in patients with negative tests (e.g. QRS-PCAstand: 0.15±0.02 vs 0.08±0.01, p=0.00004), whereas in those with positive tests the change in QRS-PCA from baseline was not significant (0.21±0.19 vs 0.16±0.15, p=0.098). Conclusion: Depolarisation heterogeneity assessed from the high but not from the standard right precordial leads is increased in symptomatic patients with positive ajmaline tests compared to those without symptoms. Heterogeneity of depolarisation exhibits different dynamics during ajmaline testing for BS in patients with positive compared to those with negative tests. PCA of the QRS can help the diagnosis and risk stratification of patients with BS.

P83

Use of ECG Quality Metrics in Clinical Trials

Martino Vaglio*, Lamberto Isola and Fabio Badilini

AMPS Llc, Montichiari, Italy

Management of large number of digital electrocardiograms (ECGs) is today a common practice in both clinical and research practice. More specifically, the need of robust quality metrics that can be useful to easily identify and classify subsets of ECGs (for example with high content of noise) has recently received growing interest and attention. We present a software package designed with the purpose to provide e viable mean to manage and automatically classify large amount of ECGs on the basis of built-in quantitative metrics, grouped into five categories:

Noise content (All frequencies, low-frequency (LF) and high-frequency (HF)) Interval annotations, based on an embedded automated algorithm (QT, PR, QRS and HR), Amplitude annotations (for example R or T wave amplitudes), Repolarization Regularity (for example, indexes of morphology of the T wave), Heart Rhythm Regularity (for example the percent of abnormal non-sinus cardiac beat contained in the ECG).

One or more combined metrics are finally used to generate ECGs subsets using, for each of the considered metric, one or more thresholds (for example, using heart rate as the single classifier, we could generate three subsets, one with the ECGs with HR < 40, a second one with the ECGs between 40 and 100, and the last one with the ECGs with HR > 100). The number of ECG subsets, as well as the thresholds to use are parameters of the system. For the metric lacking a reference values (for example for the noise scores), the distribution for the metric derived from a database of approximately 300.000 digital ECGs clinical trials is provided. Quantitative examples of the usage of ECG classifier will be provided. The use of this tool can largely improve the quality of recorded ECG in both clinical trials and common clinical ECG practice.

P83

Study of Differences in Heart Rate in Patients with Apnea and Insomnia Syndromes

Juan Guerrero, Antonio Benetó, Enriqueta Gómez, Manuel Bataller, Pilar Rubio and Alfredo Rosado*

Departamento Ingeniería Electrónica. Escuela Superior Ingeniería, Universidad de Valencia. Spain, Spain

A high percentage of patients with obstructive sleep apnea-hypopnea syndrome (OSAHS) also have chronic insomnia, particularly elderly people. Additionally, these patients usually show high levels of depression, stress and other sleep disorders. In order to quantify the potential negative impact that insomnia produces in patients with OSAHS, some studies have analyzed the usual parameters in the polysomnographic reports, although the results are inconclusive.

The aim of this paper is to study the possible effect that the combination of these pathologies might produce in heart rate (HR). We analyzed 85 polysomnograms (PSG) from two groups of patients with OSAHS, for cases without insomnia (G1, N=55, 53.4 +- 13.1 years) and with insomnia (G2, N=30, 49.1 +- 10.0 years). For each sleep stage (aWake, 1, 2, 3, REM), epochs were grouped with the presence of obstructive apnea/hypopnea (G#A) or without apneic events (G#). The obtained values (mean +- standard deviation; beats per minute) are:

P83

- W: (G1: 71.7 +- 11.9 bpm; G2: 69.4 +- 9.9 bpm).
- 1: (G1: 70.2 +- 13.0 bpm; G2: 67.8 +- 10.0 bpm), (G1A: 70.6 +- 3.0 bpm; G2A: 70.6 +- 18.5 bpm).
- 2: (G1: 67.2 +- 12.0 bpm; G2: 64.7 +- 11.0 bpm), (G1A: 69.2 +- 12.1 bpm; G2A: 66.7 +- 17.5 bpm).
- 3: (G1: 67.1 +- 12.4 bpm; G2: 64.9+- 10.8 bpm), (G1A: 70.9 +- 8.4 bpm; G2A: 67.5 +- 19.8 bpm).
- REM: (G1: 67.0 +- 11.2 bpm; G2: 65.9+- 10.9 bpm), (G1A: 67.1 +- 9.7 bpm; G2A: 68.4 +- 17.2 bpm).

Although not statistically significant, the results show that the HR in the studied PSG show higher values for G1 in all sleep stages for periods without apnea. In case of apnea, HR is also greater for G1 except for REM sleep stage.

Evaluation of Methods for Estimation of Respiratory Frequency from the ECG

Ainara Sobron, Inaki Romero* and Txema Lopetegi

IMEC

The influence of breathing on the ECG allows the estimation of respiration rate when only this signal is available. Several techniques have been proposed in literature. We compared five different methods in order to evaluate their performance under different conditions. We selected methods based on Heart Rate Variability (HRV), modulation of QRS morphology (amplitude and area), and changes on the Angle of Mean Electrical Axis (AMEA). The spectral combination of them was also studied. Methods were evaluated with signals recorded to 20 patients in different body positions and breathing patterns (free and paced breathing). Recordings doing exercise were also considered to evaluate the robustness against noise. In addition, Fantasia database was also used. Correlation in both time and frequency together with relative error between real and estimated breathing rate were computed. The modulation of QRS amplitude gave the lowest relative error for free breathing with median (mad)=0.98% (17.22%). AMEA (1.33% (22.23%)) and QRS area (1.42% (23.02%)) performed slightly worse. For paced breathing, spectral combination resulted in the lowest relative error (0.63% (2.87%)). HRV showed a good performance during paced breathing, error of 0.89% (5.80%), but gave a high relative error (39.82% (24.60%)) when breathing was free. Regarding computer complexity HRV was the best method while spectral combination required was the worst because requires previous calculations of all remaining methods. The best results were obtained for the leads placed in the middle of the chest close to V1 and V2. Recordings measured in supine positions had lower relative errors than seated or standing recordings. When the ECG noise was high due to motion artifact, the methods did not give satisfactory performance.

P83

A Body Position Detection Method by Fusing Heterogeneous Information of Surface ECG

Tsu-Wang Shen*, Fang-Chih Liu, Ya-Ting Tsao and Yi-Ling Ou

Medical Informatics, Tzu Chi University, Hualien, Taiwan

Objectives: The fall among seniors is a serious problem. The Center for Disease Control and Prevention (CDC) reported that one in four seniors, who fall and sustain hip fractures, will die within one year. Alarmingly, hip fractures are expected to exceed 500,000 by 2040. The issue is not just altruistic legislation but it addresses major economic implications. CDC also estimates that the direct costs to medical care will exceed $32 billion in 2020. Hence, determination of body position is a very important issue in both biomedical and healthcare fields, and it can be applied on various medical applications. Methods: Current fall detection systems used external signals to detect falls, such as accelerometer-based, vision-based, and wireless sensor array detectors. Instead of external signals, this proposed system is applied the heart as body internal sensor to detect body positions, including standing, sitting, and lying. Our experiment data contains 23 subjects with the similar range of ages. After signal pre-processing, the heart axis, heart rate viability (HRV), QRS areas, PR intervals, and PCA components are extracted and compared to evaluate the best factors for position detection. Finally, a soft sensor was also used to fuse those heterogeneous features for distinguishing different body positions. Results & Conclusions: Our results indicate that the heart axis is more accurate than HRV and PR intervals for posture detection. In addition, for standing and lying classification only, 99.93% training and 66.67% testing accuracy can be achieved for system performance. However, if a subjects identity is known in advance by using ECG biometrics, the performance may be further improved. Overall, ECG is potentially able to combine with other external signals to provide more reliable fall detection on homecare systems for prevention of false alarm.

P83

Design and Evaluation of an ECG Holter Analysis System

Alberto Rodríguez*, Gemma Rodríguez, Raúl Almeida, Nelvy Pina and Gisela Montes de Oca

Medical Equipment, Central Institute for Digital Research, Habana, Cuba

The aim of this paper is to discuss the design and evaluation process of a software for the analysis of ECG signal in a Holter system. The software was developed with RAD Studio 2009 using the Object Pascal language. The complete design and programming process was oriented to obtain different classes that encapsulate the needed functionality and combine them to obtain the final application.

The analysis process was organized in different steps: acquisition of the 3 channels of ECG and other recording information from the record device (up to 72 hours of ECG), filtration of ECG signal to remove movement and electrodes noises, detection and classification of QRS, detection of rhythm events and pacemaker malfunction, search of ST deviation episodes, HRV and spatial QT dispersion studies. All the processes were executed in this order and finalize with the compression and storage of the results.

Due to the large amount of data to be analyzed, all the algorithms were optimized to run fast. It was implemented a transparent buffering mechanism to manage the large ECG data files, performing reading and writing operations as if they were in memory. The rhythm events detection process was implemented using a pattern recognition algorithm that combines accuracy and faster processing. The average times to analyze recording of 24, 48 and 72 hours were 10, 30 and 70 seconds respectively.

The QRS detection and classification process was evaluated with 40 thirty-minute strips from the PhysioNet database. The 99.12% of the complexes were detected and 98.40% of complexes were well-classified. The user interface, entire system operation and analysis results were also tested and validated by specialists from the National Institute of Cardiology during a period of 4 months and 160 patients were studied. Nowadays there are 50 systems, working with good results in many hospitals.

Evaluation of a Shock Advisory System with Non-Shockable Pediatric Rhythms

JP Didon[1], I Jekova[2], V Krasteva[2]

[1]Schiller Medical SAS, Wissembourg, France
[2]Centre of Biomedical Engineering - Bulgarian Academy of Sciences, Sofia, Bulgaria

There are evidences for significant differences between pediatric vs. adult electrocardiogram (ECG). A supplementary validation of the shock advisory system (SAS) in automatic external defibrillators (AED) with pediatric ECGs is required. This study aims to assess the influence of non-shockable pediatric ECG on particular SAS criteria and to validate the SAS specificity (Sp).

The study uses an own pediatric ECG database from lead II holter recordings of 46 children - healthy and cardiac patients. A number of 10301 ten-second strips of non-shockable (N) rhythms are adopted for analysis. Adult ECG database (MIT-vfdb) is applied for derivation of reference SAS criteria values for N and shockable (S) rhythms.

Specific ECG analysis criteria of an AED SAS are evaluated: heart rate (HR), slope uniformity of positive vs. negative peaks (SU), deflections from signal extrema (SE) and signal mean (SM) in a narrow frequency band for QRS complexes enhancement.

P83

The SAS criteria are estimated in the following groups: (i) N(1-4) for N rhythms in children from 1 to 4 years; (ii) N(5-8); (iii) N(9-12); (iv) N(>18) for N rhythms in adults; (v) S(>18) for S rhythms in adults (see figure). Pediatric vs. adult N rhythms show significant differences in all criteria for groups N(1-4), N(5-8), N(9-12) compared to N(>18), $p<0.05$. Exceptions are: SE in N(5-8), N(9-12) vs. N(>18), $p>0.2$; SM in N(1-4) vs. N(>18), $p=0.12$. Comparisons in Mahalanobis space of HR,SU,SE,SM for S(>18) vs. N(1-4), N(5-8), N(9-12), N(>18) show that pediatric N rhythms are further away from S(>18) than adult N rhythms from S(>18). This is beneficial for correct recognition of pediatric N rhythms. The SAS validation for N(1-4), N(5-8), N(9-12) respectively present Sp=100%(1796/1796), 99.8%(4557/4568), 100%(3937/3937), higher than N(>18) with Sp=99.6%(2439/2448).

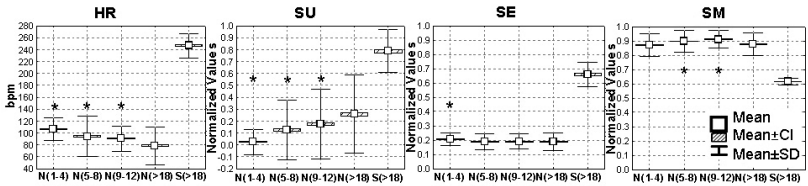

Box-Plot distribution of 4 SAS criteria for pediatric and adult rhythms.
* $p<0.05$: comparison of pediatric N(1-4),N(5-8),N(9-12) vs. N(>18)

Investigation of the Autonomic Nervous System Control of Cardiovascular Variables using fMRI and Carotid Stimulation

Giovanni Calcagnini*, Eugenio Mattei, Michele Triventi, Barbara Basile, Andrea Bassi, Marco Bozzali, Stefano Strano and Pietro Bartolini

Dept. of Technology and Health, Italian Institute of Health, Rome, Italy

Several factors make difficult in humans the study of the central processing and control exerted by the autonomic nervous system (ANS) on the cardiovascular parameters. Non invasive neuroimaging using fMRI has the potential to identify the brain regions involved. This paper illustrates the results of a fMRI event-related protocol which uses the neck suction to deliver a peripheral input to the ANS network. A dual chamber MRI-compliant neck-suction system was designed and realized. ECG, respiration and peripheral pulse signals were collected using an MRI compliant biosignal acquisition system. An event-related design was employed to randomly administer 50 efficacious (-60 mmHg) and 30 non-efficacious (-10 mmHg) stimuli, with a duration of 8 s each. Six-hundred echo-planar imaging volumes (TR=2.08 ms) with BOLD contrast, covering the whole brain, were collected in each experiment (total duration 20 min). From each MRI experiment, RR intervals were obtained from the ECG and uniformly resampled at 10 Hz. A stimulus-response curve was obtained by averaging the heart period response to each stimulation, and it was used to verify that the neck suction stimulus reached the ANS, since it is known that the individual anatomical variability in the carotid baroreceptors position may result in non efficacious stimulation. Fifteen informed volunteers underwent fMRI at 3T during neck suction stimulation. Eight subjects responded to the stimulation, whereas in seven subjects the heart period did not show a significant increase during the suction. In the responder subjects, efficacious stimuli induced an increased activation in the left posterior cingulate cortex, temporal lobe, and insula, compared to the non-efficacious condition. Our data demonstrate that, in a given number of subjects, it is possible to investigate the ANS using fMRI event-related protocols, and identify the brain regions involved in the central processing and control of signals from carotid baroreceptors.

P83

Accurate R Peak Detection and Advanced Preprocessing of Normal ECG for Heart Rate Variability Analysis

Devy Widjaja*, Steven Vandeput, Joachim Taelman, Bea Van den Bergh and Sabine Van Huffel

Department of Electrical Engineering, Katholieke Universiteit Leuven, Leuven, Belgium

Heart rate variability (HRV) analysis is well-known to give information about the autonomic heart rate modulation mechanism. In order to avoid erroneous conclusions, it is of great importance that only sinus rhythms are present in the tachogram and therefore, preprocessing the RR interval time series is necessary. R peaks have to be detected accurately in the ECG and missed peaks or false peaks have to be corrected. Also ectopic or supraventricular beats have to be removed. This paper presents an advanced automated algorithm to preprocess RR intervals obtained from a normal ECG. In case of too many (and falsely) detected R peaks, the algorithm deletes redundant R peaks by seeking the most optimal summation of consecutive small RR intervals, according to an adaptive reference RR interval which is composed of a weighted average of some previous RR intervals. The location of missed R peaks is detected if an RR interval is more than 1.8 times the reference interval and corrected by inserting new R peaks. If no optimal summation (less than 30% difference with the reference interval) of small RR intervals is possible or the RR interval is between 1.3 and 1.8 times the reference interval, the R peak is flagged for manual revision.

Validation of this algorithm was performed on one hour ECG signals of 20 pregnant women. R peaks were detected using the Pan-Tompkins algorithm after which the preprocessing algorithm was executed. R peaks before and after preprocessing were manually revised for redundant and missed R peak detections. Before preprocessing, more than 1% of the detected R peaks were incorrect while preprocessing corrected more than 94% of these errors leading to an overall error rate of 0.06%.

Our automated preprocessing technique therefore restricts the manual data check to the absolute minimum and allows a reliable HRV analysis.

P83

Blood Oxygen Level Measurement with a Chest-Based Pulse Oximetry Prototype

Collin Schreiner*, Philip Catherwood, James McLaughlin and John Anderson

NIBEC, Newtownabbey, Antrim, United Kingdom

In conjunction with ECG analysis, additional information about a patients blood oxygen level can produce safer diagnosis of any disturbance of cardiac rhythm. Reduction in blood oxygen levels can be associated with decrease in heart rate (bradyarrhythmia) or with significant reduction of a hearts pumping efficiency as a result of a myocardial infarction. Furthermore, a drastic fall in blood oxygenation could be a sign of a cardiac arrest episode. Currently, most blood oxygen measurement devices (Pulse Oximeter SpO2) require the placement of an optical sensor arrangement either on the finger, toe, earlobe or forehead. These particular positions can induce motion artefact. A previous study has revealed that the upper sternum area is most suitable for chest-based SpO2 monitoring. This paper presents a prototyped novel chest-based Pulse Oximetry system, and reports on test results from comparative trials with a commercially available finger-based Pulse Oximetry system using several human subjects. The system was iteratively optimised through adjustment of optical component alignment (angular position, component distance, photosensitive area etc.) and through fine-tuning of LED intensity and receiver sensitivity. This work is significant and timely as it provides compelling evidence that SpO2 measurements from the chest offer a genuine commercial solution for bedside and ambulatory vital-signs monitoring. Results of extensive testing clearly indicate that this system correctly records SpO2 variations from the chest for a range of adult test subjects and has been optimised to minimise signal distortion due to wearer motion. Comparison to the reference finger-based SpO2 system emphasises the prototypes commercial potential. In conclusion, we have shown SpO2 can be successfully measured on the upper sternum and the quality and repeatability of measurements are comparable to commercially available finger-based systems. This system offers reduced motion artefact due to positioning and also facilitates integration of SpO2 measurement into chest-mounted ECG monitoring systems.

Personal Sensor-System Modalities Evaluation for Simplified ECG Recording in Self-Care

Asta Krupaviciute*, Jocelyne Fayn, Eric McAdams, Christine Verdier, Chris Nugent and Paul Rubel

MTIC-EA4171, INSERM, Bron, France

Self-care is increasingly encouraged in order to detect cardiac events as early as possible. Herein, we propose a new design of a wearable sensor-system, produced in three different sizes: small (S), medium (M) and large (L), for simplified ECG recording anywhere, at anytime. It resembles a bib with four embedded electrodes which, when it is placed on the thorax, enables the recording of the three pseudo-orthogonal leads I, II and V2 according to the Mason-Likar system. Its main advantages include that it is easy to wear, it enables the measurement of the spatiotemporal ECG information while minimizing noise artefacts, it provides any given individual with a sensor-system size suitably adapted to his/her personal characteristics, and it overcomes problems associated with inter-recording variations in electrode positions, thus enabling more accurate serial ECG analysis. Our research goal is then to establish the most appropriate sensor-system size for each citizen, which thus produces ECG signals with a diagnostic information content that is closest to that of standard ECG. In order to evaluate the possible automation of this selection process, we performed a series of experiments on eight healthy volunteers. Six ECGs were recorded on each subject by using either our prototype sensor-systems or the standard and Mason-Likar recording systems. The same experiment was repeated some months later for three of the subjects to assess reproducibility. Synthesized 12-lead ECGs were computed from the 3-lead ECGs, using two patient-specific transformation models based on ANN and on regression, and compared to the recorded 12-lead ECGs, which were also compared. We present the results of the 280 ECG comparisons in terms of correlation, RMS value, changes in diagnosis probability and changes of some of the ECG measurements, and relate them to the personal characteristics of the subjects. We show that sensor-system personal adjustment can be and should be performed automatically on the basis of the ECG signal information and not of the chest/clothes size of the individuals.

P83

An Alternative to Derive the Instantaneous Frequency of the Chest Compressions to Suppress the CPR Artifact

Unai Ayala*, Elisabete Aramendi and Unai Irusta

Electronics and Telecommunication, UPV/EHU, Bilbao, Spain

The resuscitation outcome in cardiac arrest is tightly linked to minimizing interruptions in chest compression during cardiopulmonary resuscitation (CPR). Unfortunately, current automated external defibrillators (AEDs) require interruption of chest compressions for reliable rhythm analyses, as the artifacts caused by CPR corrupt the ECG signal. Filtering the artifact would allow a reliable diagnosis during CPR, thus reducing the hands-off interval and increasing resuscitation success.

Adaptive filters have been proposed to suppress the CPR artifact, either by analyzing the ECG alone or using reference signal(s). The latter provide better results than those based exclusively on the surface ECG. The instantaneous frequency of the compressions, derived from the chest compression signal, has been recently proposed to model the CPR artifact. Unfortunately, incorporating the compression depth in current AEDs involves important hardware modifications, as it should be acquired using accelerometers located in the chest compression pads.

In this work the transthoracic impedance was tested to extract the instantaneous frequency of the compressions required by an adaptive filter to suppress the CPR artifact. Transthoracic impedance signal is currently acquired by AEDs, and incorporating the suppressing system would only require software modifications.

P83

The methods were tested using a database of 380 88 shockable and 292 non-shockable records. In each record, the initial 15s were corrupted by a CPR artifact followed by 15s without artifact. Sensitivities and specificities were obtained, before and after filtering, using a rhythm analysis algorithm from a commercial AED.

The sensitivity and specificity for the corrupted intervals were 55.68% and 92.12% respectively. After filtering, the sensitivity and specificity were 92.05% and 89.38% when the frequency of the compressions was derived from the compression depth; and 95.45% and 86.30% when it was derived from the transthoracic impedance signal. It could be concluded that similar improvement was obtained with both signals.

Impact of the Approximated On-Line Centering and Whitening in OL-JADE on the Quality of the Estimated Fetal ECG

Danilo Pani*, Stefania Argiolas and Luigi Raffo

DIEE - Dept. of Electrical and Electronic Engineering, University of Cagliari, Cagliari, Italy

OL-JADE is an on-line algorithm for the separation of the Fetal ECG (FECG) from non-invasive potential recordings able to work in real-time on a DSP. It is conceived to join the separation quality of the batch JADE algorithm with the ability to follow time-varying mixing processes, with limited permutations in the order of the estimated sources, typical of sample-by-sample methods. As every Independent Component Analysis (ICA) algorithm, OL-JADE is composed of a pre-processing Second Order Statistics (SOS) stage followed by a Higher Order Statics (HOS) stage. With respect to the original JADE algorithm, OL-JADE preserves the HOS stage substituting the SOS one with a recursive sample-by-sample approximated centering and whitening. Such approximation partially violates the requirements of the JADE HOS stage so that its impact on the output quality should be carefully evaluated. This paper presents a comparison of OL-JADE with another state-of-the-art algorithm, tracking BLISS (with the HOS stage of JADE), and a manually-reordered block-by-block version of JADE. Several tests have been carried out on real trans-abdominal potential recordings in literature and on artificial mixtures of real sources either assuming time-invariant or time-variant mixing processes. The results show a substantial equivalence of OL-JADE with respect to the other algorithms with exact SOS stages. Permutations, mainly ascribable to a poor knowledge of the statistics of the noise and to unrealistic abrupt time variances, disappear enlarging the samples window for the HOS stage. Compared to tracking BLISS, which is quite similar in terms of working principle, OL-JADE presents a slightly reduced complexity and, in case of permutations due to time variances in the mixing process, permutations are confined to the involved sources but in turn these last show more distortion than in the BLISS case. The impact of the approximated SOS seems to be significant only on the noise sources.

P83

A Beat-to-Beat P-Wave Analysis in a Healthy Population

Valentina DA Corino*, Ioanna Chouvarda, Nicos Maglaveras and Luca T Mainardi

Department of Bioengineering, Politecnico di Milano, Milano, Italy

Changes in P wave morphology have been documented between patients with and without paroxysmal atrial fibrillation and in healthy subjects of different age. However, these changes were investigated using average P waves, obtained from the signal averaged ECG. Aim of this study is to explore and quantify possible beat-to-beat variations in P wave characteristics. Two-minute X-lead ECG recordings (1000Hz) of 54 healthy subjects (mean age 40 $\pm$ 14 years, range 17-69 years) were analyzed. Data were obtained from Physionet database. Beginning and end of P waves were located by means of ecgpuwave software. All P waves were aligned against a reference P wave, here defined as the first normal P wave of the ECG; waves poorly cross-correlated with the other beats were rejected. Each valid P wave was fitted by a Gaussian function (defined by three parameters: mean , standard deviation and amplitude A) whose parameter variations were investigated over two minutes window. To assess the method reliability, the normalized root mean squared error (NRMSE) between each P wave and its fitting was computed. To evaluate the variability of the estimated parameters, the coefficient of variation (CV), defined as the ratio of the standard deviation to the mean, was computed. Despite its simplicity, the proposed model was able to represent the P actual waves, being the mean NRMSE 0.047 $\pm$ 0.030 (range 0.012 0.140). A variability was found in all patients for both the parameters A and , reflecting P waves amplitude and duration, respectively. The mean CV of A was 0.087 $\pm$ 0.050 (range 0.032 0.253). CV of was 0.093 $\pm$ 0.053 (range 0.028 0.27). Finally, no correlation was found between the average model parameters and subjects age. These preliminary results lay the foundation for future beat-to-beat P wave analysis in patients with atrial conduction pathologies.

P83

ECG Motion Artefact Reduction Improvements of a Chest-based Wireless Patient Monitoring System

Philip Catherwood*, Nicola Donnelly, James McLaughlin and John Anderson

NIBEC (UU), Newtownabbey, Antrim, United Kingdom

Un-tethered patient monitors attract great interest in modern medicine. It affords patients earlier discharge, doctors increased flexibility and reduces hospital resource utilisation. With an aging population burdening healthcare services, such systems will become essential tools in overall healthcare operational strategies. However, ambulatory ECG monitoring causes motion artefact. Subsequent false positives and false negatives can effect patient management. This paper reports on a practical evaluation of motion artefact for a prototyped wireless body-worn monitoring device using multiple adult test subjects. For performance comparison, an FDA approved non-wireless system was employed and sensor leads restricted to minimise their movement. Both systems were worn concurrently, ensuring results were directly comparable. Evaluation of the device was undertaken for ranges of basic movements (bending, walking, sitting, climbing stairs) conducted under controlled conditions. This work is significant and timely as it highlights current progress in addressing key technical issues for successful implementation of smart cardiac monitors. Results indicate that the prototype system has greatly reduced motion artefact compared to the reference system. Reduction in artefact is achieved by strategic novel electrode design, optimised front-end interface and utilisation of wireless communications. In addition, heart rate and R-R intervals are of higher quality due to clearer ECG waveforms. Average heart rate difference between the prototype and the reference device is 3.8bpm with standard deviation of 12.4bpm. For R-R analysis, mean interval difference is 78.96ms with standard deviation of 123.1ms. In general, bending has highest differences due to considerable torso movement. More results for temperature, further R-R analysis etc. exist and are presented in the full paper. In conclusion, analysis of the quality of physiological data (ECG, heart rate, temperature and R-R interval) has shown the prototype system offers high fidelity recordings during basic movement. Also, due to on-chip data storage, it can be used for remote monitoring.

P83

Low-Cost Early Detection of Cardiovascular Disease in Chronic Kidney Disease Patients Based on Hybrid Heterogeneous ECG Features Including T-wave Altemans and Heart Rate Variability

Tsu-Wang Shen, Chih-Hsien Wang*, Yi-Ling Ou and Te-Chao Fang

Division of Nephrology, Tzu Chi General Hospital, Hualien, Taiwan

Objectives: According to Taiwan Society of Nephrology, there were more than 1,100,000 chronic kidney disease (CKD) patients in Taiwan. United States Renal Data System revealed that Taiwan had the highest incidence of end stage renal disease worldwide. Accumulating evidence shows that cardiovascular disease (CVD) contributes substantial burden to dialysis patients, accounting for almost 50 percent of mortality in both Chinese and Caucasian dialysis population. Traditional clinical risk factors include such as hypertension, dyslipidemia, hyperglycemia, and smoking. Unfortunately, the above factors may not totally explain and predict CVD high mortality. Hence, the research conbines heterogeneous ECG features as predictors, including T-wave altemans and heart rate variability for a low-cost prescreening tool within CKD patients. Methods: Fifty CKD hemodialysis patients were recruited and monitored over three years under IRB regulation at Tzu-Chi General hospital, Taiwan. Cardiologists categorized the population into two groups: 27 and 23 patients with and without CVD, respectively. Their ECG signals have been recorded for 5 minutes at supine for every 6 months. Potential features extracted from TWA and HRV in both frequency and time domains. For frequency analysis, basic Fourier transformation and Welch method were applied. Then, statistic analysis was followed to observe potential predictors, and then the decision-based neural network (DBNN) is used to fuse heterogeneous features. Results: Patients induced into CVD (n=23) had greater TWA magnitude (Valt: 0.24 ± 0.24 vs 0.09 ± 0.06 microvolt; P=.008) and cumulative alternans voltage (CAV: 24.21 ± 24.41 vs 9.04 ± 6.46 microvolt; P=.008) than those who has no CVD (n=27). The chi-square test showed significance between TWA and CVD (Alternans ratio$>$2.5, P=.028). The LF and LF/HF are significant smaller but the HF is higher in CVD group. The DBNN model with selected features provides 70.6% accuracy. Conclusions: Hybrid TWA and HRV successfully provide risk indicators for early CVD warning within dialysis patients for very low cost.

P83

Comparison of Voltage-Sensitive Dye di-4-ANEPPS Effects in Isolated Hearts of Rat, Guinea Pig and Rabbit

Katerina Fialova*, Jana Kolarova, Ivo Provaznik and Marie Novakova

Masaryk University, Faculty of Medicine, Brno, Czech Republic

Voltage sensitive dyes (VSDs) are used for recording of monophasic action potentials (MAPs) by optical method in cardiac preparations. Their direct influence on myocardium is not completely known. Previously we studied electrophysiological changes caused by VSD di-4-ANEPPS during staining and washout in guinea pig and rabbit hearts. However, often used animal in basic cardiology studies is rat. Therefore we decided to compare the electrophysiological effects of VSD in isolated hearts from the two abovementioned species and from Wistar rats. The hearts were perfused according to Langendorff at constant pressure (80mmHg) with Krebs-Henseleit solution (37C, 1.25mM Ca2+). Each experiment consisted of heart isolation, control perfusion, staining with VSD and washout. Touch-less 3D-electrogram was recorded, the heart rate (HR) was assessed and normalized to the end of control. The type and incidence of arrhythmias were evaluated and the hearts were assigned s.-c. Lambeth score (expressing severity of arrhythmias). Normalized HR decreased in all hearts ($p<0.01$ vs. control). During staining, this decrease was least steep in rabbit, then successively in rat and in guinea pig hearts. During washout, the highest degree of recovery was observed in rat hearts. The severity and incidence of arrhythmias did not differ significantly when rabbit and guinea pig hearts were compared. In rat, no arrhythmias appeared during staining and only one heart reached score 1 during washout (e.g. very low incidence of nonsignificant rhythm disturbances). Although the procedure of staining with the dye affects electrophysiological properties of the myocardium in all tested species, rat heart may be considered to be the most suitable for electrophysiological studies using di-4-ANEPPS. However, rat myocardium differs markedly from the human one. In order to advance towards clinically applicable research, the rabbit myocardium should be employed in such studies as the second choice. Supported by GACR 102/07/1473 and MSM 0021622402.

P84

Transcutaneous Dual Tuned RF Coil System Voltage Gain and Efficiency Evaluation for a Passive Implantable Atrial Defibrillator

Omar Jacinto Escalona, Jose Jesus Velasquez, Lawrence Chirwa, Niall Waterman* and John Anderson

CACR, NIBEC, University of Ulster, Newtownabbey, Antrim, United Kingdom

Atrial fibrillation (AF) is the most common cardiac arrhythmia, affecting 1% of the world population. Cardioversion of AF can be achieved by applying an electric shock to the heart (defibrillation). A cost-effective approach for internal cardioversion is by means of a subcutaneously implanted passive defibrillator. Methods: A circuit performance study for transcutaneous methods of atrial defibrillation is presented. A circuit design using a dual tuned resonant circuit whose capacitance also serves as a voltage booster is proposed and evaluated. Because of the rectifier network, the proposed circuit presents different secondary topological configuration for the positive and for the negative half cycles, leading to a complex theoretical analysis problem. Therefore, PSpice simulation and MatLab based modelling was implemented for circuit performance characterisation. Measurements were implemented on a hardware prototype circuit to verify the validity of the simulations and modelling results. The overall system efficiency study was carried out for several coil dimensions using a simple analytical model for the RF coils. For this particular task, a MatLab program for estimating the link efficiency was implemented. Results: The stability of output voltage across a 50 ohm heart model was evaluated by determining its variations as a function of coil separation. The circuit exhibited inherent voltage gain stability with changing separation at certain operating frequencies, with a reasonable voltage gain level >0.3 (Vrx/Vtx). Computed link efficiency modelling, estimated high link efficiency values of about 63.63% at resonant frequency (208 kHz) and 26 mm separation. Overall system efficiency was measured for the hardware prototype circuit, obtaining 59.61% in the best case, justifying the proposed circuit design. The study results would also suggest using a smaller (diameter) receiver coil on the implanted side while placing a larger coil on the transmitting side; this particular arrangement would be more suitable in an implanted passive defibrillator design.

P84

Changes of Heart Rate Complexity during Weaning from Mechanical Ventilation

Vasilios Papaioannou, Ioanna Chouvarda*, Nicos Maglaveras and Ioannis Pneumatikos

Alexandroupolis Hospital, Intensive Care Unit, Democritus University of Thrace, Alexandroupolis, Greece

Introduction: Discontinuation of mechanical ventilation in critically ill patients is a challenging task and involves a careful weighting of the benefits of early extubation and the risks of premature spontaneous breathing trial. Only a few studies have explored indices derived from heart rate (HR)and breathing pattern variability analysis for the estimation of weaning readiness.

Purpose: To investigate heart rate variability in patients with weaning failure or success, using both linear and nonlinear techniques. Materials and Methods: Thirty-two surgical patients were enrolled in the study. There were 22 who passed and 10 who failed a weaning trial. Signals were analyzed for 10 minutes during two phases: 1. pressure support (PS) ventilation (15-20 cm H2O) and 2. weaning trials with PS: 5 cm H2O. Low and high frequency (LF, HF) components and Poincaré plots of HR signals, HR multiscale entropy (MSE) and 1 exponent derived from detrended fluctuation analysis (DFA) were computed in all patients and during the two phases of PS. Results: Weaning failure patients exhibited significantly decreased LF normalized units [n.u](5.89+/-0.31 vs 6.62+/-0.10), HF n.u (4.65+/-0.30 vs 5.06+/-0.26, $p<0.001$), HR MSE (0.76+/-0.32 vs 1.09+/-0.29, $p<0.05$), and DFA 1 exponent (0.75+/-0.11 vs 1.27+/-0.16, $p<0.001$)compared with weaning success subjects. Their changes were opposite between the two phases, except for MSE that increased between and within groups, demonstrating different curve profiles ($p<0.001$). DFA A1 exponent and HR MSE predicted successfully weaning outcome. Areas under the curve were respectively: 0.791 (0.054) and 0.724(0.082, $p<0.05$ for both predictors). Conclusions: We suggest that nonlinear analysis of heart rate dynamics has a prognostic impact upon weaning outcome in surgical patients.

P85

Estimation of Stress-Strain Relationships in Vascular Walls using a Multi-Layer Hyperelastic Modelling Approach

Michel Edward Mickael*, Abbas Heydari, Roger Crouch and Sherri Johnstone

School of Engineering, Durham University, Durham, United Kingdom

Estimation of stress-strain relationships in vascular walls using a multi-layer hyperelastic modelling approach

Abstract

The World Health Organization (WHO) estimated that cardiovascular diseases were the reason behind 30% of global mortality numbers in 2005. In 2001, cardiovascular diseases caused 40% of the total deaths in the UK and led to around 10 billion dollars of productivity loss. Arteriosclerosis, atherosclerosis and hypertension are the main causes of cardiovascular diseases. Controlling blood pressure and volume could lead to saving of millions of lives and dollars.

One way of investigating and hence controlling blood pressure and volume is to use artificial mechano-sensors. These sensors would exist on molecular level to convert local stress-strain fields into electrical action potentials which can then communicate with the CNS. To understand their function in terms of measuring blood pressure, the pressure must first be transferred to a stress-strain field in the different layers -adventitia; media and intima- of the vascular wall containing mechanosentive ion channels, such that the conditions for activating mechano-sensitive ion channels in the mechano-receptors can be characterised. Previous research concluded that experimental investigations of layer characteristics have been limited to large arteries and veins , eg adult human coronary and carotid arteries, and vena cava. The mathematical model presented in this paper suggests a method of estimating the individual layer material parameters and hence stress-strain relationships for smaller vascular vessels, given only experimental data from totally intact vessels.

The model uses an existing empirically derived hyperelastic strain energy formulation to describe the individual cylindrical layer stress-strain characteristics. These are then combined assuming all the layers are thin and stress-equilibrium is conserved. Thus, an equivalent average stress, directly comparable to experimental data from an intact vessel, can be calculated. Each derived material parameter, describing the stress-strain relationship has been compared to existing experimental data from individual layers and are within previously quoted experimental error.

A New and Fast Index for the Quantification of Short-Range Self-Similarity in RR Time Series

Miguel Angel García-González*, Mireya Fernández-Chimeno and Juan Ramos-Castro

Group of Biomedical and Electronic Instrumentation, Department of Electronic Engineering, Technical University of Catalonia (UPC), Barcelona, Spain

Detrended fluctuation analysis (DFA) is becoming a usual tool in the analysis of RR time series although its computation can be very slow when dealing with long time series. We propose a new and very fast index (the frequency of sign changes of the mirrored differences or FSCMD) with good correlation with the short term scaling exponent (ALPHA-1) estimated among scales 4 to 16 of the DFA. FSCMD is the relative number of sign changes of the point-to-point differences between the RR time series and its corresponding reversed RR time series after a moving average detrending procedure is applied using a window of 30 samples. Linear regression results with simulated time series with Fractional Brownian Noise and length N show a very good relationship between both indices (Rsquare= 0.834 (N=300), Rsquare= 0.986 (N=3000), Rsquare= 0.995 (N=30000)). The linear regression results from Fantasia (FT), Normal Sinus Rhythm RR time series (NSR) and Congestive Heart Failure (CHF) databases after artifact correction also show good agreement (Rsquare= 0.822 (FT), Rsquare= 0.793 (NSR) and Rsquare= 0.937 (CHF)). Finally, Mann-Whitney Rank Sum tests applied to ALPHA-1 and FSCMD when comparing NSR and CHF databases show very significant differences ($p<0.001$) between groups for both indices. FSCMD is computed nearly 500 times faster than ALPHA-1 while analyzing NSR so FSCMD can be a fast alternative way to quantify the short term self-similarity of RR time series instead of a DFA.

P85

Prediction of Ventricular Tachycardia by a Neural Network using Parameters of Heart Rate Variability

S Joo*, KJ Choi, SJ Huh

University of Ulsan College of Medicine, Seoul, Korea

Prediction of ventricular tachycardia (VT), which is a life-threatening arrhythmic event, is an important issue for those people with heart problems. Heart rate variability (HRV) analysis has been used to find relations of parameters of HRV with not only heart problems but also other problems, such as, apnea and Parkinson's disease. In this paper, we present a method for prediction of VT by using an artificial neural network with parameters of HRV analysis.

PhysioNet's spontaneous ventricular tachyarrhythmia database, which consists of 232 RR interval (RRI) data (106 data recorded before VT events and 126 most recent (MR) data (control)), was used in this research. Each RRI was preprocessed before extracting parameters. At first, ectopic beats were removed by integral pulse frequency modulation model based correction algorithm. And then four time domain parameters (MeanNN, SDNN, RMSSD, and pNN50) and three Poincaré plot indexes (SD1, SD2, and SD1/SD2) were extracted. After detrending the RRI signal, data was interpolated with cubic splines and resampled at 7 Hz. The power spectral density of the resample data was analyzed with Welch's periodogram method. Four frequency domain parameters of VLF, LF, HF, and LF/HF were then extracted. Total 11 parameters were set for the input features of an artificial neural network (ANN) and the ANN was trained with 2/3 of the entire database. After complete training, the ANN was tested with the remaining 1/3 of the database to examine the classification performance.

P85

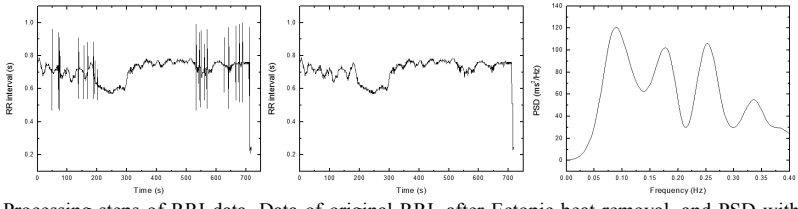

Processing steps of RRI data. Data of original RRI, after Ectopic beat removal, and PSD with Welch's periodogram

The ANN showed overall accuracy of 77.9% (60/77), 78.6% (33/42) for VT, and 77.1% (27/35) for MR data. This result shows fair success rate of VT prediction. With more number of data and improved algorithm, the developed method can be integrated into various health monitoring devices.

Frequency-domain Heart Rate Variability Analysis Performed by Digital Filters

Tsung-Chieh Lee and Hung-Wen Chiu*

Graduate Institute of Biomedical Informatics, Taipei Medical University, Taipei, Taiwan

Short-term heart rate variability (HRV) analysis based on spectral methods has been widely applied to assessment of autonomic nervous system activities for many physiological and mental disorders. Recently, homecare devices designed for heart monitoring have attempted to include HRV analysis function. These homecare devices based on some microprocessors with low computational power might encounter difficulty in implementing HRV spectral analysis for real-time applications. Therefore simple and less computation consuming methods to calculate frequency domain HRV indicators are needed. In this study, time-domain digital filters are proposed to solve this problem. The low-frequency (LF, 0.04-0.15 Hz) band and high-frequency (0.15-0.4 Hz) band signals of HRV are filtered from original 256 beats HRV signal. The variances of these two signals were considered as the equivalence of LF and HF powers derived from standard Fourier-based spectra respectively. Some finite and infinite impulse response (FIR and IIR) filters were tested to show their feasibility and find the optimal filter. The results showed that the time-domain filter with simple modification can generate comparable LF and HF power of HRV. The FIR filter-based method just uses the convolution operator thus it can simplify the design and deployment of short-term HRV analysis in homecare devices and make the real-time applications easier.

P85

Quantitative Analysis of the Relationship Between Chaotic Features of Surface ECG and an Intracardiac Electrogram

Sakineh Yahyazadeh, Mohammad Firoozabadi*, Majid Haghjoo and Saman Parvaneh

Biomedical Engineering, Islamic Azad University, Science and Research Branch,

Analysis of electrocardiogram (ECG) signal has recently become a popular non-invasive procedure to monitor the Heart activity and Heart diseases. The aim of research was to find formulas calculating chaotic features of intracardiac electrogram (EGM) using those of surface ECG. Since chaotic features of both surface ECG and EGM carry information using diagnosis, it seems finding a relation between them would be possible. This eliminates the risk of invasive procedure of EGM recording, reduces psychological stress of patients and is cost effective. An Intracardiac Atrial Fibrillation database from Physionet (IAFDB) which consists of endocardial recordings from the right atria of patients in Atrial Fibrillation (AF) was studied. A decapolar catheter was placed in four separate regions of the heart. In each region, the 5 bipolar signals were recorded (altogether 20 intracardiac signals) with 3 surface ECG leads. Open Tstool toolbox in Matlab 7.5B software was used to extract chaotic features (correlation dimension (CD), Large Lyapunov Exponent (LLE), Spatial Feeling Index (SFI)) of the signals. Coefficients of a linear formula between the features of ECG and EGM were computed for each region (bipolar) by PLS Regression method. Independent variables of this formula were chaotic features of the surface ECG and dependent variables were chaotic features of EGM. In addition, cross validation method was applied to check validation of these formulas. Using 3 ECG Leads, for each chaotic feature of 20 Heart regions a linear formula was obtained. Obtained regression formulas based on CD feature is valid with probability value (Pval) < 0.05 and Mean Square Error (MSE) <0.5. for LLE and SFI features, the regression formulas are not valid (Pval > 0.05). Moreover, it led to an important discovery, the closer bipolar electrodes were to the heart apex, the greater coefficients of lead II would be. The aim of this study was to find formulas estimating CD, LLE and SFI of intracardiac electrogram (EGM) using those of surface ECG. Formulas acquired for estimating CD of EGM using that of ECG surface in AF patients were efficient, while efforts to obtain LLE and SFI did not yield significant results.

P85

Gender-Related Effects of Sucrose Ingestion and Hypoxia on Cardiac Autonomic Modulation in Young Subjects

Tanja Princi*, Agostino Accardo, Petra Golja and Matjaz Klemenc

Department of Life Sciences, University of Trieste, Trieste, Italy

Several factors can influence the cardiac autonomic nervous system (ANS) activity, such as acute exposure to hypoxia and carbohydrate ingestion. The differences between genders in cardiac autonomic modulation in normoxia are well documented, while gender-related ANS responses following exposure to hypoxia or carbohydrate loading demonstrate dissimilar results. The aim of the present study was to assess gender-related effects of sucrose ingestion and hypoxia on cardiac ANS function in young healthy subjects by using non-linear (Poincaré plot) heart rate variability (HRV) analysis. All subjects (6 males and 8 females) were exposed to normoxia. After the first 15-min normoxic period, the subjects ingested a 10% water solution of sucrose in the amount of 4 kcal per kg body mass (4 kcal = 1 g sucrose). A 30-min acute normobaric hypoxia (FiO2 = 12.86%) followed. During the experiment, ECG, minute ventilation (V; L/min), and haemoglobin saturation (SaO2; %) were monitored. The Poincaré plot parameters (SD1 - marker of vagal influence SD2 marker of sympathetic activity) and SD1/SD2 ratio (marker of vago/sympathetic balance) were calculated on 5-10 min ECG segments. In comparison to normoxia, the sucrose ingestion and hypoxia provoked in women, but not in men, a significant reduction of vagal and sympathetic activities ($p < 0.05$) as well as a significant decrease of vago/sympathetic balance ($p < 0.03$). Haemoglobin saturation, similar between genders in normoxia, decreased significantly during hypoxia only in females ($p < 0.01$). The ventilation, in normoxia higher in males than in females, increased significantly only in females after sucrose loading ($p < 0.01$) and during hypoxia ($p < 0.02$). These results indicate a different gender-related cardiac ANS modulation after carbohydrate ingestion and acute exposure to hypoxia, suggesting a higher sensitivity to both these factors in females in comparison to males, with a shift in vago/sympathetic balance towards relatively more sympathetic and less parasympathetic activity.

P85

Perturbation in Parasympathetic Nervous System Activity Affects Temporal Structure of Poincaré Plot

Chandan Karmakar, Ahsan Khandoker* and Marimuthu Palaniswami

ISSNIP, The University of Melbourne, Melbourne, Victoria, Australia

The Poincaré plot of RR intervals is one of the most popular techniques used in heart rate variability (HRV) analysis. A novel descriptor (Complex Correlation Measure (CCM)) for measuring the variability in the temporal structure of Poincaré plot has been developed to characterize or distinguish between Poincaré plots with similar shapes. The aim of this study was to asses the changes in temporal structure of the Poincaré plot using CCM during atropine infusion (parasympathetic blockade) and transdermal scopolamine patch administration (enhanced parasympathetic activity) phases. The change in CCM values during these autonomic perturbation phases revealed the physiological relevance of the new descriptor. In this study, five subjects with normal sinus rhythm, did not smoke, had no cardiovascular abnormalities and were not taking any medications were studied. Short-term variability (SD1) (mean (ms) $\pm$ sd (ms)) was highest (69.90 $\pm$ 21.25) in Scopolamine phase and minimum (4.45 $\pm$ 2.45) in Atropine phase. Similar trend was also found for long-term variability (SD2), (103.05 $\pm$ 20.05) and (43.11 $\pm$ 13.79) in scopolamine and atropine phase respectively. CCM also showed minimum value in Atropine phase (3.88E-02 $\pm$ 1.05E-02) and maximum at Scopolamine phase (2.75E-01 $\pm$ 2.14E-02). However, Changes in mean values of CCM between study phases were higher than both SD1 and SD2. The change in CCM value indicates that CCM might correlate the parasympathetic nervous system activity as similar change in SD1 quantifies the vagal modulation of heart rate. Moreover, CCM conveys information about the temporal structure of the Poincaré plot and more sensitive to the changes in temporal structure of the plot compared to SD1 and SD2. This higher sensitivity in CCM values for Poincaré plot with small number of RR intervals might enhance the applicability of CCM to short term time series signal.

P85

Heart Rate Asymmetry (HRA) in Altered Parasympathetic Nervous System Activity

Chandan Karmakar, Ahsan Khandoker* and Marimuthu Palaniswami

ISSNIP, The University of Melbourne, Melbourne, Victoria, Australia

Heart rate asymmetry (HRA) was defined as a visible and quantifiable phenomenon in resting healthy people using Poincaré plot. In our pervious study, HRA has been defined considering geometry of the Poincaré plot to better estimate the HRA in healthy subjects. Based on the proposed definition, traditional asymmetry indices - Guziks index (GI), Portas index (PI) and Elhers index (EI) have been redefined. This study was designed to asses the changes in HRA using Poincaré plot during different phases of perturbation in parasympathetic activity. Eight subjects (age: 30.5 ± 7.3 yr) with normal sinus rhythm, did not smoke, had no cardiovascular abnormalities and were not taking any medications were studied. Parasympathetic perturbations were achieved by Atropine infusion (parasympathetic blockade) and scopolamine administration (parasympathetic enhancement) phase apart from baseline (normal) phase. The redefined Guziks index (GIp) was calculated for each subjects in each phase of the experiments. Then the asymmetry was calculated as at least 1% deviation from the symmetry value in either direction. Moreover, absolute distance from the symmetry range was calculated as Distsym to observe the changes in asymmetry index rather than subjective screening. In baseline phase the heart rate variability (HRV) of 87.50% subjects (7 out of 8) were found asymmetric which reduced to 62.50% (5 out of 8) during atropine infusion. In contrast, 100% (8 out of 8) subjects were found to be asymmetric during scopolamine administration phase. These findings suggest that screening of HRA changes harmoniously with change in parasympathetic activity of autonomic nervous system. Mean Distsym was also highest during scopolamine administration phase while it was lowest during atropine infusion phase. This suggests that mean distance from symmetric range increases with enhancement in parasympathetic activity and decreases during parasympathetic blockade. Hence, we can conclude that HRA changes with change in parasympathetic activity harmoniously.

P85

Using Cross-Correlation Function to Assess Dynamic Cerebral Autoregulation in Response to Posture Changes for Stroke Patients

Ben-Yi Liau*, Shoou-Jeng Yeh and Chuang-Chien Chiu

Department of Biomedical Engineering, Hung Kuang University, Taichung, Taiwan

Stroke has been the leading causes of mortality in Taiwan, even in the world for decades. Previous researches indicate the causes of cardiovascular diseases are highly related to the change of physiological parameters. Stroke can be resulted from rapid change or unstable cerebral blood flow due to the ineffective cerebral autoregulation (CA). The cerebral autoregulation mecha-nism refers to the cerebral blood flow (CBF) tendency to maintain relatively constant in the brain. In this study, time-domain cross-correlation function was applied to evaluate the relationship between blood pressure and cerebral blood flow velocity signals acquiring from healthy subjects and stroke pa-tients both in supine and head-up tilt positions. There are 10 stroke patients (56.0$\pm$10.6 years) and 11 healthy subjects (58.4$\pm$8.0 years) included in this study. Results revealed that the mean arte-rial blood pressure (MABP) values of stroke patients in response to posture changes were reduced (supine: 117.99$\pm$17.50 mmHg; head-up tilt: 112.25$\pm$17.68 mmHg). However, MABP values in healthy subjects were be-come higher in head-up tilt position (supine: 88.34$\pm$8.20 mmHg; head-up tilt: 95.32$\pm$11.69 mmHg). Both of MABP values of healthy subjects in supine and head-up tilt were significantly lower than those in stroke patients ($p<0.05$). On the other hand, mean cerebral blood flow velocity (MCBFV) in healthy subjects remain constant (supine: 38.85$\pm$7.94 cm/s; head-up tilt: 39.44$\pm$11.62 cm/s). However, the values in stroke patients reduced in response to head-up tilt (supine: 41.26$\pm$7.74 cm/s; head-up tilt: 37.43$\pm$7.16 cm/s). In the results of cross-correlation function (CCF) analysis, max CCF values in healthy sub-jects were significantly higher than those in stroke patients ($p<0.05$) in both supine and head-up tile positions. It might indicate correlation of MABP and MCBFV was higher in healthy subjects. The max CCF index in stroke pa-tients were close to 0 second in both positions (supine: -0.35$\pm$3.36 sec; head-up tilt: -0.29$\pm$3.20 sec). In healthy subjects, max CCF values should be around 2 seconds. Hence, it indicated the phase difference almost did not exist between MABP and MCBFV. This reveals the buffer function of CA were low in stroke patients. Therefore, CA in stroke patients might be im-paired by the results in response to posture changes.

P85

The Estimation of Arterial Stiffness Based on Analysis of Heart Rate

Alexander Fedotov* and Lev Kalakutsky

Radio Engineering, Samara State Aerospace University, Samara, Russian Federation

The estimation of arterial stiffness based on analysis of heart rate.

Hemodynamics model of human cardiovascular system has been proposed. This model allowed us to establish the relationship between index of arterial stiff-ness and pulse rate variability. We concluded that increased arterial stiffness leads to a decrease in total spectral power of pulse beat-to-beat intervals. It can be used for diagnostic evaluation. A new approach for estimation arterial stiffness by assessing the relative spectral power of pulse rate variability and heart rate variability (beat-to-beat R-R intervals) was suggested. A group of volunteers, consisting of 25 healthy people aged from 20 to 65 years were examined. ECG signal was recorded in the first standard lead. The sig-nal of peripheral arterial pulse was obtained by finger photoplethysmograph probe. The difference in magnitude of total spectral power of pulse rate variability and total spectral power of heart rate variability decrease with increasing age of subjects, which corresponds to the model evaluation and can be explained by age-related changes in arterial stiffness. Relative differences between power spectral density of pulse rate variability and heart rate variability among the older age group is shifted to lower frequencies, which may be caused by changes in temporal parameters in the secretion of vasoactive substances. Diagnostic index for estimation arterial stiffness was obtained by determin-ing relative differences in the spectral characteristics of pulse rate variability and heart rate variability. Comparative estimation between the proposed diagnostic index and arterial stiffness index, which defined by contour analysis of digital volume pulse, were presented; correlation coefficient was 0,92; $p < 0.02$.

P85

Web Site on Heart Rate Variability: Hrv-Site

Mirian Álvarez González, Xosé Antón Vila Sobrino*, María José Lado Touriño, Arturo José Méndez Penín and Leandro Rodríguez Liñares

Department of Computer Science, University of Vigo, Ourense, Spain

Heart rate variability (HRV) is an easily measurable physiological indicator that has important clinical applications. The autonomic nervous systems modulates the heart rhythm and then HRV is a good non invasive tool for evaluating diseases that affect this nervous systems, such as myocardial infarction, diabetes,... The main problem for HRV researchers is the lack of common data collections that could be used for testing their own algorithms. Moreover, free software tools for analyzing ECG records are scarce or they do not exist. Inspired by the PhysioNet Website (http://www.physionet.org), we have developed a Web portal, HRV-Site, located at http://www.hrv-site.net, and devoted to the HRV, taking into account aspects such as related papers, software, or datasets. Heart rate records included in HRV-Site are ASCII files freely and publicly accessible. We offer some additional information like age, sex or medical treatment and diagnosis. Some of them correspond to heart rate data obtained from Physionet ECG records. Another functionality provided by our Web portal is the possibility of performing online HRV analysis, employing our R-HRV software package, a plug-in for the open source statistical environment R, which can be freely downloaded from the R-CRAN repository. Users only need a web browser to use this tool and they can analyze either an heart rate record stored on the HRV-Site database, or analyze his/her proper record, stored in his/her own computer. HRV-Site is also aimed at maintaining updated documentation of both methodology and clinical applications of HRV, offering the researchers the possibility of building a growing HRV community, by forming discussion groups and adding news or advertisement. Currently, HRV-Site includes a collection of approximately 100 heart rate records, and provides information of more than 100 documents including scientific articles, books, and tutorials.

Heart Rate Variability and QT Dispersion in a Cohort of Diabetes Patients

Herbert Jelinek*, Ahsan Habib Khandoker and Marimuthu Palaniswami

Department of Electrical and Electronic Engineering, The University of Melbourne, Parkville, Victoria, Australia

QTd is associated with cardiac myopathy and heart failure. However the electrical rhythm disturbances associated QTd have not been thoroughly investigated in people with diabetes. We studied QT dispersion (QTd), an index of inhomogeneity of repolarization, and heart rate variability, a measure of cardiac autonomic modulation an indicator of rhythm disturbance in a cohort of people with and without type II diabetes and no recorded cardiac disease. Our study used a 20 minute Lead II ECG recording to obtain the tone-entropy (T-E) parameter where tone (T) represents sympatho-vagal balance and entropy (E) the autonomic regularity activity . QTd was calculated by the Welsh-Allyn ECG recorder software. The results for the tone and entropy analysis were combined using principle component analysis such that the mean$\pm$SE of for the control group (QTC$<$80msec) and high QTc (QTC$>$80msec) group were 1.009$\pm$1.009 and 0.578$\pm$0.403 respectively. 21.9% of people with diabetes fell into the $<$80msec QTd group and 25% into the $>$80msec group, giving a significant difference ($X_{33,2}=8.83$, $p<0.05$). The results for QTd and T-E indicate that the inhomogeneity of repolarization is associated with a decrease in TE reflecting a change in sympatho-vagal and a greater risk of cardiac morbidity and mortality in the diabetes cohort without any overt cardiac symptomatology.

P85

Role of the Late Sodium Current in Arrhythmias Related to Low Repolarization Reserve

Karen Cardona*, Beatriz Trenor, Lucia Romero, Jose Maria Ferrero and Javier Sáiz

I3BH, Universidad Politecnica de Valencia, Valencia, Spain

A hallmark of long QT syndrome is the prolongation of action potential duration (APD), which can be related to conditions of low repolarization reserve. An unbalance between depolarizing and repolarizing currents can fire early after depolarizations (EADs), precursor for the polymorphic ventricular tachycardia called Torsade de Pointes (TdP). This repolarizing disorder has been observed under pathological situations, such as heart failure (HF), oxidative stress, ventricular hypertrophy and/or in the presence of pure class III antiarrhythmics. Under such circumstances, there is evidence that the alteration of the late sodium current (INaL) has an important role.

The goal of this study is to evaluate the effects of INaL enhancement in the different cells of the ventricular wall under normal conditions and to analyze the role of INaL under pathological conditions prone to EADs generation. A formulation of human INaL was introduced in ten Tussher AP model, and the effects on APD and APD rate-dependency were evaluated. Simulations of EADs were also conducted under low repolarization reserve conditions.

Our results show that the increase in the maximum conductance of INaL prolongs APD in a rate-dependent manner, in agreement with experimental studies. A 10-fold increase of INaL prolongs APD in 35 %, 44 % and 80 % for a stimulation rate of 1 Hz in endocardial, epicardial and M cells, respectively. Additionally, APD rate-dependence was more pronounced in M cells (APDMax (0.5 Hz) -APDMin (0.33 Hz) yielded 123 ms versus 42 ms and 92 ms in epicardium and endocardium, respectively), especially when INaL was enhanced. Finally, the enhancement of INaL under conditions of low repolarization reserve led to EADs formation in M cells.

In conclusion, INaL enhancement is proarrhythmic in M cells with low repolarization reserve and under pathologic conditions prone to EAD generation.

P86

A Biophysical Model of Atrial Fibrillation to Simulate the Maze III Ablation Pattern

Catalina Tobon, Karen Cardona*, Jose Felix Rodríguez, Fernando Hornero, Jose Maria Ferrero Jr and Javier Sáiz

I3BH - UPV, Valencia, Spain

Atrial fibrillation (AF) is the most common cardiac arrhythmia. The Maze III ablation procedure consists of creating lines of conduction block in the atria according to a specific pattern to interrupt reentry pathways. Although a high success rate was reported, many clinical complications had been observed. An ideal pattern should be able to prevent AF with a limited number of lines. Advanced computer technology allows develop sophisticated biophysical models, which allow the simulation of the mechanisms involved in AF and opens up innovative approaches to simulate potential treatments. In this work we simulated the Maze III pattern in a tridimensional model of human atria and evaluated its efficacy for termination of an AF episode. For this purpose, we developed a 3D model of human atria, which includes the electrophysiological heterogeneity, anisotropy and fibers orientation. The electrophysiological changes caused by AF (electrical remodeling) were incorporated into a mathematical model of atrial cell and integrated in the anatomical model. An episode of AF was generated by ectopic activity in the left pulmonary veins. Unipolar pseudo-electrograms were computed in different regions of the atria. The ablation lines of the Maze III procedure were applied after 10 seconds of AF. The ectopic focus generated reentrant activity leading to fibrillatory conduction. The width of the vulnerable window for reentry was 16 ms. Figure-of-eight reentries, rotors, collisions and wave breaks were observed. The pseudo-electrograms obtained show variability in size and shape during simulated AF. When we applied the Maze III ablation pattern, the AF was finished after 200 ms. The results have been consistent with several cases reported by clinical studies. The developed model can be implemented to improve ablation patterns in order to find an ideal pattern to allow ending the arrhythmia with the least number of lines of ablation.

P86

Monophasic Versus Biphasic Stimulation of Single Cardiomyocyte Cell: a Simulation Study

Monica Caselli*, Aldo Casaleggio and Stefano Severi

University of Bologna, Vigarano Mainarda (FE), Italy

Introduction: Mechanisms involved in the initiation of fibrillation and defibrillation are very complex and still not totally understood, despite the number and varieties of theoretical and experimental approaches that have been employed to define them. This paper aims to investigate the effect of a monophasic or biphasic stimulus on a single cardiomyocite (CM).

Methods: The CM action potential (AP) is simulated using a modified Ten Tusscher model. Stimulation protocol is characterized by two following stimuli (S1-S2) of variable form and duration: the S1 is a positive pulse, S2 is like S1 in monophasic simulation, and it is a double pulse with zero mean in biphasic simulation; S1-S2 duration is variable and related to the refractory period of CM cell. To quantify the effect of S1-S2 on CM AP and the total response duration (TRD) defined as the interval between the S1 onset and the end of the action potential generated by S2 are considered. The underlying ionic currents are also analysed.

Results: With S1-S2 duration within the refractory period of the CM several simulations are considered. They indicate that, while monophasic pulse lead to very short action potential until the S1-S2 interval is closed to the end of CM refractory period, biphasic pulse lead to quasi-normal new action potential with much shorter S1-S2 intervals. The interpretation of such observation is directly obtained by the simulated current analysis: the amplitude of both calcium and fast sodium current is larger with biphasic pulse.

Conclusion: Straight-forward interpretation lead to the following conclusion: biphasic pulse, anticipating recovery from inactivation of ionic currents, allows a new action potential activation more easily that monophasic pulse.

P86

Beta-Adrenergic Modulation of Heart Rate: Contribution of the Slow Delayed Rectifier K^+ Current (I_{Ks})

R Wilders*, ACG van Ginneken, AO Verkerk

Academic Medical Center, University of Amsterdam, Dept of Anatomy, Embryology & Physiology
Amsterdam, The Netherlands

Under control conditions, the slow delayed rectifier potassium current (I_{Ks}) has little effect, if any, on the pacemaker activity of sinoatrial (SA) node cells. However, this outward current is enhanced by β-adrenergic stimulation, in which case it may affect pacing rate, either through its shortening effect on the action potential or through its inhibiting effect on diastolic depolarization. To assess the role of I_{Ks} in the β-adrenergic modulation of heart rate, we experimentally determined the effect of β-adrenergic stimulation on I_{Ks} and used the thus obtained data in computer simulations of SA nodal pacemaker activity, using the mathematical model of a primary rabbit SA node pacemaker cell by Kurata and coworkers.

Experimental data were obtained from HEK-293 cells that were transiently transfected with 1 μg wild-type KCNQ1 cDNA and 1 μg KCNE1 cDNA, encoding the α and β subunits of the I_{Ks} channel, respectively. KCNQ1/KCNE1 currents were studied at 37°C using the perforated patch-clamp technique in absence and presence of forskolin (10 μmol/L) to increase the cAMP level, thus mimicking β-adrenergic stimulation. Forskolin significantly increased the KCNQ1/KCNE1 current density by ≈25%, shifted the steady-state activation curve to more negative membrane potentials by ≈15 mV, and increased the activation rate by ≈50%.

P86

Incorporation of our experimental findings into the SA nodal cell model resulted in a 6-ms decrease in cycle length, the shortening effect on action potential duration dominating over the inhibiting effect on diastolic depolarization. The decrease in cycle length is similar to the 10-ms decrease observed upon incorporation of a +8-mV change in the voltage dependence of the HCN4-encoded hyperpolarization-activated 'pacemaker current' (I_f), reflecting our earlier experimental data on the effect of forskolin on HCN4 current expressed in undifferentiated human cardiac myocyte progenitor cells.

We conclude that I_{Ks} is an important contributor to the β-adrenergic modulation of heart rate. This may explain the impaired heart rate response to exercise observed in long-QT syndrome type 1 and type 5 patients, who carry a loss-of-function mutation in the KCNQ1 or KCNE1 gene, respectively.

Simulation of Cardiac Action Potential Propagation using Hybrid Models

Matthew J Poole*

School of Computing, University of Portsmouth, Portsmouth, Hants, United Kingdom

Mathematical models of the cardiac action potential include complex biophysically-derived ionic models, simpler generic ionic models, and phenomenologically-derived models that caricature the action potential and its propagation. Complex models are computationally demanding. To investigate spatio-temporal behaviours (e.g. reentrant arrhythmias), simpler models are more computationally effective. However, these can be insufficiently rich to represent many dynamics and pathological states.

In this study we investigate the use of hybrid models as an efficient approach to cardiac tissue simulation. Small regions of tissue modelled at a biophysically-detailed level can be embedded within a larger system (e.g. whole ventricles) represented using a simpler action potential model. Thus a region of specific interest (e.g. tissue affected by ischemia) can be realistically modelled, but with computational requirements greatly reduced for the surrounding tissue. As a case study, we consider a hybrid system in which Luo-Rudy (LR1) model cells are embedded within a surrounding tissue employing the 3-variable Fenton-Karma model.

P86

The validity of the hybrid approach is dependent upon the method used to couple cells across the interface of the two model regions. A simple approach to inter-model coupling is to allow normal (intra-model) diffusive cell-cell coupling to apply unaltered across the interface. We show that such an approach fails to cope adequately with the different action potential morphologies of the component models; e.g., instead of being preserved, the embedded Luo-Rudy model's action potential includes features characteristic of the Fenton-Karma model.

We develop an alternative method in which inter-model coupling is dependent upon the discrete action potential phase (resting - stimulated - upstroke plateau recovery) of interface cells. Our method is shown to perform well in simulations of propagation in 1D and 2D hybrid models. We conclude by considering further development of methods to support hybrid modelling, and possible future applications.

Development of a Biophysically Detailed Model of the Rapid-Delayed Rectifier Potassium Channel

Ismail Adeniran*, Jules Hancox and Henggui Zhang

Biological Physics Group, School of Physics and Astronomy, University of Manchester, Manchester, United Kingdom

The human ether-a-go-go-related-gene (hERG) encodes potassium channels responsible for the rapid-delayed rectifier current (IKr). IKr plays a critical role in the repolarisation of cardiac action potentials (AP). hERG/IKr channel mutations result in defective repolarisation, which may lead to life-threatening conditions such as the long and short QT syndromes.

To study the functional consequences of impaired hERG/IKr channel on arrhythmogenesis, models of human ventricular cells incorporating IKr channel current are often used. However, the IKr current formulation in many models simplify the inactivation process and are unable to replicate dynamic gating changes in the channel. Accurate simulation of dynamic behaviour such as the response to premature depolarising stimuli requires more complex formulations (e.g. Lu et al).

The aim of this study was to develop a model that accurately reproduces the characteristics of normal and aberrant hERG/IKr during cardiac action potential waveforms. A Markov chain model of hERG current (IhERG) was developed based on experimental (AP voltage clamp) data on its kinetic properties, particularly (1) its fast and profound inactivation upon activation by depolarisation; (2) its rectification at positive potentials; (3) the generation of transient, outward currents 'in response' to premature, depolarising stimuli.

P86

To derive the parameters of the model, the Levenberg-Marquardt algorithm and the Broyden-Fletcher-Goldfarb-Shanno method were used to minimise the residual between the experimental data and the simulated result, and obtain parameters that reproduced the experimental AP voltage clamp IhERG profile. The resulting formulation was further validated by comparing simulated results from different voltage clamp protocols activation, inactivation and deactivation against experimentally-observed results. Moreover, the model could accommodate alterations that reproduced changes to IhERG associated with short QT syndrome.

In conclusion, this work provides a new Markov chain model of hERG/IKr that can be used to investigate the functional consequences of hERG/IKr channel mutations on cardiac electrical activity.

Gender and Age Based Differences in Risk of Proarrhythmia by Dofetilide : A Computational Model Study

Rodolfo Gonzalez*, Julio Gomis-Tena, Alberto Corrias, Jose Maria Ferrero, Blanca Rodríguez and Javier Sáiz

i3bh, Universidad Politecnica de Valencia, Valencia, Spain

Male/female differences in cardiac electrophysiology have long been noted, but only in recent years has there been an increased awareness and appreciation of the influence of a patients sex on presentation of various cardiac arrhythmias. Women have higher resting heart rates than do men, but a longer rate-corrected QT (QTc) interval. However, young boys and girls have similar QTc. Many drugs associated with acquired long QT syndrome have a greater risk of inducing torsades de pointes (TdP) arrhythmia in women than in men. The aim of this study was to investigate the risk of proarrhythmia by dofetilide in gender and age based differences using action potential duration (APD) and dispersion of repolarization (DOR). Left ventricular epicardial, midmyocardial and endocardial action potentials were simulated using a modified Luo Rudy model. Sex, age and regional differences in current densities and voltage dependent parameters for ICaL, IKr, IKs, and Ito were incorporated into the model. A model of dofetilide was developed and included into a ventricular cell model. Dofetilide concentrations used were 30 and 100 nM. DOR was defined as the delay in final repolarization between shortest and longest action potential. Results shown that in all cell types, adult female cells had longer action potentials and a higher susceptibility to early afterdepolarizations (EAD) than adult male cells under control and drug induced conditions. On the other hand, young male cells had longer action potentials and higher susceptibility to EADs than young female cells under drug induced conditions. In conclusion, this study has demonstrated that gender and age based differences in ionic currents and drug induced action of dofetilide might explain in part the higher susceptibility of EADs and prevalence of TdP in adult females and the higher risk of cardiac events in males than females during childhood.

P86

An Improved Model of Ba Current through L-type Ca Channels Including Voltage- and Ion-Dependent Inactivation

Stefano Morotti*, Eleonora Grandi, Aurora Summa, Kenneth S Ginsburg, Donald M Bers and Stefano Severi

Biomedical Engineering Laboratory, University of Bologna, Cesena, Italy

Background. Inactivation of the L-type Ca channel (LTCC) is regulated by both Ca- and voltage-dependent processes (CDI and VDI). CDI is due to binding of Ca to calmodulin (CaM), which causes a channel conformational change that accelerates inactivation. To differentiate VDI and CDI, several studies have considered the inactivation of Ba current through LTCC (IBa) as a measure of VDI. However, there is evidence that Ba can weakly mimic Ca, such that IBa inactivation is still a mixture of CDI and VDI. Methods. We incorporated an existing Markov model of ICa (in which VDI was modelled to fit experimental IBa inactivation)into an excitation-contraction coupling model. We extended the LTCC model to assess whether and how experimental IBa inactivation could be recapitulated by modifying CDI to account for Ba-dependent inactivation. A weaker apparent affinity of Ba for CaM (kBa<kCa) was simulated by making ion-dependent transitions less sensitive to Ba (vs. Ca) by a factor kCa/kBa, which varied from 1 to 100. Results. Modeling results show that IBa exhibits slower inactivation as Ba affinity decreases. The modest ability of Ba to mimic Ca-dependent inactivation is negligible when kCa/kBa is larger than 10. We found that a 10-fold reduction resulted in appropriate Ba-dependent IBa inactivation. With this model we were able to reproduce the U-shaped dependence of IBa inactivation rate on voltage and the increased extent of IBa inactivation that is observed in experiments with increasing peak IBa. These results hold true if intracellular Ba accumulation is avoided during the experiment. Conclusions. The extended LTCC model should be a more faithful representation of purely VDI during ICa. This may be an important distinction when one seeks to dissect the relative roles of Ca and voltage in regulating ICa in normal and diseased conditions.

P86

Mathematical Modelling of Electrotonic Interaction between Stem Cell-Derived Cardiomyocytes and Fibroblasts

Michelangelo Paci*, Laura Sartiani, Marisa Jaconi, Elisabetta Cerbai and Stefano Severi

Biomedical Engineering Laboratory, University of Bologna, Cesena, Italy

Introduction: Human embryonic stem cell-derived cardiomyocytes (hES-CM) represent a promising tool for cell therapy. Their functional properties must be assessed.

Methods: We characterized hES-CM at their early stage of development (15-40 days) with electrophysiological, RT-PCR and modelling tools. The hES-CM action potential (AP) was simulated on the basis of the Ten Tusscher model of human adult ventricular cell, modified to incorporate all the experimentally assessed modifications of ionic currents; in particular the hyperpolarization-activated funny current was introduced following a Hodgkin-Huxley formulation with a single activation gate. This led to an in silico cell showing a spontaneous beating activity. Electrotonic coupling with one or more fibroblasts, modelled both as having an ohmic (p̈assive) membrane resistance or considering time and voltage-dependent (äctive) currents, was simulated.

Results: the uncoupled hES-CM model well fitted our experimental data in terms of APD (experimental 228+/-11; simulation 231 ms), Vmax (4216+/-611; 4778 mV/s) and beating frequency (36+/-6; 35 bpm). MDP (-47+/-7; -79 mV), APA (63+/-5; 92 mV) and diastolic depolarization rate (DDR) (22+/-5; 13 mV/s) were out of range. Electrotonic coupling was assessed: fibroblast membrane potential was more and more similar to the hES-CM when increasing the coupling conductance. Coupling the hES-CM with 1 and 2 fibroblasts caused an increment of DDR (+4, +5 mV/s respectively) and beating frequency (+3, +6 bpm) and a reduction of the AP peak (-0.4, -1.3 mV). While the correct AP features reproduced by the uncoupled model were preserved, coupling the hES-CM with 1 and 2 äctivefibroblasts led to a better fit of DDR.

Conclusions: these results suggest that our novel mathematical model can serve as a predictive approach to interpret and refine in-vitro experiments on hES-CM and that few coupled fibroblasts can significantly affect DDR while their influence on the AP amplitude is relatively small.

P86

Interplay of Potassium Channels in Modulating the Action Potential of Human Ventricular Myocytes

Chong Wang, Peter Beyerlein, Heike Pospisil, Antje Krause, Werner Dubitzky and Chris Nugent*

School of Biomedical Sciences, University of Ulster,

Potassium ion channels are key determinants of cardiac action potential (AP) activity. Their interplay in modulating the AP of human left ventricle has not been well characterized.

In the present study, our newly developed allosteric conformation model for rapid delayed rectifier (IKr) was incorporated into the ten Tusscher model for human ventricular tissue. The transmural densities of IKr, the slow delayed rectifier (IKs) and the transient outward channel (Ito) were refined based on the variable expression of underlying protein subunits. The interdependence of these channels were investigated by simulated channel block.

With an IKr density ratio of about 0.55:0.83:1 in epicardial (Epi),mid-myocardial(M) and endocardial (Endo) cells, a maximum conductance of 0.00792 nS/pF for IKr, 0.1778 nS/pF for IKs and 0.209 nS/pF for Ito, the modified model was able to reproduce an action potential duration (APD) of 311 ms in epicardial, 342 ms in M and 296 ms in endocardial cells at 1 Hz pacing. A frequency change from 1 Hz to 0.5 Hz resulted in an Epi APD difference of 20.27 ms, an Endo APD difference of 18.64 ms and an M APD difference of 31.92 ms. Blocking IKs or IKr in M cells showed that APD increased with the downregulation of Ito. Block of IKr led to a prolongation of APD90 by 9% in Epi, 23% in M and 15% in Endo cells, whereas block of IKs caused a prolongation of APD90 by 27% in Epi, 7% in M and 21% in Endo cells, respectively.

The modified ventricular model yielded the density distribution of potassium channels closer to the physiological ranges compared with that given by the previous model. The results about the response to individual channel blocks and the improved APD rate adaptation provided a basis for understanding abormal ventricular repolarization.

P86

The Role of the Transient Outward Current in Action Potential Repolarization: A Simulation Study

Beatriz Carbonell, Lázló Virág, Norbert Jost, András Varró and Chema Ferrero*

Institute for Research and Innovation in Bioengineering (I3BH), Universidad Politécnica de Valencia, Valencia, Spain

The time-course of action potential (AP) repolarization, and thus AP duration (APD), is the result of a delicate balance of currents during the AP plateau. As the potassium transient outward current (Ito) is active only during the early plateau, its role in governing APD is controversial. Recently, Virág et al experimentally showed that blocking Ito significantly lengthens APD in canine epicardium, something that could be key in arrhythmogenesis. In this work, we have combined electrophysiological experiments with simulations to study and explain the contribution of Ito to repolarization.

After isolating myocytes from dog ventricular epicardium, whole-cell patch-clamp experiments were performed to characterize the kinetic properties of Ito. An overlap region was found between the steady-state activation and inactivation curves, suggesting the potential existence of a window current in the range of -20mV to -40mV. Also, Ito inactivation was found to follow a two-exponential time course, with a slow component of tau=24ms at 20mV.

These data was used to formulate a new mathematical model for Ito, which was then inserted in the Decker (2009) model for canine epicardial AP. Simulations in control conditions yielded an APD of 202ms. Blocking IKs, only a slight prolongation of APD was observed (209ms). When an additional block of Ito was simulated, APD increased to 221ms, which is consistent with the experimental findings by Virág et al. Further IKr blocking produced EADs even at 1Hz stimulation frequency, something which could lead to lethal arrhythmias in vivo.

Inspection of ionic currents suggested that Ito reactivation (96nA/uF) due to the activation-inactivation overlap, and indirect changes exerted by Ito blockade on ICaL (110nA/uF increase during the plateau) and IKr (42nA/uF) are responsible for this paradoxical increase in APD. These novel findings emphasize the importance of Ito in repolarization and suggest a potential role of Ito blockade in arrhythmogenesis.

Slow Pulse Due to Calcium Current Induces Phase-2 Reentry in Heterogeneous Tissue

Angelina Peñaranda*

Fisica Aplicada, Universitat Politecnica Catalunya, Barcelona, Spain

Phase-2 reentry is thought to underlie many causes of idiopathic ventricular arrhythmias as, for instance, those occurring in Brugada syndrome. Reexcitation due to phase-2 reentry needs two conditions to be met: first, that a heterogeneous loss of dome is produced in tissue and, second, that the spike-and-dome regions are able to reexcitate the loss-dome areas.

We analyze the conditions that lead to very short APs, as well as possible mechanisms for reexcitation in a cable. Provided the system is in a state close to the loss of dome, very small gradients of electrophysiological properties, for instance, of the transient outward current, are enough to result in big dispersion of repolarization, giving rise to reexcitations and, eventually, reentry. The origin of reexcitation is based on the existence (often transiently) of a slow pulse (due to the calcium inward current) that propagates into the region of short action potentials (APs) until it reaches excitable tissue. We calculate the speed of the slow pulse, and also give an estimate of the minimal tissue size necessary for reexcitation. Depending on parameters this minimum tissue size may be very small, of the order of 0.5-1 cm. We then study the induction of reentrant waves (spiral waves) in simulations of AP propagation in the heart ventricles.

P86

Drugs that increase the strength of the calcium current may eventually help recovering the dome, thus decreasing dispersion of repolarization, but until this happens, they increase the probability that a reexcitation occurs. This happens because an increase in calcium strength stabilizes the slow calcium pulse, that then is able to reexcitate adjacent tissue. Thus, drugs that decrease the transient outward current would seem more suitable candidates to avoid dispersion of repolarization while maintaining a low probability of reexcitation.

Moving Window Signal Concatenation for Spectral Analysis of ECG Waves

P Augustyniak

AGH University of Science and Technology
Krakow, Poland

Spectral analysis of ECG waves is useful as a background for the medical analysis, as well as for estimating the necessary throughput of transmission channel or storage space. Recently introduced non-uniformly sampling ECG recorders also use the local bandwidth estimate to adjust the data acquisition to expected local properties of the signal. Unfortunately, the commonly applied spectral estimation methods are not directly applicable to the ECG waves due to their short duration.

We postulate replacing the averaging of successive waves spectra, by concatenation of selected type waves (P, QRS or T) in a moving time window. The window size is selected as a result of compromise between the spectrum resolution (high for long window) and temporal response (fast for short window). To avoid influence of border effect, the order of concatenated waves is optimized with regard to the maximum smoothness of resulting signal. The smoothness estimate is based on the similarity of the first and second derivatives of the adjacent signals in weighted contributions.

Evaluation of the proposed method was made experimentally and used ICE60601-2-51-complying ECG interpretation software for determining the wave borders. First attempt was made with use of the CSE Multilead Database, however the duration of records (10s) is too short to apply time sliding windows of different size. Second attempt was using custom-recorded long time 12-leads ECGs. Our results for 10s window shows a considerable drop of estimated bandwidth (defined as 5% of power spectrum density) due to limiting the border effect contribution. Using normal records from CSE Dataset3 for which the initial bandwidth value of 151Hz was calculated with P-wave spectrum averaging, we estimated the corrected limit to 107Hz only, which seems to be much more reasonable considering the physiological limitations of ECG signal generation. Similar results were observed for QRS and T waves.

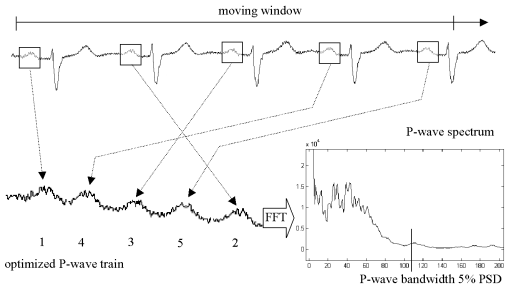

Optimizing of P-wave train for spectrum estimation.

S91

Heart Arrhythmia Detection using Continuous Wavelet Transform and Principal Component Analysis with Neural Network Classifier

Ali Ghaffari, C Nat Nataraj*, Parham Ghorbanian and Ali Jalali

Department of Mechanical Engineering, Villanova University, Villanova, PA, United States

An approach for automated heart arrhythmia detection is presented in this study. The specific aim of this study is to develop an algorithm to detect and classify six types of Electrocardiogram (ECG) signal beats including Normal (N), Atrial Premature (A), Right Bundle Branch Block (R), Left Bundle Branch Block (L), Paced (P), and Premature Ventricular Contraction (PVC or V) beat using a neural network classifier. To advance the accuracy of classification a hybrid method combining Continuous Wavelet Transform (CWT) and Principal Component Analysis (PCA) is applied. Several stages of pre-processing have been applied in order to prepare the most appropriate input vector for the neural classifier; first of all, since the collected ECG signals are so noisy, a mathematically based signal filtering method is used to remove the ECG signal baseline wandering in addition to noise. To select the suitable range of samples from the raw ECG signal, several methods have been tested and finally the best method was found to select 150 samples after R wave for all types of signals. These segments are found to be the most appropriate range of ECG signals which represent morphological differences between different types of ECG beats and include sufficient amount of data needed for accurate classification of heart arrhythmias. Continuous Wavelet Transform is then applied in order to extract features of ECG signal which are different for different types of arrhythmias. In the next step PCA method is used to reduce the size of the data. Finally, a well-known neural network architecture called Multi-Layered Perceptron Neural Network (MLPNN) is utilized as the final classifier to classify each ECG beat as one of six groups of signals under study. Finally, MIT-BIH database is used to evaluate the proposed algorithm, resulting in 99.5% Sensitivity (Se), 99.7% Positive Predictive Accuracy (PPA) and 99.2% Total Accuracy (TA).

Evaluation of Feature Models for 12-lead ECG Classification

Mariano Llamedo*, Antoun Khawaja and Juan Pablo Martínez

National Technological University, Buenos Aires, Argentina, and University of Zaragoza, Spain

Automatic ECG classification is a well-known problem with several classification models proposed in the last two decades. Those models were developed from the available two-lead ECG databases. The aim of this work is to evaluate the usefulness and robustness of multi-lead features derived from 12-lead ECG recordings, available in current databases. The St Petersburg Institute of Cardiological Technics 12-lead Arrhythmia Database (INCART) was used (available on Physionet) together with the AAMI recommendations for class labeling and results presentation. We used as reference a classification model developed and evaluated in two-lead recordings, achieving good performance in all databases available on Physionet for classification purposes. This model includes classical features based in the heart rhythm as well as features obtained from different scales of the wavelet transform (WT). This reference model was adapted to 12-lead recordings using a PCA approach, adding other features describing the VCG loop morphology. We used linear discriminant functions classifier. The performance evaluation was carried out via a 10-fold crossvalidation approach in the whole database, and specifically obtaining the global accuracy (A) sensibility (S) and positive predicivity value (P+). A 9-feature model was obtained, achieving for the normal class a S of 98% and P+ of 100%, for supraventricular beats S of 84% and P+ of 35%, for ventricular beats S of 93% and P+ of 96%. The global A was of 97% while the global S and P+ of 92% and 77% respectively. The multilead features added which describes the morphology of the VCG loop, together with the adaptation of the 2-lead features to 12-lead, resulted in an increase in the classification performance for each class with respect to the reference 2-lead classifier. The results obtained show the usefulness of extending the classification models to a 12-lead-multilead approach, but must be corroborated in other databases.

PCA-based Noise Reduction in Ambulatory ECGs

Iñaki Romero*

System Integration, IMEC, Eindhoven, Netherlands

Ambulatory cardiac monitors have experienced an increment in autonomy and functionality with the improvement of low-power microelectronics. They are able to perform some signal processing and data interpretation. However, motion artifacts can mask the ECG signal. This paper, investigates a denoising algorithm based on PCA due to its relatively low computational complexity. A database was generated by combining clean 8-lead ECG with noise signals containing motion artifacts at different levels of activity. SNR values ranging from 10 to -10 dB were considered. 8-channel PCA was applied and then inverted after selecting a subset of principal components (PC). For evaluating signal improvement, the correlation coefficient between the noise-free signal and the output after PCA filtering was computed. In addition, SNR before and after PCA was estimated. Firstly, PC that best matched the ECG was identified in function of the signal SNR. Above 0dB, the PC corresponding to highest variance gave best performance, below 0dB the best PC was the second or the third with highest variance. The number of PCs in function of the SNR was then investigated. It was observed that when SNR decreased, PCA performed better when retaining less number of PCs (4 PCs for a SNR=10dB down to 1 PC for SNR=-10dB). Reducing the number of input ECG leads did not yield to a significant difference when it was reduced from eight (median SNR improvement of 2.60 dB (MAD=2.35)) down to two (median SNR improvement of 2.06 (MAD=1.95)). Based on these results, a method for identifying the subset of PC that matches the ECG was proposed as function of input SNR and number of channels. This method gave an SNR improvement of 2.5dB-3.2dB depending input SNR.

Filtering the Cardiopulmonary Resuscitation Artifact: An Analysis of the Influence of the Signal-To-Noise Ratio in the Accuracy of the Shock Advice Algorithm

Sofia Ruiz de Gauna*, Jesus Ruiz, Unai Irusta and Unai Ayala

Electronics and Telecommunications, University of the Basque Country, Bilbao, Spain

A reliable diagnosis by automated external defibrillators (AED) during cardiopulmonary resuscitation (CPR) would avoid unnecessary hands-off time, thus increasing the resuscitation success. In the last decade, several filtering techniques have been proposed to remove the artifact induced on the ECG during CPR. The improvement of the signal-to-noise ratio (SNR) has been frequently used to test CPR cancellation filters, using artificial mixtures of ECG signals and CPR artifact. In this work, we analyze the correlation between the diagnostic results of an AED after filtering with the input SNR of the corrupted ECG, for real out-of-hospital resuscitation episodes. We processed 381 ECG records, 89 shockable and 292 non-shockable (88 asystole and 204 non-asystolic rhythms). Each record contains an initial 15.5 s interval corrupted by CPR, followed by 15.5 s free-of-artifact. The CPR artifact was suppressed using a Kalman filter and we evaluated the sensitivity and the specificity of a commercial AED. The mean input SNR for the shockable and the non-asystolic records was -1.7 $\pm$ 6.8 dB and -0.6 $\pm$ 7.8 dB, respectively. There were 52 shockable records correctly classified before and after filtering with an input SNR of 1.3 $\pm$ 5.6 dB, and 32 shockable records that changed from non-shockable to shockable after filtering, with an input SNR of -4.3 $\pm$ 6.0 dB. Therefore, the sensitivity improved from 58.4% to 94.4%. The specificity for the non-asystolic group (92.6 %) did not change after filtering; there were 178 records correctly classified before and after filtering (SNR -0.6 $\pm$ 7.8 dB); 11 records were recovered as non-shockable (SNR -3.2 $\pm$ 5.6 dB) but 11 records initially classified as non-shockable were misclassified after filtering (SNR -8.0 $\pm$ 8.0 dB). The specificity for asystole decreased from 86.4% to 81.8%. We present the first estimation of the distribution of input SNR for out-of-hospital resuscitation episodes. Filtering is positively correlated with the sensitivity for low input SNR. Non-asystolic records with low input SNR are prone to be misclassified, while those with high input SNR are recovered after filtering. The total specificity worsened after filtering, due to asystole misclassifications.

Multi-Lead Discrete Wavelet-based ECG Arrhythmia Recognition via Sequential Particle Support Vector Machine Classifiers

Mohammad Reza Homaeinezhad* and Ali Ghaffari

Department of Mechanical Engineering, KN Toosi University of Technology, Tehran, Iran

The aim of this study is to introduce a sequential heart arrhythmia classification method based on the analysis of multi-lead Discrete Wavelet Transform (DWT) derived metrics. To meet this end, after delineation of the QRS complexes, each complex and the corresponding chosen DWT scales are segmented. Next, for each resulted excerpted segment, second (variance), third (quasi-skewness), forth (quasi-kurtosis) order statistical moments and curve length (as a nonlinear moment) are calculated and used as elements of feature vector (therefore 20 measures for feature vector of each lead). The proposed features are afterwards used to tune the parameters of five sequentially operating particle Radial Basis Function (RBF)-based Support Vector Machine (SVM) classifiers implemented to multi lead records of MIT-BIH Arrhythmia Database (MITDB) for AP, NP, VE, NE, AAP, RC, VNF, PNF, NCPW, VF, PB, PVC, LBBB, RBBB and Normal categories. To increase the accuracy of the classification algorithm, the entire under study train database is divided into five groups Normal+LBBB+RBBB+APB+PB (Group#0), NP+VE+NE (Group#1), AAP+RC+PVC (Group#2), VNF+PNF (Group#3) and VF+NCPW (Group#4) and for each group a RBF-SVM classifier is tuned. In the proposed sequential particle classification algorithm, beats belonging to Group#0, Group#1, Group#2, Group#3 are recognized and isolated respectively from test database via classifier#0, classifier#1, classifier#2, classifier#3 and then arrhythmias of Group#4 are identified by the classifier#4. The proposed heart arrhythmia classification is applied to categorize the abovementioned arrhythmias and average values of Se = 99.34%, P+ = 99.60%, Sp = 99.63% and Acc = 98.64% are obtained.

Characteristics of the Standard 12-lead Holter ECG in Professional Firefighters

Mary G Carey*, Salah Al-Zaiti and Rachael Butler

University of Buffalo, Buffalo, NY, United States

Background: On-duty firefighters have twice as many cardiovascular deaths as police officers and four times as many as emergency medical responders. To date, despite the high cardiac risk for firefighters and its societal importance, there are no available high resolution continuous ECG recordings during firefighting activities that may reveal why firefighters are dying on duty. Purpose: The purpose of this study was to characterize the 12-lead ECG: resting cardiac rhythm, heart rate (HR), depolarization and repolarization patterns during ambulatory monitoring of on-duty professional firefighters. Methods: In this descriptive study, all firefighters underwent 24hr ambulatory Holter monitoring while on-duty using a standard 12-lead ECG high resolution recording (Mortara, Milwaukee WI). Results: 73 firefighters (age 45+5 yrs, mostly white males) were enrolled over a one year period. During monitoring the average 24-hr HR was 77 +11 bpm, it range from an average minimum of 47+8 to an average maximum of 144+22 bpm. Intermittent single PVCs occurred in 51 (70%) firefighters and none had life threatening arrhythmias. All were in normal sinus rhythm, however 4 (5%) had either right or left BBB and 15 (21%) had abnormal STT waves at baseline. During Holter monitoring, ST segment deviation of at least 1mm in >2 contiguous leads was detected in 12 firefighters (19%); 3 anterior wall, 3 inferior wall and 6 multiple wall involvements. Baseline QRS-T angle and QTc were 68+38 (range 8-161; 16% abnormal) and 419 +35msec (range 368-540msec; 12% abnormal), respectively. Conclusion: Although most firefighters were in sinus rhythm, some had abnormal intraventricular conduction delays or altered repolarization. Specifically, markers of annual cardiovascular mortality (e.g. abnormal QRS-T angle, prolonged QT interval) exist among professional on-duty firefighters and may contribute to their high rate of cardiovascular death.

Effects of Sotalol on T-Wave Morphology in 24-Hour Holter ECG Recordings

Thomas Brennan* and Lionel Tarassenko

Institute of Biomedical Engineering, University of Oxford, Headington, United Kingdom

This article describes the impact of sotalol, a Class III anti-arrhythmic that is known to prolong the QT interval and induce torsades de pointes, on ventricular repolarisation. Timing and T-wave morphology-based biomarkers of ventricular repolarisation are extracted from 24-hour Holter electrocardiogram (ECG) recordings from a clinical sotalol study. The results show sotalol produces a significant dose-dependent increase of QT and T-peak to T-wave end (Tpe) intervals ($p<0.0001$). The effect of sotalol tends to significantly increase the morphology-based biomarkers, with the exception of T-area and T-wave area-based symmetry. The morphology based biomarkers are shown to be more sensitive to the effects of sotalol and the maximum effect on morphology biomarkers tends to take place after the maximum effect on the heart rate, QT and Tpe intervals.

The ECG in the Normal Human Pregnancy

Muti Goloba, Scott Nelson and Peter Macfarlane*

Electrocardiology Section, University of Glasgow, Glasgow, Scotland, United Kingdom

Aims: There have been very few, if any, studies using automated 12-lead ECG measurement in uncomplicated human pregnancy. This pilot study aimed to address the shortcoming by (a) assessing a sizeable cohort of women in a cross-sectional manner to evaluate the effect of gestation and maternal characteristics, notably booking body mass index (BMI), on the ECG; (b) evaluating how ECG measures in pregnancy differ from pre-established age and gender-matched reference values; (c) assessing a subgroup of women longitudinally to determine the impact of delivery on the ECG.

Methods: Women with singleton pregnancies across varying stages of gestation, aged between 18 to 45 years, were recruited from Glasgow Royal Infirmary and assessed cross-sectionally. Patients with co-morbid cardiovascular disease were excluded. A small subset was studied before and after delivery. An Atria 6100 ECG machine and its integrated Glasgow Program were used to record and analyse ECGs. Maternal baseline characteristics, including booking BMI, were also recorded.

Results: 138 women were recruited. 50% were overweight or (morbidly) obese. Univariate analysis demonstrated a negative correlation between gestational age and the T axis ($r= -0.34$, $P < 0.001$). BMI was found to be an independent predictor of the QRS axis and the T axis when specified within a general linear model ($p=0.006$ and 0.023 respectively). The QRS axis was more superiorly directed in pregnancy at 35 degrees in the third trimester compared to 51 degreesin an age/sex matched control population ($p<0.001$). 18 women were studied longitudinally. P, QRS and T axes demonstrated a significantly more inferior direction following delivery with QRS shifting from 30 to 35 degrees ($p<0.01$) and T from 13 to 25 degrees ($p<0.001$).

Conclusions: This pilot study demonstrated that certain ECG measures are altered by pregnancy and subsequent delivery. These findings suggest that a larger longitudinal study is merited.

QTc Analysis and Comparison in Pre-Diabetic Patients

Pedro Virgilio Rivera Farina*, Javier Pérez Turiel, Francisco Javier Pagán Buzo, Enrique González Sarmiento, Alberto Herreros López and Carlos David Rodríguez Guerrero

Div de Ingeniería Biomédica, Fundación CARTIF, Boecillo, Valladolid, Spain

QT interval is a surface ECG measure which has being subject of great research interest. Its accurate measure is very relevant as a non-invasive index of cardiac risk. This is of utility for drug toxicity quantification, VF risk assessment; Ischemic cardiopathy as in diabetes mellitus because of the increased difficulty the cells have to metabolize glucose and the related QT prolongation. Usually a prolongation of the QT interval beyond the normal cause is associated with bad prognosis.

It has already been shown that many of the complications that we associate with diabetes appear in the patient in early stages of diabetes, or even before the disease is developed. The aim of this paper, then, is to check whether QTc (corrected with bazett's formula) is altered in these prior stages of diabetes (insulin resistance and/or altered glucose according to the American Diabetes Association) when compared to healthy subjects.

In this paper we revisit the wavelet transform method for delineating the ECG. We use the extreme on the second (third) derivative which first appear ahead of the inflexion point of a T-wave. The algorithm detects Q waves with the first scale of a cuadratic spline WT while detects the end of the T-wave by using the first derivative on the fourth (fifth) scale.

Results were obtained in our database (data acquired in the Ḧospital Clinico Universitario de Valladolid). This database includes 34 healthy subjects and 16 pre-diabetic patients. We found QTc to be 0.3767+/-0.03 seg for healthy subjects and 0.3901+-0.03 seg in the case of prediabetic patients. Even though there is a sligth enlargement of the QT interval in prediabetic respect to healthy subjects, the difference in the values doesn't seem to be of statistical significance.

Comparison of QRS duration in African Blacks and European Caucasians

Ibraheem Katibi, Brian Devine*, Elaine Clark, Suzanne Lloyd and Peter Macfarlane

Electrocardiology Section, University of Glasgow, Glasgow, Scotland, United Kingdom

Introduction Racial variation in QRS duration is not well defined. This study was aimed at comparing the QRS duration in a large population of healthy individuals living in Nigeria with comparative values from a Caucasian population living in Scotland.

Methods 12 lead ECGs were recorded from apparently healthy volunteers living in and around Ilorin, Nigeria, using a Burdick Atria 6100 ECG machine. The ECG data was initially stored on a PC locally and thereafter sent to Glasgow for further analysis. The West of Scotland population was recruited from students as well local government employees and included both manual and sedentary workers. All ECGs were analysed by the same version of the University of Glasgow ECG analysis program.

Results The Nigerian population consisted of 782 males and 479 females aged from 20-87 years. The Caucasian population consisted of 859 males and 637 females aged from 18-82 years.

For the Nigerian population, the overall QRS duration for males was 87.9 $\pm$ 9.4ms and for females, it was 83.4 $\pm$ 7.7ms ($p<0.001$). The upper limits of normal were 112ms in males and 100ms in females.

For the Caucasian population, the overall QRS duration in males was 93.7 $\pm$ 9.8ms and in females was 86.1 $\pm$ 7.7ms ($p<0.001$). The upper limits of normal were 114ms for males and 102ms for females.

In both populations, the mean QRS duration was higher in males than in females at each decile of age.

There was a significantly longer mean QRS duration ($p<0.001$) in white males and females compared to their Nigerian counterparts

Conclusion These are the first data from large indigenous populations in Africa and Western Europe that demonstrate a significant difference in mean QRS duration between the two racial groups. These results have important implications for routine ECG interpretation, particularly using automated methods.

Quality of Electrocardiographic Records in Population Studies: What Can We Achieve?

Siegfried Perz*, Roswitha Küfner, Karl-Hans Englmeier, Moritz F Sinner, Stefan Kääb, Christine Meisinger and H-Erich Wichmann

Institute for Biological and Medical Imaging, Helmholtz Zentrum München, Neuherberg, Germany

Measurement precision and validity of the diagnostic interpretation are to a major extent associated with the noise interference in routinely recorded electrocardiograms (ECGs), even if computerized methods for signal enhancement and noise rejection are applied. In order to provide appropriate quality in the population-based KORA-F4 study, we applied a multi-stage monitoring of the resting ECG recording. Before the beginning of the study, we conducted a comprehensive training of five technicians to enhance their skills for appropriate electrode application, artefact recognition and prevention. During the data collection period a continuous quality monitoring of the digitized ECG records was performed consisting of (1) computerized online measurement of the noise exposure, and (2) the evaluation of the technical quality of the records by physicians. Utilizable ECGs were derived from 98.3% (3027/3080) of the study participants. 0.5% of the ECG records were rated as being of limited technical quality by the physicians. Using the computerized noise level measurement (characterizing each ECG record by the maximum noise level in any of the twelve leads), overall, the distribution (m$\pm$s) of noise level measurements was 13.2$\pm$6.8 V, the median was 12 V. In 80% of the records the noise exposure was 18 V. On average, noise caused by muscle tremor was consistently increasing with age (0.14 V per year). Repeated ECG recording - applied to 6.7% of the study participants with increased noise in the first record - resulted in a 7.5 V reduction of noise. The maximum difference of the mean noise levels attributed to the five technicians was 3.0 V. The comprehensive training of the technicians and the continuous monitoring of the ECG recording provided records of predominantly good quality, which is a precondition for reliable estimates of population-based ECG characteristics, especially when valid phenotyping for serial ECG analyses and genetic association studies is required.

Repeatability Value in Heart Rate Associated with Experienced Zen Meditation

Masaki Hoshiyama* and Asagi Hoshiyama

Hoshiyama Lab, Kamakura, Japan

Zen is a traditional meditation method which utilizes unification of body, respiration and mind. Though Zen has been sophisticated highly in Japan, it is spreading widely into western world today, realizing deeper meditation with minimum body movement and distraction. While heart rate variability (HRV) during controlled breathing by the subject has been studied in the past where the variability of HRV between repeat measurements in the same subject was still very high, there remains a lack of consensus whether heart rate during Zen practice elicit consistent repeatability measures of HRV especially for experienced and practicing Zen meditator. To better understand the repeatability of hemodynamic events elicited by deep Zen meditation during Zazen, we studied heart rate in 5 experienced Zen meditators and beginners. The study took place over 8 sets of Zen meditations in a quiet, Zen practice hall in Kamakura or Tokyo. Each set of Zazen lasted for 25 minutes. The first sets were used for habituation, and the data obtained from the following seven sets were used for analysis. Population averaged results for heart rate were not significantly different between experienced and beginners. Power spectrum analysis showed distinctive change in frequency components. Very low frequency (VLF) components decreased for experienced meditators ($p=0.05$). Most notably, standard deviations from 7 sets of measurements within each subjects were significantly low for experienced meditators ($p=0.05$), showing increased repeatability. During Zen practice, we seat ourselves in a lotus posture, practice Tanden respiration, i.e., lower abdominal breathing, and keep mind free from specific state of consciousness. We attribute the decrease in VLF components to the less easily distracted meditation, and the increase in repeatability to the effective regulation of mind and body movement during experienced Zen meditation toward the edge of sleep, but not quite over it. This result suggests the possibility of HRV repeatability as a handy and quantitative evaluator for Zen meditation.

Wavelet Transform Cardiorespiratory Coherence for Monitoring Nociception

Christopher J Brouse*, Guy A Dumont, Dorothy Myers, Erin Cooke, Joanne Lim and J Mark Ansermino

Electrical and Computer Engineering, University of British Columbia, Vancouver, BC, Canada

Introduction: Heart rate variability (HRV) may provide anesthesiologists with a noninvasive tool for monitoring nociception during general anesthesia. Real-time HRV monitoring would allow dynamic drug delivery adjustment to compensate for surgical stimuli. The Fourier LF/HF power ratio is the most widely accepted HRV analysis method; however, it is incapable of analyzing the ultra short windows required in real-time analysis (5-10 s). Furthermore, recent research has cast doubt on its theoretical validity, and it malfunctions when the respiratory rate (RR) is in the LF band. A novel wavelet transform cardiorespiratory coherence (WTCRC) algorithm was used to calculate ultra short term estimates of linear coupling between heart rate and respiration. WTCRC has previously been shown to reflect autonomic balance in volunteer studies, but has never been used during general anesthesia nor have its results been compared to traditional methods. Methods: With ethics approval and informed consent, data were recorded from 9 pediatric patients during dental surgery. Patients experienced periods of nociceptive stimuli followed by an increase in depth of anesthesia. Clean data segments (388 minutes total) were manually extracted. Segments were divided into categories with normal RR (in the HF band) and low RR (in the LF band), then split into 2-minute windows. Normal and low RR categories comprised 150 and 44 windows respectively. WTCRC and LF/HF were calculated for each window. WTCRC produces estimates for every data sample (480/window); these were averaged for direct comparison with LF/HF. Results: WTCRC decreased during periods of nociception, and increased following additional anesthetic drugs. WTCRC and LF/HF showed a correlation of -0.6737 for data with normal RR, and 0.0407 with low RR. Conclusion: WTCRC and LF/HF are comparable when RR is normal, while WTCRC outperforms LF/HF when RR is low. WTCRC is also better suited to real-time monitoring, as it can analyze much shorter windows.

Respiratory Frequency Estimation from Heart Rate Variability Signals in Non-Stationary Conditions Based on the Wigner-Ville Distribution

Eva Cirugeda, Michele Orini, Raquel Bailón and Pablo Laguna*

Aragon Institute for Engineering Research (I3A), Universidad de Zaragoza, Zaragoza, Spain

Respiratory sinus arrhythmia is a modulation of heart rate synchronous with respiration, which allows the estimation of respiratory frequency from the high frequency (HF) component of heart rate variability (HRV). The extraction of the respiratory frequency from the maxima of the smoothed pseudo Wigner-Ville distribution (SPWVD) is challenging, since the time-frequency smoothing used to suppress the interference terms of the WVD introduces an estimation error which can be high both in mean and standard deviation. Additionally in non-stationary conditions the error can be augmented due to the non-linear trend of the instantaneous frequency (IF). In this study the respiratory frequency is estimated from the HF band maxima of the SPWVD of the HRV signal. The algorithm adjusts the degree of frequency filtering (time-lag window length) to the time-frequency structure of the signal, in order to reduce the estimation error of the IFs. The optimal time-lag window length, at each time instant, depends on the instantaneous amplitude estimates of the signal components as well as on the noise present in the signal. The instantaneous amplitude is estimated independently of the time-frequency smoothing by deconvolving and correcting the instantaneous power estimates. The instantaneous power of the signal components is obtained by bounded integration of the SPWVD. The method has been evaluated on simulated HRV signals with time-varying amplitudes and non-linear frequency trends, obtaining a mean amplitude error of -0.319 $\pm$ 4.694% and a mean frequency error of -0.314$\pm$4.059% (0.07$\pm$11.0 mHz) for a SNR of 20 dB. A database containing the ECG and respiratory signals simultaneously recorded for 58 subjects during the listening of different musical stimuli has been analyzed. The method estimates the respiratory frequency with a mean error of

-0.217$\pm$15.181% (-2.38$\pm$ 39.8 mHz) during musical stimuli and of

-0.262$\pm$28.542% (-6.92$\pm$73.74 mHz) during transitions between stimuli, which are highly non-stationary and non-linear.

Point Process Heart Rate Variability Assessment during Sleep Deprivation

Luca Citi*, Elizabeth Klerman, Emery N Brown and Riccardo Barbieri

Department of Anesthesia and Critical Care, Massachusetts General Hospital Harvard Medical School, Boston, MA, United States

Heart rate variability (HRV) is an important quantitative marker of cardiovascular regulation by the autonomic nervous system. Recently, links between cardiac oscillations and circadian rhythms have been reported in several correlation studies in humans and other animals. Furthermore, changes in autonomic tone are correlated with changes in states of alertness and during performance tasks, as well as during sleep deprivation.

To demonstrate the potential relationships between HRV and objective performance - subjective alertness measures, we used data from healthy young subjects participating in a 52-hour Constant Routine protocol, an extended period of enforced wakefulness (sleep deprivation) in a semirecumbent position with frequent small meals and with minimal masking from exogenous factors.

A novel point process algorithm was applied to the RR series constructed from recorded ECG. The stochastic structure in the RR intervals is modeled as an inverse Gaussian renewal process, derived directly from a physiologically-based integrate-and-fire model. The parasympathetic and sympathetic inputs to the SA node are modeled by a uniform time-sampled regression on a continuous estimate of the most recent RR intervals, allowing for spectral decomposition into classic low frequency (LF, 0.04-0.15 Hz) and high frequency (HF, 0.15-0.5 Hz) spectral components. The point process algorithm is able to estimate the time-varying behavior of each derived spectral index at any time resolution.

The results demonstrated the point process high time resolution characteristics for sympatho-vagal balance as measured by LF and HF estimates during the 52h monitoring. Correlation analysis on subjects further reveals a considerable correspondence between the LF/HF index and subjective alertness measures during the first part of the experiment. At long time awake, high correlation levels between LF/HF and objective performance indicate an increasing sympathetic drive as performance measures worsen. These exciting results point at our HRV assessment as a potential real-time physiologic predictor of performance-alertness.

Stress during Pregnancy: Is the Autonomic Nervous System Influenced by Anxiety?

Steven Vandeput, Joachim Taelman, Devy Widjaja, Marijke Braeken, Bea Van den Bergh and Sabine Van Huffel

Department of Electrical Engineering, Katholieke Universiteit Leuven, Leuven, Belgium

Recently, there seems to be more and more interest in studying all kinds of emotions by means of physiological signals. It is known that stress influences the cardiac system which is regulated by the autonomic nervous system (ANS). The goal of this study was to investigate whether anxiety during pregnancy can be linked with a different autonomic heart rate modulation.

More than 100 pregnant women were included and underwent Holter ECG monitoring, cortisol measurements and the state trait anxiety inventory (STAI) questionnaire. Based on the STAI score, subjects belong to a low, medium of high anxious group. Also a mental stress test was applied during the recording. Heart rate variability (HRV) parameters were calculated as markers of ANS functioning, as well during day as night period and during the stress test. In addition to the standard time and frequency domain methods, also nonlinear parameters were used to describe self-similarity, complexity and chaotic signatures. Statistical analysis was obtained by the Kruskal-Wallis test and Spearman correlation coefficient r.

Heart rate was not affected ($r < 0.01$). Almost all HRV parameters were negatively correlated with STAI, meaning a reduced HRV with a higher anxiety level, though not statistically significant, except the chaos level ($r = -0.26$, $p = 0.021$). This negative correlation was more expressed during day than night time. Positive correlations were only found for parameters related to sympathetic activity (LFnu and LF/HF) and for the detrended flucutation analysis (DFA) parameters. In contrast, the positive correlations were stronger at night compared to day time. Most of the significant between-group differences were found between the low and medium anxious groups. The groups did not react significantly differently on the mental stress test.

To conclude, the ANS modulation is slightly influenced by the anxiety level, but not as strongly as hypothesized before.

Analysis of the Influence of Parasympathetic Postganglionic Neurons on Cardiac Response in Ventricular Fibrillation

Juan Guerrero, Alfredo Rosado*, Antonio J Serrano, Manuel Bataller, Francisco J Chorro, Luis Such and Antonio Alberola

Departamento Ingeniería Electrónica. Escuela Superior Ingeniería, Grupo de Procesado Digital de Señal. Universidad de Valencia. Spain, Spain

Physical training modifies the sympathetic-vagal balance of autonomic nervous system. Additionally, previous studies show that this training produces intrinsic modifications of cardiac electrophysiological properties in isolated heart during ventricular fibrillation (VF).

In order to verify if these modifications are related to the activity of postganglionic parasympathetic neurons, we studied ten trained rabbits. Two records per subject were acquired during VF: before (G1) and after (G2) the infusion of atropine to inhibit the activity of neurons.

Mapping records were obtained using a 240-channel electrode array located in the left ventricle of isolated heart perfused by Langendorff system. VF was induced by stimulation at increasing frequencies.

The records were processed in 4-second consecutive segments to analyze the time course of fibrillation. For each channel and segment, the following parameters were computed: a) dominant frequency (DF), obtained by the Welch periodogram b) normalized energy (NE) in a frequency band centered at the DF; c) regularity index (RI), which analyzes the similarity of local activation waves in every segment and channel; d) coefficients of variance for DF (CVDF), NE (CVNE) and RI (CVRI).

For each segment, we obtained the average value of each of the parameters analyzed for all electrodes. The results are: a) DF (G1: 13.671+-0.509 Hz, G2: 14.783+-0.455 Hz), b) NE (G1: 0.398+- 0.014; G2: 0.380+- 0.013); c) RI (G1: 0.855+- 0.017; G2: 0.865+- 0.015), d) CVDF (G1: 0.109+- 0.009; G2: 0.098+- 0.008), e) CVNE (G1: 0.398+- 0.014; G2: 0.380+- 0.013) f) CVRI (G1: 0.084+- 0.009; G2: 0.078+- 0.008).

The results in the calculated parameters do not show significant differences between groups. Thus, the parasympathetic postganglionic neurons seem to have no effect on the cardiac response in VF due to physical training.

Stability of Bipolar and Unipolar Endocardial Electrograms

Paola Milpied*, Rémi Dubois, Pierre Roussel, Christine Henry and Gérard Dreyfus

Clinical Research Department, Sorin CRM, Clamart Cedex, France

Background: Implantable Cardioverter Defibrillators (ICDs) are widely used for sudden cardiac death prevention. In most ICD algorithms, decision making includes a morphological analysis of the unipolar and/or bipolar EGMs. The principle of such algorithms is to create a normal template by averaging normal sinus rhythm heartbeats, for comparison to each arrhythmic heartbeat. The present study addresses two major issues: (i) the stability of unipolar and bipolar EGMs with respect to the posture of the patient, and (ii) the temporal evolution of the EGM shapes.

Method: A total of 140 unipolar (RVcoil-Can) and 140 bipolar (ring-tip) 10-second EGMs were recorded by ICDs (Paradym, Sorin Group) during sinus rhythm. For 23 patients (67 $\pm$ 12.5 years, 73% men), recordings were performed in different positions (supine, prone, left and right lateral, sitting, standing). EGMs were recorded 3 ± 3 days after implant and 2 ± 1 months later (early evolution) in a subgroup of 5 patients, 10 ± 6 months and 6 ± 1 months later (late and long-term changes) in a subgroup of 8 patients. EGMs similarities are measured by the correlation coefficient on a time window of 160 ms centered on each ventricular depolarization peak.

Results: Three (resp. 2) consecutive heartbeats suffice to create a normal template for unipolar signal (resp. bipolar) ($p<0.01$). The correlation between bipolar EGMs in a given position (0.96 ± 0.06) is not statistically different from the correlation between EGMs in different positions (0.95 ± 0.06). Conversely, unipolar EGMs are affected by position changes (0.98 ± 0.04 vs. 0.97 ± 0.05). However the correlation coefficient being very high, EGMs are very similar. As expected, the time changes of unipolar and bipolar EGMs are significant during the first post-implant month (bip: 0.80 ± 0.27, uni: 0.92 ± 0.05), and very small after a few months (bip: 0.98 ± 0.02, uni: 0.94 ± 0.07).

Conclusion: The above results are significant in view of the design of a statistically solid template updating procedure for morphological algorithms in ICDs.

Spectral Analysis of Intracardiac Electrograms After PQRST Removal

Aldo Casaleggio*, Tiziana Guidotto, Vincenzo Malavasi and Paolo Rossi

Biophysics Institute, National Research Council, Genova, Italy

Aims. To investigate power spectral density (PSD) of intracardiac electrograms (EGM) after digital elimination of PQRST waves. The idea is that, outside PQRST waves, EGM should reveal heart muscle activity during its resting condition.

Methods. EGMs are recorded from implantable cardioverter defibrillators (ICD) recipients in two cases: (i) when the ICDs recognizes the onset of a spontaneous ventricular tachyarrhythmia (VT) episode, and (ii) at the Hospital for periodic follow-up to test ICD device reliability, with the patient resting in supine position. In the first case, basal rhythm preceding VT-onset is investigated, in the second a 60-seconds EGM duration is considered. EGM analysis consists of: (i) R peaks recognition using an automatic algorithm; (ii) substitution of the QRS wave with a fixed duration smooth function (ramp) connecting samples before and after QRS complex; (iii) filtering of the new signal using a third order butterworth digital bandpass filter with passband between 40 and 110 Hz (to eliminate P and T waves); (iv) computation and inspection of the filtered signal PSD.

Results. Qualitatively the following different patterns have been observed during the analysis: (i) unimodal pattern, with a PSD peak in the 40-60 Hz frequency range (similar pattern is observed in muscle contraction); (ii) more interestingly, bimodal and 3-modal patterns are observed in some cases. Power line interference was limited in most EGMs; similarly flat PSD patterns indicating that the signal PSD is typical of a gaussian noise are seldom observed.

Conclusion. This observational study , based on EGMs retrieved from ICD implanted in cardiac patients, indicates that PSD analysis of EGM during diastole (neglecting as much as possible PQRST waves), exhibit different patterns in different patients and in the two different cardiac activities of resting and pre-VT onset.

Predicting Transthoracic Defibrillation Shock Outcome in the Cardioversion of Atrial Fibrillation Employing Support Vector Machines

Jose David Diaz, Omar Jacinto Escalona, Noel Camilo Castro*, John Anderson, Ben Glover and Ganesh Manoharan

Ingenieria Biomedica, Universidad Nacional Experimental Francisco de Miranda, Coro, Falcon, Venezuela

Transthoracic DC cardioversion is a commonly performed procedure for the restoration of normal sinus rhythm in patients with atrial fibrillation (AF) with a reported efficacy of 88-95%. There is a variation in the number of shocks required for successful cardioversion and in some cases failure to cardiovert. Although there are several clinical predictors for success such as duration of AF, left atrial diameter and the presence of structural heart disease, there are no electrical predictors available at the time of the procedure. We studied the use of support vector machines (SVM) to predict if transthoracic defibrillation is likely to be successful or not in the cardioversion of persistent AF in patients. The ECG signals of 47 patients undergoing DC cardioversion were collected at the Royal Victoria Hospital in Belfast. An incremental defibrillation energy protocol was delivered until successful cardioversion or up to a maximum level of 200J or up to four shocks. Signal processing was performed on ECG segments (between 55 and 60 seconds) prior to each shock. Residual atrial activity signal (RAAS) was derived by using bandpass filtering and ventricular activity cancellation. Three electrocardiographic indexes were extracted and used as input: the dominant atrial fibrillatory frequency, estimated from the RAAS power spectrum as the dominant frequency within the 3-12 [Hz] band, the mean and the standard deviation of the R-R interval time series of the ECG segments. A total of 41/47 patients were successfully cardioverted with a total of 107 shocks. SVM could predict the outcome of 89% of low-energy shocks (100J), with a sensitivity of 87.50%, specificity of 98.8% and positive predictive value of 80.77%. The outcome of higher energy shocks (150J) could be predicted with 100% accuracy. In conclusion, non-invasive electrocardiographic parameters can be useful in predicting AF transthoracic cardioversion outcome by means of SVM.

Three-dimensional Frequency Mapping from the Non-contact Unipolar Electrograms in Atrial Fibrillation

JL Salinet Jr, A Ahmad, P Stafford, G Andre Ng, FS Schlindwein

University of Leicester
Leicester, United Kingdom

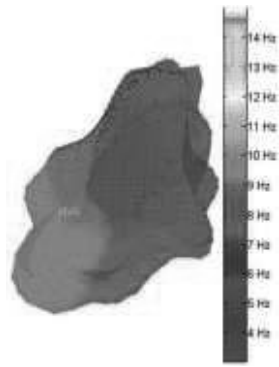

Three-dimensional (3D) colour-coded mapping of dominant frequency (DF) from noncontact unipolar electrograms in real-time can serve as a tool for identifying potential AF drives allowing the analysis and identification of re-entrant circuits sustaining atrial fibrillation (AF). The aim of this study was to develop 3D DF mapping of the inner surface of the atrium with 2048 measurement points from noncontact unipolar electrograms.

Methodology: This study was performed in 2 of 4 patients (2 paroxysmal, 2 persistent) undergoing catheter ablation guided by noncontact mapping (Ensite 3000, NavX 6.0, St. Jude Medical). 3D reconstruction of each atrial chamber, 3D electro-anatomic mapping and DF maps (and movies of 3D distribution in AVI format) during ongoing AF were performed using Matlab (MathWorks Inc., USA). Spectral analysis allowed determination of DF at each of the 2048 points in 19.5-second long segments for each protocol (baseline, after each drug, and after ablation). DF was defined as the frequency with highest amplitude within the physiological relevant range (3 to 15 Hz) using 4-second long windows. The time-domain unipolar signals were sampled at 1200 Hz and spectral resolution was 0.29 Hz. QRS subtraction was used to remove ventricular influence. We show how the spatial distribution of DF changes with time, drugs (isoprenaline and atropine), before and after ablation and compare DF areas with ablation sites.

Results: The visual analysis of the temporal evolution of the 3D DF mapping in those 2048 points showed that DF evolves its size and position in time. In addition we confirmed the effect of drugs on DF. Isoprenaline: two wide bands with DFs in (7.6 Hz and 3.5 Hz) and atropine: a narrow band with DF in 6.4 Hz. The QRS subtraction was important to reduce the power in the range of frequencies between 9 and 25 Hz on the average spectrum.

Automatic Location of Ventricular Arrhythmia using Implantable Defibrillator Stored Electrograms

Margarita Sanromán-Junquera*, Inmaculada Mora-Jiménez, Jesús Almendral, Estrella Everss, Antonio Caamaño-Fernández, Felipe Atienza, Loreto Castilla and José Luis Rojo-Álvarez

Signal Theory and Communications Department, Rey Juan Carlos University, Spain, Fuenlabrada, Madrid, Spain

Background. Electrograms (EGM) stored in Implantable Cardioverter Defibrillator (ICD) during ventricular tachycardia episodes have recently been shown to convey valuable information for the identification of the anatomical origin of the arrhythmia and subsequent ablation therapy.

Methods. We developed an automatic procedure for estimating the focal origin of the arrhythmia by analyzing the EGM waveforms. A clinical protocol was designed for validation, consisting of electrical pacing from different spatial locations in the left ventricle, in which the spatial coordinates of the pacing electrode were known by the use of a sequential navigation system. EGMs from can-coil lead configuration were stored in the ICD for 25 patients (18 ± 10.1 EGM per patient). Several machine learning classifiers (k nearest neighbors, radial basis function, and multilayer perceptron), were implemented, whose input space was given by the 201 samples (340 ms) of the template for each pacing location, and by a set of simple parameters selected according to clinical criteria. The target output was set by considering the heart division in three main planes, hence giving jointly 8 possible classification regions (octants). To estimate the generalization performance, a leave-one-patient-out strategy was implemented.

Results. Location accuracy reached, averaged over 10 runs, 73.1 ± 0.3 %, 58.4 ± 0.1 %, 57.5 ± 1.8 % (for binary classification in terms of main planes), and for octant identification with multioutput classification reached 36.3 ± 1.2 % (note that the random 8-output classifier average accuracy rate is 12.5%).

Conclusion. The estimation of the arrhythmia location can be addressed by analyzing the EGM waveform and features using learning from samples techniques.

Continuous Time Analysis Method for TWave Alternans Detection

Manuel Blanco-Velasco*, Fernando Cruz-Roldán, Eduardo Moreno-Martínez, Juan Pablo Martínez and Pedro Amo-López

Teoría de la Señal y Comunicaciones, Universidad de Alcalá, Alcalá de Henares, Madrid, Spain

Recent studies have demonstrated that T-wave alternans (TWA) is related with ventricular arrhythmias ant that its detection may help in the diagnosis of sudden cardiac death. Noise amplitudes similar to the alternant wave may make TWA detection difficult and poor SNR values lead to significant noise amplitudes that may cover the small variations associated with alternans. Limited solutions have been provided, except the inclusion of preprocessing stage for denoising. Thus, robust detection techniques against noise are welcome. Most of the detection techniques are applied over the time series obtained from the samples at the same phase taken from successive ST-T segments. The main drawback of processing temporal series obtained from ST-T complexes is that a relatively high number of beats are needed, at least from 64 to 128, which introduces a considerable delay. In this work, a new time domain method for TWA detection is presented. Its major advantage is the use of a reduced number of beats, from 16 to 32, which makes this methods less demanding in terms of signal stationarity. An extended study is performed to assess the performance of the new algorithm analyzing a wide set of long–term simulated ECG records with different SNR. The results are presented in terms of detection probability against the Alternans–to–Noise Ratio (ANR). This last parameter assesses the noise in the ventricular repolarization so that the lower the ANR, the higher the noise in the ST–T complex section of the ECG. The tests are carried out through a comparative study against the well known spectral method and different experiments are designed using muscle and motion artifact realizations. Although our method is tested with less number of heartbeats, it reports an improvement of more than 6 dB over the Spectral Method.

SA1

Automated QT Interval Measurement in Holter ECGs Recorded at 180 and 1000 Samples per Second

Gopi Krishna Panicker, Vaibhav Salvi, Dilip Karnad, Peter Macfarlane, Elaine Clark*, Arumagam Ramasamy, Snehal Kothari and Dhiraj Narula

Electrocardiology Section, University of Glasgow, Glasgow, Scotland, United Kingdom

QT interval measurement is important when studying the effects of drugs on cardiac repolarization using Holter recorders typically having sampling rates ranging from 128 to 1000 samples/sec (s/s). This study assessed the effect of sampling rate on automated QT measurements.

Methods ECGs were recorded in 16 healthy volunteers using dual snap electrodes that allowed simultaneous connection to two Holter recorders (Model H12+, Mortara Inc) recording at 180 and 1000(s/s). Thirty 10 second snapshots of ECGs were extracted at various heart rates from each subject. Recordings were resampled to 180, 500 and 1000s/s using the Antares package and also upsampled from 180 to 1000s/s using H Scribe (Mortara Inc). QT was measured by 3 algorithms: Cal ECG (AMPS LLC) which handles data at any sampling rate, the University of Glasgow (Uni-G) Program operating at 500s/s and the Veritas algorithm (Mortara Inc) operating at 1000s/s.

Results 1) QT was significantly longer (5.0 ± 6.3ms, $p < 0.001$) in the 180s/s ECGs than in the 1000s/s ECGs analysed by Cal ECG. 2) The difference decreased when ECGs were resampled to the same sampling rate before measurement, e.g 180s/s to 500s/s vs 1000 to 500s/s (2.5 ± 4.5ms by Uni-G and 1.8 ± 5.5ms by CalECG) and 180 to 1000s/s vs 1000s/s (2.6 ± 6.2ms) by Cal ECG. 3) Using Cal ECG, mean QT remained longer than the 1000s/s gold standard (345ms) in ECGs acquired at 180s/s (350ms) , even after up-sampling to 500s/s (347ms) or 1000s/s (348ms) - similarly with Veritas where there was a 5ms decrease in 180s/s data upsampled to 1000s/s vs the gold standard.

Conclusion QT measured from Holter ECGs sampled at 180s/s is longer than from ECGs sampled at 1000 s/s. Differences reduce when 180s/s data is upsampled to 1000s/s. Those involved in clinical trials where QT measurement is vital need to be aware of these findings.

SA1

Changes in the Ventricular Gradient Measured During Exercise Tests Predict Antiarrhythmic Therapy in Primary Prevention ICD Patients

S Man*, PV De Winter, AC Maan, WPM Van Meerwijk, EE Van der Wall, MJ Schalij and CA Swenne

Cardiology, Leiden University Medical Center, Leiden, Netherlands

Introduction

The clinical utility of current noninvasive predictors to identify candidates for primary prevention ICD implantation remains controversal. Exagerated reactivity of cardiac electrophysiology to changes in autonomic tone could indicate arrhythmia vulnerability. Consequently, we investigated whether changes in the ventricular gradient (VG, a measure for action potential duration (APD) heterogeneity in the heart) during exercise tests predict arrhythmias.

Methods

We studied the exercise tests of 106 primary prevention ICD patients, of whom 15 had anti-arrhythmic therapy (AT) during follow-up. Because of abundant arrhythmias during their tests, 4/15 AT patients were excluded. The remaining 11 AT patients were each matched (age, sex, etiology, EF, device) with two patients who had no AT during follow-up. Exercise ECGs were analyzed with our dedicated analysis program BEATS, that synthesizes a VCG and determines onset-QRS, end-QRS and end-T in every normal beat. Finally, intra-individual differences in VG magnitude were computed between the exercise and recovery phases of each exercise test, in the 95-110 bpm heart-rate range. Statistical analysis was done with the unpaired t-test with unequal variances.

Results

Clinical characteristics of the AT group and the non-AT group did not differ (age 58.9$\pm$12.2 vs 55.1$\pm$14.1 yrs; NYHA class 2.2$\pm$0.6 vs 2.3$\pm$0.9; EF 23.8$\pm$9.0 vs 25.3$\pm$6.7%; follow-up 3.0$\pm$0.6 vs 2.8$\pm$0.7 yrs). Changes (recovery-exercise) in the VG magnitude differed significantly: -19.9$\pm$27.2% (AT group) vs 2.8$\pm$27.1% (non-AT group), $P<0.05$.

Discussion

Autonomic influences on the heart during exercise and recovery differ dramatically. Due to the inhomogeneous innervation of the heart and due to disease this may give rise to variable changes in local APDs, thus setting the stage for reentrant arrhythmias. The observed changes in VG may denote regional changes in APD inhomogeneity. In conclusion, ICD patients whose VG is sensitive to changes in autonomic tone are more susceptible to arrhythmias than those with a stable VG.

SA1

Exercise Test Interpretation (XTI)

Willi Kaiser* and Martin Findeis

Advanced Engineering, GE Healthcare, Freiburg, Germany

An exercise test delivers a large number of measurements that are valuable in predicting morbidity/mortality, in detecting coronary artery disease and in describing the functional exercise response of a patient. However, it is very difficult to have a comprehensive knowledge of all measurements and their thresholds.

The Exercise Test Interpretation (XTI) program compares the exercise measurements against established thresholds and provides statements and reasoning texts, respectively explanation of the statements, when thresholds are exceeded. Therewith a short, clear, and accurate overview of an exercise test is provided.

XTI creates statements on risk prediction, statements on functional response, and statements on ischemia and coronary artery disease

Example: Ischemia, probably caused by coronary artery disease because ST/HR hysteresis > 0.02 mV in [V5] and HR reserve used $< 70\%$

In addition, an overall statement is created, namely: normal exercise test response, or borderline exercise test response, or abnormal exercise test response

For validation the FINCAVAS database (Tampere University, Finland), containing mortality (ICD-10 code) and angiographic data, have been used. Results: Overall mortality prediction: Hazard ratio 4, $p < 0.0001$ Cardiovascular death prediction: Hazard ratio 6, $p < 0.0001$ Ischemia (CAD) detection (upper level): Sensitivity 58%, Specificity 94%

Evaluation of a Method for Quantification of Restitution Dispersion from the Surface ECG

A. Mincholé[1,2], E. Pueyo[2,1], J.F. Rodríguez[2,1], E. Zacur[2] and P. Laguna[2,1]

[1]CIBER-BBN,
[2]Instituto de Investigación en Ingeniería de Aragón, University of Zaragoza, Zaragoza, Spain

Dynamic action potential duration (APD) restitution (APDR), expressing the relationship between APD and heart rate (HR) at different steady-state HR levels, presents spatial variations due to electrophysiological heterogeneities in the heart. Clinical studies have suggested that dispersion of APDR in the ventricle may act as a potent arrhythmogenic substrate. In this study, we evaluated a method aimed at quantifying APDR slope dispersion from the surface electrocardiogram (ECG) by computing rate-normalized differences in the T peak to T end (Tpe) interval: $d_{APDR} = \Delta Tpe/\Delta RR$.

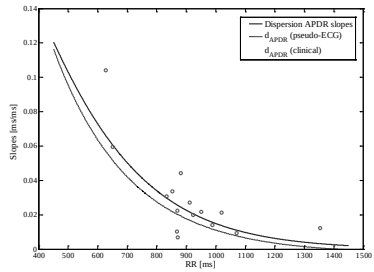

Cardiac propagation was simulated in a 2D tissue preparation representing a ventricular slice of 7.5 cm from base to apex and 1 cm from endocardium to epicardium. The ten Tusscher 2006 model was used to represent the human ventricular cell membrane. APDRs were derived from the 2D simulation to eventually compute the APDR slope dispersion, and pseudo-ECGs were calculated to compute the simulated d_{APDR} indices. These simulated d_{APDR} values were compared with values obtained from recordings of a set of healthy subjects in which pronounced HR changes were induced by a tilt-test protocol.

SA1

We found that d_{APDR} values in our simulations were in all cases within the range of clinical values measured from tilt-test recordings (mean ± std of the differences being: -0.0074 ± 0.0141 ms/ms). We then used the validated tissue model to relate the d_{APDR} index from the derived pseudo-ECG to measurements of APDR slope dispersion, and we found that the mean error relative to the slope range is 3%, being 8% the maximum and 0.02% the minimum.

We conclude that the proposed d_{APDR} index provides valuable estimates of APDR dispersion with the advantage of being able to be measured non-invasively from the surface ECG.

Evaluation of Restitution Properties using a Quasi-stationary Exercise Protocol

Joseph Starobin*, Vivek Varadarajan and Vladmir Polotski

Department of Physics & Astronomy, UNCG, Greensboro, NC, United States

Cardiac restitution portrait can be used as an effective tool for assessment of properties of cardiac electrical restitution and prediction of cardiac arrhythmias. Restitution portraits are usually measured in invasive experiments with prolonged pacing plateaus, since obtaining them from surface ECG recordings is complicated by the presence of physiological variations in QT and diastolic (DI) intervals. To overcome this problem we implement a quasi-stationary exercise protocol which minimizes exercise induced interval variations and modulates them as small fluctuations superimposed on the gradually changing QT and DI interval trends. Using such a protocol we develop an adaptive signal processing method which can be used for non-invasive assessment of restitution portraits. Firstly, we separate slow varying beat-to-beat QT and DI interval trends from high frequency fluctuations by time domain filtering of the corresponding signals. Secondly, we compute a cross correlation signal (CC) between QT and DI interval using an adaptive least-mean-square filtering algorithm. This filter provides point-to-point estimates of QT interval fluctuations that are physiologically related to DI interval fluctuations. Thirdly, we determine either correlated (CC$>$0.8) or anti-correlated (CC$<$-0.8) strips of QT and DI fluctuations longer than five beats. Finally, we compute linear regression of QT intervals on corresponding DI intervals within each correlated and anti-correlated strip. These regression lines determine S1-S2 and basic cycle length (BCL) restitution slopes, respectively. This method has been implemented for evaluation of restitution properties in seventeen normal individuals who volunteered to exercise on a treadmill. It was found that in each individual the magnitudes of S1-S2 and BCL restitution slopes increased with heart rate. It was also shown that the average S1-S2 slopes were higher for volunteers in whom peak heart rates exceeded one hundred beat per minute. These findings can be instrumental in theoretical modeling and quantification of instabilities of cardiac rhythm.

SA1

Enterprise Cardiovascular System to Support Multimodality Imaging and Clinical Effectiveness

Neil Greenberg*, Robert Cecil, Fredrick Heupler and Richard Grimm

Heart and Vascular Institute, Cleveland Clinic, Cleveland, OH, United States

Over the past several years, an enterprise cardiovascular PACs system across the Cleveland Clinic Health System has been established and enhanced to support cardiac catheterization, echocardiography, and vascular angiography and ultrasound and is evolving to support nuclear cardiology, cardiac CT and MR. The system consists of multiple departmental servers on the main campus where the procedural volume is largest and a set of distributed servers across the health system's 10 regional hospitals. The system must support the diversity and evolution of the multivendor modalities across the health system in terms of image and data storage and provide access to clinical information at all points of patient contact including procedural and operating rooms, reading rooms, exam rooms, and physician offices. Enterprise functionality in patient searching and access to prior exams is a key architectural feature of the cardiovascular PACs environment. An enterprise ADT interface allows patient data to be linked together despite multiple medical records used at the different hospital facilities through a master patient index. This capability provides enterprise searching across databases and allows for effective data comparisons. Structured reporting functionality and database warehousing of clinical data is another key system component that goes far beyond traditional image storage and review capabilities associated with PACS architecture. Patient context sharing allows integration of further applications providing access to third party applications for tasks including advanced 3D ultrasound processing, ECG waveform review, and nuclear SPECT processing. Several limited bandwidth capabilities are provided including image encoding to allow remote access with a web-based application as well as a real-time variable compression engine with local caching enabling full client functionality with remote viewing. As multimodality imaging and structured data become increasingly more important for in the delivery of high quality integrated cardiovascular patient care, continued focus on clinical effectiveness of system integration is key.

SA2

Emergency Medical Care Information System for Fetal Monitoring

Muhammad Ibn Ibrahimy*

Dept. of Electrical and Computer Engineering, International Islamic University Malaysia, Kuala Lumpur, Malaysia

This paper presents a research work that is concerned to implement an emergency medical care information system for fetal ECG (FECG) monitoring. The research work comprises of three major parts i.e. development of an abdominal ECG (AECG) data acquisition system, networking of transferring and receiving AECG data between patient (client) and physician (server), and improvement of existing techniques for fetal heart rate (FHR) monitoring. The main function of AECG data acquisition system is to acquire the mothers ECG data using a commercial chip called CARDIC and store it in a local terminal. On the other hand, the networking application serves the purpose of transferring the AECG data to the remote terminal via the established connection for remote monitoring and diagnosis purpose. Eventually, the AECG signals are processed in the remote terminal to extract the FECG from the AECG signal for efficient FHR monitoring. The networking system is a client/server application known respectively as Local Patient Monitoring System (LPMS) and Remote Patient Monitoring System (RPMS). It supports transferring of AECG data file and online chatting session. The diagnoses of the reading will be done by the specialists and action can immediately be taken in emergency cases.

SA2

An Approach Towards a Heart Beat Sound Information Retrieval System

Ehsan Safar Khorasani*, Shyamala Doraisamy, Azreen Azman and Masrah Azmi Murad

Department of Multimedia, Faculty of Computer Science, University of Putra Malaysia, Serdang, Selangor, Malaysia

Interpretation of heart sounds is a problematic and difficult skill that requires cardiology specialists. The diagnosis of heart disease from heart sound can differ between cardiologists and would require more detailed and expensive tests. However, heart disease diagnosis by heart beat is preferable and still widely used as the first step to diagnosis. Computer aided auscultation has emerged as a cost-effective technique to analyze and interpret the heart sounds. Digital Heart sound recordings with background noise, similarity among heart diseases, recording environment conditions, auscultation body points makes detection of heart diseases complicated. There are several methods for automated detection and classification of heart diseases and heart sound analysis that have been proposed. Some of them used Artificial Neural Network method for detection and classification of heart sounds. Another technique that it used for diagnosis the heart problem is Hidden Markov Model (HMM) that they suggest HMM for segmentation of heart sound recorded for clinical and classification purpose.

In this study we propose a feasible technique for developing a heart beat sound retrieval system using text based approaches useful towards automated heart disease detection. The audio format heart sound recordings are preprocessed and transcribed into the MIDI format. The MIDI files are then encoded to text strings using N-grams. These text strings are then indexed and tested for retrieval using both database and Information Retrieval (IR) systems. The Longest common subsequence (LCS) matching algorithm was used for identifying similarities from the database. With IR, full text indexing of the recordings was used and retrieved using known item searches from a search engine. The feasibility of these text based retrieval approaches are shown from retrieval experiments with around 100 digital heart sound recordings and eleven categories of heart diseases. Each recording include eight heart beat cycles and duration of ten seconds.

SA2

Distinguishing between Heart and Lung Sounds in Remote Auscultation of Patients

Nausheen Mahmood, Aafreen Mahmood and Tanveer Syeda-Mahmood*

Multimodal Imaging for Healthcare Informatics, IBM Almaden Research Center, United States

Auscultation is an early diagnostic procedure for abnormal sounds such as heart murmurs, lung sounds and gallops. Recently, it has become possible to wirelessly collect such sounds from remote patients using electronic stethoscopes that wirelessly relay the data to remote servers. Due to the inexperience of patients taking their own recordings, not all the data coming from these devices is useful. Therefore the incoming signal needs to be analyzed to extract important heart and lung sounds from the rest of the background noise arising due to stethoscope movements, incorrect positioning or even ambient noise.

In this paper, we describe a method to automatically segment and label heart and lung sounds in such recordings. The algorithm models the incoming signal as a short-time stationary process consisting of various sounds occurring in successive time segments. An overlapping window analysis is performed and evidence of periodicity is checked within each overlapping segment by approximating the sound signal using sound envelopes. Peaks in the autocorrelation function are then used to select candidate segments. A three-way classifier based on multi-class support vector machines was developed in a prior learning stage using samples of known heart, lung and other background sounds as training data. Each candidate segment is then labeled into one of the three classes using this classifier. The labeled segments are then stored as valid recordings of interest in the patients record.

A ground truth database of 675 original sound recordings taken from patients through wireless stethoscopes, was manually segmented by trained professionals into heart, lung and background sound containing regions. Of these recordings, the algorithm correctly identified respective (heart or lung) sounds in 546 cases. The average overlap of time extent with manual identification was 72.8%. The missed cases corresponded to arrhythmia cases and noise deeply intermixed with heart and lung sound recordings.

SA2

Monitoring System for Forecasting Hypotensive Episodes

Ricardo Jorge Santos[1], Jorge Henriques[1], and Jorge Bernardino[1,2]

[1]FCT – DEI – CISUC – University of Coimbra – Portugal
[2]Superior Institute of Engineering of Coimbra (ISEC) – IPC – Portugal

In critical care, hypotension (HT) may cause serious disorders, inducing severe or even lethal events. Recent studies report an increase of mortality in HT prone patients needing critical care, such as hemodialysis. If predicted in advance, staff could take action to minimize its effects or even avoid its occurrence. Most medical systems focus on monitoring and detecting current patient status, rather than finding biosignal trends or predicting patient's future status. Hence, predicting HT episodes in advance remains a challenge.

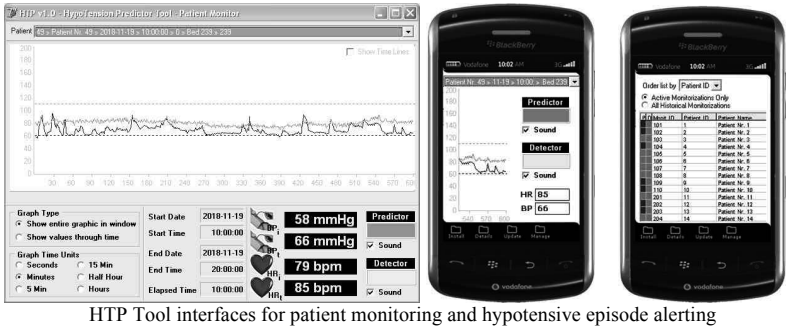

HTP Tool interfaces for patient monitoring and hypotensive episode alerting

We present a system tool that includes a real-time database for storing all patient's historical blood pressure (BP) and heart rate (HR) data, and provide applications capable of continuously monitoring each patient's status and predicting if a HT episode will probably occur during the next 60 minutes. Our system also enables medical staff mobility, using personal devices such as mobile phones/PDA's for continuous monitoring and alert purposes (see Figure). Cardiac adjustment (CA) – the heart's autonomous biological ability to modify its HR – is common for studied cases. As known, future BP values depend on the most recent past BP values, matching linearity representations when timespan of analysis is short (<=60 minutes). After thoroughly analyzing research data, we found that when a patient's heart is capable of rising its initial HR at least 20%, its CA can avoid BP values falling into HT situations. To forecast HT episodes, we developed an algorithm based on these assumptions, using linear regression on BP and HR for predicting each patient's HT status for the next 60 minutes. Our experiments, using the Physionet Challenge 2009 data, shows an accuracy of 98% in HT and non-HT prediction, scoring 49 out of 50, outperforming the 2009 challenge's winning proposal.

SA2

Matching Data Fragments with Imperfect Identifiers from Disparate Sources

Michael Craig*, Benjamin Moody, Sherman Jia, Mauricio Villarroel and Roger Mark

Harvard-MIT Division of Health Sciences and Technology, Massachusetts Institute of Technology, Cambridge, MA, United States

Patient care in modern intensive care units (ICU) relies on a rich, yet disparate, set of clinical and physiologic data. To support research aimed at improving diagnosis and treatment of ICU patients, we have captured these data in the Multiparameter Intelligent Monitoring in Intensive Care (MIMIC-II) Database, using a customized data acquisition process that does not interfere with clinical practice. MIMIC-II includes (a) waveforms and derived parameters from bedside monitors, (b) clinical data from the ICU information system, and (c) data from other hospital laboratories and archives. These data come from devices that often do not retain detailed information regarding temporal relationships between parameters, as well as from highly aggregated sources. Assembling comprehensive records from fragments that may lack common identifiers is a problem that is likely to occur in any similar project. For projects such as MIMIC-II, in which many thousands of records must be constructed, automated solutions are essential tools.

We developed software for matching data fragments with incomplete and sometimes incorrect identifiers. We found that names, medical record numbers, waveform times and durations, and ICU admission and discharge records were most helpful when available. Comparing recorded waveform data with nurse-reported vital signs, however, is less likely to lead to successful matching. Since the data we have collected are representative of ICU data, and can be analyzed only retrospectively, imprecision and inaccuracy become significant challenges, which we addressed using rule-based normalization and text edit-distance metrics. For patients whose records cannot be assembled automatically, we developed a visual verification tool. The entire process, both automatic and manual, currently matches almost 90% of the available waveform recordings to patients in the clinical database. We conclude by recommending how standards for recording both waveforms and clinical observations can be improved to increase the fraction of usable data.

SA2

Semiautomatic Quantification of Left and Right Ventricular Functions in Magnetic Resonance Imaging

L Masip*, PG Tahoces, M Souto, A Martínez, JJ Vidal

University of Santiago de Compostela (USC)
Complejo Hospitalario Universitario de Santiago (CHUS)
Santiago de Compostela, Galicia, España

The objective of this study is twofold: first, to develop a semiautomatic segmentation method to quantify left and right ventricular (LV and RV, respectively) functions in cardiac magnetic resonance (MR) imaging, and second, to compare this method with manual contour tracing (Argus, release Syngo; Siemens AG, Medical Solutions; Erlangen, Germany).

Twenty patients with cardiovascular diseases were examined using a 1.5-T MR Imaging unit (Magnetom Symphony Quantum; maximum gradient, 30 mT/m; slew rate, 125 T/m/s- Siemens Medical Systems, Erlangen, Germany). Twelve contiguous short axis slices with a thickness of 6-mm were planned to cover the entire LV and RV volumes from the base to the apex. Acquisition was performed with breath-hold cine steady-state free precession (SSFP) sequences. Several parameters such as end-diastolic and end-systolic volumes (EDV and ESV, respectively), stroke volume (SV), and ejection fraction (EF) of both ventricles were quantified using both semiautomatic and manual contour tracing methods. To start the semiautomatic method, a seed point per patient is set by hand inside the ventricular region. Next, the computer automatically segments the ventricle by means of edge detection, dynamic thresholding and region growing processes.

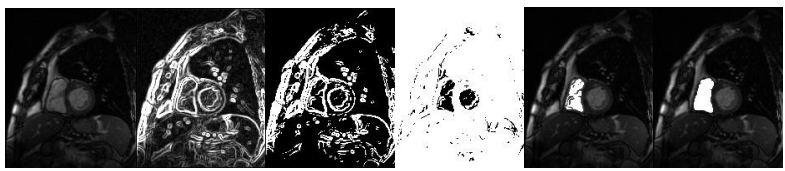

Semiautomatic segmentation of the right ventricle.

No statistically significant differences were found for the quantification of LV and RV parameters by the two methods ($p>0.05$). Correlation to estimate RV function was good ($r>0.7$) and turned to be excellent for LV function ($r>0.9$). Bland-Altman plots were used to assess the agreement between both methods.

In conclusion, semiautomatic segmentation procedures, applied to the quantification of cardiac parameters, can achieve similar results than manual procedures. Furthermore, the segmentation of the heart is less time consuming.

Three-Dimensional Analysis of Septal Curvature from Cardiac Magnetic Resonance Images for the Evaluation of Severity of Pulmonary Hypertension

Francesco Maffessanti, M Agustina Sciancaleopre, Amit R Patel, Mardi Gomberg-Maitland, Enrico G Caiani, Benjamin H Freed, Roberto M Lang and Victor Mor-Avi*

Politecnico di Milano, Milan, Italy, and University of Chicago, IL, United States

Although abnormal motion of the interventricular septum (IVS) caused by elevated right ventricular pressure in patients with pulmonary hypertension (PH) is easy to recognize visually, determination of the severity of PH relies on measurements of pulmonary arterial pressure. We hypothesized that quantitative 3D analysis of regional IVS curvature throughout the cardiac cycle could be used to differentiate patients with different degrees of PH. Cardiac MR images (Philips 1.5T) were obtained in 31 patients (14 normal controls; 17 patients with PH) undergoing right heart catheterization, who were divided into 3 subgroups according to mean pulmonary arterial pressure (mild: 25-34 mmHg, moderate: 35-50 mmHg, severe: $>$50 mmHg). Images were used to reconstruct dynamic 3D LV endocardial surfaces (TomTec 4DLV software), which were analyzed to calculate 3D IVS curvature throughout the cardiac cycle. To compensate for changes in IVS curvature secondary to changes in LV size, curvature was normalized at every phase of the cardiac cycle by mean LV curvature. In normal subjects, IVS curvature was positive, reflecting the convex septal shape and showed little change throughout the cardiac cycle. In contrast, in patients with PH, IVS curvature was lower, reflecting septal flattening, and fluctuated throughout the cardiac cycle, reflecting the abnormal bouncing septal motion. In patients with severe PH, IVS curvature reached negative values, reflecting transient concave septal shape. Dynamic 3D analysis of IVS curvature from cardiac MR images may provide an alternative for noninvasive assessment of severity of PH.

SA3

Estimation of Right Ventricular Volume, Quantitative Assessment of Wall Motion and Trabeculae Mass in Arrhythmogenic Right Ventricular Dysplasia

Massimo Lemmo*, Arshid Azarine, Giacomo Tarroni, Cristiana Corsi and Claudio Lamberti

DEIS, Universita' degli Studi di Bologna, Bologna, Italy

Cardiac MRI allows a complete overview of right ventricle(RV),it provides an anatomic,functional and morphologic approach in diagnosing arrhythmogenic right ventricular dysplasia(ARVD).The aim of this study was to gain a wide perspective of the ARVD by working out algorithms based on level-set theory.In this work we developed a semi-automatic procedure to assess the RV volumes and to quantify RV wall motion,moreover,with the increased visible details in a single MR image,a manual method to evaluate the trabeculae mass was performed.Volume estimations were executed by detecting endocardial contours with algorithm based on level-set technique.The semi-automatic procedure was applied to calculate both end-diastole volume(EDV) and end-systole volum(ESV), featuring the absence of geometric assumptions for a complex crescent-shaped as RV.RV Wall Motion,which is usually assessed by qualitative impression,was performed by sectoring the superimposition of end-diastolic(ED) and end-systolic(ES) frames,for each two-chamber view levels,that is Basal,Mid-Level and Apex.The contours were taken semi-automatically with an algorithm based on level-set technique,while the quantitative data were automatically calculated during the process by counting the spacing between ED and ES contours.The attempt of assessing trabeculae mass was carried out using a manual procedure to segment all the visible black parts inside the RV cavity,for each ED image.We applied these three tools to 6 normal subjects and 6 subjects with ARVD.A good agreement between our method and the standard manual method as reference came out from volume estimations,specifically for EDV estimations resulted $y=0.92x+6.56$ ($r=0.92$ $p<0.001$), while for ESV estimations resulted $y=0.91x+7.09$($r=0.91$ $p<0.001$). Wall Motion results showed a significant reduction of RV segmental function in patients with ARVD,Inferior Wall was the most involved with more than 80% reduction ($p<0.001$) compared with normal subjects,while RV outflow tract(RVOT) was the least involved with less than 50% reduction($p<0.001$) as regards normal subjects.A repeatability test was executed on trabeculae mass assessment, which showed an high intra observer correlation between the measures,in fact the results were significant at 95% of the cases.

SA3

Evaluation of Semi-Automated Border Detection Algorithms for the Left Ventricular Endocardium from Magnetic Resonance Images

Kun Wang*, Kieren Hollingsworth, Andrew J Sims, Andrew M Blamire and Alan Murray

Regional Medical Physics Department, Freeman Hospital, Newcastle University, Newcastle upon Tyne, United Kingdom

Accurate quantification of left ventricular (LV) volume is important for therapeutic management, risk stratification and prognostic assessment of patients with cardiovascular disease. Magnetic resonance (MR) imaging has proved to be an accurate and reproducible imaging modality for quantitative analysis of left ventricular function, and it is normally treated as the standard for left ventricular volume measurements. However, to perform accurate volume measurements on MR images, the endocardial wall surface is normally traced manually slice by slice, which requires much effort and is very time consuming. Because of large variations of MR image quality and large variations of the ventricular geometry during cardiac cycles, it is a challenge to develop automated or semi-automated techniques that can provide comparable accuracy in left ventricular volume measurements

In this study, we developed two semi-automated border detection algorithms to trace the left ventricular endocardial wall borders by examining intensity change distributions approximately perpendicular to the ventricular wall, and then calculated the left ventricular volumes. By comparing with the measurements from the manually traced endocardial borders, we evaluated the performance of each algorithm, and studied the factors that affect the automated tracing for the left ventricular endocardium on MR images.

Six patients were recruited for a MR scan. Comparing results with the manual measurement of the left ventricular volumes, the overall bias$\pm$standard deviation was 5.9$\pm$20.4ml (algorithm 1) and 23.4$\pm$6.9ml (algorithm 2, $p<0.05$) in end diastole, 6.2$\pm$4.6ml (algorithm 1, $p<0.05$) and 11.1$\pm$8.9ml (algorithm 2, $p<0.05$) in end systole and -0.3$\pm$22.8ml (algorithm 1) and 13.6$\pm$8.4ml (algorithm 2, $p<0.05$) in stroke volume. The major factors affecting the automatic tracing of endocardial wall borders are the image intensity changes caused by papillary muscles and epicardial wall borders.

SA3

3D Evaluation of Myocardial End-Systolic Wall Stress From Cardiac Magnetic Resonance Cine Data.

M Sénési, K Defrance, E Mousseaux, N Kachenoura.

Inserm U678, France/ETH Zürich, Switzerland.

Noninvasive evaluation of left ventricular (LV) function and remodeling is essential in the management of cardiovascular diseases. LV remodeling and dysfunction occur as a response to changes in LV preload and afterload conditions. This latter determines myocardial wall stress (WS). The aim of the present study was to compare the 2D against the 3D evaluation of myocardial WS. **Methods**. Two control groups C1 (10 subjects, 24±4 years) and C2 (11 subjects, 58±6 years) and a group of patients with an aortic valve stenosis (AVS) (12 subjects, 80±10 years) were studied. All subjects underwent a cardiac magnetic resonance (MR) exam with cine imaging on 10 to 12 short axis slices as well as an applanation tonometry to measure the end-systolic pressure (ESP). Regional 2DWS was calculated as a combination of the ESP and a geometrical factor calculated using myocardial wall thickness and LV cavity radius while the 3DWS included a thickness and radius correction based on the longitudinal LV curvature. **Results**. The 3D correction reduced the base to apex gradient in WS (figure) from 2.8±1.6 to 1.6±1.7 in C1, 2.9±1.2 to 2.1±1 in C2, 1.1±0.8 to 0.2±1.3 Newton.1000/m^2 in AVS. Moreover, the averaged 3D basal WS was 6.0±1.3 for C1, 4.7±1.6 for C2 and 3.3±1.3 Newton.1000/m^2 for AVS. Differences between C1 and C2 as well as between C2 and AVS were statistically significant (t-test, $p<0.05$), whereas the only significant difference was found between C2 and AVS when considering the 2DWS. **Conclusion**. The 3D evaluation corrected for the erroneous underestimation of the apical WS induced by partial volume effect that is increased in the apical region by the important curvature of the wall. Besides 3DWS was able to characterize aging and abnormal increase in afterload caused by AVS. Its addition to clinical CMR tools would enable a better characterization LV remodeling.

SA3

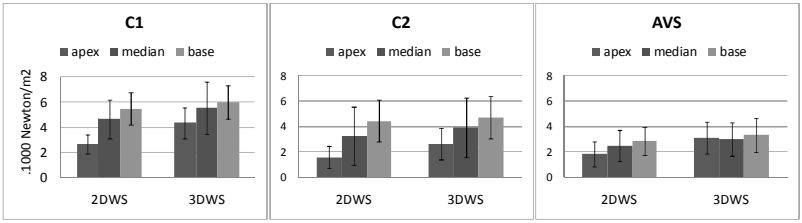

Results of 2DWS and 3DW for the 3 populations and the 3 anatomical locations.

Analysis and Improvement of a Human Ventricular Cell Model for Investigation of Cardiac Arrhythmias

Jesús Carro*, José Félix Rodríguez, Pablo Laguna and Esther Pueyo

Ingeniería Electrónica y Comunicaciones, Instituto de Investigación en Ingeniería de Aragón (I3A), Universidad de Zaragoza, Zaragoza, Spain

Background: Mathematical modeling and simulation of hearts electrical activity has become a fundamental tool to understand cardiac behavior. Different models have been proposed, each one aimed at investigating specific questions. A human ventricular action potential (AP) model was recently proposed by Grandi et al (2010). In this study we have conducted a thorough evaluation of that model, and we have proposed several improvements that render it suitable for cardiac arrhythmia investigations.

Methods: Four stimulation protocols were applied to the original and improved models, and a number of cellular arrhythmic risk biomarkers were computed, including: steady-state AP and [Ca2+] transient properties, AP duration (APD) restitution curves, APD adaptation to abrupt changes in heart rate, and intracellular [Ca2+] and [Na+] rate dependence.

Results: In its original version the Grandi model proved to adequately reproduce AP triangulation (APD90-APD50=59.3ms), and maximum normalized systolic [Ca2+] and [Na+] levels (180% and 132%), outperforming other previous models. However, APD rate adaptation did not show the biphasic behavior (with characteristic fast and slow adaptation phases), and the maximum slope of the S1S2 restitution curve was out of physiological range (S_S1S2=10.18). Based on those results, we reformulated the L-type calcium current (ICaL) to include both fast and slow voltage-dependent inactivation gates, we updated the inward rectifier K+ current (IK1) based on recent experimental data, we shifted the voltage-dependence curve of the Na+ current inactivation gates, and we adjusted the conductance of the slow delayed rectifier K+ current (IKs) and maximal value of the Na+/K+ pump. Our modifications led to: a) further improved AP triangulation (64.7ms); b) APD rate adaptation curves characterized by fast and slow time constants within physiological ranges (8.92s and 84.21s); c) S1S2 restitution slope in accordance with experimental data (S_S1S2=1.6).

Conclusions: An improved human ventricular cell model has been developed and validated for cardiac arrhythmia investigations.

SA4

Systems Biology in Drug Safety Assessment: Use of a Recalibrated Hund-Rudy Model to Predict the Effect of Novel Drug Compounds on Action Potential Duration

Mark Davies*, Hitesh Mistry, Leyla Hussein, Najah Abi-Gerges, Chris Pollard and Jonathan Swinton

Advanced Science and Technology Laboratory, AstraZeneca, Macclesfield, United Kingdom

Objective: Drug-induced ion channel modulation in ventricular myocytes can prolong action potential duration (APD), which is seen on the electrocardiogram (ECG) as a prolongation of the QT interval. This is associated with a cardiac arrhythmia and therefore QT interval duration is carefully monitored in animal and man. Therefore, all candidate drugs are screened in an in vivo model of QT duration. This is however a late-stage, low throughput assay and also not entirely predictive for cardiac toxicity. For this reason, and much earlier in the drug discovery path, AstraZeneca screens compounds using IonWorksTM technology for their effects in vitro on several key cardiac ion channels. This information by itself is insufficient to infer APD change however.

Results: We have taken a publicly available model of cardiac action potentials (Hund Rudy) and calibrated it against a series of DMSO-control experiments from a voltage-sensitive dye based assays on isolated canine ventricular myocytes (VM). This calibration allows us to capture the variation in inter- and intra-experimental drift and create an ensemble of parameter sets, differing only in the ion-channel current parameters which are consistent with variations observed in electrophysiology experiments. We have then simulated the anticipated change in APD for a series of compounds with known channel inhibition profiles and compared this to experimentally derived estimates in order to assess the predictivity of the model.

Conclusions: Using a mathematical model of cardiac action potentials, we are able to integrate potency estimates from a range of ion channels and assess the potential cardiac risk that a particular compound may pose. This risk assessment can be performed at a much earlier stage in the drug pipeline and with the intention of improving and speeding up drug decision making.

SA4

In-silico Evaluation of β-adrenergic Effects on the Long-QT Syndrome

DUJ Keller, A Bohn, O Dössel, G Seemann

Institute of Biomedical Engineering, Karlsruhe Institute of Technology, Karlsruhe, Germany

Patients suffering from the congenital Long-QT syndrome react highly sensitive to the presence of β-adrenergic agents that are produced by the sympathetic nervous system. In this work we use an anisotropic and electrophysiologically heterogeneous in-silico model to reproduce wedge experiments in which the Long-QT syndrome was induced pharmacologically. Although different research groups have tried this in the past, they were only partially successful as the effects of the β-adrenergic agents could not be considered. Recently we integrated a description of the β-adrenergic signaling cascade into a model of human ventricular cells. Using the bidomain reaction-diffusion equations we calculated transmural pseudo ECGs which could be compared to the wedge experiments. For LQT1, the in-silico model predicted a QT prolongation in the transmural ECG without an increase in transmural dispersion of repolarization (TDR). For LQT2 and LQT3 the QT prolongation was accompanied by an increased TDR (+20%, +13% respectivley). β-adrenergic stimulation always shortened the APD of epicardial cells (4%-21%). In case of LQT1 and LQT2, β-adrenergic stimulation increased the APD of the M cells (+21%, +7% respectivley), whereas no significant change was observable for LQT3. This leads to an increase in TDR under adrenergic influence. Except for the increase in TDR under adrenergic influence for LQT3, the results of the in-silico model are consistent with the experimental reports. However, there are crucial differences between the features of LQT1 and LQT2 in the wedge experiments and clinical ECG recordings. In case of LQT1, patients show broad-based T Waves which are not easily reproducible if a reduction of the heterogeneous current I_{Ks} is assumed. In contrast to that, wedge experiments of LQT2 show an increased TDR leading to broad T Waves of high amplitude which are unlike the low-amplitude T Waves seen clinically.

SA4

Modelling of Intracellular Ca2+ Alternans and Ca2+-Voltage Coupling in Cardiac Myocytes

Qince Li and Henggui Zhang*

The School of Physics and Astronomy, The University of Manchester, Manchester, United Kingdom

In cardiac tissue, Ca2+ cycling plays the most important role in regulating mechanical contraction and the membrane potential (voltage). Intracellular Ca2+ transient alternans may produce not only mechanical contraction alternans, but also action potential duration (APD) alternans via Ca2+-Voltage coupling, which is pro-arrhythmic. The aim of this study was to investigate the interaction between Ca2+ and APD alternans by using computer simulations.

The mathematical model of canine ventricular action potential developed by Shiferaw et al. was used in the study. In the model, a cell was divided into 75 sarcomeres elements, which were coupled together via Ca2+ diffusion. In each element, ionic channels were modelled by equations of Fox et al.. At the cellular level, Ca2+ and APD alternans were produced either by rapid pacing (3.57 Hz), or by slow pacing (2.5 Hz) with an increased stiffness of the relationship between SR Ca2+ content and cytoplasimc Ca2+ concentration, which were consistent with experimental observations. In the spatially extended (75 elements) cell model, spatially discordant Ca2+ alternans was observed under the condition of strong Ca2+-induced L-type Ca2+ channel inactivation, while Ca2+ alternans tended to be concordant for weak Ca2+ induced inactivation. APD alternans with concordant Ca2+ alternans is more significant than that with spatially discordant and fragmented Ca2+ alternans, which leads to approximately identical total L-type Ca2+ current of the whole cell during successive stimulations and thus suppressing APD alternans.

This study indicates that Ca2+ alternans can be induced under both rapid and relatively slow pacing rates via different mechanisms, each of which may produce concordant or discordant Ca2+ alternans. The coupling between Ca2+-Voltage may reduce the amplitude of APD alternans, though Ca2+ distribution is spatially heterogeneous in the cell.

SA4

Mechano-Electrical Feedback during Cardiac Resynchronization Therapy?

Nico Kuijpers*, Evelien Hermeling and Frits Prinzen

Dept of Biomedical Engineering, Maastricht University, Maastricht, Netherlands

Cardiac Resynchronization Therapy (CRT) has emerged as an important therapy to improve pump function in patients with left bundle branch block (LBBB). Electrical excitation of the ventricles is synchronized by simultaneously pacing both ventricles. It is known that long-term asynchronous activation leads to a form of electrical remodeling, referred to as T-wave memory. T-wave memory is known to occur after a period of ventricular pacing, but its role during CRT is unclear. Evidence is growing that T-wave memory is induced by altered mechanical load, and thus is a form of mechano-electrical feedback (MEF). We hypothesize that this kind of MEF leads to local changes in the expression of L-type calcium channels, aiming at (partial) correction of local workload in the asynchronous ventricle, but also affecting local action potential duration (APD). The aim of the present simulation study was to investigate the effects of MEF during LBBB and CRT using a multi-scale computer model. The model described cellular electrophysiology and calcium handling as well as cardiac mechanics and hemodynamics. Ventricular electromechanics was represented by a single cardiac fiber, while physiological pressure-volume loops were obtained by simulating the systemic circulation. LBBB was simulated by stimulating the fiber at one end (activation time 108 ms) and CRT by simultaneous stimulation at both ends (activation time 54 ms). During chronic LBBB, MEF lead to a reduction in local differences in external work as well as in dispersion of repolarization. During acute CRT, systolic function was acutely increased as was dispersion of repolarization. As a consequence diastolic function (reflected by E/A-ratio) was reduced. With chronic CRT, dispersion of repolarization decreased and diastolic function improved. We conclude that MEF may lead to an increase in dispersion of repolarization during the early phase of CRT, which may lead to impaired diastolic function and to ventricular arrhythmia.

SA4

Enhanced Computer Modeling of Cardiac Action Potential Dynamics using Experimental Data-Based Feedback

Laura Munoz* and Niels Otani

Department of Biomedical Sciences, Cornell University, Ithaca, NY, United States

Mathematical models of cardiac action potential (AP) dynamics are useful for studying the formation of dynamically significant patterns such as alternans and conduction block. A closed-loop observer is an augmented version of a mathematical model, in which experimental data, such as microelectrode measurements of membrane potential, are supplied to the model through a feedback algorithm. An observer can reconstruct unmeasured quantities, such as AP durations (APDs) at locations away from sensing electrodes. These reconstructed quantities can be used to gain insight into AP behavior within an experiment, or provide enhanced information to anti-tachyarrhythmic stimulus protocols that depend on real-time measurements. In this study, tools for observer analysis and design were applied to a two-variable Karma model of AP dynamics. Observability Grammians were computed for a single-cell Karma model, and it was determined that the membrane potential variable, rather than the refractory variable, is the better choice for reconstructing the initial state of the model. Next, a two-cell Karma model was augmented with Luenberger observer feedback, and a restricted search of stabilizing observer gain values was used to determine gains that were optimal in the sense of minimizing the 2-norm of the closed-loop eigenvalues. A practical extension of these results is presented, in which a 106-cell Luenberger observer was used with membrane-potential data from microelectrodes at 0.3, 0.9, and 1.5 cm from the proximal end of a 2.1-cm in vitro canine Purkinje fiber. Compared with the Karma model by itself, the observer was able to reduce the mean absolute APD error from 69.5 ms to 12.9 ms, averaged over three locations (0.6, 1.2, and 1.8 cm) where the observer was not supplied with electrode data. This shows that observer feedback can help the Karma model to reproduce measured APDs, even when the correct model parameters are not known precisely.

SA4

ECGSIM: Interactive Simulation of the ECG for Teaching and Research Purposes

PM van Dam*, TF Oostendorp, A van Oosterom

Radboud University Medical Center, Nijmegen, the Netherlands

The expression of the electric activity of the heart in the ECG waveforms is complex. The understanding of this relation can be facilitated by using an interactive tool, enabling introduction of changes in the electrical activity of the heart and observing their effect on the ECG. **ECGSIM** (version 1.3) is such an interactive simulation tool. It has been found to be effective both in teaching and basic research. A new version (2.0) of **ECGSIM** has been designed in which the expression of atrial activity has been included and its functionality has been optimized.

ECGSIM is based on a mathematical model that links the ECG at the body surface to the local transmembrane potential (TMP) at the surface of the myocardium (epicardium and endocardium). It includes atrial, ventricular and torso geometries, reconstructed from human MR images. The user may change any of a set of parameters describing the TMP such as the depolarization time, the timing of repolarization and the TMP magnitude. These changes may be introduced at any section of the heart surface or globally; their effect on the ECG is displayed instantaneously. In the new version, several cases (heart and thorax models) can be selected. Currently, cases of healthy subjects and of a WPW patient are included. This collection will be extended by including additional cases. In this way the applicability of this tool in clinical education and research will be enhanced.

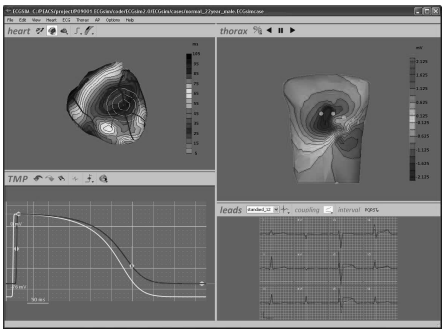

Main type of ECGSIM display

By using **ECGSIM** it is easy to intuitively induce abnormalities such as bundle branch block and infarction, and observe their effect on the ECG, version 2.0 will be even more helpful in teaching and research applications. **ECGSIM** may be downloaded of free of charge from http://www.ecgsim.org.

PB1

Refined Estimate of the Dominant T Wave

Roberto Sassi* and Luca T Mainardi

Dipartimento di Tecnologie dell'Informazione, Università degli Studi di Milano, Crema, Italy

The Dominant T-wave (DTW) offers an overall view of the repolarization phase in the ventricula. While being only a conceptual entity, it derives directly from an equivalent surface source model (ESSM). Once postulated that the conductive properties of the thorax are linear and that the shape of the repolarization curve of each myocytes is identical, although with different time intervals between firing and repolarization, it can be shown that the T waves of all leads on the thorax are, in first approximation, a scaled version of a single waveform shape.

Generally, the DTW reflects the first-order derivative of the repolarization phase of the transmembrane potential of the myocytes. An increased dispersion of the repolarization times is linked to pathological conditions. In this case the second-order derivative starts to play a relevant role. Unfortunately the method proposed so far only consider the first-order derivative.

In this work we first proposed an algorithm to estimate the DTW taking into account the second-order derivative of the repolarization curve. It is based on the minimization of the Frobenius norm of the residual matrix. This results in a set of non-linear equations and this difficulty is overcame by iteratively solving two linear sub-parts of the system.

The algorithm was tested on synthetic ECG recordings. The shape of the repolarization curve and the scaling factors which accounts for the geometry of the sources were derived from ECGSIM, a freely available software implementing the ESSM. When the dispersion of the sources is varied from 20 to 60 ms, the new technique shows an average improvement in the precision of the estimate of the repolarization curve of about 5.1% over previous methods. This hints that the new method might permit to employ the DTW formalism in a larger set of applicative contexts.

PB1

Simulation of Fractionated Electrograms at Low Spatial Resolution in Large-Scale Heart Models

Mark Potse* and Nico HL Kuijpers

CARIM, Department of Biomedical Engineering, Maastricht University, Maastricht, Netherlands

Computation of extracellular potentials from transmembrane potentials is a common problem in cardiac electrophysiology. It is part of many bidomain reaction-diffusion models, and is also used to compute (intracardiac) electrograms from membrane potentials simulated by monodomain models. Computation of electrograms requires the solution of an elliptic boundary-value problem which, when discretized, can be written as a system of linear equations. Because extracellular potentials must be solved at a spatial resolution of 0.2 mm or better to avoid spike artefacts, these linear systems can have tens or hundreds of millions of equations for a whole-heart model. Such large systems are hard to solve and require in the order of 10-100 GB memory. Faster and less memory-intensive solutions are often desirable.

Artefacts in low-resolution solutions are related to the restriction operator that is used to translate the source data from the high-resolution to the low-resolution mesh. Typically, this restriction is done by injecting transmembrane potentials. We propose to use transmembrane current as a source, with trilinear weighting rather than simple injection.

We tested this method in a large-scale model of the human ventricles, which consisted of 90 million nodes at 0.2-mm resolution. A good visual match was obtained between electrograms computed at 1-mm and at 0.2-mm resolution, even in regions where strong sub-millimeter heterogeneity in tissue conductivity was present. Peak potential values were well reproduced, but the slope of steep deflections was underestimated at low resolution. The solution at low resolution was more than proportionately faster than that at high resolution.

Our method is easy to implement in an existing bidomain solver and is useful to rapidly compute electrograms intended for visual inspection at thousands of sites simultaneously. The scheme may also be valuable as a restriction operator in multigrid methods.

PB1

Implantable Cardioverter Defibrillator Predictive Simulation Validation

Jess D Tate*, Jeroen G Stinstra, Thomas A Pilcher and Rob S MacLeod

Dept. of Bioengineering, University of Utah, Salt Lake City, UT, United States

Despite the growing use of implantable cardioverter defibrillators (ICDs) in adults and children, there has been little progress in optimizing device and electrode placement. To facilitate effective placement of ICDs, especially in unique cases of children with congenital heart defects, we have developed a predictive model that evaluates the efficacy of a delivered shock. Most recently, we have also developed and carried out an experimental validation approach based on measurements from clinical cases. We have developed a method to obtain body surface potential maps of ICD discharges during implantation surgery and compared these measured potentials with simulated surface potentials to determine simulation accuracy.

Each study began with an full torso MRI or CT scan of the subject, from which we created patient specific geometric models. Using a customized limited leadset applied to the anterior surface of the torso away from the sterile field, we recorded body surface potentials during ICD testing. Subsequent X-ray images documented the actual location of ICD and electrodes for placement of the device in the geometric model. We then computed the defibrillation field, including body surface potentials, and compared them to the measured values.

Comparison of the simulated and measured potentials yielded very similar patterns and a typical correlation between 0.8 and 0.9 and a percentage error between 0.2 and 0.35. The high correlation of the potential maps suggest that the predictive simulation generates realistic potential values. Ongoing sensitivity studies will determine the robustness of the results and pave the way for use of this approach for predictive computational optimization studies before device implantation.

PB1

A Chaotic Model for Generating Heart Rate Variability Signal using Integral Pulse Frequency Modulation

Mahdi Lak, Nader Jafarnia Dabanloo* and Seyed Kamaledin Setarehdan

Bioelectrics, Biomedical Engineering Faculty, Science and Research branch, Islamic Azad University, Tehran, Iran

Heart Rate Variability (HRV) is a very useful signal to investigate the activity of the Autonomic Nervous System (ANS), which affects and the heart function. Constructing a mathematical model for producing artificial HRV signal is needed to get a conceptual understanding of how ANS controls the heart rate (HR). In addition, an accurate HRV model can be used to drive an Electrocardiogram model for producing artificial ECG. The Integral Pulse Frequency Modulation (IPFM) structure is employed in this paper to model the Sino-Atrial Node (SAN). Considering the complexity and nonlinear dynamics in the real HRV signal, a chaotic input is used in the proposed model. Also, the effects of both Respiratory Sinus Arrhythmia (RSA) and Mayer waves were incorporated in the proposed model. Instead of using a fixed threshold in IPFM model as in most previous works, we applied an appropriate variable signal, which has nonlinear chaotic dynamics. After implementation and running the model, the power spectrum of the output signal is extracted, which was then followed by calculating the nonlinear characteristics. The simulation results showed that the calculated power spectrum and the nonlinear parameters of the output HRV signal are closely correlated with the real ones which confirm the effectiveness of the proposed model.

PB1

Towards the Cardiac Equivalent Source Models in ECG and MCG Problems: A Simulation Study

Guofa Shou, Ling Xia*, Huilong Duan and Mingqi Qian

Department of Biomedical Engineering, Zhejiang University, Hangzhou, Zhejiang, China

The cardiac equivalent source model is very crucial in the electrocardiogram (ECG) and magnetocardiography (MCG) problems. Many source models have been proposed and applied to explain and calculate the cardiac electromagnetic signals, in which the dipole, equivalent double layer (EDL) and epicardial potential (EP) models are commonly used. However, the performance of three source models have not been explored and compared into a unified framework. In this study, we presents a thoroughly investigation of these three models in terms of the ECG/MCG forward problem. Based a virtual heart model with electric excitation, the cardiac electromagnetic field is cal-culated with boundary element method (BEM). The numerical performance and the properties of the three source models are studied detailed for electric and magnetic fields. For the three source models, three different resolutions of dipole and two of EP and EDL models are studied. The dipole and EDL source models are directly calculated from the heart model, while the EP source is from the dipole or EDL models. Besides, the effect of the volume conductor model is also studied. The simulation results demonstrated that the resolution of the source models shouldn't be too small, otherwise some in-formation about the cardiac activities will be lost as shown in the single di-pole model situation. The effect of the resolution on the MCG is larger than that on BSP. The higher resolutions of the source, the larger effect of the vol-ume conductor happened for each source. While for the EDL source, the lung has little effect on the MCG. The EDL source can generate the similar per-formance compared to the dipole source, while the largest difference hap-pened at the time when the ventricle start or finish the activation. The pre-sented study suggests that the EDL source is a good choice as source model for ECG/MCG problem.

PB1

The Inverse Problem of Phase Singularity Distribution: An Eikonal Approach

V Jacquemet

Université de Montréal
Montréal, QC, Canada

Phase singularity analysis provides a tool to quantify the complex spatio-temporal behavior observed in electrophysiological models of cardiac arrhythmia. The associated inverse problem consists in constructing an initial condition for a reaction-diffusion system with a given spatial distribution of anatomical/functional reentries. We aim to tackle this problem by solving an eikonal-diffusion equation that generates phase maps.

The eikonal-diffusion was extended to handle anatomical/functional reentries and wavefront collisions. Boundary conditions on activation times were used to specify pathways of reentry. A dedicated finite-element-based method was developed to solve this equation on a triangular mesh. The resulting phase maps served to construct an initial condition for a propagation model through a mapping between phase and cell state. Cardiac propagation was then simulated from this initial condition in the monodomain framework. Evolution of phase singularities was tracked.

Our approach was applied to initiate reentries in an atrial model. Anatomical and functional reentrant circuits were placed at 24 different locations in the atria. For each reentrant circuit, the eikonal-diffusion equation was solved on a coarse triangular mesh representing the epicardium and a phase map was reconstructed. Monodomain simulations (Courtemanche model; L-type calcium current reduced by 75%) were run on a finer 3D mesh after interpolation of the initial condition. In two cases, the reentry self-terminated within 3 s. In the other cases, the phase singularity meandered in the vicinity of the desired location specified in the eikonal problem.

The results suggest that this tool could help in the development of dedicated models aimed at better understanding clinical case reports, as well as in the creation of a library of different forms of simulated arrhythmias.

PB1

Estimating the Influence of Cardiac Motion on Simulations of Electrical Excitation

Stefan Fruhner*, Harald Engel and Markus Bär

Fak. II - Institut für Theoretische Physik, EW 7-1, Technische Universität Berlin, Berlin, Germany

In simulations realistic heart models often include detailed physiological knowledge about ionic dynamics of cardiac cells and accurately account for anatomical details like fibre orientation or heterogeneity of heart tissue. Additionally describing the feedback between propagating waves of electrical activity and cardiac contraction might be essential for a deeper understanding of the mechanism of cardiac arrhythmias like tachycardia and fibrillation.

Using time resolved magneto-resonance images two-dimensional finite-element meshes have been generated in order to perform simulations of waves of electrical activity propagating in a beating human heart. Therefore, the intracellular and extracellular domain are treated separately. This approach is commonly known as bidomain approach. Cardiac motion is extracted from the images by following a set of control points visualised using a tagged MRI protocol.

Different ionic cellular models have been applied to analyse the differences between a static and a moving heart. To characterize these differences in simulations the activation times of the excitation have been computed. These are given as the time difference between initial stimulation and the first activation of some region. For the moving heart, in some regions activation times up to 20 ms smaller than in the static case have been obtained. At the same time other regions became activated 25 ms later. The impact of cardiac motion can also be demonstrated in artificially generated biosignals like the electrocardiogram (ECG).

The approach also offers the opportunity to calculate the mechanical stresses during cardiac contraction from experimental data without using detailed models on calcium dynamics and stress-activated channels in cardiac myocytes.

PB1

Role of the Fast Conduction System in Electrical Activation in Simple and Detailed Biophysical Heart Models

Ali Pashaei*, Daniel Romero, Rafael Sebastian, Oscar Camara and Alejandro F Frangi

Computational Imaging and Simulation Technologies in Biomedicine (CISTIB), Universitat Pompeu Fabra, Barcelona, Spain

Electrical activation in the ventricles follows a complex pattern which involves propagation through both specialized fast conduction tissues and contracting myocardium. Modelling the effects of the conduction system is essential to obtain meaningful simulation results. This is especially critical for in silico planning and optimisation of certain therapies such as Cardiac Resynchronisation Therapy (CRT), where events such as the retrograde Purkinje activation might play an important role.

There exist several models with different degree of complexity to simulate cardiac electrical activation. The complexity is usually selected as a function of the final application and has a great impact in computational times. It is not fully clear whether simple models that include the most important anatomical structures can reproduce results of complex biophysical models.

In this paper a comparison between simplified and complex electrical propagation models was carried out over a patient-specific anatomical model of the left ventricle from an asymptomatic patient, in which main substructures were mathematically modelled, i.e. the Purkinje network and myocardial fiber orientation. Complex biophysical modelling used ion kinetic dynamics at cellular level and reaction-diffusion equations for tissue propagation, whereas a simple model was based on Eikonal equations solved with a Fast Marching Method (FMM).

Anisotropic conductivity of the tissue was modelled in the electrical equations throughout the domains. Electrophysiological activation and propagation was modelled as a 3D conductive domain coupled to a 1D fast conductive structure. Coupling between the myocardium structure and fast conductive systems was provided on the terminals nodes.

The electrophysiological signal propagation on the myocardium was compared between both models by looking at local activation times and activation sequences. Results showed that simpler electrophysiology models coupled with a fast conductive system might provide results valid in applications where the focus is in the activation sequence of ventricles, such as CRT.

PB1

Moving Equivalent Dipoles Derived from the Body Surface Potential Map by Solving the Inverse Problem

Vito Starc*

Institute of Physiology, University of Ljubljana, Faculty of Medicine, Ljubljana, Slovenia

Hypothesis/Objective: The aim of this study is to determine instantaneous 3-D locations of moving equivalent dipoles (ED) corresponding to singular value decomposition (SVD) components obtained from body surface potential map (BSMP) of the CINC/Physionet Challenge 2007 database. Mehtod: The proposed method is based on the relationship between SVD components and ED parameters derived for this purpose. Here we use a dipole model in a bounded spherical homogenous conductor (Geselowitz and Ishiwatari 1965), with the dipole moment and dipole spatial parameters separated. Dipole parameters are obtained in two steps: first (forward problem formulation), the dipole moment parameters are calculated from each SVD component for a dipole with the known location,, and second (inverse problem formulation), dipole location is varied until reaching the optimal one at the minimum in the selected objective function. Our method was successfully tested using Gabor Nelson method. In calculations, we used BMSP of 71 anterior leads (of the Dalhouise 120 torso leads), assuming a standard thorax dimensions (homogenous and isotropic thorax conductance distribution) approaching the spherical surface in the applied region. All BMSPs were first divided into short intervals (4 ms in the QRS, and 20 ms in the T wave region). These parts of BMSP signals were then decomposed, and from 3 biggest SVD components the corresponding EDs were determined. Results: Each set of BMPS data was represented with sequential arrays of EDs, each with changing dipole moment, spatial orientation, and a 3D location, thus providing additional information for the interpretation of ECG. This representation enabled a relatively precise reconstruction of all 71 BMSP signals used: in four BMPS cases mean deviations of the reconstructed BMSP from the original one were 0.025, 0.020, and 0.0195 mV (in all SE of +-0.002mV), when EDs of the first one, two and first three SVD components, respectively, were used.

PB1

Study of the Static and Dynamic Characterization of the Biological Tissue to Obtain the Temperature Estimation in RF Aablation using Computer Modeling

José Alba*, Macarena Trujillo, Ramón Blasco and Enrique J Berjano

Electronic Engineering Department, Biomedical Synergy, Torrent, Valencia, Spain

Radiofrequency ablation has been used to treat some types of cardiac arrhythmias. We have previously proposed an ARMAX model (non structural) to estimate the temperature in the tissue during ablation. Computer modeling has allowed us to study the temperature distribution by means of solving numerically theoretical models based on partial differential equations, which represent physical phenomena. Now our objective is to consider the biological tissue as a system with an input (applied voltage) and output (tissue temperature), and thus to search for a transfer function between these variables. The final aim is to have a simple model that could estimate the temperature at each point of the tissue. We solved the model using the finite element method and identified the transfer function between the temperature at 4 mm depth and an applied voltage using a 7Fr and 4 mm electrode. We used COMSOL Multiphysics to solve the electro-thermal problem and MATLAB to obtain the transfer function. The results showed that the variation in the electrical conductivity of cardiac tissue affected only the static gain of the system, while the variation in the specific heat produced a change only in the dynamic system response. However, the variation in thermal conductivity modified both the static gain and the dynamic system response. These results are a first step towards the development of a macroscopic model based in physical principles, which would lead to better temperature estimation during ablation.

PB1

Three-Dimensional Analysis of Regional Left Ventricular Endocardial Curvature from Cardiac Magnetic Resonance Images

Francesco Maffessanti*, Enrico G Caiani, Hans-Joachim Nesser, Johannes Niel, Regina Steringer-Macherbauer, Roberto M Lang and Victor Mor-Avi

Politecnico di Milano, Milan, Italy, Publich Hospital Elisabethinen, Austria, and University of Chicago, IL, United States

Left ventricular (LV) remodeling is usually assessed using changes in LV volume. Because this methodology disregards regional changes that may occur independently of volume, we hypothesized that 3D analysis of regional endocardial curvature could provide useful information on localized remodeling, and tested this approach on cardiac magnetic resonance (CMR) images. CMR images (Siemens 1.5T) were acquired in 44 patients: 14 normal controls (NL), 15 with dilated cardiomyopathy (DCM), and 15 with ischemic heart disease (IHD). LV endocardial surface was semi-automatically reconstructed throughout the cardiac cycle (TomTec). Custom software was used to calculate for each point on the surface the curvedness, normalized to take into account instantaneous LV size, Cn. Normalized curvedness was compared between groups of segments: NL (N=401), DCM (N=255) and IHD (N=92). While in NL segments, both maximum and minimum Cn values were comparable in basal and mid-ventricular segments, they were significantly higher in the apical segments. Additionally, percent change in Cn was higher in mid and apical compared to basal segments ($p<0.05$). At all LV levels, Cn values in IDC segments were lower ($p<0.05$) than in NL and IHD segments. In contrast, percent change in Cn was significantly lower in both IHD and DCM segments compared to NL. 3D analysis of regional LV endocardial curvature from CMR images provides quantitative information, which is consistent with the known pathophysiology, and may thus prove clinically useful in the evaluation of LV remodeling.

PB2

Characterization of Degenerative Mitral Valve Disease using Morphologic Analysis of Real-Time 3D Echocardiographic Images

Sonal Chandra, Ivan S Salgo, Lissa Sugeng, Lynn Weinert, Masaaki Takeuchi, Wendy Tsang, Roberto M Lang and Victor Mor-Avi*

University of Chicago, IL, United States

Pre-surgical planning of mitral valve (MV) repair in patients with Barlows disease (BD) and fibroelastic deficiency (FED) is challenging due to inability to accurately assess the complexity of MV prolapse. We hypothesized that the etiology of degenerative MV disease (DMVD) could be objectively and accurately determined using morphologic analysis of MV geometry real-time 3D echocardiographic (RT3DE) images. Eighty-eight patients underwent transesophageal RT3DE study: 58 patients with DMVD studied intra-operatively (29 BD, 29 FED classified during surgery) and 30 patients with normal MV who were used as controls (NL). MVQ software (Philips) was used to measure parameters of annular dimensions and geometry, and leaflet surface area, including billowing volume and height. Patients were divided into a study group (34 DMD; 20 NL) used to define cutoff values of MV billowing parameters for differential diagnosis of NL vs FED vs BD using ROC analysis, and a test group (24 DMVD; 10 NL) to test the accuracy of these criteria in an independent sample when compared with surgical inspection. In the study group, morphologic analysis revealed a progressive increase in multiple parameters from NL to FED to BD, which allowed accurate diagnosis. 3D billowing height with cutoff of 1.3 mm differentiated DMVD from NL without overlap, and billowing volume with cutoff of 1.4 ml differentiated between FED and BD without overlap. The accuracy of this approach was confirmed in the test group, as reflected by high sensitivity and specificity for both parameters. Morphologic analysis as a form of decision support of assessing MV billowing revealed significant quantifiable differences between NL, FED and Barlow, allowing accurate classification of the etiology of MV prolapse and determination of the anticipated complexity of repair.

PB2

Identifying Fetal Heart Anomalies using Fetal ECG and Doppler Cardiogram Signals

Ahsan Habib Khandoker*, Yoshitaka Kimura, Marimuthu Palaniswami and Slaven Marusic

Department of Electrical and Electronic Engineering, The University of Melbourne, Parkville, Victoria, Australia

The principal aim of fetal welfare testing is to identify fetuses with heart anomalies so that these adverse outcomes can be prevented. This study presents an automated and non-invasive technology using an integrated fetal transabdominal electrocardiogram system and Doppler cardiogram (DCG) to identify fetal heart anomalies. Simultaneous recording of the abdominal ECG signals and DCG signals from 5 pregnant women at the gestational age of 2836 weeks with normal single pregnancies and 5 pregnant women who were diagnosed to have fetal heart anomalies collected from Tohoku University Hospital. A total of 10 recordings (each of 1 min length) were sampled at 1,000 Hz with 16-bit resolution. Multiresolution wavelet analysis and Jensen-Shannon divergence (JSD) methods were used to identify the frequency contents of the Doppler signals to be linked to the opening and closing of the heart's valves (Aortic and mitral) and two wall motions (ventricular and atrial contraction). The JSD is a measure of distance between probability distributions which were defined from the wavelet decompositions of the DCG signals. For the normal fetuses, PEP (Pre-ejection period), VET (Ventricular ejection time), ICT(Isovolumic contraction time) and IVRT (Isovolumic relaxation time) were found to be 75.0$\pm$11.9 (msec), 153.2$\pm$18.9 (msec), 50.0$\pm$15.9 (msec) and 69.6$\pm$9.7 (msec) respectively. On the other hand, for fetuses with heart anomalies, these timing intervals were found to be 89.0$\pm$10.3 (msec), 168.6$\pm$25.0 (msec), 52.2$\pm$17.2 (msec) and 51.6$\pm$13.7 (msec) respectively. PEP, VET and IVRT values are significantly ($p<0.01$) different between the two groups. The ability of the newly developed system to accurately detect opening and closing timing in fetal cardiac valves has be confirmed using B-Mode and M-mode pulsed Doppler images of aortic and mitral valves. Figure 1 (see pdf). Example of simultaneously recorded fetal ECG and Doppler ultrasound data.

PB2

Magnetic Resonance Imaging-induced heating on patients with Implantable Cardioverter-Defibrillators and Pacemaker: Role of Lead Structure

E Mattei, G Calcagnini, F Censi, M Triventi and P Bartolini

ISS - Italian National Institute of Health, Rome, Italy.

Magnetic Resonance Imaging (MRI) induced heating on patients with metal implants can pose severe health risks and careful evaluations are needed for pacemaker (PM) or implantable cardioverter-defibrillator (ICD) leads to be labeled as 'MRI conditionally'.

Experimental studies in this field have shown a great variability in results and revealed that several aspects can affect the amount of heating induced at the lead tip. The structural parameters of the lead are one of these.

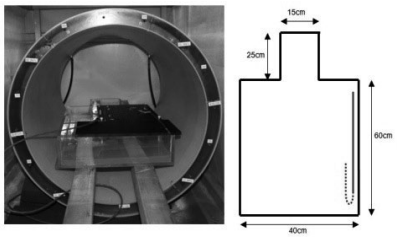

RF coil and human trunk simulator and sketch of the lead positioning inside the phantom

In this study we performed in-vitro temperature measurements of PM/ICD leads inside a human trunk simulator exposed to the RF field of a 1.5T MRI scanner. Aim of these measurements is to investigate the role of the lead structure on the induced heating at the lead electrodes (tip and ring). The exposure system was a 64 MHz birdcage coil delivering a whole-body SAR on 1W/kg and temperature was measured by fluoroptic® porbes. The trunk simulator was filled with a gelled saline solution that minimized the heat transfer by convection, as described in the international standards ASTM F2182–02a.

A total of 26 commercial leads from 7 manufacturers were tested (23 PM leads, 3 ICD leads) and the temperature increases induced by the RF field ranged from 2.1°C to 15.0°C. Significant heating was observed not only at the lead tip, but also at the ring (as high as 4.2°C), even if not in all the bipolar leads tested. Active-fix leads showed higher temperature increases than passive-fix ones (4.7°C versus 7.4°C).

In conclusion, the lead structure plays an important role in the MRI-induced heating. It must be carefully considered to interpret the widely varying results reported in literature and to define safe conditions to extend MRI to patients with metal implants.

PB2

Assessing Cardiac Phase Retrieval in Intravascular Ultrasound

Aura Hernàndez-Sabaté*, Monica Mitiko Soares Matsumoto, Sergio Shiguemi Furuie and Debora Gil

Computer Science Dept, Computer Vision Center, Bellaterra, Barcelona, Spain

A good reliable approach to cardiac triggering is of utmost importance in obtaining accurate quantitative results of atherosclerotic plaque burden from the analysis of IntraVascular UltraSound. Although, in the last years, there has been an increase in research of methods for retrospective gating, there is no general consensus in a validation protocol. Many methods are based on quality assessment of longitudinal cuts appearance and those reporting quantitative numbers do not follow a standard protocol. Such heterogeneity in validation protocols makes faithful comparison across methods a difficult task.

We propose a validation protocol based on the variability of the retrieved cardiac phase and explore the capability of several quality measures for quantifying such variability. An ideal detector, suitable for its application in clinical practice, should produce stable phases. That is, it should always sample the same cardiac cycle fraction. In this context, one should measure the variability (variance) of a candidate sampling with respect a ground truth (reference) sampling, since the variance would indicate how spread we are aiming a target. In order to quantify the deviation between the sampling and the ground truth, we have considered two quality scores reported in the literature: signed distance to the closest reference sample and distance to the right of each reference sample. We have also considered the residuals of the regression line of reference against candidate sampling.

The performance of the measures has been explored on a set of synthetic samplings covering different cardiac cycle fractions and variabilities. From our simulations, we conclude that the metrics related to distances are sensitive to the shift considered while the residuals are robust against fraction and variabilities as far as one can establish a pair-wise correspondence between candidate and reference. We will further investigate the impact of false positive and negative detections in experimental data.

PB2

Noninvasive 4D Blood Flow and Pressure Quantification in Central Blood Vessels via PCMRI

S Meier*, A Hennemuth, O Friman, J Bock, M Markl, T Preusser

Fraunhofer MEVIS
Bremen, Germany

Introduction. Local vessel anatomy and haemodynamics is a key factor for diagnosis and therapy planning in patients with aortic aneurysma and congenital heart diseases. Recent progress in MRI technology has facilitated time- and spatially resolved (4D) PCMRI velocity-encoded measurements in reasonable scan times. Purpose of this work is the demonstration of new methods for noninvasive assessment of detailed haemodynamical parameters in central blood vessels based on advanced postprocessing methods.

Methods. The semi-automatic image processing chain of the 4D PC data consists of an eddy current correction and phase unwrapping , followed by PC-MRA calculation in order to extract the vessel lumen. The pressure calculation is done by solving the Pressure-Poisson equation with Neumann boundary conditions via the finite-element method directly in the segmented flow volume. The algorithm was validated by comparison with Lattice-Boltzmann flow simulations of a turbulent flow jet in a stenotic vessel phantom and tested on 4D PCMRI measurements from a 3T system covering the entire thoracic aorta (spatial resolution $1.8 \times 1.8 \times 2.6\,\mathrm{mm}^3$, temporal resolution 40 ms, venc 150 cm/s).

Results. The CFD validation showed that the pressure drop along a stenosis can be well predicted by our algorithm. A first evaluation of the method on invivo data of patients with aortic aneurysma as well as patients that underwent Fontan procedure was successfully performed.

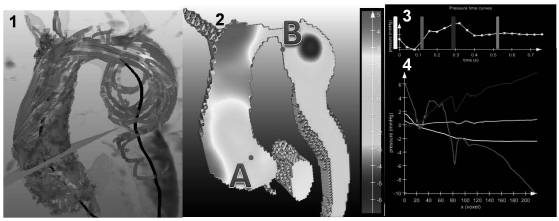

1,2) Flow pathlines and pressure in aortic aneurysma at late systole. 3) Pressure difference between A and B over the cardiac cycle. 4) Pressure along centerline (black line in (1)) at different times.

Conclusions. The proposed noninvasive methods yield valuable information on local haemodynamic parameters and can improve diagnosis and therapy planning.

PB2

A Computational Tool for Coronary Atherosclerotic Plaque Analysis of Virtual Histology Images

Fernando Sales*, João Falcão, Breno Falcão, Sergio Furuie and Pedro Lemos

Centro de Engenharia, Modelagem e Ciências Sociais Aplicadas (CECS), Universidade Federal do ABC, São José dos Campos, Brazil

Histopathological studies have shown an association between sudden death from acute coronary syndromes and the presence of ruptured plaques. This way, several efforts have been made for identifying profiles of rupture-prone atherosclerotic lesions. Diagnosis tools for in-vivo assessment of arterial wall composition have been playing a major role in this context. Virtual Histology (IVUS-VH) is an image modality, derived from intravascular ultrasound (IVUS), which allows the identification of atheromatous components, providing a frame-by-frame tissue classification into four classes: Fibrotic (FT), Fibro-Fatty (FF), Necrotic-Core (NC) and Dense Calcium (DC). According to current pathology consensus, intra-plaque spatial distribution of tissue elements has become an important issue for lesion classification. However, there is not an available environment to realize previously described analysis. To attend this demand, a computational tool has been developed in this work. ImageJ has been used as development framework, due to be an open-source platform for image processing built in Java language. Morphological operations and labeling algorithms of binary images were used to determine neighborhood relations between confluent sets of pixels, such as to measure distance to the arterial lumen. In order to attend the current classification scheme, automatic plaque type identification has been implemented as a new functionality. Automatic segmentation of grayscale IVUS images have also been implemented using active contours techniques. A sample test of 495 IVUS frames have been used to evaluate the accuracy of segmentation algorithms. For luminal contour, an average true positive rate (TPR) of 72.3% has been achieved. For adventitia contour, the average TPR was 80.9%. These are encouraging results, once we visualize some possible modifications in order to improve our methods. In the next months, we intend to distribute this tool for download under request.

PB2

Automated Heart Localization for the Segmentation of the Ventricular Cavities on Cine Magnetic Resonance Images

Constantin Constantinides*, Yasmina Chenoune, Elie Mousseaux, Frédérique Frouin and Elodie Roullot

Laboratoir d'Imagerie Fonctionnelle, INSERM UPMC, Paris, France

The automated segmentation of the ventricular structures is necessary for the routine evaluation of clinical parameters such as the ejection fraction or the left ventricular mass. Thus, a region of interest around the heart is essential but, in most cases user-defined. We propose an automatically defined region to reduce manual interactions. First, the hearts beating was exploited. Borderline pixels of the cavities have a higher gray level variation than pixels inside the cavities during the cardiac cycle. A rectangular function was chosen to model these variations. An image containing only the pixels showing movement (i.e. with gray level variations) over time was then produced. However, if the patient moves during data acquisition then falsely detected pixels that do not normally correspond to the beating heart can appear in this image. Thus, the second step consisted of taking advantage of the connected components throughout the slices with a 3D labeling followed by 2D labeling in each slice to keep only the pixels that truly correspond to the heart. This method was tested on the MICCAI 2009 challenge database of 45 subjects with various pathologies. Overall, detection of the whole cardiac structure was successfully achieved on almost all subjects except 2 subjects suffering from hypertrophy where failure on detecting the whole cardiac structure due to reduced motion and thickening of the left ventricle was noticed. The method was designed for the regions to always enclose the whole myocardium even if this may result in a region larger than necessary. Knowing that, only 17.5% of the total number of slices for all subjects was found to have an overgrown region of interest that needed reducing. Our method is simple, built with few plausible assumptions, and robust compared to other methods due to the accumulation of variability information from all slices.

PB2

A Method for Fast Browsing of Coronary Angiography Studies

Aafreen Mahmood and Tanveer Syeda-Mahmood*

Monta Vista High School, CA, United States

Cardiologists interpreting 2D coronary angiography videos often have to browse thousands of medical images for visual interpretation and diagnosis. Angiography studies are organized into several (20-30) video runs depicting the coronary arteries from different viewpoints. Currently, a specialist successively opens up each of the video run, and examines all the frames in the sequence for vessel anomaly-depicting images. Fast browsing methods that allow visually indexed navigation of the content, can help lower the burden on clinicians and reduce the time to diagnose.

We present a method to organize images from video runs of a coronary angiogram study into a storyboard by deriving a set of key images that represent the relevant coronary arteries being depicted. Specifically, a measure of vessel visibility is developed based on the number of tube-like vessel structures detected within images of the sequence. Curves extracted from edge-filtered images are paired to form tube-like structures using a variant of dynamic time warping. Changes in the vessel visibility measure are then tracked through the sequence to identify salient peaks and their corresponding images are chosen as key frames. Each key frame is annotated by its study, run and image number so that the section of the raw video sequence between consecutive key-frames from the same run can be displayed by selecting the key frame, thus serving as a visual index.

Using a ground truth database of 3647 video runs with 85022 images corresponding to 91 studies for 70 patients with various forms of coronary artery disease, we recorded the reduction in diagnosis time by physicians using the storyboard-based browsing. We recorded an 84.3% reduction in time for diagnosis using our method in contrast to raw browsing of video runs of coronary angiogram studies, thus proving the value of fast browsing methods in reducing the diagnosis time.

PB2

Transmural Changes in Fibre Helix Angle in Normal and Failing Canine Ventricles

Richard Clayton*, Samia Abdalhamid, Ryan Bloor, Kanna Kotagiri, Georgios Kyprianou, Jaeson Lee, Amruta Mane and Robert White

Department of Computer Science, University of Sheffield, Sheffield, United Kingdom

BACKGROUND: Ventricular myocytes are arranged in fibres, and it is well known that the fibre orientation relative to the base-apex axis (the helix angle) varies across the ventricular wall. Fibre orientation is important for propagation of the action potential, and for mechanics. Diffusion tensor MRI (DT-MRI) images fibre orientation in the heart, and the aim of this study was to examine transmural helix angle in a group of normal and failing canine hearts imaged using DT-MRI by Patrick Helm and colleagues at Johns Hopkins University. METHODS: We included DT-MRI images of 6 normal canine hearts, and 4 canines with heart failure. We examined transverse slices close to the base, midway between apex and base, and close to the apex. In each slice we measured the helix angle at locations in the left ventricular (LV) free wall, the septum, and the right ventricular (RV) free wall. RESULTS: In the normal hearts, the helix angle across the LV free wall and septum changed smoothly from between 50 and 60 degrees in the epicardial layer (RV endocardium in the septum) to between -50 and -60 degrees in the LV endocardial layer. However, close to the epicardium and within an endocardial layer around 3 mm thick we observed abrupt changes in helix angle. Close to the insertion of the RV and the septum, fibre orientation was much more variable. In the failing hearts, the change in helix angle across the LV and RV free walls as well as the septum was much less well defined. CONCLUSION: The transmural change in helix angle is often characterised as smooth, with a total rotation of 120 degrees. Our findings are consistent with this, but show that the helix angle is more variable close to the ventricular endocardium, at the insertion of the RV, and in failing hearts.

PB2

Poincaré Plot in Ischemic Rabbit Hearts

Oto Janoušek*, Marina Ronzhina, Marie Nováková, Ivo Provazník and Jana Kolářová

Department of Biomedical Engineering, Brno University of Technology, Brno, Czech Republic

BACKGROUND Heart rate variability may be evaluated by Poincaré plot. Its parameter SD1 describes short-term variability which is mainly caused by respiratory sinus arrhythmia, whereas long-term variability is described by SD2. Ischemia is believed to influence non-autonomic mechanism of the heart control and consequently HRV. Moreover, ischemia affects both SD1 and SD2 parameters significantly even in isolated denerved hearts.

METHODS Seven isolated New Zealand rabbit hearts were perfused at Langendorff setup. After control perfusion (15 min), each heart underwent three 15-minutes long episodes of coronary artery occlusion, followed by three reperfusion periods of the same duration. These six periods were compared to control. ECG signals were recorded by three orthogonal leads positioned orthogonally around the heart. Signals were amplified and digitized with sampling rate 2 kHz by 16-bit AD converter. Signals were further analysed by non-linear HRV parameters SD1 and SD2 by Kubios HRV software. The differrences among control, ischemic and reperfusion periods have been evaluated, because this approach allows comparing results from all examined rabbit hearts.

RESULTS The Poincaré plot indexes measured from control periods were smaller than those measured during ischemic periods. The Poincaré plot of the reperfusion periods exhibited greater dispersion of points than that of the ischemic periods. Parameter SD1 was set-up at 100% at control period. SD1 showed 584%, 439% and 220% decrease against control at three ischemic periods. There were 678%, 590% and 1150% changes against control in three reperfusion periods. Parameter SD2 exhibited 550%, 552% and 543% change against control period at three ischemic periods. There were 1170%, 1096% and 1023% changes against control period in three reperfusion periods.

CONCLUSIONS Ischemia significantly influences HRV even in isolated hearts.

PB3

HRV in Isolated Rabbit Hearts and In Vivo Rabbit Hearts

Oto Janoušek*, Marina Ronzhina, Peter Scheer, Marie Nováková, Ivo Provazník and Jana Kolářová

Department of Biomedical Engineering, Brno University of Technology, Brno, Czech Republic

BACKGROUND There is evidence that heart rate variability persists in denervated hearts. However, the mechanism of HRV in isolated heart is not known. Only a few studies have been published on this topic, mainly because presence of heart rate variability in conditions of completely denervated heart can be studied only at patients with transplanted heart. In this study HRV parameters in isolated rabbit hearts were compared with those from heart in vivo, which might help clarify the origin of HRV in denervated hearts.

METHODS Seven isolated New Zealand rabbit hearts were perfused at Langendorff setup. ECG signals were recorded by three orthogonal leads positioned around the heart. Leads were situated at borders of small bath, where the heart was placed. It allows touch-less recording of ECG. Signals were amplified and digitized with sampling rate 2 kHz by 16-bit AD converter. Signals were further analyzed by time, frequency and non-linear HRV methods by Kubios HRV software.

RESULTS Twenty six standard HRV parameters have been used for evaluation of differences between HRV of Langendorff-hearts and in vivo hearts. In the isolated, denervated heart HRV showed a broadband fluctuation, different from the well-known oscillation peaks at specific frequencies in in vivo hearts. Most significant difference was in mean RR - 491.0$\pm$13.4ms in the Langendorff hearts and 284.6$\pm$5.1ms in in vivo hearts.

CONCLUSIONS There are attempts to use HRV in the assessment of brain death and/or depth of sedation. Detailed analysis in this area may bring significant contribution to diagnostic possibilities. Our data provide evidence for the presence of HRV in isolated, denerved rabbit hearts. It was shown that intracardiac mechanisms regulating heart function affect the main parameters of heart rate variability. Variability of the rhythm of Langendorff-perfused isolated rabbit hearts is significantly different from that of in vivo hearts.

PB3

Determination of the Frequency Bands for Heart Rate Variability: Studies on the Intact and Isolated Rabbit Hearts

Marina Ronzhina*, Oto Janousek, Marie Nováková, Peter Scheer, Ivo Provazník and Jana Kolářová

Department of Biomedical Engineering, Brno University of Technology, Brno, Czech Republic

INTRODUCTION Many authors use in their studies the standards of the HRV frequency bands for human intact hearts, sincethese standards for animal's isolated hearts are still missing. However, there are other oscillations of HRV spectrum present in isolated heart, although there is no general consensus, what is their origin. Thus, it is important to define and compare the frequency bands of the intact and isolated hearts.

METHODS Twelve New Zealand rabbits were included in this study. The isolated hearts of 7 rabbits were perfused according to Langendorff. The ECG signals were recorded by touch-less method from three orthogonal leads. Moreover, the ECGs of the intact hearts of remaining 5 rabbits were recorded by 4 electrodes placed in such a way that the resulting records were comparable with those of isolated hearts. The RR-series were computed with own designed R-wave detector and detrended by smoothness prior procedure with the regularization parameter = 800. The detrended data were interpolated and resampled with frequency 15Hz. The limits between low and high frequencies (LF and HF) were defined on the basis of the spectral indices calculated from the accumulated power spectra of the HRV.

RESULTS The limits between LF and HF bands are defined as 0.86Hz and 1.47Hz for isolated and intact rabbit hearts, respectively. The HRV of the isolated hearts included in the present study have a different character of the power spectra: there are the spectra with one or two dominant oscillators or with no dominant oscillators. The pattern of the HRV spectrum of the isolated heart is determined by mechanisms, which differ from the phenomena occurring in the intact heart. These mechanisms are still unknown and are a very important topic for future studies.

PB3

Time Domain BRS Estimation: Least Squares versus Quantile Regression

Sónia Gouveia*, Conceição Rocha, Ana Paula Rocha and Maria Eduarda Silva

Centro de Matematica da Universidade do Porto e Departamento de Matematica, Universidade de Aveiro, Portugal

The estimation of baroreflex sensitivity (BRS) has been shown useful in the study of cardiac-pathological states, with lower BRS values associated with increased dysfunction. BRS is quantified from the joint analysis of systolic blood pressure (SBP) and RR intervals and it can be estimated by the ordinary least squares (OLS) slope between SBP and RR values in baroreflex events. Using OLS, the linear relation between two variables is described by the conditional mean. Quantile regression (QR) provides a more robust slope estimate, using the conditional median. Additionally, QR is able to provide different slope estimates B(tau), $0<tau<1$, by simply considering other quantile values besides the median (tau = 0.50). The aim of this work is to investigate if QR is able to provide new insights into BRS characterization.

OLS and QR estimation procedures are applied to the 46 EuroBaVar records (23 paired records in Lying and Standing positions). In 7/46 records, B(OLS) and B(0.50) exhibit significant differences (Wald test, $p<0.05$). In these records, few but influent SBP-RR pairs (associated with the highest SBP and RR values) lead to B(OLS)>B(0.50). In respectively 4/46 and 6/46 records, B(0.25) = B(0.50) = B(0.75) and B(0.05) = B(0.25) = B(0.50) = B(0.75) = B(0.95) were rejected ($p<0.05$), indicating that for most records the SBP and RR dispersion around the median line is fairly symmetric. Regarding L and S discrimination, it is expected that $R>1$, with R being the L to S ratio of B. Similarly to R(OLS) also R(0.25), R(0.5) and R(0.75) distinguish L from S in all the 23 paired records. Finally, R(0.5)>R(OLS) in 15/23 cases.

In conclusion, for most recordings the EuroBaVar slopes at other quantiles besides 0.5 do not provide different information. However, B(0.50) is more robust than B(OLS) to influent SBP-RR pairs and therefore QR may provide a more adequate BRS estimate.

PB3

Relationship between Fractal Dimension and Power-Law Exponent of Heart Rate Variability in Normal and Heart Failure Subjects

Monica Cusenza, Agostino Accardo*, Gianni D'Addio and Graziamaria Corbi

DEEI-University of Trieste, Trieste, Italy

Among the plethora of methods proposed to study the fractal-like behavior of heart rate variability (HRV), the power-law exponent (beta) and the fractal dimension (FD) have gained wide acceptance. Since HRV behaves like self-similar fractional Brownian motion (fBm) process, the linear relationship existing between beta and FD indices for fBm is often used to express one parameter in terms of the other. Objective of the study was to check the reliability of fBm in modeling HRV, focusing on the possible differences between normal (NR) and heart failure (HF) series. To this aim, 50 NR-HRV series and 50 HF-HRV series, extracted from 24-h Holter recordings, were analyzed. FD was estimated with Higuchis algorithm. Power-law beta exponent was calculated as the slope of the periodogram on a log-log plot within three different common narrow low-frequency bands as well as in the whole HRV frequency range. Both parameters were estimated every hour. Preliminary results showed that a linear relationship can be found only when beta is calculated in the whole HRV frequency range, being the two parameters almost independent in the considered narrow low-frequency bands. The relation is different for NR and HF populations and it differs from the theoretical one (beta=5-2D) valid for fBm series, suggesting no true self-similar behavior. In conclusion, the common practice of estimating beta from FD values for HRV series using the theoretical linear relation, should be reconsidered. A linear relation between the two parameters, though different from the theoretical one, can be found, in fact, only when beta is calculated in the whole HRV band. Moreover, the relationship seems not to be unique for NR and HF subjects. Finally, being the HRV beta exponent potentially less than or equal to 1, the linear relationship saturates to a FD value of 2.

PB3

Ventilatory Threshold Prediction by Spectral Analysis of Heart Rate Variability in Incremental Maximal Tests

Adolfo Benítez-Herrera, Miguel A García-González*, Rosa Angulo-Barroso, Ferran Rodríguez-Guisado, Xavier Iglesias-Reig, Raul Bescós, Michel Marina and Josep M Padullés

Electronic Engineering Department, Technical University of Catalonia (UPC), Barcelona, Spain

Ventilatory thresholds (VT1 and VT2) are useful in many fields of medicine and sports. Nevertheless, their measurement is cumbersome and needs trained personnel. This work proposes an alternative method to predict VT1, VT2 and maximum loads in incremental maximal tests based on heart rate variability (HRV) analysis of the RR time series obtained while performing the test. Twelve competitive male cyclists (34.1 +/- 5.7 years old) executed an incremental exhaustive test (25W/min) in the upright position on an electronically braked cycle ergometer. HRV data were collected with a Polar RS800 and the gas measurement was performed with a Cosmed Quark PFT-Ergo gas analyzer. An expert doctor annotated VT1 and VT2 loads from the gas measurements. After artifact correction, the power spectrum of the RR time series was estimated in a sliding window and central frequency (CF) and bandwidth that contains half the total power (BW) were computed. These indices dont need a band definition and are useful for analysis during exercise because the physiological changes associated with physical effort cause a radical modification of the power spectrum. An automatic algorithm recognized the loads at where CF and BW experiment a significant change. These loads were used as inputs in linear regression models to predict VT1, VT2 and maximum loads. The standard errors of the estimates were 24.3 W for the maximum load, 23.6 W for VT2 and 22.6 W for VT1 so the errors of the predictions are comparable to the resolution of the load (25 W). Moreover, the abrupt changes in BW and CF happened always in advance of the first ventilatory threshold so this methodology can be applied in real time and the test can be stopped once the abrupt changes in CF and BW are detected.

PB3

Modifications of Autonomic Activity and Baroreceptor Response During Tilt-induced Vasovagal Syncope

Chun-An Cheng*, Jiunn-Tay Lee and Hung-Wen Chiu

Graduate Institute of Biomedical Informatics, Taipei Medical University, Taipei, Taiwan

Vasovagal syncope (VVS) is diagnosed by medical history and confirmed by head-up tilt (HUT) test. The acceptable pathophyisiological mechanism for VVS is the simultaneous induction of the enhancement of vagal activity and the withdrawal of sympathetic activity. But the recent studies discover the parasympathetic activity could be inhibited during VVS. Therefore, in this study we attempted to examine this controversial by heart rate variability and baroreceptor sensitivity. Twenty positive HUT patients and twenty negative HUT patients were enrolled in this study from 2005 to 2009 in Taiwan. The baseline hemodynamic data of patients were checked with impedance cardiography. The spontaneous activity of the baroreceptor was determined by using the sequence method, rising sequences (rising systolic blood pressure, prolonged RR-interval) and falling sequences (falling systolic blood pressure, shorter RR-interval). Frequency domain analysis of heart rate variability was performed for assessment of autonomic activities. The results showed the VVS subjects had lower total peripheral vascular resistance in baseline. During HUT test the VVS subjects had increased LF/HF (7.585 ± 6.20 vs. 3.45 ± 1.21, $P=0.0083$) and decreased baroreceptor sensitivity (7.986 ± 2.34 vs. 11.88 ± 3.34 ms/mmHg, $P<0.001$). In conclusion, patients with VVS have the characteristics of baseline vascular sympathetic dysfunction and postural cardiac hypersympathetic activity. The decreased baroreceptor sensitivity revealed that the VVS subjects could not respond the sufficient heart rate to compensate blood pressure because of baroreflex impairment.

PB3

Respiration Signal as a Promising Diagnostic Tool for Late Onset Sepsis in Premature Newborns

Xavier Navarro*, Fabienne Porée, Alain Beuchée and Guy Carrault

INSERM, U642, Université de Rennes I, Rennes, France

The diagnosis of late onset sepsis in premature infants (PI) remains difficult because clinical signs are subtle and non-specific and none of the laboratory tests have high predictive accuracy. This lack of reliability of laboratory tests often results in anticipatory antimicrobial treatment. Heart rate variability (HRV) analysis emerges as a promising diagnostic tool. Entropy and long-range fractal correlation are decreased in PI with proven sepsis and presenting frequent and severe bradycardias. We shown last year that respiration and its relationship to HRV can participate as a diagnosis tool. As apneas and bradycardias are more severe and recurrent when a systemic infection is present in the PI, we investigated here only the respiratory signal. It has been analyzed using statistical, signal processing and chaos techniques in order to nd any relationships between the breathing pattern and infection. The tests were performed on a cohort study of 13 septic and 13 non septic infants (post-menstrual age $<$33 weeks and chronological age $>$72 hours), hospitalized in the neonatal intensive care unit at the university Hospital of Rennes who presented severe (need of bag and mask to resuscitate) or frequent (more than 1 per hour) bradycardias. From the respiratory signal, the statistical analysis reported some signicance in the ratio between the inspiratory ti and expiratory te times (p value=0,002), while the other parameters were not signicant. Analyzing the respiratory variability with chaos techniques, it has been found that the Hurst exponent is lower in the infected population (0,64 against 0.66 in healthy with p value$<$0.03), which implies a more complex breathing pattern. Moreover, we observe that the duration of central apneas have a different distribution in each group : the infected newborns exhibit generalized extreme value (GEV) distribution, the non infected trend to lognormal distribution.

PB3

Identification of Sympathetic and Parasympathetic Nerves Function in Cardiovascular Regulation using NARX Model

Ali Ghaffari, C Nat Nataraj*, Ali Jalali, Parham Ghorbanian and Fatemeh Jalali

Department of Mechanical Engineering, Villanova University, Villanova, PA, United States

In this study, a new nonlinear system identification approach for dynamical quantification of cardiovascular regulation is developed. This approach is specifically focused on the identification of Heart Rate (HR) baroreflex mechanism. The specific aim of this study is to improve the model accuracy in the estimation of HR by proposing a modified nonlinear model. The proposed HR baroreflex model is based on inherent features of autonomic nervous system. A Nonlinear Auto-Regressive Exogenous (NARX) model is employed to estimate the HR series as the output of the HR baroreflex mechanism. Also, an Adaptive Neuro-Fuzzy Inference System (ANFIS) structure is developed to estimate the NARX model. This method allows incorporation of physiological understandings about the sympathetic and parasympathetic nerves through selection of membership functions in the ANFIS structure. Membership functions are selected so as to represent the sympathetic and parasympathetic nerve functions. The hybrid learning method is applied as a learning algorithm of the ANFIS structure. Finally, an A-Information Criterion (AIC) is applied in order to select the appropriate order of the model. Required data for system modeling, training and testing are collected from the Physionet database. The model is trained by data obtained from four subjects and tested with the data acquired from eight subjects. The mean Normalized Root Mean Square Error (NRMSE) resulted in this study is 0.191. The results show significant improvements in HR prediction by calculating NRMSE in comparison with other developed methods. It is shown in this study that for cardiovascular system regulation, as a complicated system, our proposed nonlinear model is more accurate than other recently developed methods. Such accurate HR baroreflex modeling would enable clinicians to have more reliable information for their patients.

PB3

Tone-Entropy Analysis as a Cardiac Risk Stratification Tool

Herbert Jelinek, Ahsan Habib Khandoker* and Marimuthu Palaniswami

Department of Electrical and Electronic Engineering, The University of Melbourne, Parkville, Victoria, Australia

Improving risk assessment to provide evidence for preventative intervention has recently become more of a focus in cardiovascular medicine with atherosclerosis as an early manifestation of cardiovascular disease. There are many cardiac risk factors including cholesterol level, gender, age, diabetes and systolic blood pressure as well as coronary calcium screening or scintigraphy usingSPECT for identification of preclinical atherosclerosis. However coronary calcium screening or SPECT are not suitable for population screening purposes. Sudden cardiac deaths or acute myocardial infarctions in previously asymptomatic individuals, are linked to autonomic nervous system dysfunction as a causative factor in the development of atherosclerosis and augmenting arrhythmic events. We propose an algorithm to determine autonomic nervous system dysfunction that calculates the sympathetic-parasympathetic balance and allows stratification of individuals at higher risk of atherosclerosis that would benefit from coronary calcium screening or scintigraphy. Three hundred and seventeen study participants had a 20 minute lead II ECG recording taken and analysed for heart rate variability using the tone-entropy (T-E) algorithm. Tone (T) represents sympatho-vagal balance and entropy (E) the autonomic regularity activity. Of the 317 participants, 274 had TC/HDL ratios of below 5mmol/L indicating normal levels. The mean$\pm$SE of TC/HDL in the control versus elevated risk group were 3.514$\pm$0.047 and 5.809$\pm$0.11 respectively. The results for the tone and entropy analysis were combined using principle component analysis such that the mean$\pm$SE control group and elevated risk group were 1.433$\pm$0.712 and 0.189$\pm$0.236 (95% CI -2.303, 4.791; $p<0/05$). Our results suggest that T-E is a sensitive tool to identify heart rhythm disturbance associated with possible early risk of developing atherosclerosis. T-E does not require multiple tests to determine risk and can be used for patient stratification for coronary calcium screening to identify atherosclerotic plaques and lead to more timely intervention and better treatment outcomes.

PB3

A New Parameter in the Nonlinear Dynamics of the Heart: The Higher Reconstruction Step

Antônio Carlos da Silva Filho*, Fátima MHSP da Silva, Lourenço Gallo Júnior and Júlio Cesar Crescêncio

Departamento de Matemática, Centro Universitário de Franca, Ribeirão Preto, São Paulo, Brazil

Nonlinear dynamics has been playing an outstanding role in the study of heart in the last decades. It not just helped our understanding of the cardiac system but also brought many parameters that improved the diagnostic methods, as the Correlation Dimension or Lyapunov Exponents. In this work we propose a new of these parameters, The Higher Reconstruction Step (HRS), an extension of the Time Lag obtained from the Autocorrelation Function (ACF) in order to reconstruct the possible chaotic attractor that lies behind the dynamics. It is computed as usual, looking for the time lag in an ACF, but the difference is that it is calculated many times, increasing the number of points in the data set used until the whole time series is swept. As the data set used is increased, new time lags are found, forming a new sequence. The HRS is just the biggest of them, for each time series. In order to verify if the HRS parameter is or is not a good one to help the doctor or the researcher to discriminate between states (its potential diagnostic use), we collected R-R time series from two groups of men: one group with a cardiac chagasic disease (24 individuals) and a second one of healthy people (21 individuals). The series, for each individual, were collected in two positions: supine and after passive 70 degree head-up tilting, with volunteers seated in a saddle (dismissing the initial transient changes). Typical values of HRS are in the range 1-5, but there are some outliers. After removing the outliers greater than 50 the HRS is significantly smaller in the healthy group, with $p < 0.01$ in a t-test for the supine position. The same result happens if we remove the outliers greater than

10. SUPPORT OF FAEPA-HC-FMRP-USP AND FAPESP AND CNPq

PB3

Statistical Properties and Memory of Excursions in Heartbeat Intervals

Israel Reyes Ramirez

Lab. Sistemas Complejos, UPIITA IPN, Del. G.A. Madero, Mexico, D.F., Mexico

We study the statistics of excursions, defined as the number of beats to return to a local mean value, in heartbeat interval time series from healthy subjects and patients with congestive heart failure (CHF). We find that the cumulative distributions of excursions are consistent with a stretched exponential function of the form $G(t)\ exp(a * t^b)$ with a=1.09+/- 0.15 (mean value +/- SD) and b=0.91+/- 0.11 for healthy subjects and a=1.31+/- 0.23 and b=0.77+/- 0.13 for CHF patients. Besides, we study the statistics of return intervals between long excursions above certain threshold Q for both groups to explore the possibility of memory in the time organization of the extreme-size excursions. We find important differences in return intervals for both groups. We also apply the detrended fluctuations method (DFA) to excursions sequences to confirm the presence of correlations in healthy data while for CHF records the scaling exponent is characterized by a crossover, indicating that for short scales the sequences resemble uncorrelated noise.

PB3

Towards a Data Fusion Model for Predicting Deterioration in Haemodialysis Patients

Yasmina Borhani*, Susannah Fleming, David Clifton, Sheera Sutherland, Lyndsay Hills, David Meredith, Chris Pugh and Lionel Tarassenko

Institute of Biomedical Engineering, University of Oxford, Oxford, United Kingdom

Patients with Chronic Renal Failure are given three 4-hour haemodialysis treatments per week in order to maintain fluid and biochemical homeostasis. The accumulation and relatively rapid removal of fluid is often accompanied by adverse events, the most prominent of which is hypotension. Current patient monitoring during dialysis treatment includes intermittent measurements of tympanic temperature, blood pressure and haematocrit. However, this information is mostly used retrospectively rather than as a means for preventing adverse events.

We continuously monitored the vital signs of 40 haemodialysis patients during 8 sessions over a 6-month period in the Oxford Renal Unit in order to establish whether data fusion techniques could assist in predicting hypotension and which parameters would be most suitable for this purpose. The study involved non-invasively monitoring the ECG, heart rate, blood oxygen saturation and photoplethysmograph (PPG) waveform, as well as the haematocrit and tympanic temperature throughout each dialysis session.

The 4-dimensional vital sign data (heart rate, blood pressure, oxygen saturation and tympanic temperature) was initially visualized on 2D maps using the Neuroscale algorithm. The training data consisted of a data subset acquired from patients labelled by clinicians as physiologically stable patients and therefore considered to reflect normal physiology during dialysis. The maps show a clear distinction between unstable from and stable patients, with adverse hypotensive events outside the region corresponding to normal physiology.

A data fusion model based on a Parzen windows estimator of the probability density function of normal data was then created using the same training data. With this model, instabilities in patient physiology can be identified with, in some cases, the adverse event being predicted ahead of time.

PB3

Heart Rate Variability Using Poincaré Plots in 10 Year Old Healthy and Intrauterine Growth Restricted Children with Reference to Maternal Smoking Habits During Pregnancy

Taher Biala*, Michael Dodge, FS Schlindwein, Michael Wailoo

University of Leicester, Leicester, United Kingdom

The diagnosis of intrauterine growth restriction (IUGR) is given to children considered small for their gestational age. IUGR is associated with diseases later in adulthood, including hypertension, diabetes and stroke. ECG data taken from a cohort of 73 children at 10 years of age, using a Holter monitor, was analysed to investigate the heart rate variability during sleep. The cohort was split into 4 groups depending on the maternal smoking during pregnancy habits as well as IUGR or normal birthweight status. Beat to beat RR-interval analysis preceded the production of Lomb periodograms. Following this, Poincaré plots were created. The actual sleeping hours were decided from analysis of RR-intervals and the power of spectra in the high frequency region (indicating respiratory sinus arrhythmia) on the Lomb periodograms. This analysis enabled low frequency to high frequency (LF/HF) ratios to be found during waking and sleeping hours. During waking, the LF/HF ratio showed that IUGR children whose mothers did or did not smoke parent during pregnancy have elevated levels (2.67, 2.90) respectively, compared to the normal groups (2.23, 2.19) during waking. During sleep the LF/HF ratio was (0.70, 0.80) for IUGR, and (0.52, 0.53) for normal children. Among children whose mothers smoked during pregnancy, the Poincaré plot analysis of long-term variability during sleep found less long term HRV in IGUR (SD2=148.53ms) than in healthy children (SD2=182.87ms, p=0.02). Poincaré plot testing suggested that asthmatic children were consistently returning different results compared to the other children in their groupings. Following this, a Poincaré plot analysis was employed from which significantly lower short-term variability was found for IUGR asthmatic children whose mothers smoked. It is suggested that smoking during pregnancy can have adverse implications for the development of autonomic nervous system of the IUGR child.

PB3

QRS Morphological Analysis using a Two-Layered Self-Organizing Map for Heartbeat Classification

Mutsuo Kaneko*, Fumiaki Iseri, Takafumi Gotoh, Hidehiro Ohki, Naomichi Sueda and Tatsuya Yoneyama

R&D center, Fukuda Denshi Co, Ltd, Tokyo, Japan

Purpose: QRS complex classification in Holter electrocardiogram have been developed using the correlation coefficient methods. However, the accuracy of this traditional classification is not fully satisfied the clinical needs. In this paper, we propose an application of a two-layered self -organizing map (SOM) to classify QRS complexes to improve the accuracy. Methods: Our two-layered classification is performed in a slice SOM classification layer and a beat SOM one successively. First, each beats is divided in 10 sections. The characteristics of the section (slice wave) are calculated. An average level, height, amplitude of a peak, maximum slope and minimum slope are used for the characteristics. By learning these characteristics in the first SOM (slice SOM), the slice waves are classified in a qualitative attributes (flat line, up slope, down slope, mountain, valley etc). Second, QRS complexes are reconstructed as a line of the classified qualitative attributes and classified by the second SOM (beat SOM). We evaluated our method using MIT-BIH Arrhythmia Database of 17 cases 33,362 beats and compared with the accuracy of a standard cross correlation coefficient method. Five kinds of beat cords of normal, VPC, right bundle branch block, left bundle branch block and WPW are used for the comparison. We defined the error rate Er by the following equation for a qualitative result comparison,Er = Eb/Tb where Eb is the number of the classification error beats and Tb is the total number of beats. Results: The classification error rate Er in the case of the correlation coefficient method is 0.75% and proposed method is 0.41%. We confirmed that the accuracy in our method for the QRS complex analysis is significantly improved.

PB4

Robust Delineation of High-Resolution Ambulatory Holter ECG Events via False-Alarm Controlled Segmentation of a Wavelet-Based Geometrical Decision Statistic

Mohammad Reza Homaeinezhad* and Ali Ghaffari

Department of Mechanical Engineering, KN Toosi University of Technology, Tehran, Iran

In this study, a new long-duration holter electrocardiogram (ECG) major events detection-delineation algorithm is described which operates based on the false-alarm error bounded segmentation of a decision statistic with simple mathematical origin. To meet this end, after implementation of the required pre-processings, a uniform length window is slid sample to sample on the synthetic scale and in each slid, six features namely as summation of the nonlinearly amplified Hilbert transform, summation of absolute first order differentiation, summation of absolute second order differentiation, curve length, area and variance of the excerpted segment are calculated. Then all feature trends are normalized and superimposed to yield the newly defined geometric index (GI) metric for the detection and delineation of ECG events. In the next step, a -level Neyman-Pearson classifier (which is a false-alarm probability-FAP controlled tester) is implemented to detect and delineate QRS complexes. To show advantages of the presented method, it is applied to MIT-BIH Arrhythmia Database, QT Database, and T-Wave Alternans Database and as a result, the average values of sensitivity and positive predictivity Se = 99.96% and P+ = 99.96% are obtained for the detection of QRS complexes, with the average maximum delineation error of 5.7 msec, 3.8 msec and 6.1 msec for P-wave, QRS complex and T-wave, respectively.

PB4

A Wavelet-based Algorithm for Delineation and Classification of ECG Waves

Lars Johannesen*, Ulrik Silvanus Lerkevang Grove, Jens Stampe Soerensen, Mick Lykkegaard Schmidt, Jean-Philippe Couderc and Claus Graff

Health Science and Technology, Aalborg University, Aalborg, Denmark

Quantitative analysis of the electrocardiogram (ECG) requires delineation of the individual ECG waves. Fiducial points are important markers that can be used in clinical practice to guide diagnosis. We therefore propose a robust delineation algorithm to identify important onsets, offsets and peaks for the P, QRS, J, and T-wave. Furthermore, we investigated whether the identified fiducial points could be used to classify the configuration of a given wave i.e negative, positive, biphasic or absent. Annotated ECG records (n=105) of the QT database (Physionet) were used in this study and all ECG waves were classified manually according to their configuration. A quadratic spline wavelet was used to identify fiducial points. These fiducial points were subsequently used to automatically determine the configuration of the individual waves in the ECG. The difference between annotated and automatically identified points was calculated and the accuracy for correct wave configuration was determined. Classification accuracy for wave configurations were: 74% (P-wave), 94% (QRS complex) and 82% (T-wave). The average difference between manual and automatic delineation of the P-wave (onset/offset) was -5.6 ms (std. = 26.7 ms). For points involved in the QRS complex this difference was -1.2 ms (12.2 ms) on average. The difference between automatic and annotated T-wave (peak and offset) was 1.8 ms (32.5 ms). We have shown that it was possible to use automatically identified fiducial points for classification of wave configurations. This technique may potentially be used to assist clinicians in identifying abnormal beat configurations in long term Holter recordings.

PB4

Predicting Effectiveness of Cardiac Resynchronization Therapy Based on the Analysis of QRS Components using the Meyer Orthogonal Wavelet Transformation

Xiaojuan Xia*, Jean-Philippe Couderc, Scott McNitt, and Wojciech Zareba

University of Rochester, Rochester, NY, United States

Introduction: Cardiac Resynchronization Therapy (CRT) has shown clinical benefit for patients with heart failure. However, 20% to 30% of patients do not response to CRT. We investigated whether QRS morphology of cardiac patients prior to CRT could predict the level of response of patients to CRT. We used data from the MADIT-CRT study and developed a method to decompose time-frequency features of the QRS complex to identify characteristics common to CRT responders and non-responders.

Methods: The study evaluated 12-lead ECG recordings obtained from Fifty-eight CRT recipients (mean age = 65 $\pm$ 11 years, 41 male and 17 female) with left bundle branch block (LBBB) before CRT. The digital ECGs had 1000 Hz sampling frequency and 16-bit amplitude resolution. We developed a signal averaging algorithm to produce a representative of QRS complex (avQRS), the number of cardiac beats used for the avQRS was set in order to reach a noise level of 0.5 microvolt. Then, a Meyer orthogonal wavelet transformation was applied on the avQRS signal Thirty-four wavelet coefficients located inside the QRS were analyzed corresponding to time frequency range equal to 8-125 Hz from the onset of the QRS to 150 ms after. We compared the distribution of energies across the transformation between the two groups to identified time-frequency cells discriminating responder from non-responder to CRT.

Results: Nonparametric two-sample tests were performed on the measured thirty-four coefficients from each of three Frank orthogonal leads. The tests showed that two coefficients from lead X and three coefficients from lead Z were significantly different ($P < 0.05$) between responder and non-responder. No coefficient from lead Y shows significantly different. Receiver Operating Characteristic (ROC) curve analysis of these coefficients analysis of these parameters provided levels of sensitivity and specificity equal to 64%-72% in lead X and 64%-73% in lead Z, respectively. The level of sensitivity and specificity using QRS duration was 59% and 47%.

Discussion/conclusion: We studied the baseline surface ECG in LBBB patients with narrow QRS interval (QRS $<$ 150 ms before CRT). The time-frequency analysis of the surface ECG permitted to distinguish the CRT responder and non-responder.

PB4

Automatic Electrocardiogram Delineator Based on the Phasor Transform of Single Lead Recordings

Arturo Martínez*, Raúl Alcaraz and José Joaquín Rieta

Innovation in Bioengineering Research Group, University of Castilla-La Mancha, Cuenca, Spain

The surface electrocardiogram (ECG) provides a widely used and comfortable way to study the heart function, being a conventional tool for the diagnosis of cardiac diseases. Given that most of the clinically useful information in the ECG is found within the intervals and amplitudes determined by its fiducial points, the development of accurate and robust methods for automatic ECG delineation is a very interesting challenge. The present work introduces a new ECG delineator which is able to operate in single lead recordings, based on the Phasor Transform, which is characterized by its robustness, low computational cost and mathematical simplicity.

The method converts each instantaneous ECG sample into a phasor, thus being able to deal very precisely with P and T waves, which are of notably lower amplitude than the QRS complex. Initially, the method relies on the detection of R peaks and, next, onset and offset of the QRS complex are identified. Finally, taking the QRS as a reference, P and T waves are detected and delineated.

This delineator was validated with the QT database, which is available in Physionet, providing average values of sensitivity higher than 98.60% for the detection of all the significant ECG waves and fiducial points. Concretely, sensitivity for the P wave was 98.65% for the onset, peak and offset. The QRS onset and end achieved a sensitivity of 99.85% and, finally, the T wave provided a sensitivity of 99.20% both for its peak and offset. Additionally, the average maximum time delineation error was lower than 6 ms and its standard deviation was in agreement with the accepted tolerances for expert physicians in the onset and offset identification for QRS, P and T waves. As a consequence, this new algorithm is able to achieve a performance similar to the top rated ECG delineators, but with notably lower computational cost.

PB4

An Efficient Approach for Heartbeat Classification

Stevan Jokić, Srd;an Krčo, Dejan Sakač, Zoran Lukić, Vlado Delic and Tatjana Loncar Turukalo*

Faculty of Technical Sciences, Novi Sad, Serbia

In this paper an efficient heart beat classification algorithm for mobile devices is presented. A simplified ECG model is used for feature extraction in the time domain. QRS complex is modeled by two straight lines while P and T waves are modeled by parabolas. The T wave asymmetry is achieved using a fourth degree parabola, whereas the P wave is modeled by the second degree parabola. The model parameters are estimated by minimizing the root mean square (RMS) of the model error. Heart beats are classified as one of the following: normal (N), supraventricular (S) and ventricular (V) ectopic beats. Classification of model parameters is done using a feed-forward neural network. The inputs used by the classifier are: QRS slopes and duration, P wave coefficients, adjacent and averaged RR intervals. Patient specific adaptation is achieved using a dominant heart beat as an additional classifier input. A series of tests have been performed to evaluate the classification algorithm. Three model sets were used for that purpose. The first one contains QRS parameters only. The second one contains the dominant QRS model as well and in the third model set the P wave and appropriate dominant P wave model are included. Training and testing is done using the MIT-BIH arrhythmia database ECG signals subset and expressed in sensitivity (Se), specificity (Sp) and accuracy (Acc). It can be concluded that the best results are achieved when applying the classification algorithm on the third model set. The following results were obtained: SeN = 0.9915, SpN = 0.9750, AccN = 0.9865; SeS = 0.9208, SpS = 0.9641, AccS = 0.9448; SeV = 0.9469, SpV = 0.9566; AccV = 0.9531. Additionally, the proposed algorithm has been implemented as a J2ME mobile application. It has been tested on signals recorded by a telemedicine health care system and have achieved average accuracy above 93%

PB4

Long-Duration Ambulatory Holter ECG QRS Complex Geometrical Templates Extraction by Non-Parametric Clustering of the QRS Virtual Close-up Extracted Feature Space

Mohammad Reza Homaeinezhad* and Ali Ghaffari

Department of Mechanical Engineering, KN Toosi University of Technology, Tehran, Iran

The presented study concentrates on description of the new feature extraction and clustering techniques for the QRS geometrical templates extraction. To meet this end, first the original holter ECG signal is segmented into QRS and non-QRS regions. Then, each QRS region and also its corresponding discrete wavelet transform are supposed as virtual images and each of them is divided into eight polar sectors. Next, the curve length and the polar area of each excerpted segment are calculated and are used as elements of the feature space, (therefore, for each detected QRS complex, 32 features are computed). Afterwards, applying the Principal Components Analysis (PCA), the dimension of the feature space is reduced to 2, and the joint probability density function (pdf) of the mapped features is estimated via Parzen approximation. Afterwards, using a n-dimensional adaptive smoothing method, the obtained joint pdf is smoothed as far as the number of its local maximums is reached to the desired user-defined template number. After assigning the detected peaks as the cluster centers, to estimate the border of each cluster, each center is assigned as a local search origin and in all directions, investigations are conducted to find the best minimum slope-height locations. For each boundary sample in the 2-D histogram, its corresponding QRS complex Kendall tau rank correlation coefficients with the QRS of all cluster centers are calculated and consequently each candidate border location is added to the cluster with the maximum correlation coefficient. After determination of borders, the median QRS waveform of each cluster is extracted and is assigned as the cluster template. The method was applied to DAY general hospital high resolution holter data (more than 1,500,000 beats including BBB, PVC and Junctional contractions) and average values of Se=99.87% and P+=99.84% are obtained for QRS waveshape classification.

PB4

A Fast and Robust Time-Series Based Decision Rule for Identification of Atrial Fibrillation Arrhythmic Patterns in the ECG

Omar Jacinto Escalona* and Mauricio Enrique Reina

NIBEC, CACR, University of Ulster, Newtownabbey, Antrim, United Kingdom

Atrial fibrillation (AF) is a pathologic arrhythmic behaviour of the heart which occurs when the myocardium of the atrial chambers enter into a sustained chaotic and fractionated muscular contraction dynamic. AF is the major contributor to strokes in the elderly and nearly 34% of the hospitalizations by arrhythmias are AF. Reliable detection of AF episodes in long term ECG monitoring devices, such as in implantable cardioverters, is required for early treatment and health risks reduction. Methods: A decision rule for identifying AF arrhythmic patterns was derived from RR-intervals analysis of time-series generated from ECG recordings before, during and after AF episodes. Time-series elements were obtained by consecutive RR intervals time differences (deltaRR=presentRR-previousRR). The proposed decision rule used for the analysis of the deltaRR time-series consisted in two arguments to be satisfied for the identification of an AF episode. The first consisted in determining the number of deltaRR elements above 50ms absolute value within a window of 35 beats, and the first argument is satisfied if the quantity exceeds 10. Then, the second argument is operated within the same window of 35 beats which satisfied the first argument. For this, uniform dispersion of all the corresponding RR-interval elements within the window is evaluated. The latter is particularly aimed to rule out cases of type 2:1, 3:1 and 4:1 arrhythmias. Results: To assess the reliability of the AF identification scheme, two publically accessible databases were used: the MIT AF Database (N=25) and the MIT-BIH Arrhythmia Database, from which 10 non-AF ECG recordings were randomly chosen. Identification of AF using the proposed decision rule was achieved with 96% accuracy, 93% sensitivity and 97% specificity. In the computer program implementation, the processing time per ECG beat was of 129 ms. This manageable computing time requirement can enable real-time ECG processing for AF identification.

PB4

Segment Clustering for Holter Recording Analysis

Jose Luis Rodríguez-Sotelo, Diego Peluffo-Ordóñez, David Cuesta-Frau, Germán Castellanos-Domínguez and Lina Sepúlveda*

Departamento de eléctrica, electrónica y computación, UNAL, Manizales, Colombia

Holter electrocardiography (ECG) is useful to detect transitory and irregular pathologies that are hard to diagnose in short-time ECG. The problem of this test is the wide amount of information which complicates the manual inspection. For this reason, computer analysis tools have been developed and are commonly used as diagnostic support. In general, these systems work off-line taking into account several factors that affect signal quality. Then, it is necessary to process each heartbeat, to detect some specific types of heartbeats. Therefore, unsupervised classification is preferred in this approach, being clustering the most frequently used technique. In addition, processing time and unbalanced classes are other important issues to be taken into consideration.

In this work, a methodology for segment grouping is presented that reduces the computational cost and sensitivity to unbalanced classes. Proposed method includes stages for preprocessing, characterization and clustering. All these stages are developed in a sequential scheme, where similar clusters are grouped into new clusters per couple of contiguous segments taking into account exclusion and merger criteria based on dissimilarities. For unsupervised grouping, the estimation of the number groups employing spectral techniques is first performed. Next, to avoid the problem of convergence into a local minimum, JH-means and sum of squares criteria are used. Clustering stage is developed by using a general iterative model for center-based clustering with soft membership functions.

The method is assessed over a set of records from MIT/BIH arrhythmia database with different types of heartbeats recommended by the AAMI, such as, normal, ventricular extra systoles, branch bundles blocks among others. The results are assessed by means the sensitivity and specificity measures, taking advantage of the database labels. Also, unsupervised performance measures are used. Finally, the performance of the algorithm is in average 95%, improving results reported by previous works of the literature.

PB4

Optimal Delineation of Ambulatory Holter ECG Events via False-Alarm Bounded Segmentation of a Wavelet-Based Principal Component Analysis Decision Statistic

Mohammad Reza Homaeinezhad*

Department of Mechanical Engineering, KN Toosi University of Technology, Tehran, Iran

The aim of this study is to develop and describe a new ambulatory holter electrocardiogram (ECG) events detection-delineation algorithm with the major focus on the bounded false-alarm probability (FAP) segmentation of an information-optimized decision statistic. After implementation of the appropriate pre-processings, a uniform length sliding window is applied to the synthetic scale and in each slid, six feature vectors namely as summation of the nonlinearly amplified Hilbert transform, summation of absolute first order differentiation, summation of absolute second order differentiation, curve length, area and variance of the excerpted segment are calculated. Then all feature trends are normalized and utilized to construct a newly proposed principal components analyzed geometric index (PCAGI) by application of a linear orthonormal projection. In the next step, the -level Neyman-Pearson classifier (which is a FAP controlled tester) is implemented to detect and delineate QRS complexes. To show advantages of the presented method, it is applied to MIT-BIH Arrhythmia Database, QT Database, and T-Wave Alternans Database and as a result, the average values of sensitivity and positive predictivity Se = 99.96% and P+ = 99.96% are obtained for the detection of QRS complexes, with the average maximum delineation error of 5.7 msec, 3.8 msec and 6.1 msec for P-wave, QRS complex and T-wave, respectively showing marginal improvement of detection-delineation performance.

PB4

Long-Duration ECG Signal Events Detection-Delineation via Segmentation of a Wavelet-Based Independent Components Analyzed Metric

Mohammad Reza Homaeinezhad* and Ali Ghaffari

Department of Mechanical Engineering, KN Toosi University of Technology, Tehran, Iran

The aim of this study is to describe the development procedure of a new ambulatory long-duration holter electrocardiogram (ECG) events detection-delineation algorithm with the major focus on the bounded false-alarm probability (FAP) segmentation of an information-optimized decision statistic. After implementation of an appropriate pre-processing scheme, a uniform length sliding window is applied to the modified signal and in each slid, six feature vectors namely as summation of the nonlinearly amplified Hilbert transform, summation of absolute first order differentiation, summation of absolute second order differentiation, curve length, area and variance of the excerpted segment are calculated. Then all feature trends are normalized and utilized to construct a newly proposed independent components analyzed geometric index (ICAGI) by application of a blind source separation (BSS) method. The ICAGI metric is then used as decision statistic and -level Neyman-Pearson classifier (which is a FAP controlled tester) is implemented to detect and delineate QRS complexes. The presented method was applied to MIT-BIH Arrhythmia Database, QT Database, and T-Wave Alternans Database and as a result, the average values of sensitivity and positive predictivity Se = 99.97% and P+ = 99.97% were obtained for the detection of QRS complexes, with the average maximum delineation error of 5.6 msec, 3.8 msec and 6.1 msec for P-wave, QRS complex and T-wave, respectively.

PB4

Linear and Non-Linear Features for Intrapartum Cardiotocography Evaluation

Václav Chudáček*, Jiří Spilka, Petr Janků and Lenka Lhotská

Dept. of Cybernetics, CTU in Prague, Praha 6, Czech Republic

Cardiotocography (CTG), consisting of fetal heart rate (fHR) and tocographic (TOCO) measurements, is used to evaluate fetal well-being during the delivery. It provides real-time information of fetal status and allows clinicians to detect ongoing hypoxia.

In this work we tried to confront new (from the obstetricians point of view) descriptive features with day-to-day clinical praxis.

In the data preprocessing phase 20-minute segments preceding the deliveries were selected. Artifacts were removed and the fHR signal was interpolated to equidistant 4Hz sampling frequency.

Final data set consisted of 476 recordings each annotated by three expert obstetricians into FIGO-like categories: normal; suspect and pathological.

Then linear and nonlinear features were computed. Many of these features are known in the field of HRV processing, but completely unknown in obstetrics and their benefits there has yet to be proven. The linear features computed were: description of the fHR baseline using mean, median and SD measures, SDNN, RMSSD, mean of RR interval, and NN50 from the time domain. The non-linear features computed were: Fractal dimension of attractor, fractal dimension of waveform, entropy, and complexity. The particular methods used to compute the features were: correlation method for estimation of attractor dimension; Higuchi's, variance, and box counting method for estimation of waveform fractal dimension; approximate and sample method for estimation of entropy and the Lempel Ziv Complexity.

Two fold evaluation of the features was employed. All features were investigated for their informational gain and feature selection was performed resulting into several sets of features. These feature sets were used for data classification using decision tree algorithm.

Promising new features were identifyied: baseline standard deviation; sample entropy and Higuchi's fractal dimension. Features useful for everyday use in the obstetrician wards since our classification mehtod outperformed the FIGO guidelines classifier while matching expert panel interobserver variability.

PB4

Hidden Markov Tree-based Arrhythmia Classification

Samar Krimi, Kaïs Ouni* and Noureddine Ellouze

LSTS, ENIT, Tunis, Tunisia

The electrocardiogram (ECG) is the recording of the electrical property of the heartbeats. Several approaches that automatically classify heartbeats have been proposed in the literature using a variety of features to represent the ECG. This paper aims at providing new insights on the electrocardiogram classification problem through an original concept of combining Hidden Markov Tree (HMT) model with the (HTK) recognition toolkit. This HMT recognition framework is based on different parameters like Morphological Descriptors (MD), Higher Order Cumulants (HOC) and Synchronous Wavelet Transform Energy (SWTE) which is a new parameterisation technique. The assessment of performances is achieved using the benchmark public QT database from Physionet that makes a cross validation method: the training stage (10mn) about 2/3 of the data and the test stage (5mn) about the last 1/3.

The recognition results of 8 arrhythmia classes extracted from QT database, while varying each time the states (5 to 7) and the gaussian numbers by state (2 to 5) of the HMT model are presented and discussed. For morphological descriptors (MD), every heart beat is characterized by 10-elements vector representing information of the amplitude, the area, specific interval durations and slopes. For (HOC) descriptors, every heart beat is characterized by 15-elements vector, five for each cumulant (the second, the third and the fourth order cumulants) and finally 8-elements vector for the (SWTE) descriptors in the fourth scale with a first derivative gaussian wavelet having a standard deviation =0,25. To evaluate the performance of the classifier, a comparative study of recognition rates in terms of average sensitivity (SE) and average specificity (SP) and other statistical indices are used. These indices obtained with morphological descriptors for our recognition system having 6 states and 4 gaussians per state were a sensitivity (SE) of 94,95%, a specificity (SP) about 98,65%. By using higher order cumulants, we obtained a sensitivity (SE) of 97,22% and a specificity (SP) about 99,12% with the same model having 5 states and 3 gaussians per state. Synchronous wavelet transform energy allows a sensitivity (SE) of 95,20% and a specificity (SP) of 99,03% for a HMT model having 6 states and 3 gaussians per state.

PB4

P Wave Delineation using Spatially Projected Leads from Wavelet Transform Loops

Rute Almeida, Juan Pablo Martínez, Ana Paula Rocha and Pablo Laguna*

University of Zaragoza, Zaragoza, Spain

The visible P wave boundaries vary with the considered lead (view point) in spite of the atrial depolarization onset/end being a unique/global features. In [Almeida et al, IEEE TBME 56(8)] we have proposed an automatic delineation strategy for multilead (ML) location of wave boundaries which provides a unique lead independent mark. A transformed lead is obtained from VCG loops, by projecting the wavelet transform (WT) spatial loop into a direction (derived lead) that optimizes the SNR and so the delineation. Single-lead based delineation (SL) is then applied to the synthesized lead, providing unique locations for wave boundaries. The system was implemented and validated regarding QRS complex and T wave. In this work the methodology was extended to P wave boundaries. The Sensitivity (Se), mean (m) and standard deviation (s) of errors in P wave onset and end locations were evaluated over the CSE database (CSEDB, 27 annotated P waves, 12 standard and 3 Frank leads) using spatial loops defined by the Frank leads (F) and by the leads derived by inverse Dower transformation (D). Results were compared with SL over each lead available and with the global marks obtained by post-processing rules (SLR). 2-dimentional loops were also considered as subsets from F and D to quantify the performance loss. The 2D approach was applied over QT database files (QTDB, 2983 annotated P waves, 2 leads) and Se, average across files of the delineation errors mean (m) and deviation (s) were calculated. [Se%, m—s (ms)] of [100,-7.9—19.3]/[96,3.1—15.8] were obtained for onset/end, respectively, using F; [96,-2.8—11.0]/[93,5.2—8.2] using D, while SLR achieved [85,3.0—5.3]/[89,1.8—6.7]. None of the s values for SL results was, both for onset and end, lower than using D. Moreover, using just X and Y leads (2D) [100,-6.8—18.8]/[96,2.5—15.8] were obtained for F and [100,-2.1—7.4]/[100,5.9—6.9] for D. Regarding QTDB the results obtained were [94, 6.15—22.3]/[94, 4.59—17.45]: a higher Se and lower s than in any of the two leads itself with SL. Thus, we can conclude that ML strategy is appropriated for P wave delineation; D allows achieving lower s than SL result, with higher Se that SLR, and 2D loops were enough, allowing a more efficient processing when compared to SLR.

PB4

BEATS: An Interactive Research Oriented ECG Marker System

S Man*, AC Maan, EE van der Wall, MJ Schalij and CA Swenne

Dept. of Cardiology, Leiden University Medical Center, Leiden, Netherlands

We have developed BEATS (Beat Editing And T-wave marker Software) using MATLAB. The purpose of BEATS is to detect QRS complexes and interactively mark features of the ECG at different heart rates. BEATS will accept 8-channel ASCII data ECG recordings (leads I, II, V1-V6) of any length. A corresponding Vector Cardiogram (VCG) is computed from the ASCII data by matrix multiplication. Beats are detected from the spatial velocity by means of a user-adjustable threshold. Noise can be rejected, missed beats can be inserted and incorrectly detected fiducial points can be adjusted. The VCG is displayed using X, Y and Z leads. Also, spatial velocity, vector magnitude and the first derivative thereof can be displayed. Since recordings can show a wide range of heart rates, initial guesses for a number of markers are made: the user has to mark at least 5 isoelectric points (IEP) at different heart rates. The intervals between these markers and their corresponding fiducial points are used to calculate, by interpolation, all IEPs in the recording. These IEPs are used as anchor points for a linear baseline correction. The user then marks onset and end of the QRS complex and the T apex at different heart rates to globally calculate these values for each beat. Each individual T apex is calculated by a 2nd degree polynomial fit, T end is calculated as the intersection of the tangent to the steepest slope and the isoelectric line. Any outliers in heart rate, QT interval and all other markers are flagged to facilitate easy checking and editing. BEATS generates files with all estimated and calculated markers with respect to their fiducial points and the baseline corrected ECG. After a one-time carefully processing of the recordings, other programs can run unattended to extract features like T-Wave alternans in exercise tests.

PB4

Radial Basis Function Networks Applied to QRST Cancellation in Atrial Fibrillation Recordings

Jorge Mateo, Ana Torres, César Sánchez and José Joaquín Rieta*

Innovation in Bioengineering Research Group, University of Castilla-La Mancha, Cuenca, Spain

Atrial fibrillation (AF) is the most common type of human cardiac arrhythmia. Due to the much higher amplitude of the electrical ventricular activity (VA) on the surface ECG, cancellation of the ventricular involvement is crucial in the study of AF from the ECG. Two approaches are generally used to perform this task: source separation algorithms and average template subtraction. Source separation algorithms try to find uncorrelated components using a principal component analysis (PCA), or to find independent components in an instantaneous linear mixture using an independent component analysis (ICA). On the other hand, the methods based on average beat subtraction (ABS) obtain a median template that is then used to subtract the VA. In this contribution, a QRST cancellation method using a radial basis function (RBF) network is proposed. This RBF network has been developed like a hierarchically layered structure. It starts with a small number of RBFs and then adds new RBFs if the approximation error is larger than some predetermined threshold and there is no existing RBF that can efficiently represent the current input. The adaptation strategy for the weight matrix of the RBF network is developed using the Lyapunov approach. This proposed approximation strategy guarantees uniform ultimate boundedness of the approximation error, which is proved using the second Lyapunov method. The cancellation system has been developed using Gaussian RBF (GRBF) and the outcomes compared with ICA-based methods and ABS techniques using cross correlation (CC), mean square error (MSE), ventricular depolarization reduction (VDR) and similarity the similarity index(S). Both real and synthetic signals have been used to reach a total amount of 400 recordings in the study. Average Results for the RBF method applied to the synthetic signals are (mean$\pm$std) CC=0.95$\pm$0.021 and MSE=0.356$\pm$0.102 in contrast to the previous published methods that, for the best case, yielded CC=0.86$\pm$0.031 and MSE=0.491$\pm$0.213. For real signals VDR and S obtained for RBF were VDR=7.01$\pm$2.23 and S=99,39%$\pm$0.33, and the classical techniques provided, in the best case, VDR=4.23$\pm$3.02 and S=92,23%$\pm$0.44. The results prove that RBF based methods are able to obtain a very accurate reduction of VA, thus providing high quality atrial activity extraction in AF recordings.

PB5

Ectopic Beats Canceler for Improved Atrial Activity Extraction from Holter Recordings of Atrial Fibrillation

Arturo Martínez*, Raúl Alcaraz and José Joaquín Rieta

Innovation in Bioengineering Research Group, University of Castilla-La Mancha, Cuenca, Spain

Ectopic beats are a frequent and challenging problem in atrial fibrillation (AF) long time monitoring that still is unsolved. Moreover, they provoke important ventricular residua in the atrial activity (AA) signal when methods based on average QRST cancellation are used for its extraction from the ECG. In this work, a new method for ectopic removal in a template-based cancellation technique is proposed.

The first step consists in distinguishing between normal and ectopic beats through a forward/backward level windowing strategy. Next, for each ectopic under cancellation, the most similar 15 ectopic beats are clustered by using an adaptive correlation index, which provides a robust and efficient measure of morphological similarity among signals than Pearson correlation. Next, the eigenvector matrix of the selected beats is obtained by singular value decomposition (SVD). Finally, the highest variance eigenvector (HVE) is considered as the ventricular template for the ectopic beat cancellation.

In order to evaluate the proposed methods performance, an index called reduction ectopic rate (RER) was defined. Concretely, this index was obtained by computing the root mean square value of the ratio between each ectopic in the original ECG and its residue in the AA signal after ectopic cancellation. Through this metric, the proposed technique was compared with a previously published average QRST cancellation technique, in which ventricular template was also generated by applying SVD to normal beats. Twenty 5 hour-length segments extracted from Holter ECG recordings of 20 different AF patients, with a high percentage of ectopic beats, were used for the comparison. Results for the proposed ectopic cancellation provided maximum RER values of 5.76 and minimum of 1.67 being, in average, of 3.57 ± 0.25. In contrast, when ectopic beats were considered as normal beats, maximum RER was 1.49 and minimum 0.88, being in average 1.11 ± 0.25. As a consequence, the proposed ventricular ectopic cancellation method is able to improve notably the AA extraction from Holter ECG recordings by reducing notably the residua provoked by the presence of ectopic beats.

PB5

Simulation of Monitoring Strategies for Atrial Fibrillation Detection

Federica Censi*, Giovanni Calcagnini, Eugenio Mattei, Michele Triventi and Pietro Bartolini

Dept Technologies and Health, Italian National Institute of Health, Italy

Paroxysmal atrial fibrillation (PAF) is a difficult disorder to investigate because of its intermittent and sometimes asymptomatic nature. The monitoring strategies usually adopted for a PAF patient include sporadic ambulatory ECG control, transtelephonic monitoring, event monitor, sporadic 24h Holter, 7-days Holter. Given the intermittent nature of both arr-hythmic events and current monitoring methods, the ability of monitoring strategy to diagnose PAF is highly dependent on whether or not the moment selected for monitoring coincides with the occurrence of PAF episodes. The aim of this study was to simulate several daily ECG monitoring strategies applied on data reporting date, time and duration of mode switch episodes, extracted from Burden II Study (patients implanted with pacemaker for Brady-Tachy Syndrome). Starting from this database of 98 patients, daily monitoring strategies were simulated by varying the hour of beginning and the duration of each daily recording, and the number of monitoring con-secutive days. The first important result is that the number of detected pa-tients varies depending on the hour of the day when the monitoring starts, with peaks in the morning (9-10 A.M.). The lowest number of detected pa-tients is obtained at late evening (10-11 P.M.). We found that an optimized 2-hour monitoring for 60 consecutive days can detect almost 60% of patients experiencing PAF episodes in the observational period; when performed on 30 consecutive days the percentage of detected patients de-creases to about 48%. A shorter monitoring (half-an-hour) allows to detect up to 35% (for 60 consecutive days). One-day and 7-days Holter monitoring turned out to detect about 10% and 35% of patients with AF episodes, respectively. The number of detected patients from our database could be an underestimation of the potential detectable patients from a real population, given the limited number of logged AF episodes on pacemaker memory. In conclusion, these results represent an important indication for the optimization of ECG daily monitoring for PAF or post-ablated patients.

PB5

Organization Analysis of Atrial Fibrillation Applied to the Improvement of Electrical Cardioversion Protocols

Raúl Alcaraz, Fernando Hornero and José Joaquín Rieta*

Innovation in Bioengineering Research Group, University of Castilla-La Mancha, Cuenca, Spain

The development of non-invasive tools able to provide valuable information about the effectiveness of a shock in external electrical cardioversion (ECV) is clinically relevant to enhance these protocols in the treatment of atrial fibrillation (AF). The present contribution analyzes the ability of a non-linear regularity index, such as sample entropy (SampEn), to follow-up noninvasively AF organization under successive attempts of ECV and to predict the effectiveness of every single shock.

To this respect, the atrial activity (AA) preceding each delivered shock was extracted by using a QRST cancellation method. Next, the main atrial wave (MAW), which can be considered as the fundamental waveform associated to the AA, was obtained by applying a selective filtering centered on the dominant atrial frequency (DAF). Finally, the MAW organization was estimated with SampEn and two thresholds (Th1=0.1223 and Th2=0.0832) were established to predict the ECV outcome.

Results indicated that, prior to the first attempt, all the patients who only needed one shock to restore normal sinus rhythm (NSR) were below Th1. In addition, most of them were above Th2 in case of AF relapsing during the first month. Regarding several shocks, all the patients who maintained NSR more than one month were below Th2 after the first shock. Moreover, all the patients who relapsed to AF during the first month were between Th1 and Th2 and, finally, all the patients with ineffective ECV were above Th1. After each unsuccessful shock, a SampEn relative decrease was observed for the patients who finally reverted to NSR, but the largest variation took place after the first attempt, thus indicating that this shock plays the most important role in the procedure. Indeed, by considering jointly the patients who needed only one shock and the patients who needed several shocks, 91.67% (22 out of 24) of ECVs resulting in NSR, 93.55% (29 out of 31) of ECVs relapsing to AF during the first month and 100% (10 out of 10) of ECVs in which NSR was not restored were correctly classified. As conclusion, the MAW organization analysis via SampEn could provide useful information that could improve the effectiveness of conventional external ECV protocols used in AF treatment.

PB5

Study of Sample Entropy Ideal Computational Parameters in the Estimation of Atrial Fibrillation Organization from the ECG

Raúl Alcaraz, Daniel Abásolo, Roberto Hornero and José Joaquín Rieta*

University of Castilla-La Mancha, Cuenca, Spain

Sample Entropy (SampEn) is a nonlinear regularity index that requires the a priori selection of three parameters: the length of the sequences to be compared, m, the patterns similarity tolerance, r, and the number of samples under analysis, N. Given that no guidelines exist for the selection of that values, a thorough analysis on the optimal values for m, r and N is presented within the context of noninvasive atrial fibrillation (AF) organization estimation. Recently, the evaluation of AF organization, through SampEn, has revealed clinically useful information that could be used for a better treatment of this arrhythmia. This work analyzes optimal SampEn parameters within two scenarios, such as the prediction of paroxysmal AF termination and the electrical cardioversion outcome in persistent AF.

As a result, recommendations about the selection of m, r and N, together with the relationship between N and the sampling rate (fs) will be given. More precisely, (i) the proportion between N and fs should be higher than one second and fs higher than 256 Hz, (ii) overlapping between adjacent N-length windows does not improve organization estimation and (iii) values of m and r maximizing classification should be considered within a range wider than the proposed in the literature for heart rate analysis, i. e. m = 1 and m = 2 and r between 0.1 and 0.25 times the standard deviation of the data. Thus, for paroxysmal AF, the maximum accuracy was 96%, which was obtained with m=3 and r=0.4 (p=3.4567*e-13) for fs=256Hz and m=2 and r=0.35 (p=4.2134e-13) for fs=1024Hz, respectively. Regarding persistent AF, maximum accuracy of 82.54% was achieved for fs=256Hz, m=3 and r=0.3 (p=5.2483e-3) and, for fs=1024 Hz, with the pairs m=2 and r=0.4 (p=9.3892e-4) and m=3 and r=0.25 (p=8.7756e-4), respectively. Finally, both the methodology and the outcomes provided by this study could serve, not only in AF studies, but also as a startup framework in the application of SampEn to other biomedical signal processing scenarios.

PB5

Sensitivity of T-Wave Alternans Identification Algorithms to Residual Physiological Noise Affecting the ECG after Preprocessing

Silvia Bini*, Laura Burattini and Roberto Burattini

Department of Biomedical, Electronics and Telecommunication Engineering, Polytechnic University of Marche, Ancona, Italy

Residual physiological noise is likely to survive the ECG preprocessing-stage providing the input to T-wave alternans (TWA) identification algorithms. To address the issue as to how and at what extent this residual noise affects TWA detection and quantification, a test was performed here on three different methods known in literature as fast-Fourier-transform spectral method (FFTSM), modified-moving-average method (MMAM), and adaptive-match-filter method (AMFM). These techniques were applied to four synthetic ECG tracings respectively affected by no TWA, stationary TWA, and time-varying TWA characterized by either smoothed-step or sinusoidal trend. These synthetic ECGs were considered in the absence of noise or after adding each one of the six recordings of electrode-motion noise, muscular noise and baseline wandering, belonging to the MIT-BIH noise stress test database (PhysioNet), with normalized maximum amplitude of 50 V or 100 V. In the absence of noise, all three competing methods did not provide false-positive TWA when applied to no-TWA tracings. Stationary TWA was detected and quantified with no error, while, in the presence of time-varying TWA, the FFTSM, the MMAM and the AMFM quantified TWA amplitude with maximum root-mean-square-error (RMSE) of 9 V, 7 V and 3 V, respectively. In the presence of the two considered noise levels, the FFTSM provided the same output as in the absence of noise. Instead, the MAMM and the AMFM quantified TWA with increased RMSE (up to 12 V and 5 V, respectively), and detected false-positive TWA cases in all twelve and one no-TWA tracings, respectively. In conclusion, the FFTSM is robust to noise but has an intrinsic limitation in the precision of TWA quantification in the presence of time-varying TWA. Noise significantly affects the behavior of the MMAM, while the AMFM offers a good compromise between robustness to noise and ability to identify both stationary and time-varying TWA.

PB6

Signal Processing Subsystem Validation for T wave Alternans Estimation

Rebeca Goya-Esteban, Inmaculada Mora-Jiménez*, Manuel Blanco-Velasco, Óscar Barquero-Pérez, Antonio Caamaño-Fernandez, Arcadi García-Alverola and José Luis Rojo-Álvarez

Signal Theory and Communications Department, Rey Juan Carlos University, Madrid, Spain, Fuenlabrada, Madrid, Spain

Background. A number of methods have been proposed to estimate microvolt T-Wave Alternans (TWA), which typically include several ECG processing subsystems. However, there is no systematic procedure for analyzing the robustness of each whole estimation system in terms of these processing subsystems, hence making the standarization difficult.

Methods. We used a basic TWA estimation temporal system to study the effect of some relevant preprocessing subsystems. The subsystem inclusion and its parameters tuning were analyzed. TWA episodes were included in real ECG signals by adding an alternan waveform with different patterns, namely, in the 0%, 10%, 50%, and 100% of the signal. Additional and different noise sources were also added to the signals. In each experiment, two estimation systems were evaluated, which were different in just one preprocessing characteristic. We randomly obtained 50 semi-synthetic signals, and for each one, the TWA amplitude and area estimation errors were computed. To evaluate the differences between each pair of systems, different statistics (mean M, power P, and others) were obtained, and their increase (dM, dP; Mean [95% Interval Confidence]) was evaluated with bootstrap resampling.

Results. (a) Baseline cancellation subsystem: for noise-free signals, when this subsystem was not included, TWA estimation improved sigificantly, dM = 0.76[0.46,1.06], dP = 22.88[15.50,30.43]; for SNR=25 dB, estimation improved, dM = 0.80[0.15,1.46], dP = 29.97[7.24,52.66]; and for SNR=15 dB, estimation performance decreased dM = -0.01 [-0.02,-0.002], dP = -0.01 [-0.03,-0.003]. Including this subsystem, the use of a median filter, instead of a mean filter, significantly improved the estimation. Different filter window lengths (T) were tested, obtaining significantly better results with T=1500 ms. (b) High frequency noise filter subsystem: for noise-free signals, when this subsystem was not included, TWA estimation improved, dM = 1.86[0.78,2.94], dP = 55.11[27.22,83.92]; however, for SNR=25 dB, estimation did not improve, dM=1.55[-2.18,5.69], dP = 152.40[-50.10,382.21]; and for SNR=15 dB, estimation performance decreased dM = -25.16[-32.67,-18.70], dP = -2154.2[-3037.8,-1417.3].

PB6

T Wave and QRS Complex Alternans During Standard Diagnostic Stress ECG Test

Ivaylo Christov*, Giovanni Bortolan, Iana Simova and Tzvetana Katova

Centre of Biomedical Engineering, Bulgarian Academy of Sciences, Sofia, Bulgaria

Background: T wave and QRS complex alternans (TWA&QRSA) is an electrophysiological phenomenon associated with the change in the shape of the T wave and QRS complex, appearing in alternation on every other beat basis. These changes may be predictors of complex ventricular arrhythmias and sudden cardiac death. The objective of the present work is to study the presence of wave alternans during standard diagnostic stress ECG test. Methods: Principal component analysis, and wave amplitude computation on a combined lead, were used for TWA&QRSA quantification. The method successfully participated in the Physionet/CinC Challenge 2008. Global (entire record) and local intervals (64 RR) were used in combination for the detection of TWA&QRSA. Wave Alternans index was obtained (range from 0 to 4), and 3 classes were defined: negative (<2), borderline (2) and positive (>2). 44 patients (age of 63 $\pm$ 12 years, 21 male, 8 with a history of myocardial infarction, 2 with a history of ventricular tachycardia) have been considered for this study. Angiographically significant coronary artery disease (AS_CAD) was found in 17 patients. Digital 12-lead electrocardiograms (ECG) were acquired during stress ECG test using veloergometer (GE Marquette Stress PC ECG Application Version 4.312, Medset Medizintechnik GmbH) 2-min stages 25W incremental workload. Results: Stress ECG test was positive (evidence of inducible myocardial ischemia) in 16 patients (36%). Positive TWA was found in 7 patients (6 male, age 62 $\pm$ 10 years) and negative in 10 (3 male, age 67 $\pm$ 13 years). Positive QRSA was found in 4 patients (3 male, age 63 $\pm$ 3 years) and negative in 23 (11 male, age 66 $\pm$ 11 years). Patients with positive stress ECG test had significantly higher TWA&QRSA compared to patients with negative stress test (2.4 $\pm$ 0.6 and 1.7 $\pm$ 0.6, $p < 0.001$ for TWA and 1.8 $\pm$ 0.8 and 1.2 $\pm$ 0.9, $p = 0.03$ for QRSA). Patients with AS_CAD (50% stenosis of at least 1 epicardial coronary artery) had significantly higher TWA values compared to patients without such disease (2.22 and 1.77, $p = 0.037$); Conclusions: Both TWA&QRSA indices show statistical significant difference in patients with positive/negative stress ECG test, and TWA index in patients with/without AS_CAD.

PB6

T-Wave Alternans Quantification: Which Information from Different Methods?

Laura Burattini*, Silvia Bini and Roberto Burattini

Department of Biomedical, Electronics and Telecommunication Engineering, Polytechnic University of Marche, Ancona, Italy

Several computerized methods have been proposed in the literature for detection and quantification of T-wave alternans (TWA), an ECG phenomenon consisting of every-other-beat changes in the T-wave morphology. In the absence of a standardized quantitative definition of TWA, a question arises about the quantitative information provided by each TWA identification method. In the effort to identify differences in TWA quantification, three methods were considered in the present study, namely, the fast-Fourier-transform spectral method (FFTSM), the modified-moving-average method (MMAM), and our heart-rate adaptive match filter method (AMFM). These techniques were applied to two synthetic ECG tracings affected by stationary TWA having: 1) a triangular profile (TRI_TWA), characterized by an alternans mostly localized around the T-wave apex, with T-waves maximum-amplitude difference (AMAX) of 100 V and mean-amplitude difference (AMEAN) of 50 V; and 2) a uniform profile (UNI_TWA), characterized an alternans uniformly distributed over the T waves, with AMAX= AMEAN=100 V. When analyzing TRI_TWA, TWA quantification by the FFTSM, the MMAM, and the AMFM was 57 V, 100 V, and 50 V, respectively. Instead, when analyzing UNI_TWA, all three methods provided 100 V TWA amplitude. Comparing these estimates with the simulated values of AMAX and AMEAN, we can infer that the FFTSM and the AMFM provide TWA quantification in terms of AMEAN, while the MMAM provides AMAX. Thus, an equivalent quantification of TWA amplitude can be expected from the three different methods only in the presence of the ideal case of uniformly distributed TWA. In more realistic conditions, like the one simulated here by a triangular profile, quantification more properly related to mean TWA amplitude is provided by the FFTSM and the AMFM, whereas maximum amplitude information is provided by the MMAM. These differences in TWA quantification have to be taken into account for objective comparison of TWA identification methods.

PB6

Assessment of Autonomic Cardiac Control in Women with Cardiac Syndrome X using Time Related Autonomic Balance Indicator

Mikhail Matveev, Svetlin Tsonev*, Rada Prokopova and Temenuga Donova

Centre of Biomedical Engineering, BAS, Sofia, Bulgaria

In our previous studies we indicated that the various CVD have a different circadian profile of heart autonomic balance (HAB), compared to the profile in healthy subjects. In this study we analyze the specific abnormalities in HAB circadian changes in patients with cardiac syndrome X (CSX). The study comprised of 26 women (mean age 55.3±9.5) with CSX and 22 healthy women (45.8±10.9). All patients are with fulfilled criteria for CSX at the period of pre- or postmenopause and with c̈learc̈oronary arteries verified from angiography or multi-slice CT. Stratification by risk factors, comorbidity and pharmacological management have been done using a standardized protocol. The HAB changes were assessed by HRV indices from ECG recordings in resting state (RS) and by parasympathetic (Valsalva manoeuvre; VM), or sympathetic (handgrip test; HT) stimulation. In Computers in Cardiology 2003:30 we proposed the Time Related Autonomic Balance Indicator (TRABI) a non-parametric criterion for estimating the changes in HAB by any HRV indices. In this study, TRABI was used for evaluation of the specific changes in HAB in the women with CSX. The mean value of TRABI for the HRV indices in the study in RS versus HT in healthy subjects is 0,103; in patients with CSX is 0.059 ($p = 0.062$; n.s.). The mean value of TRABI in the study in RS versus VM in healthy women is 0,167; in patients with CSX is 0.072 ($p = 0.049$) see Fig. 1 and Fig. 2. The results indicated that: i) both components in HAB are suppressed in women with CSX; ii) the parasympathetic circadian characteristic is more decreased from the sympathetic one; iii) although the autonomic cardiac control has suppressed activity circadian profile of HAB in women with CSX is similar to profile in healthy women.

PB7

Discrete Wavelet-Aided Delineation of PCG Signal Events via Analysis of an Area Curve Length-Based Decision Statistic

Mohammad Reza Homaeinezhad* and Ali Ghaffari

Department of Mechanical Engineering, KN Toosi University of Technology, Tehran, Iran

The aim of this study is to describe a new false-alarm probability (FAP) bounded unified framework for segmentation of the phonocardiogram (PCG) signal sounds registered by an electronic stethoscope board. To meet this end, first the original PCG signal is pre-processed by application of an appropriate bandpass finite-duration impulse response (FIR) filter and then by implementation of a trous discrete wavelet transform (DWT) to the filtered signal for extracting several dyadic scales. Then, after choosing a proper scale, a fixed sample size sliding window is moved on the selected scale and in each slid, the area under the excerpted segment is multiplied by its curve-length to generate the Area Curve Length (ACL) metric to be used as the segmentation decision statistic (DS). Next, using an adaptive smoothing filter (ASF), the obtained metric is modulated and is freed from the fast fluctuations occurring in the vicinity of the events onset and offset locations which consequently results enhancement of edges detection accuracy. Afterwards, histogram parameters of the filtered DS metric are used to regulate the -level Neyman-Pearson classifier for FAP-bounded delineation of the PCG events. To assess performance quality of the proposed PCG segmentation algorithm, the method was applied to all 85 records of Nursing Student Heart Sounds database (NSHSDB) including stenosis, insufficiency, regurgitation, gallop, septal defect, split sound, rumble, murmur, clicks, friction rub and snap disorders with different sampling frequencies. Also, the method was applied to the records obtained from an electronic stethoscope board designed for fulfillment of this study in the presence of high-level power-line noise and external disturbing sounds and as the results, no false positive (FP) or false negative (FN) errors were detected. High robustness against measurement noises of the electronic stethoscopes, acceptable detection-segmentation accuracy of PCG events in the presence of severe heart valvular and arrhythmic dysfunctions within a tolerable computational burden (processing time) and having no parameters dependency to the acquisition sampling frequency can be mentioned as the important merits and capabilities of the proposed ACL-based PCG events detection-segmentation algorithm.

PB7

Robust Arterial Blood Pressure Events Detection-Delineation via Segmentation of a Wavelet-Derived Stationary-Baseline Metric

Mohammad Reza Homaeinezhad* and Ali Ghaffari

Department of Mechanical Engineering, KN Toosi University of Technology, Tehran, Iran

The major focus of this study is to describe the structure of a solution designed for robustly detecting and delineating the arterial blood pressure (ABP) signal events. To meet this end, first, the original ABP signal is pre-processed by application of a trous discrete wavelet transform (DWT) for extracting several dyadic scales. Then, a fixed sample size sliding window is moved on the appropriately selected scale and in each slid, six features namely as summation of the nonlinearly amplified Hilbert transform, summation of absolute first order differentiation, summation of absolute second order differentiation, curve length, area and variance of the excerpted segment are calculated. Then, all feature trends are normalized and utilized to construct a newly proposed principal components analyzed geometric index (PCAGI) (to be used as the segmentation decision statistic (DS)) by application of a linear orthonormal projection. After application of an adaptive-nonlinear transformation for making the DS baseline stationary, the histogram parameters of the enhanced DS are used to regulate the -level Neyman-Pearson classifier for false alarm probability (FAP)-bounded delineation of the ABP events. In order to illustrate the capabilities of the presented algorithm, it was applied to all 18 subjects of the MIT-BIH Polysomnographic Database (359,000 beats) and the end-systolic and end-diastolic locations of the ABP signal as well as dicrotic notch pressure were extracted and values of sensitivity and positive predictivity Se = 99.85% and P+ = 99.96% were obtained for the detection of all ABP events.

PB7

Elimination of the Respiratory Effect on the Thoracic Impedance Signal with Whole-body Impedance Cardiography

Pavel Jurák*, Josef Halámek, Vlastimil Vondra, Ivo Viščor, Jolana Lipoldová and Martin Plachý

Institute of Scientific Instruments of the ASCR, Brno, Czech Republic

Introduction: We are presenting technology for elimination of the respiratory effect on the thoracic impedance signal and stroke volume computing beat-to-beat. We used a multichannel bioimpedance monitor to measure the impedance signal from the thorax, neck and extremities simultaneously. Thoracic impedance cardiography (TIC) is a widely-used method for noninvasive stroke volume computation. Unfortunately, breathing not only modulates systemic blood pressure, but also strongly affects the impedance signal (IS). Consequently, we measure an artificial variability. In such circumstances it is not possible to evaluate stroke volume beat-to-beat, and averaging over a larger number of heartbeats is necessary. TIC provides completely incorrect results in the case of the Valsalva or Mueller maneuver.

Methods: We used measurements with 18 simultaneously scanning impedance signal locations, each left and right: carotid artery, chest, thigh, calf, abdomen and the abdominal artery, the upper part of the chest, arm, forearm, and the chest at the level of the heart. Simultaneously with IS, we also recorded 12-lead ECG, continuous blood pressure, phonocardiography, and breathing rate and depth. We filtered IS in the pass band 0.514 Hz. We detected maxima dZ/dtmax from negative derivative IS. We obtained a time series of maxima from the thorax, neck and extremities. Elimination of breathing is based on the assumption that neck and limb IS measures only the variability in systemic blood pressure and is not affected by respiration.

Results: Mean -dZ/dtmax variability (six subjects) from thorax = 100%, neck 60, arm 57, forearm 31, thigh 64, calf 31. Respiration increases the variability of

-dZ/dtmax parameter from thorax 1.7 times in comparison with neck, forearms and thigh.

Conclusion: Whole-body IS measurements and processing reflect changes in the hemodynamic system not affected by respiration. By using retrospective reconstruction we can eliminate the influence of respiration on the impedance signal from the chest.

PB7

Estimation of Hemodynamic Parameters from Seismocardiogram

Kouhyar Tavakolian, Andrew Blaber, Brandon Ngai, Bahman Yari
Saeed Khanloo, Alireza Akhbardeh and Bozena Kaminska*

Simon Fraser University, Burnaby, BC, Canada

Biosignals such as seismocardiogram (SCG), ballistocardiogram and apexcardiogram represent the mechanical vibrations of the body as the result of heart beating and have their main components in the infrasound range. SCG, in particular, is recorded from the sternum and represents the acceleration that heart creates on the surface of the body in an axis perpendicular to it.

In this paper it is shown that SCG can be used to estimate two important hemodynamic parameters of stroke volume and left ventricular ejection duration. In this study, recordings of suprasternal pulsed Doppler and Impedance cardiogram (ICG) were used as the reference methods for comparison to the values estimated by SCG.

Simultaneous SCG and ICG and Doppler were recorded from eight male subjects between 20-30 years old. Linear regression analysis was used to estimate the stroke volume from features extracted from SCG and Bland and Altman method was used to compare the results to values estimated by the Doppler method. The average of the correlation coefficients between the two methods and over all the subjects was 0.74 and the upper and lower confidence intervals were estimated to be 6.1 and -6.6 mL. The mean of differences between the two methods were less than 0.1 mL. The linear regression estimator gave us similar results as the support vector machine (SVM). For the same subjects the left ventricular ejection time estimated by SCG was compared to the same parameter estimated from simultaneous ICG signal.

The goal of this study was to prove the possibility of using the vibrations recorded from the sternum to estimate two important hemodynamic parameters, stroke volume and left ventricular ejection time, and to identify the possibilities that such an inexpensive methodology can provide for monitoring of the cardiac dynamics non-invasively and as an compliment to the methods that already exist.

PB7

Mitral Valve Modelling in Ischemic Patients: Finite Element Analysis from Cardiac Magnetic Resonance Imaging

CA Conti, M Stevanella, F Maffessanti*, F Trunfio, E Votta, A Roghi, O Parodi, EG Caiani, A Redaelli

Department of Bioengineering, Politecnico di Milano, Milano, Italy

Introduction. Biomechanical data of the mitral apparatus could serve as a basis for finite element (FE) analyses of the mitral valve (MV) in ischemic patients. Previously FE models were mostly based on simplifying assumptions on MV symmetrical shape, idealized leaflets free-edge profile and neglected papillary muscles (PMs) contraction. To overcome these limitations, we aimed at developing a framework for the quantitative analysis of time-varying MV geometry from cardiac magnetic resonance (CMR) imaging, and to integrate these data in a patient-specific structural simulation of MV closure.

Methods. CMR imaging of 18 long-axis planes (one every 10 degrees) was performed on three ischemic patients with a temporal resolution of 55 time-frames per cardiac cycle. Three-dimensional MV annulus geometry, leaflets surface and PMs position were manually obtained using custom software. Leaflets extent and 3-D orientation were set consistently with the MRI-derived leaflets free-edge profile. Hyperelastic anisotropic mechanical properties were assigned to the MV tissues, and a physiological pressure load curve was applied to the leaflets.

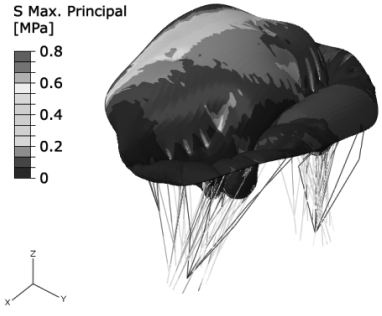

Maximum principal stress distribution at peak systole.

Results. In the studied subjects, preliminary results concerning different aspects of MV biomechanics, such as valve dynamics, leaflets coaptation, leaflets strains and chordae tendineae tensions, were in good agreement with in vitro observations.

Conclusion. In this study, we introduced a novel approach for developing a FE model of the MV based on patient-specific data obtained from CMR. This technique allows for high time-resolution imaging in adequately large field of view, even in subjects with enlarged annulus due to MV pathologies. This approach could constitute the basis for accurate evaluation of MV pathologic conditions and for the planning of surgical procedures.

PB7

Long-Term Characterization of Arterial Blood Pressure Series

Juan Carlos Perfetto*, Graciela Aurora Ruiz and Carlos Enrique D'attellis

Instituto de Ingenieria Biomedica, Universidad Buenos Aires, Capital Federal, Buenos Aires, Argentina

OBJECTIVE: To study how arterial pressure values increases and decreases during the so-call till test, which is the tool universally used to evaluate people with faint episodes. Not only what is happening but how, that is calculating the angle of the pressures ramps. This is achieved from smoothed versions of systolic pressure series.

METHODS: Ten-minute segments of arterial blood pressure recorded during tilt test procedures were selected. Those studies were done to fifty subjects (33 females and 17 males) at Fernandez Hospital using a non invasive continuous blood pressure monitor at the radial artery.A method is used to detect systolic points from continuous arterial blood pressure. Depending on test results, they are classified as positives or negatives. Those from healthy subjects are controls. A five order Butterworth low pass filter is applied to time series. The inflection points that have different sign in their slopes are the endpoints of the segments and we call them breakpoints. If they are link together, a simpler representation of the original series can be obtained. To this simplified version of the original time series we can apply different computations to extract some parameters which can serve as discrimination factors. For each record four parameters were extracted: the maximum pressure (MP) difference and the maximum angle (MA) between breakpoints for both signs.

RESULTS: MP+ was 14.56 $\pm$ 5.78 mmHg. in controls, vs. 17.93 $\pm$ 10.39 mmHg and 17.86 $\pm$13.26 mm Hg in positives and negatives respectively. MP- was -13.53 $\pm$ 6.12 mmHg in controls, vs. -17.71 $\pm$ 6.50 mmHg and -15.67 $\pm$ 9.61 mmHg in positives and negatives respectively. MA+ was 27.52 $\pm$ 10.86 degrees in controls vs. 30.44$\pm$11.84 degrees and 33.63 $\pm$ 17.41 degrees in positives and negatives respectively. MA- was -23.36 $\pm$ 8.54 degrees in controls versus -31.58 $\pm$11.50 degrees and -31.87 $\pm$18.58 degrees in positives and negatives respectively. In all the cases controls have lower values and lower standard deviations, but due to the greater dispersion in positives and negatives, significant differences cannot be reached.

CONCLUSION: These parameters were preliminary chosen for their simplicity. Although they are not significantly different, many others can be tested starting from this approach.

PB7

Displaying Computerized ECG Recordings and Vital Signs on Windows Phone 7 Smartphones

Stefan Klug*, Kai Krupka, Hartmut Dickhaus, Hugo A Katus and Thomas Hilbel

Cardiology, University of Heidelberg, Heidelberg, Germany

Introduction: Because smartphones are popular in all age groups, one could posit that they might be useful as a portable health monitor for physiological parameters and as an ECG imaging device. Smartphones support many communication standards like GSM, WIFI and Bluetooth so physiologically monitored parameters could be sent wireless from anywhere in the world to telemedicine healthcare centers. But due to the rapid evolution in the mobile market existing software is often not reusable for the new upcoming mobile devices. Therefore a new mobile biomedical application was developed to test and to judge the suitability of the new Windows Phone 7 mobile platform as an ECG imaging device and a vital sign viewer in the future. Methods: Visual Studio 2010 Express for Windows Phone was used to develop the new mobile ECG and vital sign viewer. The application does run on the Windows Phone 7 Emulator. The software emulator was released by Microsoft to allow new software development prior to the release of the Windows 7 smartphones. Silverlight (a mix of C# and XAML) was used for coding. The graphical user interface was designed to display continuous, digitally recorded ECG data and also discrete values of blood pressure and oxygen saturation. Results: Using the latest Windows Phone 7 development tools a mobile biomedical ECG viewer application on the smartphone could be developed with minimal effort. The limiting factor of monitoring and viewing the ECG tracings was the small smartphone display size. Especially for elderly people the small touchscreen may be difficult to see and operate. Because of the small display it is not feasible to display a reasonable 12 lead ECG. Nevertheless, smartphones can be useful for the mobile transmission of physiological data to telemedicine healthcare centers or personalized health or fitness portals due to their multiple wireless communication capabilities.

PB8

Transmural Exchange of Cardiology Related Information Between Two Academic Centres and Referring Hospitals using XDS(-I)

Arnold Dijk*, Jan Peter Busman, Niek van der Putten and Willem Dassen

Thoraxcenter, University Medical Center Groningen, Netherlands

More than 50% of the patient population undergoing a therapeutic invasive procedure in an Academic Centre has undergone diagnostic based procedures in a referring hospital. These procedures generate the data that forms the basis for the policy to propose therapeutic treatment in our department. Until recently the information was paper- and CD-based. It is widely recognised that an electronic system leads to better patient care. In this paper we describe two different IHE-XDS(-I) (Integrating the Healthcare Enterprises Cross- enterprise Document Sharing (for Images)) solutions based on a network that facilitates the exchange of documents as well as images. XDS is based on existing medical standards like HL-7 and DICOM , industrial standards like ebXML and SOAP and internet standards like HTTP(S) and JPEG. The existing systems, a variety of PACS systems and Hospital information systems, were easily interfaced to the XDS network, due to the on standards based infrastructure. The recently adapted nationwide patient ID serves as unique patient identifier in the XDS infrastructure. Conversion to locally used ID numbers is incorporated. Using IHE-XDS(-I), cardiologists from the regional hospitals can share rather than exchange their angiographic, echocardiographic and ECG data sets. Additionally they can include various reports and forms. After treatment, the Academic Centre can share back information to the referring cardiologist. Preliminary data has shown that the time between a patient presenting in the physicianss office and the case review in the intervention centre has decreased by 1 to 2 days.

PB8

Library for Managing and Processing ECG Signal Data: Design and Implementation in Delphi and C#

Alberto Rodríguez*, Raúl Almeida, Gemma Rodríguez, Nelvy Pina and Gisela Montes de Oca

Medical Equipment, Central Institute for Digital Research, Habana, Cuba

Software development of systems for displaying and analyzing ECG signal data is often very repetitive because they generally consist of the same modules: acquire, display, filter, detect QRS, make measurements and propose an interpretation or diagnosis. That's why it's necessary to design a way to group and make easy to reuse the functionalities of these modules. The aim of this paper is to present the design of a class hierarchy for working with ECG signal data, and its implementation, using Delphi and C#. The base classes are: TFileHandler, TProcessor and TECGBrowser. TFileHandler is use as base in many classes for managing and processing very large ECG files and other related data, as QRS, Rhythm Event and ST segment information, which allow to create, read, write, sort, and perform searches and other specific operations on these files, having very small access times and improving the systems performance. Other classes were developed, using as base the TProcessor class, for detecting QRS complexes, making rhythm analysis, filtering, classifying and ST segment processing, allowing placing the process execution code on a different thread and maintaining a continuous feedback of the progress. On the other hand the TECGBrowser class has all the properties and methods needed to display an ECG on screen: the signal itself, different marks, any kind of grids and text labels. All of these classes became a library which was used in the development of three systems: a holter, a rest ECG study system and other for remote acquisition and diagnosis of ECG. The development times were reduced in a high percent comparing with the older versions, and results are very homogeneous, consistent and nowadays are working with good results. This library helps developers and investigators to focus their efforts on the main goal of their research, having the basic issues solved.

PB8

A Personalised Self Management System for Chronic Heart Failure

William P Burns*, Richard J Davies, Chris D Nugent, Paul J McCullagh, Huiru Zheng, Norman D Black and Gail A Mountain

University of Ulster, Newtonabbey, Antrim, United Kingdom

Within our current work we are developing a home based Personalised Self-Management System (PSMS) for persons suffering from Chronic Heart Failure (CHF). Users of the PSMS have the ability to record and monitor their vital health information such as blood pressure, heart rate and weight in addition to gross levels of activity. In consultation with their Healthcare Professional (HP) an initial set of life goals are identified. Each of these goals will require some form of physical activity for example walking. Through the use of a touchscreen PC and smartphone in addition to a suite of telehealth devices it is possible for the PSMS to record health information whilst providing summative feedback on gross activity.

A touchscreen PC and smartphone are used for reviewing and entering information. Using the in-built accelerometer and GPS module, the smartphone can be used to monitor the movement of the user whilst recording how much activity is undertaken while outside of the home. The phone can also provide real time, motivational, feedback regarding the users goal achievement. Through the use of a suite of sensor technology such as PIRs, door, chair and bed sensors it is possible to record gross levels of activity within the home. Any information either entered into the system or acquired directly from sensors can be made available to healthcare professionals for review via a customisable web portal. Should any abnormalities or potential problems arise, the HP has the ability to adapt the users goals or alter other parameters under the systems control.

To date the PSMS has been evaluated by 8 persons suffering from CHF in a supervised user evaluation. Results from this evaluation have provided positive feedback on the User Interface and health information feedback although users did report negative features of the system in relation to the presentation of health information over long periods and the responsiveness of the smartphone touchscreen. Feedback following user evaluations has been used to guide ensuing cycles of technical development.

Long-term plans for the PSMS are to conduct user evaluations with 20 sufferers of CHF within their own home environment.

PB8

Nonhyperemic Intracoronary Pressure Waveform Analysis Predicts the Fractional Flow Reserve

Peter Lugosi, Peter Santa, Zoltan Beres, Balazs Tar, Janos Santa and Zsolt Koszegi*

Invasive Cardiology Laboratory, Jósa András County Hospital, Nyíregyháza, Hungary

It has been regarded that the nonhyperemic resting pressure ratio (RPR) was not appropriate for exact evaluation of the functional severity of coronary lesion. However, some studies suggest that the comparison of the proximal and distal resting waveform of the stenosis may predict the fractional flow reserve (FFR), because the intracoronary waveform has such a high-frequency pressure signal at the closing of aortic valve (notch) that can be decreased by the filter-effect of the stenosis. Deriving the resting pressure waveforms, an attempt was made to identify such a nonhyperemic parameter that correlated directly with the severity of coronary artery stenosis. We studied 22 patients (age: 61+10.2 years. On 31stenosed vessels (15 LAD, 2 LCx, 11 RCA, 2 I. diagonal, 1 OM) 40 pressure measurements were carried out by PressureWire Certus (Radi Medical) (9 times after PCI). The pressure curves were exported through the RadiView software to a JAVA program developed by us and the dp/dt were calculated (dt=1/100 sec). In order to characterize the ascending slope of the dicrotic notch, the difference between the local minimum and maximum values of the derivated pressure waveform was calculated (derivated delta notch: delta dpN/dt). There was a significant correlation between the delta dpN/dt and FFR, as well as the RPR and the FFR ($r= 0.59$, $p < 0.001$ and $r= 0.65$, $p= 0.004$, respectively). By using the Receiver Operating Curve (ROC) analysis, the value of 3>delta dpN/dt (sensitivity 100%, specificity 91%), and an RPR=0.87 (sensitivity 88%, specificity 84%), was found to be the optimal cut-off values for predicting FFR<0.75. The area under the ROC was 0.99 in case of delta dpN/dt and 0.92 in case of RPR. The delta dpN/dt can be a new useful nonhyperemic parameter for the assessment of the coronary artery stenosis during the intracoronary pressure measurements.

MC

Development and Validation of Automated Endocardial and Epicardial Contour Detection for MRI Volumetric and Wall Motion Analysis

Enrico G Caiani*, Alberto Redaelli, Oberdan Parodi, Emiliano Votta, Francesco Maffessanti, E Tripoliti, Gaetano Nucifora, Daniele De Marchi, Giacomo Tarroni, Massimo Lombardi and Cristiana Corsi

Biomedical Engineering Dpt., Politecnico di Milano, Milan, Italy

Magnetic resonance imaging (MRI) represents the gold standard for left ventricular (LV) volumes and mass analysis, as well as for the diagnosis of regional LV dysfunction. However, volumetric measurements based on multiple contour tracings are cumbersome, and visual interpretation of cine images suffers from inter-observer variability. Our aim was to develop a technique for combined automated endo and epicardial border detection from MRI throughout the cardiac cycle, and to validate it. Methods. Dynamic, ECG-gated, steady-state free precession short-axis images were obtained (GE Healthcare, 1.5T) in 812 slices in 15 patients with previous myocardial infarction. An expert cardiologist provided the gold standard for: 1) LV dimensions and mass, by manually tracing endo and epicardial contours; 2) regional wall motion (WM) interpretation, by grading (normal, abnormal) three slices selected at apical, mid and basal level. Custom software based on image noise distribution (for LV endocardial detection) and level-set (for epicardial detection) was applied, from which end-diastolic (ED) and end-systolic (ES) volumes and mass were computed, as well as regional fractional area change (RFAC), from which automated classification of regional WM abnormality was defined for RFAC$<$50%. Comparison with gold standard was performed by: 1) linear regression and Bland-Altman analyses for LV volumes and mass; 2) levels of agreement between the cardiologist WM grades and the automated classification. Results: Optimal correlations (r2$>$.97) and no bias were found for ED and ES volumes, while LV mass resulted in a good correlation (ED: r2=.81; ES: r2=.74) with a minimal overestimation (ED:15.2g; ES:8.7g) and narrow 95% limits of agreement (ED: $\pm$ 30 g; ES: $\pm$ 33 g). The automated interpretation resulted in high sensitivity, specificity, and accuracy (78%, 85%, 82%, respectively) of WM abnormalities. Conclusion. Combined automated endo and epicardial border detection from MRI provides reliable measurements of LV dimensions and regional WM classification.

MC

Polysomnography in Extreme Environments: the MagIC Wearable System for Monitoring Climbers Ascending on Mount Everest Slopes

Paolo Meriggi*, Paolo Castiglioni, Carolina Lombardi, Francesco Rizzo, Andrea Faini, Marco Di Rienzo and Gianfranco Parati

Polo Tecnologico (Biomedical Technology Department), Fondazione Don Carlo Gnocchi, Milano, Italy

We recently developed a textile-based wearable system (called MagIC) for monitoring ECG, thoracic respiratory movements, body accelerations and posture in unrestrained subjects. This study presents results on the applicability of MagIC for polysomnographic recordings at very-high altitude in climbers on Mt. Everest slopes. Five professional mountaineers were provided with MagIC modified for the HIGHCARE expedition by integrating a finger pulse oximeter (Nonin Xpod) and by substituting cotton with polypropylene, a yarn for thermal underwear which facilitates transpiration. Signals were recorded continuously for more than 10 hours at night, first at sea level (SL), and then during the ascent on Mount Everest slopes, at 6000m (Camp1) and 6800m (Camp2). Each climber found MagIC comfortable to wear and completed the monitoring set-up without need of help, even in the most challenging environment of Camp2. After having visually scored the signal quality, the average artefacts rate (ratio between cumulative duration of artefacts and length of the recording) resulted to be lower than 5%. This allowed the identification of central sleep apneas and the calculation of tachogram-derived parameters. The mean R-R interval (RRI) and its standard deviation (SDNN) were obtained on the last 4 hours of sleep, easily identified from the accelerometric signals. During night RRI tended to decrease from SL (956.2±50.1ms, mean±SEM) to Camp1 (938.3±39.1 ms) and Camp2 (894.3±41.2ms). SDNN increased significantly from SL (110.7±15 ms) to Camp1 (159.6±14.0 ms) and from Camp1 to Camp2 (186.5±18.8 ms). Central apneas, absent at SL, occurred frequently at high altitude and the oxygen saturation was lower at Camp2 (69%±5%) than at Camp1 (75%±3%). MagIC demonstrated to be suitable for cardiorespiratory monitoring in such extreme environments, being comfortably used by climbers and offering high quality recordings. Our results provide the first description of cardiorespiratory changes during sleep in climbers exposed to hypobaric hypoxia at very high altitude.

MC

Investigation of Drowsiness while Driving utilizing Analysis of Heart Rate Fluctuations

Gabriela Dorfman Furman* and Anda Baharav

Tel Aviv University, Rehovot, Israel

Complex regulatory and biofeedback systems rule human function and behavior. Sleep is vital, ruled by homeostatic balance and circadian oscillations. Sleepiness is a main causal factor for accidents and daytime malfunction. In this study we check the feasibility of a new non-invasive method, ECG based, to detect drivers propensity to fall asleep mainly while driving. 10 healthy volunteers, under conditions of increasing sleep deprivation (up to 34 hours), were asked to alternately undergo a standard, passive, 45 minute Maintenance of Wakefulness Test, and a 90 kilometer driving simulation test, every 2 hours while ECG, EEG, EMG, eye movement and video were recorded and later analyzed off-line. Microsleeps (MS) lasting for 3-15 seconds and falling asleep events lasting 15-120 seconds were detected from electroencephalogram analysis. The ECG was analyzed using R-R interval (RRI) behavior in the time domain, time-frequency decomposition of the RRI series (TFD), and entropy and Poincare plots n+1 of the RRI. Significant changes occurred in the RRI behavior in the time domain after the first MS using windows of 30 seconds and longer. TFD showed a significant change in low frequency (LF), high frequency (HF), and LF/HF after the first MS. The Entropy of the RRI and certain measures of Poincare plots also changed after the first MS. The first accident on the simulator task occurred 2-7 minutes after the first MS. We can thus conclude that the first MS represents a cutoff point in the behavior of HRV based on a number of calculated parameters in the time and time frequency domains. There are clear HRV markers that indicate sleepiness in sleep deprived subjects. Provided some of these variables show the same trends, a threshold should be defined as to imminent danger while driving and when a subject should be stopped from continuing a task.

MC

Features of Arterial Blood Pressure as Indicators of Impending Acute Kidney Injury in ICU Patients

Li-wei Lehman*, Mohammed Saeed, George Moody and Roger Mark

Harvard/MIT Division of Health Sciences & Technology, MIT, Cambridge, MA, United States

In the context of critical illness, hypotension may be associated with acute kidney injury (AKI). We studied the relationship between arterial blood pressure and the development of AKI using the MIMIC II Database (release v2.4). We defined AKI as an increase in creatinine of at least 50%, to 1.2 mg/dL or more, within a period of 12 - 48 hours.

Among the 17,202 adult ICU stays that had at least 3 creatinine measurements without elevated (>5 mg/dL) admission creatinine, AKI occurred in 1,506 (8.75%) of these cases. The remaining 15,696 cases were identified as the controls. Nurse-verified systolic intra-arterial blood pressure (SBP) measurements obtained at intervals of an hour or less, were recorded for approximately 80% of the AKI cohort, and 45% of the controls.

We examined six features of the SBP time series for each ICU stay, including minimum, median, fractions of samples below 90 and 110 mmHg, and mean and minimum sample-to-sample differences. We calculated each feature using SBP samples for up to four 24-hour windows (beginning at 24, 48, 72, and 96 hours) before T, where T was defined as either the time when the AKI criterion was met, or (for controls) the time of the penultimate creatinine measurement.

Significant differences between the AKI cohort and controls emerge as early as the third day before AKI onset. Using Student's t-test, we found significantly lower median and minimum SBP values in the AKI cohort ($p < 0.0009$ and $p < 0017$ respectively) over the period from 72 to 48 hours before T. There is a significantly higher fraction of SBP less than or equal to 110 mmHg in this time window for the AKI cohort ($p < 0.0004$). Our results suggest that patterns in intra-arterial blood pressure may contain useful features in developing early warning signs of AKI.

MC

Development and Clinical Validation of a Physiological Data Acquisition Device Intended for Monitoring and Exercise Guidance of Heart Failure and Chronic Heart Disease Patients

Athina Kokonozi, Alexander Astaras, Panagiotis Semertzidis, Emmanouil Michail, Dimitris Filos, Ioanna Chouvarda*, Olivier Grossenbacher, Jean-Marc Koller, Leopoldo Rossini, Jacque-André Porchet, Marc Correvon, Jean Luprano, Auli Sipilä and Chryssanthos Zambou

Lab of Medical Informatics, Medical School, Aristotle University of Thessaloniki, Thessaloniki, Greece

The HeartCycle project is a european biomedical engineering research effort aiming to provide disease management solutions for heart failure and chronic heart disease patients, including co-morbidities such as hypertension, diabetes and arrhythmias. Developed by some of the authors within HeartCycle, IMAGE is a microcontroller-based, power-autonomous, 3-lead wearable device, capable of acquiring 2-channel ECG, 2-channel bioimpedance, 3-channel gyroscopic acceleration and oxymetry measurements. The acquired signals are stored in onboard memory and processed, while the results are transmitted in real time via a wireless IEEE 802.15.4 link to an interface base station, such as a properly equipped PC or PDA. Processed data is available to clinicians wishing to continuously monitor their patients, as well as to patients requiring real-time feedback during safety-sensitive recuperation exercise periods (guided exercise). IMAGE is worn by the patient using purpose-designed undergarment vests while design choices allow for smart fabric washable electrode development in the future. While development of IMAGE continues, evaluation of existing prototypes performance in clinical, domestic and outdoors environments is also well underway in three HeartCycle partner sites. In the Medical School of the Aristotle University of Thessaloniki (Greece) IMAGE was initially evaluated by means of outdoors exercise routines involving 4 healthy volunteers, followed by similar experimentation entailing indoors exercise. Subsequently, gold standard BRUCE protocol treadmill stress test experiments were performed using a commercial portable device (Zephyr Bioharness BT) for comparative analysis. Parallel testing involving gold standard hospital equipment and chronic heart disease patients is planned next. Results to date show good correlation of the heart rate and breathing rate signals from the two devices, using both the onboard and off-line Matlab algorithms (typical mean HR difference < 4.48, BR < 0.87).

MC

Time-Frequency Analysis of Cardio-Respiratory Response to Mental Task Execution

Luigi Yuri Di Marco*, Roberto Sottile and Lorenzo Chiari

Department of Electronics, Computer Science and Systems (DEIS), University of Bologna, Bologna, Italy

OBJECTIVE: Heart rate, heart rate variability (HRV) and respiratory effort have been proposed in numerous studies with the goal of correlating physiological parameters with mental workload. Aim of this study was to analyze the cardio-respiratory response to a mental task (Sternberg Task) from a single lead ambulatory ECG recording, in healthy subjects. METHODS: Under no assumptions on stationarity, short-term HRV was analyzed in the time-frequency domain by means of the Hilbert-Huang Transform (HHT). Results were compared with the power spectral density (PSD) estimate based on Welch periodogram. HHT marginal energy spectrum was computed to estimate normalized LF and HF energy evolution over time. A surrogate respiratory signal (SRS) was extracted from the ECG by means of an established principal component analysis (PCA) based method, and its spectrum was computed in the range 0-0.5 Hz for respiratory rate and power analysis. SRS was extracted from the same sliding window of ECG data used for HRV, to allow synchronous and consistent analysis. RESULTS: HRV analysis in the time-frequency domain and in the frequency domain lead to similar results in terms of normalized LF and HF components (LF: $r^2 = 0.63 \pm 0.17$, HF: $r^2 = 0.54 \pm 0.20$) evolution, the first being more evident and also the most relevant in literature to the characterization of the cardio-respiratory response to a mental task in healthy subjects. A significant though not sustained increase in LF was found in this study in most subjects in response to the mental task start. Frequency domain PSD analysis of SRS showed a dominant respiratory rate between 0.20 Hz and 0.35 Hz (12 rpm and 20 rpm, respectively) in most subjects, which in some cases was associated with a transient lower frequency component (0.15-0.20 Hz) with higher power in proximity of the task start.

NN

Author Index